Commercially scalable fish collagen processing

A thesis presented in partial fulfilment of the requirements for the

degree of

Doctor of Philosophy

in

Food Technology

at Massey University, Palmerston North,

New Zealand.

Suchima Tharangi Gonapinuwala

2023

MASSEY UNIVERSITY
TE KUNENGA KI PŪREHUROA
UNIVERSITY OF NEW ZEALAND

Abstract

Fish collagen has a potential for high-value applications in the biomedical industry due to its excellent biocompatibility, biodegradability and low antigenicity properties. It is also a viable alternative for mammalian collagen due to its high availability, having no risk of disease transmission or religious barriers and the low cost of raw material. However, its utilisation is limited due to the non-availability of industrial-scale processing methods. Maintaining the native triple-helical structure in collagen molecules and the native D-banding pattern in the collagen fibrils are the requisites for biomedical collagen, therefore the existing industrial fish collagen extraction methods for food or cosmetic applications cannot be used. Unlike mammalian-origin collagen, fish-origin collagen differs due to fish species differences, and it is not practical to develop by trial and error, collagen extraction methods for every individual fish species of interest. Therefore, this study was carried out to interpret how the fish skin structure and composition relate to the physico-chemical processes that occur during collagen extraction, to develop a biomedical collagen extraction method based on this understanding, and to present guidelines to use this method for other fish species at industrial-scale.

This collagen extraction process was developed through three main steps: pretreatment, extraction, and fibrillogenesis, and important determinants at each step, in relation to the fish skin structure and composition were identified. The focus of the pretreatment step is to remove non-collagenous proteins and fats, and the swelling of the skin in the pretreatment medium was also found to be a critical aspect in this tissue due to the structure of fish skin. The focus of the extraction step is to solubilise collagen molecules into the extraction medium in its native triple-helical conformation. Using a hydrochloric acid medium at an initial pH of 2 was found to be important in preserving the native triple-helical structure of collagen molecules. In addition, four processing objectives were presented based on the underpinning knowledge, to apply this method to any fish species of interest: (i) an upper limit of pH 4 for the extraction solution; (ii) maximum swelling; (iii) a manageable viscosity of the extraction solution; and (iv) as few undissolved pieces of skin as possible. A second extraction was introduced as a pigment removal step to improve the purity and colour of collagen while still preserving the collagen native structure.

The ultimate focus of the whole collagen extraction process is the formation of collagen fibrils with the native D-banding pattern, which is achieved in the fibrillogenesis step. An initial collagen concentration of 0.30% in 0.01 M hydrochloric acid solution, adding 0.1 M Sodium hydroxide until pH 9.3 with gentle mixing, and keeping undisturbed for 24 h at 4°C are recommended as processing conditions to obtain collagen fibrils with native D-banding pattern. The initial collagen concentration is critical for molecular availability and the mixing speed is critical for molecular mobility during fibrillogenesis.

With this understanding of the behaviour of fish skin during the extraction process, and the knowledge on how it can be applied to any fish species of interest, the future processing of biomedical collagen from fish skin at the industrial level will be possible.

Acknowledgements

This PhD journey has been a truly life-changing experience for me, and it was a challenging time with the unexpected hit of COVID-19 after six months of starting my PhD. I am grateful to everyone who was with me during this time, without whose help completion of my PhD would not be an easy task. Thank you all for contributing to making my PhD a very special time in my life.

First, I am extremely grateful to my supervisory panel: main supervisor Prof. John Bronlund, and co-supervisors Prof. Jim Jones, Dr Steve Kirk and Prof. Dileepa de Croos. It was a lifetime opportunity to be supervised by you all, thank you for accepting me as a PhD student and for extending trust and confidence in me. I learned a lot from you, experienced new disciplines of science and realised more about my passion for research. Your patience and kindness were so much influential to me. I express my sincere gratitude to John for all the opportunities and challenges, I admire the freedom given to me to conduct my research independently which helped me to shape into the person I am today. Thank you, John, for your understanding, and life advice and for being such a great mentor to me. Similarly, I am deeply grateful to Jim, for your constructive comments, invaluable suggestions, and dedicated support, especially during writing. I am thankful to Steve for providing me with hands-on experience in industrial processes, and being available at every time despite his busy schedule. Thank you Steve for helping me by every possible means. Dileepa, I am deeply thankful for your mentorship and generous help, especially during the period I stayed in Sri Lanka.

Next, I would like to acknowledge the PhD scholarship from the World Bank through the government of Sri Lanka under the scheme Accelerating Higher Education Expansion and Development (AHEAD) operations. At the same time, I would like to take this opportunity to thank the free education system of Sri Lanka which helped me and many others to thrive well through education and gain the benefits of higher education.

My PhD project involved various work in different labs, and without the great help of the technical staff, it would not have been possible to complete all work without delay. I would like to thank the technical staff of the School of Food and Advanced Technology, Massey University: John Sykes and Ann-Marie Jackson for being available for any need and always approving after-hours lab work; Inge Merts, Kylie Evans, Steve Glasgow, Michelle Tamehana, Warwick Johnson, and Garry Radford for teaching and assisting me in lab analysis. I am grateful to John Edwards for helping me in designing and making some apparatus in the lab and thank you for your joyful personality. I also appreciate my labmates for their questions about my research, their enthusiasm and for bearing the fishy odour.

I specially thank Prof. Geoff Jameson for allowing me to use the circular dichroism spectrometer at the School of Natural Sciences, Massey University and for helping me with analysis. Thank you for your time and guidance. I thank Trevor Loo and Bruce Chilton for providing me with the hands-on experience of using the instrument. I also thank the staff of other outside laboratories for providing me with the training to use different equipment and assisting me with analysis. Thank you to Graham Freeman for the Fourier transform infrared spectrometer at the School of Natural Sciences; Maggie Zou and Sihan for the Zerasizer at the 'Te Ohu Rangahau Kai'-joint food science facility of AgResearch, Massey University and

Riddet Institute; Raoul Solomon and Yanyu He for the scanning electron microscope and transmission electron microscope at the Manawatu microscopic and imaging centre. Thank you to Niki Hazelton at the University of Otago for agreeing to conduct transmission electron microscopy work in a much-needed time and for your quick responses. I thank Vijitha, Kumarasinghe, Jayantha and the lab staff for assisting me with lab work at the Department of Aquaculture and Fisheries, Wayamba University of Sri Lanka during my short stay.

This work involved processing many kilos of fish waste. I acknowledge the friendly staff at fish shops in Palmerston North for providing me with fish waste and their kind cooperation.

I would like to thank my friends I met in New Zealand: Isuri, Muditha, Umani, Harshana, Nuwan, Joanna, Hien, Christine, How, Achinthya, Aslan, Soumya, Sonia, Rehan, Merit, Aiman, Sebastian, Alex, Gieun, Akmal, Natasha, Maheeka, Maru, Rupsa, Magda, Reshab and Farah. Your joyful friendship and kind help made my three-year stay in New Zealand a wonderful and memorable one. I also thank my friends from Sri Lanka: Charitha, Senani and Thilini for their continuous encouragement.

I owe a debt of gratitude to Dilantha and Amal. Thank you for being home away from home, your kindness, being available at any time for any need and also for life advice.

I sincerely acknowledge my colleagues at the Wayamba University of Sri Lanka for their support and flexibility provided me during my study period.

Finally, I want to present my dearest gratitude to my family. I am highly indebted to my brother for taking care of my parents, tremendous understanding and efforts to keep me smiling. My aunt Puncha, Gigi, Ruchika, Yanu, Senu, and Denu, you all deserve my wholehearted thanks as well. My parents - Amma and Thaththa, thank you for your patience, kindness, love and care. I dedicate this thesis to you!

Table of contents

List of tables

List of figures

List of abbreviations

AFM	Atomic force microscopy
ANOVA	Analysis of variance
ATR-FTIR	Attenuated total reflectance-Fourier transform infrared
CD	Circular dichroism
DSC	Differential scanning calorimetry
ECM	Extra cellular matrix
m/v	Mass to volume
pI	Isoelectric pH
R_{pn}	Positive to negative peak ratio
SEM	Scanning electron microscopy
ΔH	Denaturation enthalpy
T_d	Denaturation temperature
TEM	Transmission electron microscopy
UV	Ultraviolet
v/v	Volume to volume ratio
w/v	Weight to volume ratio

Conference abstracts, presentations and prizes

Oral presentations

- **Gonapinuwala, ST.,** Kirk, S., Jones, J., de Croos, MDST., & Bronlund, J. (2020). Measurement of swelling behaviour of fish skin during collagen extraction pretreatment. Massey University Postgraduate Food Science Symposium. Palmerston North, New Zealand.
- **Gonapinuwala, ST.,** Kirk, S., Jones, J., de Croos, MDST., & Bronlund, J. (2022). Native collagen from fish waste - a study of extraction conditions. NZIFST Annual Conference, Rotorua, New Zealand.

Poster presentations

- **Gonapinuwala, ST.,** Kirk, S., Jones, J., de Croos, MDST., & Bronlund, J. (2021). Biomedical collagen from fish skin - Adding value to fisheries waste. NZIFST Annual Conference, Palmerston North, New Zealand.
- **Gonapinuwala, ST.,** Kirk, S., Jones, J., de Croos, MDST., & Bronlund, J. (2022). Effect of treatment conditions on extracting fish collagen for biomedical applications. NZIFST Annual Conference, Rotorua, New Zealand.

Scholarships and prizes

- Registration scholarship to attend the New Zealand Institute of Food Science and Technology (NZIFST) Annual Conference – Rotorua, New Zealand (July 2022)
- Food Tech Solutions Prize for the poster at the NZIFST Conference 2022 that best demonstrates both good science and commercial viability.

Chapter 1. Introduction and thesis outline

1.1 Research background

Marine collagen which can be extracted from fish skins has the potential for high-value applications in the biomedical field. Uses include wound dressings, drug delivery systems, gene delivery systems, and tissue engineering systems. Key to its use are its excellent biocompatibility, biodegradability and low antigenicity properties (Riaz et al., 2018, Sun et al., 2017; Zhu et al., 2018). It is made up of predominantly type I collagen, like currently sourced mammalian-derived collagen. Mammalian sources such as bovine and porcine have been widely utilised to extract collagen, however there is a need of alternative sources due to some concerns associated with mammalian sources. The rising costs of mammalian sources, and the challenges in the geography of supply due to the risk of transmission of zoonotic diseases such as bovine spongiform encephalopathy (BSE), foot and mouth disease (FMD) and transmissible spongiform encephalopathy (TSE) are associated problems (Liu et al., 2014, 2015; Pal & Suresh, 2017). Additionally, mammalian-derived collagen is associated with religious concerns. Muslim and Hebrew faiths do not accept pig related products and Hindus do not accept cow related products in general (Nurilmala et al., 2019).

On the other hand, industrial processing of fish recovers only 20-50% of the original raw material as edible portions and discards 50-80% as waste (Wasswa et al., 2007). Fish skin constitutes the major component of fish by-products with type I collagen accounting for the highest component of protein within it (Xu et al., 2017). Therefore, fish skin-origin collagen is a viable alternative due to its high availability, no risk of disease transmission, no religious barriers and low cost of raw material. However, this valuable resource has not been utilised by the biomedical industry to its optimum potential mostly due to the non-availability of industrial-scale processing methods that can extract collagen in native form with the tipl-helical structure and D-banding pattern preserved in it. This D-banding pattern is required for cellular responses such as cell proliferation, cell migration, cell differentiation, and cell adhesion (Zhu et al., 2018), and mineralisation of the collagen matrix (Li et al., 2009).

Industrial methods are available for collagen extraction from mammalian sources; however, they cannot be directly applied to fish due to structural and compositional differences between fish and mammalian sources. For example, the isoelectric pH of collagen extracted from bovine hide wastes is slightly acidic (pH 5.38) (Li et al., 2008) compared to pH 9.3 (Pati et al., 2012), and pH 6-9 (Li et al., 2013) reported for fish skin collagen. Lower thermal stability of fish collagen is a major barrier due to less cross-links compared to mammalian collagens, however cross-linking methods could be applied to attain the required stability in making biomedical materials.

Kerecis, a company in Iceland has developed a skin substitute from intact cod fish skin without isolating the collagen from the skin. This device has applications in surgeries and wound healing. Jellagen, a company in United Kingdom has developed biomedical materials such as liquid collagen, hydrogels, flowable matrix, scaffolds and dressings from jellyfish which is a marine invertebrate. There are also industrial methods available to extract collagen from fish skin for food and cosmetics applications. Collagen is extracted in the form of gelatin for food applications and in the form of peptides for cosmetic applications. Both the gelatin

and peptides are hydrolysed forms of collagen which are not suitable for biomedical applications due to the loss of D-banding pattern. There are no industrial extracted microfibril biomedical collagen products that are derived from fish skin.

Many studies have been done on the extraction and characterisation of fish skin collagen, however, they have not been progressed beyond the laboratory level. Unlike mammalian-origin collagen, the properties of fish-origin collagen differ due to the inter and intra-fish species differences. This important factor has not been considered in laboratory methods. Therefore, the adoption of the same method on all fish species is not appropriate for valorising applications in the biomedical field. In addition, these methods are complex, time-consuming and not cost-effective to use by the industry. Therefore, modifying industrially relevant methods by considering fish species differences is of high importance. It is not practical to develop methods experimentally for all fish species of interest, therefore a strong mechanistic knowledge is required on how the biology of fish and biochemistry of fish skin structure relate to the physico-chemical processes of collagen extraction, to optimise processing parameters for any fish species with minimal experimentation.

Therefore, this study is built on the hypothesis 'optimum parameters that preserve the collagen native structure for biomedical applications will depend on the fish skin properties'. To test this hypothesis, different analytical and characterisation techniques were used to understand the behaviour of fish skin during different stages of the collagen extraction process.

1.2 Aims and objectives

The overall aim of this work was to develop an industrially relevant method for biomedical collagen extraction from fish skin. This aim was achieved through the following objectives:

- Interpret how the fish skin structure and composition relate to the physico-chemical processes that occur during collagen extraction.
- Present guidelines for collagen extraction from variable fish species at industrial level.

The overall aim of the thesis can be seen in Figure 1.1. The knowledge developed from the research would be used to take the characteristics of the raw material fish skin and the desired structural properties of the product and identify the processing conditions required to deliver these outcomes.

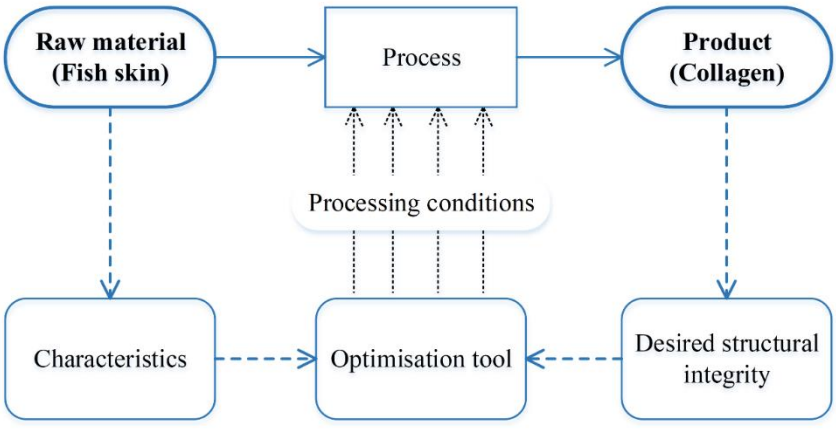

Figure 1.1 Graphical representation of the overall aim of the thesis.

1.3 Research approach

This research was conducted through preliminary experiments followed by major experiments and finally proposing an industrially relevant method for biomedical collagen extraction from fish skin. The structural characteristics required for biomedical collagen are considered, but the biological tests to assess biocompatibility are not considered in this study.

Preliminary experiments were conducted to become familiar with collagen extraction processes both from fish and mammalian sources, and to set up key equipment. A commercial bovine collagen extraction method was modified in preliminary experiments which formed the basis for the collagen extraction method proposed in this thesis. In addition, the experiments under three major experimental chapters; pretreatment, extraction, and fibrillogenesis were designed based on the overall knowledge gained from preliminary experiments. The analysis and characterisation techniques were employed to determine the structural integrity that should be preserved in biomedical collagen. Finally, a method was proposed and how it should be adopted to varying fish species was discussed.

A summary of the work done under each chapter is listed below.

- **Chapter one** describes the research background, aims and objectives, and the research approach.
- **Chapter two** contains a comprehensive review covering all the aspects of research including biomedical applications of collagen, differences between fish and mammalian collagen, collagen extraction methods from fish skin, and the characterisation of collagen for biomedical applications.
- **Chapter three** demonstrates a laboratory scale implementation of a commercial bovine collagen extraction process, and the application of this process to fish skin, and identifies key areas where modifications are required.
- **Chapter four** includes preliminary experiments that developed a fish collagen extraction method for biomedical applications based on the understanding of the Chapter three results and available literature on fish collagen extraction.
- **Chapter five** introduces the degree of swelling as a quantitative measure of the behaviour of fish skin during collagen processing in relation to different processing conditions.
- **Chapter six** develops a pretreatment process based on experiments which determined the effect of different treatment conditions on the removal of non-collagenous proteins and fats, and the understanding of how fish skin behaved in the pretreatment medium.
- **Chapter seven** develops an extraction process on the understanding of the collagen solubilisation process from the fish skin into an acidic solution, the factors affecting that process and the characteristics to determine the native triple-helical conformation of collagen.
- **Chapter eight** develops a fibrillogenesis process based on the experiments which assessed the conditions affecting the isoelectric precipitation method used in this study.
- **Chapter nine** concludes this thesis by presenting and discussing an industrially applicable biomedical collagen extraction method from fish skin and suggesting possible directions for future research.

Chapter 2. Literature review

2.1 Introduction

To develop an industrial process for preparation of marine collagen for biomedical applications, the research literature on the following aspects was reviewed; collagen as a biomaterial including molecular structure and biomedical applications, fish as a source of type I collagen for biomedical applications, the chemistry behind collagen extraction processes and how it relates to the biochemistry of fish skin structure, and the characterisation techniques to determine the applicability of collagen in biomedical applications. The structural characteristics required for biomedical collagen were considered, but the biological tests such as biocompatibility, biodegradability, and cell viability and the toxicity tests were not considered in this study. Further, the hygienic practices required for the safety aspects were not considered.

2.2 Collagen as a biomaterial

2.2.1 Molecular structure of collagen

Collagen is the most abundant protein in vertebrates (Li et al., 2013; Xu et al., 2017) accounting to 25-30% of total body proteins (Arumugam et al., 2018; Li et al., 2013; Muralidharan et al., 2013; Singh et al., 2011) and 20-30% of total body proteins in mammals (Li & Douglas, 2013; Ricard-Blum, 2011; Woo et al., 2008). About half of the total body collagen is in the skin (Lee et al., 2001).

Collagen is an extracellular matrix protein (Ikoma et al., 2003; Jiang et al., 2004; Maroušek et al., 2015; Shoulders & Raines, 2009; Zhu et al., 2018;) and it is the major constituent protein of tissues primarily responsible for the mechanical functions (Lee et al., 2001) such as skin, tendons, cartilage, bones (Schmidt et al., 2016), and other types of tissues like blood vessels and cornea (Silvipriya et al., 2015). Collagen plays structural roles (Chen et al., 2016; Li et al., 2013; Maroušek et al., 2015) and contributes to mechanical properties (Ricard-Blum, 2011; Zhu et al., 2018), organisation, and shape of tissues (Ricard-Blum, 2011). Collagen is involved in the formation of tissues and organs (Lee et al., 2001), cell attachment (Jiang et al., 2004) and functional expressions of cells (Lee et al., 2001). About 70% of the composition other than water in the dermis of skin and tendons of mammals is collagen (Lee et al., 2001).

At least 28 known genetically different types of collagen have been identified in vertebrates (Gómez-Guillén et al., 2011; Green et al., 2016), numbered with Roman numerals such as type I, type II, type XII (Ricard-Blum, 2011). Each type differs in its amino acid composition and sequence, molecular structure, and function (Gómez-Guillén et al., 2011; Liu et al., 2012; Pal et al., 2015). Some scientists say there are 29 types under the collagen family (Chen et al., 2016; Gómez-Guillén et al., 2011; Pal et al., 2015; Riaz et al., 2018; Silvipriya et al., 2015). An epidermal collagen type has been proposed as type XXIX (Rodhouse et al., 1998), but its acceptance is under debate because the coding gene COL29A1 of type XXIX is identical to the coding gene COL6A5 of type VI (Gara et al., 2008; Hinderer et al., 2016), therefore the α1(XXIX) chain corresponds to the α5(VI) chain (Gara et al., 2008).

These 28 types of collagen are categorised as fibril-forming collagens, fibril-associated collagens, network-forming collagens, membrane collagens, and multiplexins (Ricard-Blum, 2011). Fibril-forming or fibrillar collagens contain one major triple-helical domain. In contrast, fibril-associated collagens contain interrupted triple-helices. Membrane collagen subfamilies and multiplexins contain several triple-helical domains. Fibril-associated collagens or (fibril-associated collagens with interrupted triple-helices) do not form fibrils by themselves but are found covalently linked to the surface of fibril-forming collagens. For example, type XII and type XIV collagens are linked to the surface of type I collagen, whereas type IX is linked to type II collagen (Ricard-Blum, 2011).

Molecular structure is common to all collagen types, i.e., the key feature or the structural unit is characterised by the presence of a triple-helix, composed of three polypeptide chains called α-chains, having a repeating amino acid sequence (Gelse et al., 2003; Riaz et al., 2018; Ricard-Blum, 2011) in at least one region of the molecule (Gelse et al., 2003). The fraction of the molecule in the triple-helix structure varies from 96% in type I to less than 10% in type XII (Ricard-Blum, 2011). These α-chains are numbered with Arabic numerals such as α1, α2 (Ricard-Blum, 2011). In this repeated sequence of amino acids (Gly-X-Y)n, Gly is glycine, X is mostly proline and Y is mostly hydroxyproline (Addad et al., 2011; Gelse et al., 2003; Gómez-Guillén et al., 2011; Pal et al., 2015; Ramı´rez-Rodrı´guez et al., 2014; Ricard-Blum, 2011; Yang et al., 2014).

The presence of glycine in every third position of the amino acid sequence is important for the assembly of a right-handed super helix (Gelse et al., 2003). The presence of proline and hydroxyproline residues is important for the conformation and stability of the triple-helix. It is caused by the steric hindrances originating from the pyrrolidine rings of these two imino acids (Jenkins & Raines, 2002; Nagai et al., 2008) and hydrogen bonding effects due to the hydroxyl group of hydroxyproline (Gelse et al., 2003). In addition, interchain hydrogen bonds, and electrostatic interactions, involving lysine and aspartate are important to stabilise the triple-helix (Ricard-Blum, 2011).

In the first step of fibril-formation *in vivo*, collagens are synthesised as procollagen molecules (Figure 2.1) comprised of an amino-terminal propeptide (N-propeptide) followed by a short, non-helical, N-telopeptide, a central triple-helix, a C-telopeptide and a carboxy-terminal propeptide (C-propeptide) (Ricard-Blum, 2011).

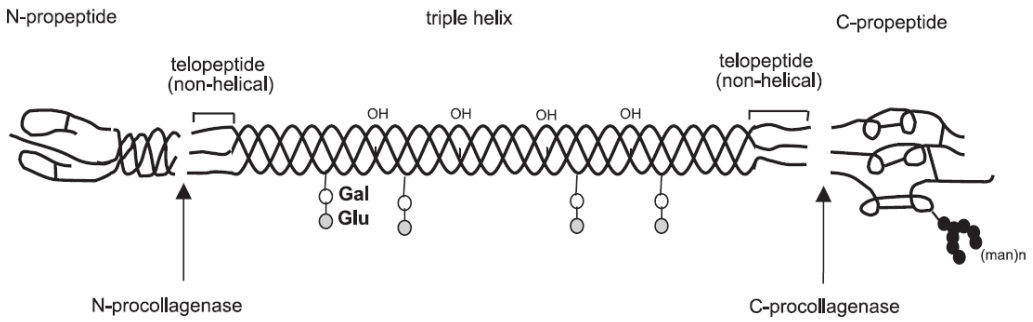

Figure 2.1 Molecular structure of the procollagen molecule with various subdomains and cleavage sites (source: Gelse et al., 2003).

During the first step of fibril-formation *in vivo*, pro-α-chains undergo various modifications such as hydroxylation of proline and lysine residues, glycosylation of lysine and hydroxylysine residues, sulfation of tyrosine residues (Myllyharju & Kivirikko, 2004) to form the triple-helix procollagen molecule, and this process stops once heat shock proteins 47-HSP47 are bound to this procollagen molecule (Makareeva & Leikin, 2007). C-propeptides are important in the initiation of triple-helix formation, while N-propeptides are important in the regulation of primary fibril diameters (Bateman et al., 1996). These propeptides are cleaved during the maturation process to form tropocollagen molecules, the structural unit of collagen with dimensions of 300 nm in length and 1.5 nm in diameter (Kadler et al., 1996) corresponding to about 1,000 amino acids (Bateman et al., 1996) (Figure 2.1).

During the second step of fibril-formation *in vivo*, five of these tropocollagen molecules combine to form one microfibril (Hulmes, 2002; Orgel et al., 2001) of tens to hundreds of nm in diameter (Zhu et al., 2018) (Figure 2.2). In the first 14 amino acid residues from the N-terminus and in the first 10 amino acids from the C-terminus of the tropocollagen molecule, which are termed telopeptides, the repetitive occurrence of glycine amino acids does not occur (Wong, 1989), therefore these two ends are non-helical. These telopeptide regions are important in a collagen molecule to form covalent cross-links between collagen molecules (Nalinanon et al., 2011; Ricard-Blum, 2011) and form cross-links with other molecular structures of the surrounding matrix (Gelse et al., 2003). The mechanical properties of fibril-forming collagens depend on this covalent cross-linking that occurs due to lysine and hydroxylysine amino acids (Ricard-Blum, 2011). These cross-links are formed by different pathways (Hofman et al., 2012). These cross-links cause a decrease in collagen solubility (Nalinanon et al., 2011). Cross-linking is tissue-specific rather than collagen-specific (Ricard-Blum, 2011). The form of cross-linking and its chemical properties depend on the animal species and tissue type (Hofman et al., 2012). Meanwhile, these fibrils are covalently bound to each other in a staggered manner (Zhu et al., 2018) with a distinctive periodicity of about 67 nm (the D-period) (Gelse et al., 2003; Lee et al., 2001; Li & Douglas, 2013). One D-period refers to 234 amino acid residues (Zhu et al., 2018).

During the last step of fibril-formation *in vivo*, these collagens assemble into well-packed, highly-orientated supramolecular aggregates or fibrils, which present a suprastructure with the same D-banding pattern (Gelse et al., 2003; Lee et al., 2001; Li & Douglas, 2013), and a typical quarter-staggered fibril-array with diameters between 25 and 400 nm (Gelse et al., 2003), and length less than 1 cm (Shoulders & Raines, 2009). A typical collagen fibril consists of 4.4D periods (Li & Douglas, 2013). These collagens are called fibril-forming collagens due to their ability to assemble into D-periodic cross-striated fibrils (Zhu et al., 2018) (Figure 2.2).

Fibril-forming collagens are the most abundant collagens in vertebrates (Gelse et al., 2003; Pawelec et al., 2016; Ricard-Blum et al., 2000), accounting for about 90% of all collagens (Zhu et al., 2018). They have a structural importance as they contribute to the molecular architecture and shape, and a mechanical importance as they maintain tensile strength in skin and resistance to traction in ligaments (Ricard-Blum et al., 2000). In addition, fibril-forming collagens regulate cell growth, differentiation and migration by interacting with cells through several receptors (Ricard-Blum et al., 2000). D-periodicities provide the structure template for calcification where minerals are primarily deposited in these gap zones

of fibrils (Li et al., 2009; Li & Douglas, 2013). This D-periodicity or D-banding pattern is the key requisite for biomedical-grade collagen because cellular responses such as cell proliferation, cell migration, cell differentiation, and cell adhesion depend on this D-banding pattern (Zhu et al., 2018).

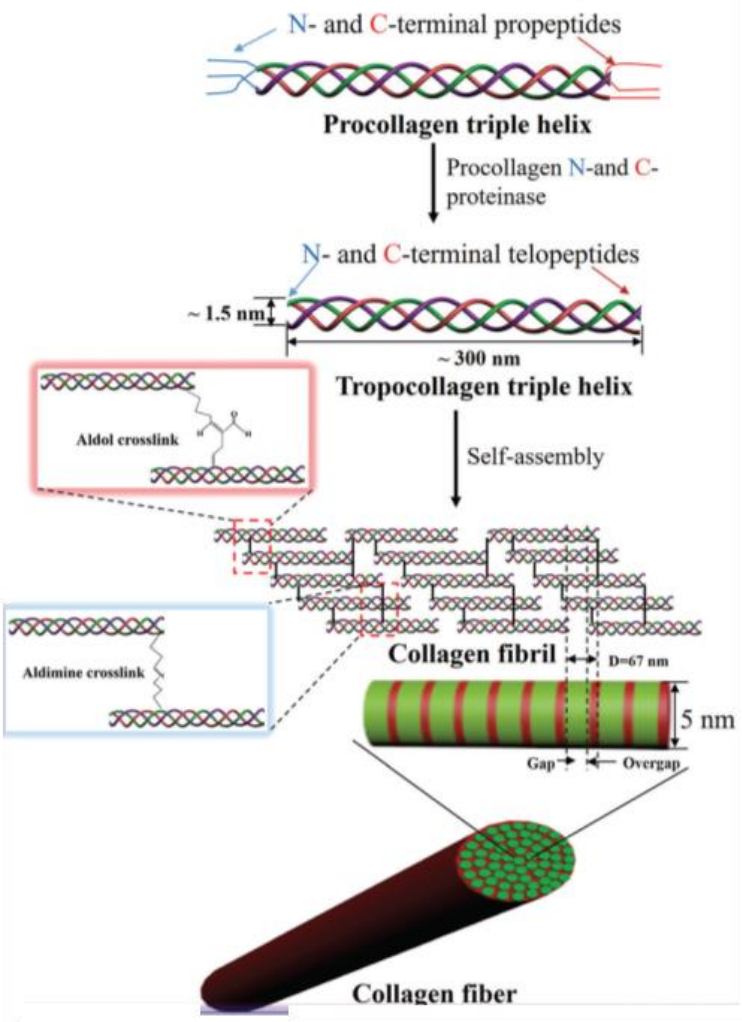

Figure 2.2 Schematic representation of fibril-forming *in vivo* showing the characteristic D-banding pattern (source: Zhu et al., 2018).

2.2.2 Type I collagen

Collagen type I is a fibril-forming collagen, (with types II, III, V, XI, XXIV, XXVII) (Ricard-Blum, 2011). Type I collagen is the most abundant collagen type (Gelse et al., 2003; Pal & Suresh, 2017; Pawelec et al., 2016).

Type I collagen similar to all other collagen types, in that it has a triple-helix structure containing three α-chains. Type I collagen is usually formed as a heterotrimer by two identical α1(I) chains and one α2(I) chain: $\alpha1(I)_2\alpha2(I)$ (Gelse et al., 2003; Nalinanon et al., 2011; Ramı´rez-Rodrı´guez et al., 2014; Yang et al., 2014). The structural differences between α1(I) chain and α2(I) chain are shown in Figure 2.3. Collagen type I forms super-twisted microfibrils

of five molecules that interdigitate with neighbouring microfibrils, leading to the quasi-hexagonal packing of collagen molecules (Ricard-Blum, 2011).

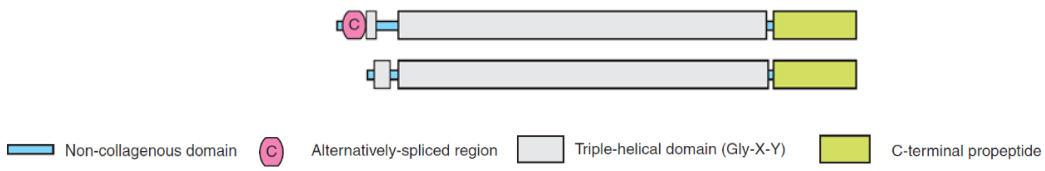

Figure 2.3 Domain composition of α-chains in type I collagen (source: Ricard-Blum, 2011).

Type I collagen is found in connective tissues such as skin, bones, dermis, tendon, ligaments, cartilage, and cornea (Gelse et al., 2003; Krishnamoorthi et al., 2017; Li et al., 2009; Li et al., 2013). Insoluble networks of fibrous bundles of type I collagen provide shape (Li et al., 2009), mechanical support (Gobeaux et al., 2008; Li et al., 2009) and stability in tissues (Gobeaux et al., 2008), and strain energy storage in bone by being mineralised in vertebrate tissues (Li et al., 2009). Type I collagen is also found as a major structural protein in invertebrates (Gobeaux et al., 2008). Type I collagen extracted from mammalian, fish or any other source can be used for biomedical applications in humans or animals as the molecular structure is not source dependant.

2.2.3 Biomedical applications of type I collagen

Collagen has a wide variety of applications in food, pharmaceutical, nutraceutical, medical, biodegradable packaging, cosmetic and biomedical industries (Arumugam et al., 2018; Liu et al., 2015; Muralidharan et al., 2013; O'Sullivan et al., 2006; Pal & Suresh, 2016, 2017; Shoulders & Raines, 2009; Xu et al., 2017; Zeng et al., 2009) due to properties such as biocompatibility, biodegradability and low immunity response (Riaz et al., 2018; Sun et al., 2017; Zhu et al., 2018). In addition, properties related to surface behavior, such as emulsification, foam formation, stabilisation and adhesion are advantageous in biomedical applications (Coppola et al., 2020).

Low immunogenicity or weak antigenicity is a characteristic for use of type I collagen for biomedical applications (Lee et al., 2001; Stamov & Pompe, 2012). Antigenicity of collagen is due to the non-helical telopeptides attached to both ends of the collagen molecule (Lee et al., 2001; Stamov & Pompe, 2012). Weak antigenicity is achieved by producing atelocollagen by cleaving the telopeptides of collagen molecules while retaining the triple-helical structure of collagen, using a proteolytic enzyme like pepsin (Lee at al., 2001; Stamov & Pompe, 2012).

Collagen has several applications in the biomedical field as;

- a drug delivery system (Cheng et al., 2008; Gómez-Guillén et al., 2011; Kim & Mendis, 2006; Lee et al., 2001; Pal & Suresh, 2016; Zhu et al., 2018),
- a protein and gene delivery system (Cheng et al., 2008; Gómez-Guillén et al., 2011; Kim & Mendis, 2006; Pal & Suresh, 2016),
- a substitute for human skin, blood vessels and ligaments (Gómez-Guillén et al., 2011; Kim & Mendis, 2006),

- tissue engineering devices (Bak et al., 2018; Cheng et al., 2008; Jiang et al., 2004; Lee et al., 2001; Muralidharan et al., 2013; Zhu et al., 2018),
- inhibitors of angiogenic diseases (Muralidharan et al., 2013), and
- wound healing devices (Pal & Suresh, 2016).

2.2.3.1 Collagen-based wound dressings

Collagen-based dressings have been used in wound healing (Zhu et al., 2018) and burn coverage applications (Geesin et al., 1996; Riaz et al., 2018;). Physical properties, such as high surface area, efficient exudate absorption, regulation of the wound's humidity, ability to produce scaffolds with optimum porosity suitable for effective cell respiration via air permeability and to protect from bacterial infections (Zhu et al., 2018), and biological properties like promotion of fibroblast production (Cheng et al., 2008), acceleration of wound and burn healing efficiency (Lee et al., 2001), make collagen a suitable candidate in wound healing applications.

2.2.3.2 Collagen-based drug delivery systems

Natural drug carriers are recently being used over synthetic carriers due to their safety profiles and degradability *in vivo* (Zhu et al., 2018). The most important feature of an efficient drug delivery system is the release kinetics, which is the controlled release of the drug at the target site. It is controlled by the collagen matrix characteristics such as cross-linking density and composition, and properties of the drug molecule such as size and composition (Zhu et al., 2018). Other important characteristics of type I collagen in this application include withstanding sterilisation, flexibility upon hydrolysis, good strength to resist manipulation and biocompatibility (Lee et al., 2001).

Collagen is used in various forms such as films, discs, sheets, sponges, membranes, fibres, hydrogels and nanoparticles in drug delivery systems. Collagen films, discs or sheets as drug delivery systems to treat tissue infections are capable of maintaining drug concentrations, particularly antibiotics or anti-cancer agents at target sites for a relatively long period (Lee et al., 2001). Telopeptide-free reconstituted collagen films can deliver drugs with slow-release profiles (Rubin et al., 1973). Bloomfield et al. (1978) used collagen films as alternatives to liquid and ointment vehicles in eye treatment. The compatibility of collagen with polymers such as chitosan is advantageous to make films by cross-linking, enabling design for the controlled release of incorporated drugs (Lee et al., 2001).

Collagen sponges have been used as short-term antibiotic and steroid delivery systems. The advantages of collagen sponges as drug carriers include the controlled release of drugs and reducing the tissue-irritation activity. Disadvantages of collagen sponges include poor mechanical strength (Lee et al., 2001).

Collagen's ability to be cross-linked with natural and synthetic polymers is advantageous in making hydrogels as drug carriers. The combination with a synthetic polymer improves mechanical stability and biological acceptability. Controlled release of drugs such as anti-cancer drugs, contraceptive steroids, and growth hormones has been successful in hydrogels made of collagen and synthetic polymers. Hydrogels have the advantages of ease of manufacturing and self-application (Lee et al., 2001). Minipellets of collagen were used

successfully as drug delivery carriers due to their ability to be injected into subcutaneous space through a syringe needle (Lee et al., 2001).

2.2.3.3 Collagen-based gene delivery systems (proteins, genes)

Collagen is used as a gene delivery system in promoting bone formation. Collagen film or matrix serves as the carrier of bone cells and provides anchorage to bone cells during cell differentiation (Lee et al., 2001). Films made of collagen cross-linked with chitosan have been successfully used in the long-term survivability of cells in gene delivery systems (Park et al., 2000). Collagen implants in the form of sponge have been used as vehicles to transport skin cells to replace skin (Lee et al., 2001). Minipellets of collagen were successful as gene carriers and in carrying plasmid DNA due to biocompatibility and controlled release rates. Carrying large molecular weight proteins can also be achieved with minipellets of collagen (Lee et al., 2001). Collagen hydrogels are used as gene carriers in clinical applications due to low antigenicity. One example is carrying human tracheal epithelial cells and chondrocytes to repair cartilage defects (Lee et al., 2001). Collagen hydrogels have raised great interest as protein delivery systems due to porosity, high water content and high resemblance to the extra cellular matrix (ECM) (Zhu et al., 2018).

Collagen's ability to cross-link with liposomes provides the advantages of formulation stability and controlled release of entrapped materials. Liposome-collagen combined systems can be used to carry insulin and growth hormone into the circulatory system (Lee et al., 2001). Collagen provides the substrate for cell attachment and proliferation while antimicrobials or cell growth factors entrapped within liposomes provides enhanced cell growth and prevention of infection (Weiner et al., 1985). Collagen-based matrices are also used as a lattice for tissue culture systems to study the mechanisms behind human tumour progress (Lee et al., 2001).

2.2.3.4 Collagen-based tissue engineering systems

Mechanical and biological properties of type I collagen make them useful candidates in tissue engineering applications to make scaffolds, artificial tendons, and skin under *in vitro* conditions (Pal & Suresh, 2017). Type I collagen is superior to any natural biological polymer for tissue engineering applications, as it is the major structural component of the native ECM in living tissues (Pawelec et al., 2016) and due to its ability to resemble ECM by self-aggregation into a three-dimensional (3D) network *in vitro* (Zhu et al., 2018). Self-aggregation and cross-linking abilities are mostly useful as a biomaterial to form fibres with high strength and stability (Lee et al., 2001) which is useful in tissue engineering applications. Characteristic features of type I collagen for tissue engineering applications include excellent biocompatibility (Lee et al., 2001; Zhu et al., 2018), safety (Lee et al., 2001), osteoconductive activity (Lee et al., 2001), biodegradability *in vivo*, large surface area for cell attachment, support of vascularisation processes (Lee et al., 2001), and low immunity response (Zhu et al., 2018). It can be combined with other polymers like chitosan and elastin to improve chemical and mechanical properties (Pawelec et al., 2016).

Disadvantages of collagen in tissue engineering include poor mechanical strength, ineffectiveness in the management of infected sites, and the inability of adequate supplies. These drawbacks can be overcome by improving the chemical, physical and biological

properties of collagen, for example, by adjusting the collagen matrix structure or the addition of other proteins, or polymers (Lee et al., 2001).

Applications of collagen as bioengineered tissues include the use of 3D collagen scaffolds as artificial blood vessels, heart valves or cell transplant devices (Lee et al., 2001), connective tissues, adipose tissue, mammary glands and in osteochondral defects (Pawelec et al., 2016). Type I collagen provides the collagen component in making biomimetic scaffolds due to its ability to mimic real tissue (Li et al., 2009).

2.3 Sources of type I collagen for biomedical applications

Collagen has been extracted from a range of sources for use as biomaterials. Bones, tendons and skin of bovine and porcine sources have been mainly utilised for collagen extraction and further applications (Zeng et al., 2009). However, due to outbreaks of bovine spongiform encephalopathy (BSE), foot and mouth disease (FMD) and transmissible spongiform encephalopathy (TSE), people have concerns about using mammalian-origin collagen and collagen-based products (Liu et al., 2014, 2015; Pal & Suresh, 2017) as there is a risk of getting these diseases transmitted to human beings (Arumugam et al., 2018; Gauza-Włodarczyk et al., 2017; Muralidharan et al., 2013; Pal & Suresh, 2016; Woo et al., 2008; Zeng et al., 2009). Use of poultry sources for collagen extraction has concerns due to avian influensa (Chen et al., 2016; Schmidt et al., 2016). In addition, Muslims and Hebrew faiths do not accept pig-based products (Arumugam et al., 2018; Chen et al., 2016; Kittiphattanabawon et al., 2005; Li et al., 2013; Muralidharan et al., 2013; Pal & Suresh, 2016; Schmidt et al., 2016; Zeng et al., 2009) while Hindus do not accept cow-based products (Muralidharan et al., 2013; Pal & Suresh, 2016).

2.3.1 Fish as a source of type I collagen

During the past few years, increasing attention on alternative sources for the replacement of mammalian collagen has been paid, fish collagen, and invertebrate collagen such as jellyfish, sponges, squids, and molluscs being better alternatives (Pal & Suresh, 2016; Zhang et al., 2009).

Fish collagen has become a viable and an attractive source due to its high availability (Li et al., 2013; Pawelec et al., 2016), no risk of disease transmission (Li et al., 2013), no religious barriers (Li et al., 2013), high yield (Li et al., 2013) and low cost of raw material (Pawelec et al., 2016). Fish is the most genetically distant animal from mammals, therefore the possibility of disease transmission from fish to mammals or humans is not found. This makes fish a safer source for collagen extraction (Yamamoto et al., 2015).

Industrial processing of seafood recovers only 20-50% of the original raw material as edible portions while 50-80% is generated as non-edible by-products or leftover raw materials (Chi et al., 2014; Kittiphattanabawon et al., 2005; Li et al., 2013; Pal & Suresh, 2016; Woo et al., 2008; Xu et al., 2017). Fish processing by-products include skin, head, viscera, bones, and scales (Li et al., 2013; Xu et al., 2017). These by-products are either underutilised for cheap applications such as manufacturing of fertiliser, feed and fuel (Li et al., 2013; Nagai & Suzuki, 2000; Pal & Suresh, 2016; Schmidt et al., 2016; Xu et al., 2017) or wasted causing environmental problems (Kittiphattanabawon et al., 2005; Li et al., 2013; Pal & Suresh, 2016) and increasing the cost of disposal.

Either through wastage or underutilisation, a potential source of income is lost (Schmidt et al., 2016). If these low-value by-products are utilised properly, they can be converted to a product with a highly added value that can increase the economic return to the seafood processing industry by covering the costs of processing and disposal (Arumugam et al., 2018; Chi et al., 2014; Schmidt et al., 2016; Xu et al., 2017). In addition, it supports the sustainable utilisation of natural aquatic resources and reduces environmental problems (Arumugam et al., 2018; Schmidt et al., 2016; Xu et al., 2017).

There is a growing market to extract collagen and gelatin-like proteins, peptides, oils, fatty acids, chitin, vitamins, minerals, enzymes, pigments, flavours, and minerals from these seafood by-products (Pal & Suresh, 2016; Schmidt et al., 2016). Recently, there has been great interest in fish by-products such as bones, scales, fins, and skin as potential alternative sources of collagen (Liu et al., 2014, 2015; Pal & Suresh, 2016; Schmidt et al., 2016; Skierka & Sadowska, 2007; Xu et al., 2017).

Excellent bioactive properties such as biocompatibility (Addad et al., 2011; Cho et al., 2014, Pal & Suresh, 2016; Subhan et al., 2015; Yamamoto et al., 2015), high biodegradability (Pal & Suresh, 2016; Subhan et al., 2015; Yamamoto et al., 2015), weak antigenicity (Pal & Suresh, 2016; Subhan et al., 2015; Yamamoto et al., 2015), high cell growth potential (Subhan et al., 2015), high cell adhesion properties (Pal & Suresh, 2016; Yamamoto et al., 2015) and high cell proliferation potential (Yamamoto et al., 2015) are the favourable characteristics of fish-origin collagen for biomedical applications (Subhan et al., 2015). The main differences between fish and mammalian collagen include high biological value, high essential amino acid content and low hydroxyproline content (Muralidharan et al., 2013). However, source dependant composition variation and low denaturation temperature are associated with fish collagen as drawbacks.

2.3.2 Fish skin as a source of type I collagen

Fish skin constitutes the major component of fish by-products from fish processing industry (Xu et al., 2017) and it contains 50-95% of protein (Xu et al., 2017), collagen being the highest component (Nalinanon et al., 2011; Xu et al., 2017). Fish skin collagen has been extracted and characterised from several fish species (Table 2.1). However, only a few researchers have analysed the potential of fish skin collagen for use in biomedical applications (Table 2.2). Fish skin has not been rationally utilised up to now by the collagen manufacturing industry and many research studies have ended up without progressing to industrial-level processing.

Table 2.1 Fish and other seafood sources used for extraction and characterisation studies.

Fish species used	Reference
Sole fish (*Aseraggodes umbratilis*)	Arumugam et al., 2018
Tilapia (*Oreochromis niloticus*)	Chen et al., 2016
Hammerhead shark (S*phyrna lewini*)	Chi et al., 2014
Common carp (*Cyprinus carpio*)	Duan et al., 2009
Skate (*Raja kenojei*)	Hwang et al., 2007
Brownstripe red snapper (*Lutjanus vitta*)	Jongjareonrak et al., 2005

Fish species used	Reference
Jellyfish (*Acromitus hardenbergi*)	Khong et al., 2018
Bigeye snapper (*Priacanthus tayenus*)	Kittiphattanabawon et al., 2005
Blacktip shark (*Carcharhinus limbatus*)	Kittiphattanabawon et al., 2010a
Brownbanded bamboo shark (*Chiloscyllium punctatum*), Blacktip shark (*Carcharhinus limbatus*)	Kittiphattanabawon et al., 2010b
Splendid squid (*Loligo formosana*)	Kittiphattanabawon et al., 2015
Squid (*Illex argentinus*)	Kolodziejska et al., 1999
Spanish mackerel (*Scomberomorous niphonius*)	Li et al., 2013
Grass carp (*Ctenopharyngodon idella*)	Liu et al., 2015
Leather jacket (*Odonus niger*)	Muralidharan et al., 2013
Skipjack tuna (*Katsuwonus pelamis*), Japanese seabass (*Lateolabrax japonicus*), Ayu (*Plecoglossus altivelis*), Yellow sea bream (*Dentex tumifrons*), Chub mackerel (*Scomber japonicus*), Bullhead shark (*Heterodontus japonicus*), Horse mackerel (*Trachurus japonicus*)	Nagai and Suzuki, 2000
Jellyfish (*Stomolophus Meleagris*)	Nagai et al., 1999
Ocellate puffer fish (*Takifugu rubripes*)	Nagai et al., 2002
Ornate threadfin bream (*Nemipterus hexodon*)	Nalinanon et al., 2011
Black drum (*Pogonia cromis*), Sheepshead seabream (*Archosargus probatocephalus*)	Ogawa et al., 2004
Nile Tilapia *(Oreochromis niloticus)*	Potaros et al., 2009
Baltic cod (*Gadus morhua*)	Sadowska et al., 2003
Striped catfish (*Pangasianodon hypophthalmus*)	Singh et al., 2011
Baltic cod (*Gadus morhua*)	Skierka & Sadowska, 2007
African Catfish (*Clarias gariepinus*), Salmon (*Salmo salar*), Baltic Cod (*Gadus morhua*)	Tylingo et al., 2016
Marine eel-fish (*Evenchelys macrura*)	Veeruraj et al., 2013
Deep-sea redfish (*Sebastes mentella*)	Wang et al., 2008
Yellowfin tuna (*Thunnus albacares*)	Woo et al., 2008
Southern catfish (*Silurus meridionalis* Chen)	Xu et al., 2017
Nile tilapia (*Oreochromis niloticus*)	Zeng et al., 2009
Largefin longbarbel catfish (*Mystus macropterus*)	Zhang et al., 2009

Table 2.2 Fish and other marine sources investigated for use in biomedical applications.

Fish species used	Biomedical application	Reference
Antarctic squid (*Kondakovia longimana*), Sub-Antarctic squid (*Illex argentines*)	hybrid scaffolds for tissue engineering	Coelho et al., 2017
Jellyfish (*Rhopilema esculentum*)	cartilage tissue engineering	Hoyer et al., 2014
Irish cod (*Gadus morhua*), Irish ling (*Molva molva*), New Zealand hoki (*Macruronus novaezelaniae*), New Zealand ling (*Genypterus blacodes*)	biopolymer films	O'Sullivan et al., 2006
Pacific cod (*Gadus macrocephalus*)	sponge as a biomedical material	Sun et al., 2017
Tilapia (*Oreochromis* sp.)	sponge as a biomedical material	Yamamoto et al., 2015

2.3.3 Characteristics governing the species differences in fish-origin collagen

2.3.3.1 Denaturation temperature (Td)

Denaturation temperature depends on the collagen origin and generally it is higher in mammalian-origin collagen (Gauza-Włodarczyk et al., 2017). There are a few perspectives for this difference, for example, according to Liu et al. (2014) and Pal & Suresh (2016), a higher frequency of interactions by the higher content of proline and hydroxyproline amino acids in bovine skin collagen contributes to a comparatively higher Td than fish skin collagen, but according to Gauza-Włodarczyk et al. (2017) it is due to higher content of hydroxyproline.

In the case of fish collagen, denaturation temperature depends on the fish species it originates from (Gauza-Włodarczyk et al., 2017; Muralidharan et al., 2013; Pal & Suresh, 2016) and is a result of many factors such as;

- temperature of feeding ground of the fish (Gauza-Włodarczyk et al., 2017),
- water content in fish tissue (Gauza-Włodarczyk et al., 2017),
- degree of cross-linking (Gauza-Włodarczyk et al., 2017),
- hydroxyproline content (Gauza-Włodarczyk et al., 2017; Yamamoto et al., 2015),
- content of both proline and hydroxyproline (Li et al., 2013; Liu et al., 2014; Nalinanon et al., 2011; Xu et al., 2017; Zeng et al., 2009),
- degree of hydroxylation of proline residues (Coelho et al., 2017; Li et al., 2013; Xu et al., 2017;),
- body temperature of fish and environmental temperature of their habitat (Gauza-Włodarczyk et al., 2017; Li et al., 2013; Nalinanon et al., 2011; Xu et al., 2017).

Some scientists argue that the thermal stability of fish collagen is a function of proline and hydroxyproline content rather than hydroxyproline content alone (Muralidharan et al., 2013; Muyonga et al., 2004). According to this argument, thermal stability is associated with its superhelical structure which is maintained by the conformational restrictions by pyrrolidine

rings of proline and hydroxyproline (Woo et al., 2008), and the involvement of hydrogen bonding through the hydroxyl group of hydroxyproline is only a partial attribution (Liu et al., 2015; Nalinanon et al., 2011; Pal & Suresh, 2016, 2017). However, some researchers describe the denaturation temperature as a function of hydrogen-bonded networks mediated by water molecules which connect the hydroxyl group of hydroxyproline in one strand to the main chain amide carboxyl of another chain (Li et al., 2013). According to Pal & Suresh (2016, 2017), it is directly correlated with the body temperatures of fish species and their habitat temperatures. Generally, the Td of collagen from warm-water fish species is higher than that of cold-water species (Liu et al., 2015; Nagai & Suzuki, 2000). Studies reported similar Td values in fish collagen extracted from fish living in similar environmental temperatures.

- Td of skin collagen from subtropical and tropical fish showed similar values: Unicorn leatherjacket (29.33-31.98°C) (Ahmad & Benjakul, 2010); Striped catfish (39.3-39.6°C) (Singh et al., 2011); Ornate threadfin bream (33.35°C) (Nalinanon et al., 2011); Eagle ray (34.1°C) (Bae et al., 2008); Bigeye snapper (28.68-31°C) (Kittiphattanabawon et al., 2005); Bigeye snapper (32.5°C) (Nalinanon et al., 2007); Channel catfish (32.5°C) (Liu et al., 2007); Black drum (34.2°C) (Ogawa et al., 2003); Sheepshead seabream (34°C) (Ogawa et al., 2003).
- Td values of skin collagen from cold-water fish from temperate regions reported lower values: Cod (15°C) (Duan et al., 2009); Arabesque greenling (15.7°C) (Nalinanon et al., 2010); Deep-sea redfish (16.1°C) (Wang et al., 2008); Pacific whiting (21.7°C) (Kim & Park, 2004).
- Nagai & Suzuki (2000) reported similar Td values for skin collagen from Japanese seabass (26.5°C), Chub mackerel (25.6°C), and Bullhead shark (25°C) living in habitats with relatively similar temperatures.

Akita et al., (2020) showed a correlation between the denaturation temperature of type I collagen with habitat temperature of fish. Six warm-water fish species where their habitat temperatures ranged from 16.6°C to 28.0°C recorded Td values ranging from 23.5°C to 34.9°C. Five cold-water fish species where their habitat temperatures ranged from 0.4°C to 12.8°C recorded Td values ranging from 18.0°C to 20.2°C.

Denaturation temperature of collagen also depends on the state of the sample. In solid state it depends mainly on the method of measurement, the presence of admixtures and water among many other factors (Gauza-Włodarczyk et al., 2017). Effect of hydration level is related to the loss of structural water (Gauza-Włodarczyk et al., 2017). Chemical composition of the sample plays only a limited role (Gauza-Włodarczyk et al., 2017). According to the study of Gauza-Włodarczyk et al. (2017) using *Salmo salar* skin collagen, different Td values were obtained depending on the state of the sample. When collagen was used in the form of gel, lower Td values (23-35°C) and when it was used in solid freeze-dried form higher Td values (150°C) were obtained. Zeugolis & Raghunath (2010) reported higher Td values for dry-state mammalian collagen (102-116°C) than that for wet-state mammalian collagen (49-53°C).

Low denaturation temperature is a drawback associated with fish collagen in tissue engineering applications and reported poor stability in mammals *in vivo* (Yamamoto et al., 2015). But this drawback can be overcome by the use of various methods. According to the study of Liu et al. (2014) using the skin of Snakehead (*Channa argus*) Td became much higher

when the heating rate increased. This indicates that the denaturation process can be kinetically controlled in part (Liu et al., 2014). Introduction of covalent bonds or cross-links between individual fibrils is another method to improve the thermal stability of fish collagen (Pawelec et al., 2016; Subhan et al., 2015). Examples of cross-linking agents that have been successful with fish collagen include neutral buffers such as 1-ethyl-3-(3-dimethylaminopropyl)-carbodiimide (EDC), 1-ethyl-(3-3-dimethylaminopropyl) carbodiimide hydrochloride/N-hydroxysuccinimide (EDC/NHS), and genipin under high pressure of carbon dioxide (Subhan et al., 2015). Composite of marine collagen with biomaterials such as chitosan and calcium hydroxyapatite is another method of increasing the thermal stability (Subhan et al., 2015). Fish skin collagen can be used instead of mammalian collagen on the condition that the process will not require a temperature higher than Td depending on the state of collagen (Gauza-Włodarczyk et al., 2017).

2.3.3.2 Amino acid composition

Collagen contains 19 amino acids irrespective of its origin (Gauza-Włodarczyk et al., 2017). The combination of amino acids in collagen is different from other proteins. Proline, hydroxyproline and hydroxylysine are unique amino acids available in collagen (Gauza-Włodarczyk et al., 2017; Li et al., 2013). Type I collagen is rich in glycine, alanine and proline (Nalinanon et al., 2011), glycine being the most dominant amino acid (Muyonga et al., 2004). When the content of amino acids is expressed as residues per 1,000 total amino acid residues, the highest amount accounted for is glycine as recorded by researchers using various fish species, for example, Leather jacket (352.0-356.8 residues/1,000 residues) (Muralidharan et al., 2013), Spanish mackerel (341.6-352.6 residues/1000 residues) (Li et al., 2013). Type I collagen contains no cysteine and tryptophan, and relatively low contents of tyrosine and histidine. This is under the findings using various fish species, such as Ornate threadfin bream, Common horse mackerel, Yellow sea bream, Tiger puffer fish, Black drum, Sheepshead seabream, Brownstripe red snapper and Arabesque greenling (Nalinanon et al., 2011). The property of absence or presence of only negligible amounts of tryptophan and tyrosine is used in analysing the purity of collagen using the ultra-violet (UV) absorption spectrum.

The content of hydroxyproline in collagen depends on its origin, but when the origin is fish it varies depending on their environment. Generally, cold-water fish have a lower content of hydroxyproline compared to warm-water species (Gauza-Włodarczyk et al., 2017). Similarly, differences in imino acid content in different fish species are associated with their habitat (Muralidharan et al., 2013; Muyonga et al. 2004; Xu et al., 2017; Zeng et al., 2009).

- Imino acid content of fish skin collagen is lower than that of mammalian collagen. Studies reported higher imino acid contents in mammalian-origin collagen, for example, calf skin collagen (215 residues/1000 residues) (Ogawa et al., 2003; Xu et al., 2017); calf skin collagen (216 residues/1000 residues) (Li et al., 2013) and pig skin collagen (220 residues/1000 residues).
- Imino acid content of skin collagen from warm-water species is higher than that of cold-water species, for example, Bigeye snapper (193-200 residues/1000 residues) (Nalinanon et al., 2011); Shark (204-207 residues/1000 residues); Nile perch (192-200 residues/1,000 residues (Muralidharan et al., 2013); Southern catfish (197 residues/1000 residues)

(Xu et al., 2017); Bighead carp (181 residues/1000 residues) (Xu et al., 2017); Grass carp (186 residues/1000 residues) (Xu et al., 2017).

- Conversely, imino acid content is lower in fish skin collagen obtained from cold-water species, for example, imino acid content of Arabesque greenling (Nalinanon et al., 2011), Cod (Duan et al., 2009), Deep-sea red fish (Nalinanon et al., 2011) and Pacific whiting (Nalinanon et al., 2011) ranged between 154 and 165 residues/1000 residues; Spanish mackerel (177-180 residues/1000 residues) (Li et al., 2013), Leather jacket (161.4 residues/1000 residues) (Muralidharan et al., 2013); Toad fish (170 residues/1,000 residues) (Muralidharan et al., 2013). The higher content of imino acids is important to have higher thermal stability (Pal & Suresh, 2016) by strengthening the triple-helix structure of collagen (Pal & Suresh, 2017; Nalinanon et al., 2011; Xu et al., 2017).

The degree of hydroxylation of proline is important for better functional properties by also stabilising the triple-helical structure of collagen (Muralidharan et al., 2013; Xu et al., 2017; Woo et al., 2008). Proline content is generally higher than hydroxyproline content in fish collagen (Muralidharan et al., 2013). This can also be interpreted as the degree of hydroxylation of proline. It is lower than mammalian collagen, for example, Japanese flounder (40.0%); Bigeye snapper (39.9%); Ocellate puffer fish (39.4%) and Nile perch (40.1%) compared to calf skin collagen (43.91%) (Li et al., 2013). Lysine hydroxylation is important to improve the cross-links in collagen (Li et al., 2013).

The content of hydroxyproline in collagen is used for quantitative estimation of collagen properties (Gauza-Włodarczyk et al., 2017). After determining the conversion factor of hydroxyproline content to collagen, it can be used to estimate the collagen in raw fish skin, the yield of collagen and the purity of extracted collagen (Nalinanon et al., 2011). This conversion factor depends on the fish species and body part, for example, Ornate threadfin bream (12.7), Baltic cod backbone (15.7) and skin (14.7) (Nalinanon et al., 2011). Nalinanon et al. (2011) in their study using the skin of Ornate threadfin bream found a 1.46-fold increase in hydroxyproline content in the extracted collagen (72.3±0.5 mg/g dry weight) compared to that of raw skin (49.5±0.4 mg/g dry weight) suggesting effective removal of non-collagenous materials from fish skin before collagen extraction.

2.4 Collagen extraction and isolation process from fish skin

2.4.1 Structure and composition of fish skin

The structure and composition of fish skin are important determinants of collagen pretreatment and extraction steps. Thickness and cell composition of fish skin depend on the species, sex, life stage, reproductive status, body region, nutritional status, water quality, the season of the year and health (Paterson, 2008). The generalised structure of fish skin is shown in Figure 2.4.

A fatty tissue layer (hypodermis) connects the skin to underlying muscles or bones (Paterson, 2008). Fat content varies from species to species (see Table 2.3), for example, Tarakihi (18.4%); Ling (1.3%); Trevally (5.8%); Hake (6.1%); White warehou (44.0%) in fish species from New Zealand (www.fao.org). In the same fish it varies in different body parts, for example, head (13.5%); viscera (24.8%); bones (12.8%); skin (18.4%); fillet (2.9%) in

Tarakihi fish (www.fao.org). Fat content also varies within the skin. Fish use their tail end for swimming and therefore contains more connective tissues, and hence more collagen and less fat compared to the head region.

Chromatophores or pigment cells give colour to fish skin for camouflage and communication. They are found mainly at boundaries between the epidermis, dermis and hypodermis. There are five types of chromatophores responsible for colours in fish skin; black or brown colour by melanin in melanophores, yellow colour by xanthophylls in xanthophores, orange or red colour by carotenoids in erythrophores, white colour by guanine or purine in leucophores, reflective or iridescent appearance by guanine in iridophores. Sometimes colour is determined by more than one pigment type (Paterson, 2008). The colour of a particular fish species is affected by water quality, temperature, salinity, mechanical pressure, and UV radiation (Paterson, 2008).

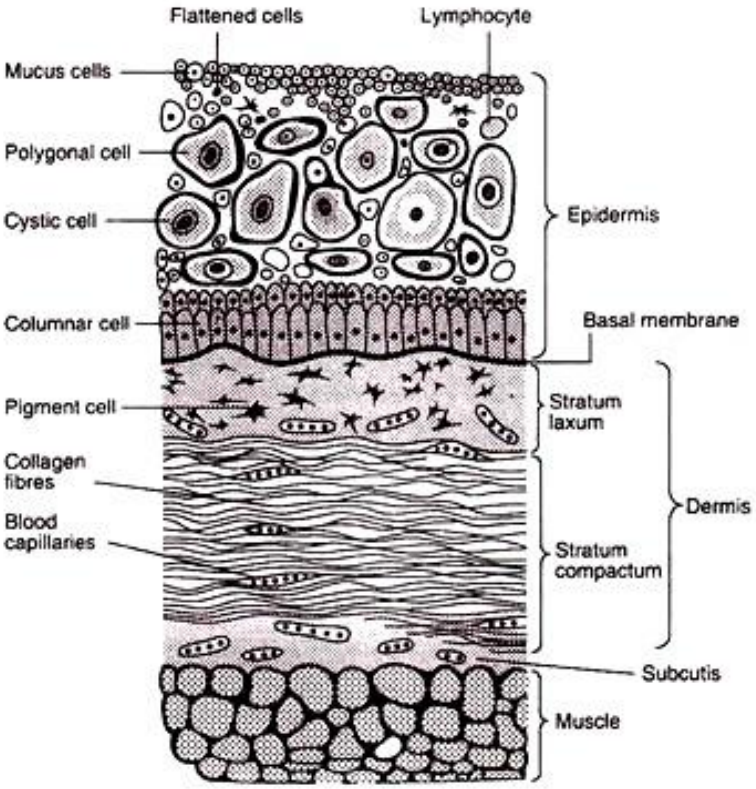

Figure 2.4 Generalised structure of fish skin showing the distribution of collagen fibres, fat (subcutis), and pigments (source: www.slideshare.net).

Table 2.3 Protein, fat and ash composition in the skin of three selected fish species used for the study (picture source: wikipedia.com).

Proportion of the total body composition	**Tarakihi (*Nemadactylus macropterus*) (from New Zealand)**	**Ling (*Genypterus blacodes*) (from New Zealand)**	**Yellowfin tuna (*Thunnus albacares*) (from Sri Lanka)**
	Pictures are not in proportion		
			
Protein (%)	20.8	22.2	27.1
Fat (%)	18.4	1.3	8.9
Ash (%)	4.2	1.6	1.0
Reference	www.fao.org	www.fao.org	Karunarathna and Attygalle (2010)

2.4.2 Skin pretreatment for collagen extraction

The effectiveness of the whole collagen extraction process is determined by the proper selection of pretreatment methods of the raw material (Skierka & Sadowska, 2007). Pretreatment involves the removal of non-collagenous components such as non-collagenous proteins, fats, and pigments, before collagen extraction to increase the collagen yield and purity of the final extracted collagen (Pal & Suresh, 2016; Xu et al., 2017). Pure, colourless and odourless collagen is required for practical applications (Sadowska et al., 2003).

Generally, pretreatment of fish skin involves the removal of non-collagenous proteins, fats and pigments in a series as practised by Xu et al., (2017). This depends on the fish species and the chemicals used. Some researchers, such as Liu et al., (2014); Zhang et al., (2007) have done the pigment removal step before fat removal. Kittiphattanabawon et al., (2010c), have used only a non-collagenous protein removal step in the absence of fat and pigment removal steps (Table 2.4).

Table 2.4 Examples of procedures used in collagen extraction from fish skin reported in the literature.

Fish species	**Pretreatment method**	**Extraction method**	**Reference**
Sole fish (*Aseraggodes umbratilis*)	Non-collagenous protein removal: 0.3 M NaOH at 1:10 (w/v) for 4 h with solution change every 1 h, at 10°C Fat removal: 20% butanol at 1:10 (w/v) ratio for 30 h with solution change every 10 h, at 10°C Pigment removal: not used	acetic acid (0.4 M, 0.6 M, 0.8 M) for time (24 h, 36 h, 48 h), at 10°C	Arumugam et al., 2018
Tilapia (*Oreochromis niloticus*)	Non-collagenous protein removal: 0.1 M $NaHCO_3$ 1:10 (w/v) ratio for 6 h, 4°C	0.5 M acetic acid for 24 h	Chen et al., 2016

Fish species	Pretreatment method	Extraction method	Reference
	Fat removal: not used Pigment removal: not used		
Hammerhead shark (S*phyrna lewini*)	Non-collagenous protein removal: 0.1 M NaOH in 1:15 (w/v) ratio for 24 h at 4°C, changing the solution every 6 h Fat removal: 15% (v/v) butyl alcohol with in 1:20 (w/v) ratio for 48 h with change of solution every 12 h Pigment removal: not used	0.5 M acetic acid with in 1:15 (w/v) for 24 h	Chi et al., 2014
Common carp (*Cyprinus carpio*)	Non-collagenous protein removal: 0.1 M NaOH at 1:8 (w/v) for 6 h with solution change every 3 h Fat removal: 1.0% detergent (dish drops, Amway Inc., Guangzhou, China) at sample/detergent solution ratio of 1:10 (w/v) overnight Pigment removal: not used	0.5 M acetic acid for 3 days	Duan et al., 2009
Skate (*Raja kenojei*)	Non-collagenous protein removal: 0.1 M NaOH at 1:10 (w/v) ratio for 24 h Fat removal: not used Pigment removal: not used	0.5 M acetic acid at 1:10 (w/v) ratio for 24 h	Hwang et al., 2007
Brownstripe red snapper (*Lutjanus vitta*)	Non-collagenous protein removal: 0.1 M NaOH at 1:30 (w/v) for 24 h with solution change every 8 h, at 4°C Fat removal: 10% (v/v) butyl alcohol at 1:30 (w/v) for 24 h with change of solution every 8 h Pigment removal: not used	0.5 M acetic acid at 1:30 (w/v) for 24 h	Jongjareonrak et al., 2005
Jellyfish (*Acromitus hardenbergi*)	Non-collagenous protein removal: 0.1 M NaOH Fat removal: not used Pigment removal: not used	0.5 M acetic acid at 1:1 (w/v) for 3 days, extraction was repeated twice at 4°C	Khong et al., 2018

Fish species	Pretreatment method	Extraction method	Reference
Bigeye snapper (*Priacanthus tayenus*)	Non-collagenous protein removal: 0.1 M NaOH at 1:10 (w/v) for 6 h with solution change every 2 h, at 4°C Fat removal: 10% butyl alcohol at 1:10 (w/v) for 18 h with solution change every 6 h, at 4°C Pigment removal: not used	0.5 M acetic acid at 1:30 (w/v) for 24 h, at 4°C	Kittiphattanabawon et al., 2005
Blacktip shark (*Carcharhinus limbatus*)	Non-collagenous protein removal: 0.1 M NaOH at 1:10 (w/v) for 6 h with solution change every 2 h, at 4°C Fat removal: not used Pigment removal: not used	0.5 M acetic acid at 1:15 (w/v) ratio for 48 h, at 4°C	Kittiphattanabawon et al., 2010a
Splendid squid (*Loligo formosana*)	Non-collagenous protein removal: 0.1 M NaOH at 1:10 (w/v) ratio for 6 h with solution change every 2 h, at 4°C Fat removal: 10% (v/v) butyl alcohol at 1:10 (w/v) for 18 h with solution change every 6h, at 4°C Pigment removal: not used	0.5 M acetic acid at 1:250 (w/v) in the presence of porcine pepsin (10 g/100 g freeze-dried skin) for 72h, at 4°C	Kittiphattanabawon et al., 2015
Spanish mackerel (*Scomberomorous niphonius*)	Non-collagenous protein removal: 0.1 M NaOH at a 1:10 (w/v) for 2 days with solution change every 6 h at 4°C Fat removal: 10% butyl at 1:20 (w/v) for 2 days with solution change every 6 h Pigment removal: not used	0.5 M acetic acid at 1:15 (w/v) for 24 h	Li et al., 2013
Grass carp (*Ctenopharyngodon idella*)	Non-collagenous protein removal: NaOH concentration (0.05, 0.1, 0.2 or 0.5 M) at temperature (4, 10, 15 or 20°C) and time (1, 2, 4, 8 or 12 h) Fat removal:	0.5 M acetic acid at 1:40 (w/v) ratio for 72 h	Liu et al., 2015

Fish species	Pretreatment method	Extraction method	Reference
	10% (v/v) butyl alcohol at 1:10 (w/v) ratio for 24 h with change of solution every 12 h, at 4°C Pigment removal: not used		
Leather jacket (*Odonus niger*)	Non-collagenous protein removal: 0.8 M NaCl at 1:6 (w/v) ratio for 10 min, repeated 3 times, to remove impurities 0.1 M NaOH at 1:10 (w/v) for 3 days Fat removal: not used Pigment removal: not used	0.5 M acetic acid for 3 days	Muralidharan et al., 2013
Skipjack tuna (*Katsuwonus pelamis*), Japanese seabass (*Lateolabrax japonicus*), Ayu (*Plecoglossus altivelis*), Yellow sea bream (*Dentex tumifrons*), Chub mackerel (*Scomber Japonicus*), Bullhead shark (*Heterodontus japonicus*), Horse mackerel (*Trachurus japonicus*)	Non-collagenous protein removal: 0.1 M NaOH at 4°C Fat removal: 10% butyl alcohol for 1 day Pigment removal: not used	0.5 M acetic acid for 3 days	Nagai and Suzuki, 2000
Ocellate puffer fish (*Takifugu rubripes*)	Non-collagenous protein removal: 0.1 M NaOH at 4°C Fat removal: 10% butyl alcohol for 2 days with solution change every 1 day at 4°C Pigment removal: not used	0.5 M acetic acid for 3 days at 4°C	Nagai et al., 2002
Ornate threadfin bream	Non-collagenous protein removal:	0.5 M acetic acid at 1:100 (w/v) for 48 h, at 4°C	Nalinanon et al., 2011

Fish species	Pretreatment method	Extraction method	Reference
(*Nemipterus hexodon*)	0.1 M NaOH at 1:10 (w/v) for 6 h with solution change every 2 h at 4°C Fat removal: 10% (v/v) butyl alcohol at 1:10 (w/v) v) for 18 h with solution change every 6 h, at 4°C Pigment removal: not used		
Nile Tilapia *(Oreochromis niloticus)*	Non-collagenous protein removal: 0.1 M NaOH at 1:10 (w/v) ratio for 4 h, at 4 - 6°C Fat removal: not used Pigment removal: not used	0.5 M acetic acid at 1:70 (w/v) ratio for 24 h, at 4-6°C	Potaros et al., 2009
Baltic cod (*Gadus morhua*)	Non-collagenous protein removal: 0.45 M NaCl or 0.01 M NaOH at 1:6 (w/v) for 3 min, mixtures homogenised in the same solutions for 4 min at 6000 rpm, repeating the whole process twice Fat removal: 0.5 % detergents Pigment removal: 10% NaCl solution at room temperature for 24 h and then bleaching with 1% H_2O_2 solution in 0.01 M NaOH (not successful) or repeated homogenisation of skins with 0.4 M NaCl (not successful) or leaching with 0.5 M acetic acid at 4°C for 24 h, followed by homogenisation and centrifugation (successful)	0.1-0.5 M acetic acid solution at 0°C; homogenised after 2 h, stirred for 24 h, homogenised again, then centrifugation	Sadowska et al., 2003
striped catfish (*Pangasianodon hypophthalmus*)	Non-collagenous protein removal: 0.1 M NaOH at 1:10 (w/v) ratio for 6 h at 4°C with change of solution every 2 h Fat removal: 10% butyl alcohol at 1:10 (w/v) ratio for 48 h with solution change every 8 h, at 4°C Pigment removal: not used	0.5 M acetic acid at 1:15 (w/v) for 24 h	Singh et al., 2011

Fish species	Pretreatment method	Extraction method	Reference
African catfish (*Clarias gariepinus*), Salmon (*Salmo salar*), Baltic Cod (*Gadus morhua*)	Non-collagenous protein removal: 0.1 M NaOH at (1:6, w/v) for 48 h, at 4°C Fat removal: not used Pigment removal: 3% H_2O_2 for 24 h, at 4°C	0.5 M acetic acid for 72 h, at 4°C	Tylingo et al., 2016
Yellowfin tuna (*Thunnus albacares*)	Non-collagenous protein removal: 0.5–1.3 M NaOH at 1:5 (v/w) at 9°C Fat removal: not used Pigment removal: not used	pepsin digestion with 0.6–1.4% at 1:20 (v/w) HCl solution (pH 2.0)	Woo et al., 2008

2.4.2.1 Pretreatment to remove non-collagenous proteins

Alkali treatment is the most widely applied method of removing non-collagenous proteins from fish skin, NaOH being the mostly used alkali agent. Sodium hydroxide swells the skin to facilitate the removal of non-collagenous proteins from fish skin (Liu et al., 2015; Woo et al., 2008), in addition this swelling is useful to remove fats (Woo et al., 2008) and pigments (Liu et al., 2015; Pal & Suresh, 2016) and to eliminate the effects of endogenous proteases on collagen during manufacturing (Liu et al., 2015).

Calcium hydroxide ($Ca(OH)_2$) is also used as an alkali pretreatment agent, and it has shown similar effectiveness in removing non-collagenous proteins from fish skins (Liu et al., 2015). However, NaOH causes significant swelling of fish skin during pretreatment, thus facilitating the following acid extraction of collagen by increasing the mass transfer rates in the tissue matrix, whereas $Ca(OH)_2$ does not swell the skin (Liu et al., 2015).

The effectiveness of removing non-collagenous proteins depends on the concentration of NaOH and the temperature used. A study by Liu et al., (2015) evaluated the effect of alkaline pretreatment on the extraction of acid-soluble collagen from the skin of grass carp (*Ctenopharyngodon idella*). The NaOH concentrations ranging from 0.05 to 0.1 M were effective in removing non-collagenous proteins without causing a significant loss of collagen. Higher concentrations like 0.2 M and 0.5 M NaOH caused a significant loss of collagen and structural modifications at 15 and 20°C. However, some researchers have used 0.3 M NaOH effectively, such as Arumugam et al. (2018) treating Sole (*Aseraggodes umbratilis*) fish skin in the ratio of 1:10 (w/v) for 4 h with solution changes every hour.

Pretreatment with NaOH at 0.1 M has been used in several studies to treat fish skin:

- Pal et al., (2015) using Catla (*Catla catla*) and Rohu (*Labeo rohita*);
- Kittiphattanabawon et al. (2010b) using Brownbanded bamboo shark (*Chiloscyllium punctatum*);
- Zeng et al. (2009) using Nile tilapia (*Oreochromis niloticus*);
- Nagai & Suzuki (2000) using Japanese seabass (*Lateolabrax japonicus*), Chub mackerel (*Scomber japonicus*), Bullhead shark (*Heterodontus japonicus*);

- O'Sullivan et al. (2006) using Irish cod (*Gadus morhua*) and Ling (*Molva molva*); and
- Nalinanon et al. (2011) using Threadfin bream (*Nemipterus hexodon*). However, the weight to volume ratio between the skin and NaOH solution, and soaking time were different in these examples.
- Zeng et al. (2009) in their experiment with Nile tilapia (*Oreochromis niloticus*) skin used 0.1 M NaOH solution at 1:30 (w/v) for 48 h at 4°C with a gentle stirring to remove non-collagenous proteins and pigments, with solution changes every 8 h.
- O'Sullivan et al., (2006) used 0.1 M NaOH solution at 1:7 (w/v) at 9°C for Irish cod (*Gadus morhua*) and Ling (*Molva molva*).
- Nalinanon et al. (2011) used 0.1 M NaOH in 1:10 (w/v) ratio for 6 h with continuous stirring and solution changes every 2 h in treating Ornate Threadfin bream (*Nemipterus hexodon*).

In some studies, neutral salt solutions were used to remove non-collagenous proteins, for example, Chen et al. (2016) used Sodium bicarbonate ($NaHCO_3$), and Ciarlo et al. (1997); Muyonga et al. (2004); Wang et al. (2007) used Sodium chloride (NaCl). According to some researchers, uneven swelling can occur when using NaOH treatment which is not effective in subsequent degreasing, decolouring and extraction steps. Therefore, an alkaline solution is replaced by a weak alkaline salt to facilitate even swelling of collagen fibres (Xu et al., 2017). However, newly synthesised uncross-linked collagens can be removed by neutral salt solutions, leading to a low yield of collagen (Liu et al., 2015).

2.4.2.2 Pretreatment to remove fats

The need of a fat-removing agent depends on the fat content in fish skin, therefore fish with low-fat content in the skin may not require an additional pretreatment agent other than NaOH to remove fats. For skins with high-fat content, a degreasing agent is required to further facilitate the loosening of collagen fibres to remove more fat, and to increase the yield and purity of the extracted collagen (Xu et al., 2017).

The most widely used degreasing agent to treat fish skin in laboratory methods is butyl alcohol at different concentrations, different ratios and different time durations depending on fish species.

- Nalinanon et al. (2011) used 10% (v/v) butyl alcohol at 1:10 (w/v) for 18 h with solvent changes every 6 h for Ornate threadfin bream (*Nemipterus hexodon*).
- Zeng et al. (2009) in their experiment with Nile tilapia (*Oreochromis niloticus*) skin used 10% (v/v) butyl alcohol solution at 1:30 (w/v) for 24 h at 4°C with solution changes every 8 h to remove fats.
- Arumugam et al., (2018) used 10% (v/v) butyl alcohol solution at 1:10 (w/v) ratio for 30 h with solution changes every 10 h for Sole fish (*Aseraggodes umbratilis*).
- O'Sullivan et al. (2006) used 10% (v/v) butyl alcohol solution at a 1:7 (w/v) ratio for 1 h for Irish cod (*Gadus morhua*) and Ling (*Molva molva*).

Some researchers have used a non-ionic detergent instead of butyl alcohol to remove fats while some others have used both depending on the fat content of fish skin. For example, Zhang et al. (2007) used a 0.5% non-ionic detergent for 18 h with solution changes every 6 h for Grass carp (*Ctenopharyngodon idella*).

Xu et al. (2017) in their experiment with Southern catfish (*Silurus meridionalis* Chen) skin, analysed the effectiveness of degreasing agents to remove fats in 2 steps. Treating the skin with 10% Sodium carbonate (Na_2CO_3) as an agent to remove non-collagenous proteins was effective to remove fats by 69.37%. Use of a 15% (v/v) isopropyl alcohol treatment after Na_2CO_3 treatment as the first degreasing agent was effective to remove fat up to 80.95% (further removal of 11.58%), and 6% (v/v) non-ionic degreasing agent as the second degreasing agent was effective to remove fats up to 90.24% (further removal of 9.29%). Kittiphattanabawon et al. (2010b) used only the non-collagenous protein removal step in the absence of a fat removal step for Brown-banded bamboo shark (*Chiloscyllium punctatum*).

2.4.2.3 Pretreatment to remove pigments

Presence of pigments in extracted collagen affects the colour (O'Sullivan et al., 2006; Xu et al., 2017) and purity (Xu et al., 2017), therefore a decolouring process is needed to remove pigments. Melanin is the pigment found in many species of fish.

Several studies focused on hydrogen peroxide (H_2O_2) treatment to remove pigments from fish skin (Xu et al., 2017), using different concentrations, different ratios and different time durations. Hydrogen peroxide especially under alkaline conditions oxidises pigments to achieve decolourisation (Xu et al., 2017). Xu et al. (2017) experimented to find an effective H_2O_2 treatment to remove pigments from Southern catfish (*Silurus meridionalis* Chen) skin by using different alkaline conditions: 0.5%, 1%, 2% and 4%; different pH levels: 8, 9, 10, 11 at a sample: solution ratio of 1:20 at 4°C for 24 h by changing the solution after 12 h. Using 0.5% H_2O_2 at pH 10 was found as the most effective treatment. Zhang et al. (2007) used 3% H_2O_2 for Grass carp (*Ctenopharyngodon idella*). However, H_2O_2 treatment was not successful in some studies. The experiment of O'Sullivan et al. (2006) using 0.2%-5% (v/v) H_2O_2 for 4 h at 4°C-20°C for Irish cod (*Gadus morhua*) and Irish ling (*Molva molva*), failed to decolourise fish skin.

Some studies have focused on combining H_2O_2 treatment with NaCl to improve the efficiency of pigment removal. Sadowska et al. (2003) experimented this combining treatment with Baltic cod (*Gadus morhua*) skin by treating with 10% NaCl solution at room temperature for 24 h and then bleaching with 1% H_2O_2 solution in 0.01 M NaOH. In addition, Sadowska et al. (2003) used repeated homogenisation of skins with 0.4 M NaCl. However, both methods did not provide successful results. According to Sadowska et al. (2003) the most effective method to remove pigments from Baltic cod skin was leaching with 0.5 M acetic acid at 4°C for 24 h, followed by homogenisation and centrifugation. In the experiment of Nagai et al. (2001) using cuttlefish (*Sepia lycidas*) in the absence of a decolouring step, produced collagen with a pink colour (Xu et al., 2017).

2.4.3 Extraction of collagen

After the pretreatment, the next step is the extraction of collagen into a soluble form. The method should be able to extract collagen at a high yield with the required purity. Further, the

method should be capable of preserving the native form of collagen for biomedical applications.

Collagen can be extracted by using different methods. Collagen is categorised based on the extraction method such as salt-soluble collagen (SSC), acid-soluble collagen (ASC), pepsin-soluble collagen (PSC) and ultrasound-assisted collagen (UAC) (Pal & Suresh, 2016). In addition, deep eutectic solvent and supercritical fluid (SF) extractions are used (Jafari et al., 2020). These methods are used alone or in combination at laboratory and industrial-scales (Bak et al., 2018).

To prepare a collagen extract, it is necessary to remove numerous covalent intra and intermolecular cross-links, primarily involving residues of lysine and hydroxylysine, ester bonds and other bonds with saccharides, to solubilise the collagen. This makes the process of collagen extraction quite complex (Schmidt et al., 2016; Skierka & Sadowska, 2007).

Collagen is insoluble due to covalent crosslinks, therefore chemical hydrolysis or proteolytic cleavage is needed to solubilise them (Skehel, 2004). Collagen should only be subjected to partial hydrolysis by this treatment to achieve the cleavage of cross-links, maintaining the polypeptide chains of collagen molecules intact in the triple-helix conformation (Schmidt et al., 2016). Partial hydrolysis can be achieved by a mild chemical treatment using diluted acids and bases (Schmidt et al., 2016) or enzymatic treatment.

The method of extraction influences the collagen yield, length of the polypeptide chains and functional properties such as viscosity, solubility, water retention and emulsification capacity (Pal & Suresh, 2016; Schmidt et al., 2016). In addition, extraction conditions of a particular method are important determinants of yield and the resulting properties of the extracted collagen (Skierka & Sadowska, 2007). Extraction parameters include weight to volume ratio of raw material and acid solution, temperature (Pal & Suresh, 2016; Schmidt et al., 2016), time (Pal & Suresh, 2016; Schmidt et al., 2016), pH (Schmidt et al., 2016).

As described previously, pretreatment conditions affect collagen yield and properties to a greater extent. The yield and properties of extracted collagen are impacted by fish species (Pal & Suresh, 2016), age (Pal & Suresh, 2016; Skierka & Sadowska, 2007), and biological and chemical properties of the raw material (Pal & Suresh, 2017; Schmidt et al., 2016). The storage conditions of raw material should also be considered (Schmidt et al., 2016).

2.4.3.1 Acid-soluble collagen

In the acid-soluble collagen extraction method, raw material is immersed in an acidic solution until the solution penetrates throughout the material. As the solution penetrates the structure of the skin at a controlled temperature it swells to two or three times its initial volume due to hydration and the cleavage of non-covalent inter and intramolecular bonds (Schmidt et al., 2016). The dominance of positive charges in collagen molecules under acidic conditions causes enhanced repulsion among collagen molecules which lead to increased solubilisation (Pal & Suresh, 2016). The process of solubilisation determines the structural organisation and mechanical features of the collagen matrix (Achilli & Mantovani, 2010).

Several factors affect the solubility of collagen in acid solutions. The concentration or pH of the acid is one factor (Sadowska et al., 2003). This effect can be explained by considering different aspects. According to Qi et al. (2015), the effect of pH has a relationship

with the chosen acid as well. They have found that the ionisation behaviour of the acid is important. They have studied the solubility of collagen in two types of acids: an acid with complete ionisation; perchloric acid ($HClO_4$) and an acid with incomplete ionisation; acetic acid (CH_3COOH). The complete ionisation of $HClO_4$ acid provides H^+ ions to the solution. The collagen molecule is amphoteric which means it has both acidic-side chain radicals (-COOH) and (-NH2). The H^+ ions available in the medium adsorb to the -NH2 and form NH_3^+. Other H^+ ions are available in the solution in free form. The adsorption of H^+ to collagen molecules can be represented as;

$R\text{-}NH_2 + H^+ \rightarrow R\text{-}NH_3^+$ where R- represents the main part of collagen molecules.

There should be an equilibrium between the adsorption and desorption of H^+ which is dependent on temperature. The adsorption of H^+ to collagen molecules depends on the concentration of free H^+ ions in the solution, which means if more H^+ ions are present more H^+ adsorbed to collagen molecules. Then the zeta potential increases which means the electrostatic repulsion between collagen molecules increase. This leads to the depolymerisation of collagen colloidal particles into smaller ones. This is the reason for having higher solubility in higher $HClO_4$ concentration or lower pH. When the amount of dissolved collagen increases in the solution more H^+ ions are adsorbed onto the collagen molecules. This results in a decrease of free H^+ in the solution. If the $HClO_4$ concentration is high, it can provide enough H^+ ions and continue the collagen solubilisation process. However, if the concentration of free H^+ ions is not enough as in the case of lower $HClO_4$ concentrations, adsorption of H^+ to collagen decreases to keep the equilibrium. Then the electrostatic repulsion decreases and repolymerise the smaller collagen colloidal particles into larger ones. This is the reason for higher solubility in higher $HClO_4$ concentration (or lower pH) and vice versa (Qi et al., 2015).

This solubility behaviour is different for acetic acid. It is only incompletely ionised in solutions. The concentration of H^+ produced by incomplete ionisation and the remaining acetic acid molecules in the acid solution at different pH levels depends on the ionisation constant (Ka). A ratio of the concentration of acetic acid to the concentration of H^+ can be calculated. The ratio is 5.7, 57 and 570 for pH 4, 3 and 2 respectively. At a lower ratio such as 5.7 (at pH 4), the adsorption of H^+ is the main process and it acts like dissolving collagen in $HClO_4$. However, at a higher ratio such as 570 (at pH 2), the adsorption of acetic acid molecules to the collagen molecules occurs reducing the sites for H^+. Hence, it decreases the zeta potential, increases the collagen colloidal particle sizes and ultimately reduces the solubility. This has been shown in the results of Qi et al. (2015), where the solubility is highest for pH 3, and it decreased from pH 3 to 2, and also from pH 3 to 4.5.

Swelling of the skin is important for collagen solubility. The pH of the chosen acid affects the swelling of collagen. If the pH is very low, positively charged amine groups of protein bind with anions, for example, Cl^- from hydrochloric acid (HCl), which reduces the electrostatic repulsive forces. As a consequence, the tightening or shrinking of collagen fibres occur, making less space for water molecules and decreasing the binding ability of water to collagen (hydration). In this way swelling of collagen decreases and reduces collagen solubility (Skierka & Sadowska, 2007).

Duration of the acid extraction step is also important. If duration is shorter than the optimum time, poor yield is obtained due to incomplete solubility of collagen in the acid. This

happens due to the incomplete removal of intermolecular cross-links between collagen fibres (Skierka & Sadowska, 2007). If extraction duration is longer in a strong acid, chemical hydrolysis or complete breakage of bonds between three polypeptide chains of collagen molecules occurs. This leads to the denaturation of collagen (Skierka & Sadowska, 2007).

Organic acids such as acetic acid, chloroacetic acid, citric acid, and lactic acid and inorganic acids such as HCl have been used to extract collagen (Pal & Suresh, 2016; Skierka & Sadowska, 2007). Among them acetic acid has been widely utilised to extract collagen from marine sources. However, the literature on the extraction of collagen by different acids is limited (Skierka & Sadowska, 2007) (Table 2.4).

Acetic acid at 0.5 M concentration causes only partial hydrolysis of collagen which is desirable (Bak et al., 2018). Some studies reported alterations in the structural and thermal properties of type I collagen by acetic acid (Bak et al., 2018). If complete hydrolysis occurs, it results in the decomposition of collagen fibres and fibrils into small aggregates of collagen monomers dispersed in the acid solution (Achilli & Mantovani, 2010).

The use of HCl acid to extract collagen from fish skin is not widely found in literature, however, Sankar et al. (2008) used 2.81 N HCl in 1:1 (w/v) ratio for 24 h at room temperature (34±2°C) to produce a collagen sheet from Barramundi (*Lates calcarifer*) scales.

2.4.3.2 Enzyme-soluble collagen

Enzymes such as pepsin, trypsin, and collagenases have been used to extract collagen. Of these, pepsin has been widely utilised to extract collagen from marine sources (Pal & Suresh, 2016). Generally, pepsin treatment is used either alone or in combination with acetic acid (Pal & Suresh, 2016) (Table 2.4).

The use of pepsin treatment in collagen extraction has main three advantages; increased purity, increased yield, and reduced antigenicity (Pal & Suresh, 2016). Pepsin hydrolyses non-collagenous proteins which can later be removed by salt precipitation and dialysis to improve collagen purity (Pal & Suresh, 2016; Skierka & Sadowska, 2007). Enzymatic extraction processes yield a higher amount of collagen than acid extraction processes (Pal & Suresh, 2016). The lower solubility of acid-soluble collagen due to the interchain aldehyde crosslinks with lysine and hydroxylysine amino acids at the telopeptide region of collagen molecules results in lower yield (Pal & Suresh, 2017). A higher yield is achieved by cleaving telopeptide regions of collagen molecules by enzyme treatment, mostly by pepsin in fish collagen extraction, which is not achievable with acetic acid, thereby increasing solubility without altering the triple-helical structure of collagen molecules (Bak et al., 2018; Coelho et al., 2017; Li et al., 2013; Pal & Suresh, 2017; Skierka & Sadowska, 2007). These cross-links at telopeptide regions of collagen molecules occur in β and γ chains and cleavage by pepsin converts these chains to α1-chains (Bak et al., 2018; Nalinanon et al., 2011). This has been reported in several studies of collagen extraction from fish; the skin of Deep-sea redfish (Wang et al., 2007), Black drum, and Sheepshead seabream (Ogawa et al., 2003). This conversion is evident by the increase of α1/α2 proportion in Sodium dodecyl sulphate-polyacrylamide gel electrophoresis (SDS-PAGE) analysis (Nalinanon et al., 2011). The antigenicity of collagen is due to the telopeptide region, so cleavage of this region by pepsin can reduce antigenicity (Pal & Suresh, 2016).

Despite these advantages, the alteration of collagen structure due to pepsin treatment affects the physico-chemical properties of collagen (Skierka & Sadowska, 2007), particularly by reducing the thermal stability of collagen (Li et al., 2013) and negatively affects fibrillogenesis.

2.4.4 Fibrillogenesis or recovery of collagen after extraction

According to the published literature, isolation or recovery of fish collagen after extraction involves salt precipitation or salting-out, centrifugation, dialysis, and freeze-drying (Pal & Suresh, 2016). Collagen extracted into the acetic acid solution is precipitated using NaCl, usually involving a concentration of 2.6 M, but different concentrations have been used to maximise collagen recovery. In some studies, salting-out is performed in the presence of tris(hydroxymethyl)aminomethane at pH 7.5. Precipitated collagen is separated using centrifugation at 4°C to avoid denaturation, but different rpm values and time durations have been reported. Centrifugation at 10,000-20,000 rpm, for 60 min has been used by many studies. After that dialysis is done by dissolving precipitated collagen in a minimum volume of acetic acid and then dialysing against distilled water. Dialysis is used to obtain purified collagen by removing impurities or residues of acids. Finally, the resultant dialysate is freeze-dried and milled to obtain collagen powder (Pal & Suresh, 2016).

This is the process used in all laboratory-based protocols available in the literature. However, this process is associated with drawbacks, especially, if the extracted collagen is to be used in biomedical applications. Bak et al. (2018) reported structural and conformational changes in type I collagen occurred due to the presence of acetic acid residues after dialysis with acetic acid. This was confirmed in their study by the Fourier transform infrared (FTIR) spectrum: a peak at 1647 cm^{-1} and a low 1240 cm^{-1}/1445 cm^{-1} ratio suggesting denaturation of collagen by acetic acid dialysis. A band appeared at the higher wavelength in measured X-Ray diffraction (XRD) spectra, indicating the weakening of hydrogen bonds between triple-helix molecules and suggesting the denaturation of collagen. Therefore, the removal of acetic acid residues from the final product is essential to have a highly ordered structure with strong hydrogen bonding (Bak et al., 2018). This study further indicated lower thermal stability of collagen influenced by acetic acid residues. According to differential scanning calorimetry (DSC) thermograms, weak denaturation enthalpy in acetic acid dialysed collagen indicates strong thermal disruption of collagen and the formation of random chains of gelatin (Bak et al., 2018). Bak et al. (2018) used acetic acid dialysed collagen to make collagen scaffolds by freezing, freeze-drying and cross-linking. These scaffolds were associated with larger pore sizes than required due to induced repulsion between collagen molecules by acetic acid residues. In addition, increases in ice crystal size by acetic acid during the freezing process causes large pore sizes and weak pore walls in scaffolds. Collagen scaffolds free of acetic acid residues are needed to support the long-term culture of cells and to provide a stable environment for cells and cell-therapy-related applications (Bak et al., 2018).

2.4.4.1 *In vitro* fibrillogenesis mechanism

There are two models which describe fibrillogenesis; the nucleation and propagation model, and the liquid crystalline model. The nucleation and propagation model refers to the formation of a nucleus of a triple-helix which grows in length and diameter into a mature fibril. The

liquid crystalline model refers to precipitation from a solution of bulk collagen with a liquid-like structure when collagen concentration is high. However, these two assembly mechanisms coexist in the same system (Zhu et al., 2018).

Fibrillogenesis *in vitro* is a time-dependent multi-step process and occurs in three phases; lag phase, growth phase, and plateau phase (Li et al., 2009). During the lag phase, collagen fibrils in solution associate together to form the nucleus of a triple-helix structure. This nucleation is a stepwise process, starting with the formation of dimers and trimers of collagen fibrils, and then leading to triple-helices. However, this process is quite different at high collagen concentrations, in which collagen fibrils or monomers first aggregate leading to a high local concentration of monomers, thus forming the initial nuclei. Once a critical number of nuclei are reached collagen fibrils begin to grow laterally. This process yields fibres with the characteristic D-banding similar to native collagen by a self-assembly process (Pawelec et al., 2016) while linear growth occurs through a fusion of individual fibres themselves in order along the fibre length (Li et al., 2009; Pawelec et al., 2016). This characteristic D-banding is a key feature as it marks a key difference between collagen and gelatin networks (Pawelec et al., 2016).

When this collagen is used in biomedical applications, particularly for tissue engineering applications, cellular responses to the scaffold material, in this case collagen, is important. Cellular responses such as cell proliferation, cell migration, cell differentiation, and cell adhesion depend on the architecture and strength of collagen, which are closely related to the self-assembly process of fibrillogenesis (Zhu et al., 2018). Thus, regulation of the factors affecting fibrillogenesis is of particular importance (Pawelec et al., 2016).

2.4.4.2 Factors affecting fibrillogenesis

Fibrillogenesis depends on the collagen source, method and conditions of fibrillogenesis. Maintenance of optimal conditions during *in vitro* fibrillogenesis similar to *in vivo* conditions is important, otherwise, it results in a variety of polymorphic aggregates in addition to the native fibrils (Li & Douglas, 2013).

Fibrillogenesis is an entropy-driven self-assembly process which is favoured by a large positive entropy contribution due to the release of structured water around collagen molecules (Li et al., 2009; Li & Douglas, 2013; Pawelec et al., 2016). Collagen fibrillogenesis is regulated by hydrophobic interactions between non-polar residues of adjacent collagen molecules (Li et al., 2009; Li & Douglas, 2013; Ramı´rez-Rodrı´guez et al., 2014), electrostatic interactions (Li et al., 2009; Li & Douglas, 2013; Pawelec et al., 2016) and hydrogen bonding between polar residues between collagen monomers (Ramı´rez-Rodrı´guez et al. 2014; Zhu et al., 2018), however energy assignable to electrostatic interactions is lower than that of hydrophobic interactions (Zhu et al., 2018).

Aggregation of collagen molecules due to hydrophobic attractions between non-polar regions of adjacent collagen molecules are determined by the negative temperature coefficient of collagen solubility (Li & Douglas, 2013; Zhu et al., 2018) and the endothermic nature of *in vitro* fibrillogenesis (Li et al., 2009; Li & Douglas, 2013). Electrostatic interactions are determined by the formation of net charges between collagen molecules of neighbouring fibrils (Li & Douglas, 2013). Some studies indicate that optimised electrostatic interactions between adjacent triple-helices facilitate the maximum contact between hydrophobic regions

(Li & Douglas, 2013). Electrostatic attractions affect the stability of the collagen matrix (Li & Douglas, 2013) while its effect on fibril size and morphology is weak (Li et al., 2009). Water-mediated hydrogen bonds between polar residues are important determinants of the lateral alignment of collagen fibrils during fibrillogenesis (Li et al., 2009; Li & Douglas, 2013).

Factors governing the fibrillogenesis of collagen include; pH (Li et al., 2009; Pal & Suresh, 2017; Pawelec et al., 2016; Zhu et al., 2018), temperature (Li et al., 2009; Pal & Suresh, 2017; Zhu et al., 2018), ionic strength (Li et al., 2009; Pal & Suresh, 2017; Pawelec et al., 2016; Zhu et al., 2018), ion species (Li et al., 2009), concentration of collagen (Zhu et al., 2018), non-collagenous components (Zhu et al., 2018) like saccharides (Li et al., 2009), ionic species (Li & Douglas, 2013; Zhu et al., 2018), extraction method (Li et al., 2009; Li & Douglas, 2013; Pawelec et al., 2016); surfactants (Li et al., 2009); inhibitors (Zhu et al., 2018), and interactions (Zhu et al., 2018).

2.4.4.2.1 pH

When the pH of the fibrillogenesis medium reaches the isoelectric pH (pI), the surface charge of collagen monomers is reduced, thus minimising the electrostatic repulsion and favouring collagen fibril aggregation (Li et al., 2009). Electrostatic interactions are sensitive to the pH of the medium (Li & Douglas, 2013; Pawelec et al., 2016). Fibrillogenesis is slow or incomplete resulting in a loss of the D-banding pattern at pH values far away from the isoelectric point (Pawelec et al., 2016). At these pH values, fibrils tend to gather to form sub-fibrils without a D-banding pattern in highly concentrated collagen solutions (Zhu et al., 2018).

In fibrillogenesis methods, the rate of pH change in addition to the final steady pH, affects fibril morphology, particularly the size and kinetics of fibril formation (Pawelec et al., 2016; Zhu et al., 2018). A high rate of pH change in the system reduces the lateral growth of fibres, thus forming thinner fibres as it provides only a shorter period for molecules to spend around the isoelectric point, so electrostatic interactions become weak. On the other hand, a gradual increase of pH in the system promotes lateral growth but inhibits the formation of collagen fibres in length thus causing the loss of some D-banding resulting in a more heterogenous collagen fibrils compared to native ones (Pawelec et al., 2016; Zhu et al., 2018).

This effect of pH on collagen morphology; diameter and the D-periodicity of fibrils has been reported by Li et al. (2009) in their study with commercial purified type I pepsin-treated adult bovine dermal collagen. At low pH values, fibrils of variable sizes were formed without the D-banding pattern. More uniform fibres interwoven into a network were formed with increasing pH. In the pH range from 6.0 to 6.9, no fibrillogenesis occurred, instead a gel of non-fibrillar collagen was formed. It was reported that it took three days to form fibrils of 85 nm diameter at pH 6.6, while fibrils of 200 nm diameter were formed within one day when the pH increased from 6.9 to 8.0.

2.4.4.2.2 Ionic conditions: species and strength

The ionic strength of the buffer solution in combination with pH has a profound effect on fibrillogenesis (Pawelec et al., 2016) by regulating electrostatic interactions between amino acid residues (Li & Douglas, 2013). In systems with pH values far away from the isoelectric point, additional ions or charge-altering molecules can shift collagen's isoelectric point to initiate fibril formation (Pawelec et al., 2016). Lower ionic strength induces faster collagen

fibrillogenesis by inhibiting the salting-in effect and enhancing electrostatic interactions between charged amino acid side chains (Zhu et al., 2018).

The presence of an environment similar to *in vivo* conditions is important for better fibrillogenesis. Ions and molecules other than collagen present in the environment for *in vivo* fibrillogenesis help to stabilise the collagen fibres and act as molecular crowders to affect many biological processes. Similarly, crowders under *in vitro* conditions reduce the time to initiate nucleation and increase the fibrillogenesis rate (Pawelec et al., 2016).

Ion preferential binding accelerates the fibrillogenesis rate and fibril growth due to screening of the surface charge of soluble collagen (Zhu et al., 2018). Different types of ions or salts are capable of binding to collagen thus affecting electrostatic interactions (Li et al., 2009). Divalent phosphate ions bind with collagen molecules and form salt bridges in the regions of high excess positive charge, thus affecting electrostatic interactions (Li et al., 2009; Zhu et al., 2018). Sulphate ions have also reported the same effect (Zhu et al., 2018). The effect of phosphate ions highly depends on temperature, telopeptides and additives in the system (Zhu et al., 2018). Phosphate ions play a critical role in forming native fibrils with characteristic D-banding pattern, increasing the fibrillogenesis rate and increasing the critical concentration for fibrillogenesis (Li & Douglas, 2013). However, chloride ions are superior to phosphate and sulphate in the formation of native fibres with the characteristic D-banding pattern (Zhu et al., 2018). Harris et al. (2013) reported better fibrillogenesis of acetic acid soluble collagen with chloride ions in phosphate buffers than water alone. Different ion species in buffer solutions behave differently in the same fibrillogenesis conditions (Pawelec et al., 2016). Freudenberg et al. (2007) reported shifting of the isoelectric point of pepsin-soluble type I collagen from pH 7.5 to 5.3 when the ionic strength of KCl was increased from 0.1 mM to 10 mM, however with the same concentration of $CaCl_2$, the isolectric point increased above pH 9. Calcium and magnesium ions inhibit fibril formation due to salt bridging with carboxylic groups (Zhu et al., 2018).

2.4.4.2.3 Temperature

Temperature affects the hydrophobic interactions between collagen molecules and therefore the kinetics of fibrillogenesis (Li & Douglas, 2013). Collagen is denatured when heated above its denaturation temperature (Zhu et al., 2018). Collagen fibrillogenesis is a thermally driven process governed by a large positive entropy contribution due to the displacement of structured water around collagen molecules. Therefore, increasing the temperature of the fibrillogenesis system within the respective denaturation temperature increases the fibrillogenesis rate, thus forming more compact and thinner fibres compared to those that can be produced at lower temperatures (Zhu et al., 2018). This justifies the possibility of protocols with different fibrillogenesis temperatures to produce collagen with varying fibril strength and morphology; thickness, porosity and length (Zhu et al., 2018).

2.4.4.2.4 Concentration

The concentration of collagen solutions affects fibrillogenesis through the mechanism of hydrogen bonding. Collagen fibril size has a strong, but non-linear relationship with the concentration of the collagen solution (Zhu et al., 2018). This non-linear relationship is a result of competition between the availability of collagen molecules and the viscoelasticity of dense solutions. For example, according to the study by Gobeaux et al. (2008), fibril diameter and

concentration were linear in the 10 to 80 mg mL^{-1} concentration range, but lower than the dilute concentration of 5 mg mL^{-1}. Again, in the intermediate range from 90-150 mg mL^{-1}, fibril diameter significantly increased with the increasing concentration, and the diameter dropped when concentration increased above 200 mg mL^{-1}. Therefore, collagen with different architectures can be obtained by varying the concentration (Zhu et al., 2018).

2.4.4.2.5 Extraction method

Acid-soluble or enzyme-soluble extraction methods or combinations of them are used to extract collagen before the fibrillogenesis step. N- and C-termini telopeptide regions of tropocollagen molecules are important to form cross-links between collagen fibrils (Li & Douglas, 2013), thereby stabilising the collagen network during the self-assembly process of fibrillogenesis. During the extraction step, enzymes cleave these telopeptide regions thus increasing the solubility, however it is not favourable for the self-assembly of fibrils with the characteristic D-banding pattern (Li & Douglas, 2013; Pawelec et al., 2016). The presence of more cross-links remaining after the extraction step shortens the time for fibrillogenesis (Pawelec et al., 2016).

2.4.4.2.6 Other molecules

Large molecules, such as glycosaminoglycans (GAGs) and small leucine-rich proteins regulate the fibril size during fibrillogenesis *in vivo* (Pawelec et al., 2016). Incorporation of these types of molecules into the *in vitro* system can have effects on the final collagen structure (Pawelec et al., 2016) due to effects on electrostatic interactions. Different types of proteoglycans act in different ways (Zhu et al., 2018). Decorin reduces the fibril diameter, whereas biglycan has a modest effect. GAG (glycosaminoglycan)-containing decorin strongly inhibits fibrillogenesis compared to non-glycosylated decorin (Zhu et al., 2018).

2.4.4.2.7 Cross-linking agents

Physical, chemical or biological cross-linking agents can be employed to stabilise collagen networks during fibrillogenesis, through covalent interactions with collagen molecules (Zhu et al., 2018). Chemical cross-linking agents such as organic aldehydes, carbodiimides, polyepoxy compounds and inorganic polyvalent cations bind to specific groups such as the, lysine, hydroxylysine or carboxyl residues of collagen molecules. This may affect fibril formation to some extent, however, aldehydes promote faster fibril formation (Zhu et al., 2018). Hexamethylene diisocyanate (HMDC), sorbitol, glycerol, glutaraldehyde (GTA), k-carageenan (kCGN), transglutaminase (TG) (Riaz et al., 2018), 1-Ethyl-3-diaminopropyl-carbodiimide (EDC), N-hydroxysuccinimide (NHS), Genipin (Englert et al., 2007) are a few examples of chemical cross-linking agents that can be used to promote collagen fibrillogenesis.

2.4.5 Method scalability

Collagen extraction for biomedical applications does not require mass-scale production as the quantities required are low compared to applications in food or cosmetic industries. Therefore, scalability from laboratory scale to small or medium scale production should be considered. Collagen extraction for biomedical applications involve initial sample preparation, pretreatment, extraction, fibrillogenesis and freeze-drying as main steps. Preservation of the

native triple-helical structure and the d-banding pattern are the important aspects that should be considered in scale-up.

2.5 Characterisation of type I collagen for biomedical applications

2.5.1 UV absorption spectroscopy

UV absorption spectroscopy is a qualitative technique to analyse the purity of extracted collagen with respect to the absence of non-collagenous proteins. Pure type I collagen gives the maximum absorption peak in the 220 nm to 240 nm range (Pal & Suresh, 2017), mostly at 230 nm (Nalinanon et al., 2011; Pal et al., 2015; Pal & Suresh, 2017). This peak is associated with the C=O, -COOH, and $CONH_2$ groups in polypeptide chains of the collagen molecule (Pal & Suresh, 2017; Zeng et al., 2009). If amino acids are present as impurities, it provides an additional small peak at 280 nm corresponding to tryptophan and tyrosine (Pal & Suresh, 2017; Xu et al., 2017; Zeng et al., 2009). The UV absorption spectrum of most seafood by-product-derived collagens reported a maximum absorption peak at 230-240 nm and a little absorption peak at 280 nm (Pal & Suresh, 2016). The presence of amino acids as impurities can further be confirmed by the amino acid content analysis (Table 2.5).

Table 2.5 UV absorption data and amino acid analysis data (tyrosine) from studies on fish skin collagen extraction.

Collagen source	Maximum absorption peak (nm)	Peak at 280 nm	Tyrosine (residues per 1,000 total amino acid residues)	Justification on purity	Reference
Southern catfish (*Silurus meridionalis* Chen)	220	Absent	4	Pure	Xu et al., 2017
Nile tilapia (*Oreochromis niloticus*) skin	210	Absent	3	Pure	Zeng et al., 2009

2.5.2 Attenuated total reflectance-fourier transform infrared (ATR-FTIR) spectroscopy

ATR-FTIR spectroscopy is a vibrational spectroscopic technique which provides molecular-level information allowing investigation of functional groups, bonding types, and molecular conformations (Riaz et al., 2018; Talari et al., 2017). Spectral bands in this spectrum are molecule specific and provide direct information about the biochemical composition (Riaz et al., 2018; Talari et al., 2017). These spectral bands are relatively narrow, easy to resolve and sensitive to molecular structure, conformation, and environment (Talari et al., 2017). All vibrational spectroscopic techniques including FTIR spectroscopy techniques are relatively simple, reproducible, non-destructive to the tissue, only small amounts of material (usually micrograms to nanograms) with minimal sample preparation are required, fast, affordable and provide reliable results (Riaz et al., 2018; Talari et al., 2017).

FTIR spectroscopy is a measurement of the wavelength and intensity of the absorption of IR radiation by a sample (Kong & Yu, 2007). There are nine characteristic IR absorption

bands, namely, amide A, B, and I−VII corresponding to different vibrational types of protein are available (Tables 2.6 and 2.7).

The FTIR spectroscopy is used in collagen analysis to confirm its type, hence in fish skin collagen to confirm type I. Type I collagen is confirmed by the presence of amide A, amide B, amide I, amide II and amide III bands in the FTIR spectrum. Amide I and II bands are correlated to the protein secondary structure. The amide I band has a higher protein conformational sensitivity than its counterpart amide II because the amide I band is due almost entirely to the C=O stretching vibrations (approximately 80%). In contrast, the amide II band is due partly to the in-plane NH bending (40-60% of the potential energy) and CN stretching vibration (18-40% of the potential energy) (Kong & Yu, 2007). The absorption ratio close to 1, between the amide III band and the 1450 cm^{-1} band, indicates the maintenance of the integrity of the triple-helical structure of collagen. The position of bands can shift to lower frequencies indicating the involvement of hydrogen bonding (Xu et al., 2017).

Table 2.6 FTIR peak locations and assignment of fish skin collagen (data are from studies available in the literature).

Designation	**Approximate frequency (cm^{-1}) based on literature**	**Source of collagen and reference**		
		Sole fish (*Aseraggodes umbratilis*)	Spanish mackerel (*Scomberomorous niphonius*)	Southern catfish (*Silurus meridionalis* Chen)
		Arumugam et al., 2018	Li et al., 2013	Xu et al., 2017
Amide A	3440 – 3400	3310	3433	3420
Amide B	App. 2920	2362	2926	2926
Amide I	1700 – 1600	1651	1641	1655
Amide II	1600 – 1550	1542	1549	1550
Amide III	1300 – 1230	1238	1240	1240
Absorption ratio for peak near 1450 cm^{-1}			1	0.903

Table 2.7 Characteristic infrared bands of peptide linkages not belonging to type I collagen **(**source: Kong & Yu, 2007).

Designation	**Approximate frequency (cm^{-1})**	**Description**
Amide IV	625−767	OCN bending
Amide V	640−800	Out-of-plane NH bending
Amide VI	537−606	Out-of-plane C=O bending
Amide VII	200	Skeletal torsion

More detailed information about protein secondary structure is obtained through X-ray crystallography analysis concerning the position of individual atoms in the protein,

however all proteins cannot form quality crystals and also crystallographic data of a protein cannot be easily extrapolated to the dynamic properties of the proteins in solutions, hence FTIR spectroscopy is commonly used to analyse the secondary structure of proteins (Kong & Yu, 2007). Peptide linkages have another four spectral bands which do not belong to type I collagen (Table 2.7). Their presence in a spectrum would indicate contamination or low purity of collagen.

2.5.3 Differential scanning calorimetry (DSC)

DSC is superior to other methods of thermal denaturation measurements due to the appreciable heat absorption when denaturation occurs (Liu et al., 2014). The process of denaturation is a phase transition. During this phase transition, the native form of collagen is transformed to denatured form and simultaneously structured water is released. This phase transition is mainly determined by the state or phase of particular components of the sample, and indirectly inform about the chemical composition of the sample. However, DSC curves do not provide information about the type of reaction that has taken place in the sample. The physical properties of collagen depend on its water content. Water molecules participate in different ways in collagen structure, therefore the release of water at phase transition is a complex process. The amount of free and bound water depends on relative humidity (Gauza-Włodarczyk et al., 2017).

Free water moves in and out of the fibre structure with changes in relative humidity, whereas bound water is attached to the protein molecules. The amount of free water varies with the physical state of the skin, such as porosity and the presence of chemicals. Structural water is present in the form of an integral part of the collagen structure and affects its physical and chemical properties. Heating of collagen also leads to the release of free and bound water, whose content affects both the thermal and electrical conductivity of collagen (Gauza-Włodarczyk et al., 2017).

DSC permits the investigation of thermal effects accompanying different processes taking place on heating or cooling of a given substance and thermal effects taking place under isothermal conditions at a certain time (Gauza-Włodarczyk et al., 2017). This process can be explained using DSC thermograms. For example, DSC thermograms recorded by Gauza-Włodarczyk et al. (2017) in their study with fish skin collagen in a form of hydrogel made of *Salmo salar* skin, loss of free water and bound water occurred in 25-87°C temperature region, the process of denaturation occurred in 107-147°C region and thermal decomposition occurred above 147°C.

Generally, the enthalpy of denaturation: the energy needed for the phase transition of fish collagen is lower than that of bovine collagen, hence the denaturation temperature of fish collagen is low (Liu et al., 2014). The processing temperature of collagen should be below the denaturation temperature (Gauza-Włodarczyk et al., 2017). Therefore, measurement of Td is important in this study to know which processing temperatures should be regulated to avoid the denaturation of collagen during extraction and further applications.

2.5.4 Circular dichroism (CD) spectroscopy

Circular dichroism spectroscopy is used for the structure determination of peptide bonds, aromatic amino acid side chains, and disulphide bonds in the wavelength ranges of less than

240 nm, 260-320 nm, and around 260 nm respectively (Kelly et al., 2005). Circular dichroism spectroscopy is considered the gold standard for estimating the secondary structure of proteins among other techniques like FTIR and DSC due to the easy identification of the native and denatured conformations (Gopinath et al., 2017). The secondary structure determination by this technique is based on the measurement of differential absorption of left and right-handed polarised light by peptide bond chromophores in a protein (Drzewiecki et al., 2016; Qi et al. 2015; Zhou et al. 2018), in the far UV range, generally from 250 to 190 nm (Rodger & Marshall, 2021). The spectrum is recorded as dichroism measured as a function of wavelength (Kelly et al., 2005). The native triple-helical structure of collagen in a solution is characterised by the presence of a negative peak at around 198 nm related to the content of the α-helix structure, a cross-over at 214 nm and a weak positive peak at around 220 nm due to the π-π* transition of peptide bonds (Liu et al., 2016; Zhou et al., 2018). The easy identification of the native structure from the denatured structure is based on the presence or absence of the positive peak as it disappears upon denaturation (Drzewiecki et al. 2016). The calculated value of the 'positive/negative ratio' (R_{pn}) from the CD spectra is used as a measure to estimate the degree of denaturation or the triple-helical content (Akita et al. 2020; Perez-Puyana et al. 2019). A higher R_{pn} ratio implies a more denatured protein and shows a positive value above zero, and a lower R_{pn} ratio below zero implies a native protein (Perez-Puyana et al., 2019). Sun et al. (2020) reported a R_{pn} ratio of -0.123 for native collagen and 0.120 for thermally denatured collagen.

The solvent and the pH of the medium should be selected appropriately for dissolving collagen. The use of HCl as a solvent is not a good choice as Cl^- is an achiral molecule which absorbs light and reduce the photons available for the analyte to absorb (Rodger & Marshall, 2021). Therefore, the most suitable solvent for collagen secondary structure analysis is acetic acid. However, the pH of the medium should not be below 3.0, due to the irreversible unwinding of triple-helices into random polypeptide chains by the higher amount of H^+ (Zhou et al., 2018). Therefore, an acetic acid concentration of 0.05 M is used (Zhou et al., 2018). The dynode voltage of the samples should also be checked. It is an instrument parameter that increases with the increasing optical density of the samples (Drzewiecki et al., 2016). For highly absorbing samples only a few photons are reaching the detector causing weak signals in the spectrum (Rodger & Marshall, 2021). Therefore, the dynode voltage of the samples should be confirmed to be below 600 V (Drzewiecki et al., 2016).

2.5.5 Scanning electron microscopy (SEM)

Scanning electron microscopy images are used to describe the morphology of freeze-dried collagen. These collagens appear as sponges and typically consist of interwoven fibril network found as sheets, and pores between the spaces (Arumugam et al., 2018; Liao et al., 2018;). Features of these sponges, such as specific surface area, pore size, pore volume and fibril distribution are important for biomedical applications (Arumugam et al., 2018; Pal et al., 2016; Wu et al., 2010;). This porous structure is a result of freeze-drying, and the pore size depends on the water content during preparation (Ikoma et al., 2003).

2.5.6 Zeta potential

The zeta potential or surface charge of collagen is used to measure the isoelectric pH (pI). The pI can be used to study the electrostatic interactions of collagen during fibrillogenesis (Li et al., 2009). Collagen precipitation or fibrillogenesis occurs at isoelectric pH (pI) attributing to the aggregation of collagen molecules due to hydrophobic interactions among collagen molecules, which increases at pI, where the total net charge of protein molecules becomes zero (Pal & Suresh, 2016).

When the pH of the collagen solution is higher or lower than the pI, the repulsive forces between charged residues of collagen molecules increases, thereby increasing the solubility of collagen. At pI, the total charge of collagen is almost zero, thereby increasing the interactions between hydrophobic sites of collagen molecules leading to aggregation and precipitation (Li et al., 2013; Pal & Suresh, 2016; Woo et al., 2008).

The pI depends on the source of collagen, hence the species of fish (Pal & Suresh, 2017), method of collagen extraction and fibrillogenesis. Pepsin treatment in the collagen extraction step can alter the pI by reducing the content of high molecular weight cross-links due to the cleaving of the telopeptide region (Li et al., 2013). The presence of ions or added salts in collagen solution during fibrillogenesis alter pI of fish collagen (Li et al., 2009). Studies have reported different pI values for different fish species: pH 9.3 (Pati et al., 2012); pH 6-9 (Li et al., 2013); pH 6.6 (Woo et al., 2008); pH 5.5-9.5 (Pati et al., 2012).

2.5.7 Turbidity measurement

Turbidity measurement is widely used to study the self-assembly process of collagen fibrillogenesis due to its simplicity of operation and providing multiple kinetic parameters (Zhu et al., 2018). Fibrillogenesis occurs in three phases and changes are sigmoidal, measurement of optical density at 313 nm during lag, growth and plateau phases are assessed. During the lag phase, the assembly of collagen monomers into fibril intermediates are initiated, therefore no detectable change in turbidity is observed. During the growth phase, the formation of mature collagen fibrils from the fibril intermediates occurs, and therefore a significant increase in turbidity is observed. During the plateau phase a constant level of turbidity is observed (Li et al., 2009; Zhu et al., 2018). The turbidity method has some drawbacks including failure to reveal details of the fibre number and size at the microscale (Zhu et al., 2018). In some studies, atomic force microscopy (AFM) or transmission electron microscopy (TEM) images are used together with turbidity measurements to describe the results.

2.5.8 Atomic force microscopy (AFM)

AFM is an imaging technique to visualise the surface topography of a sample (Zhu et al., 2018). Compared to electron microscopy, AFM can be used in aqueous solutions thereby preserving their physiological conformations, and functions. A high signal-to-noise ratio permits the resolution of surface structural details down to less than 1 nm (Jiang et al., 2004). AFM can be used to investigate the self-assembly process and network formation of collagen in biological systems (Jiang et al., 2004) as it enables the study of both individual molecules and the interaction between molecules (Zhu et al., 2018). Therefore, AFM is an effective tool to analyse the morphology of collagen fibrils, such as typical D-periodicity and dynamics of

collagen fibrillogenesis under different conditions. D-periodicity can also be obtained using complementary electron microscopy methods and XRD spectra (Zhu et al., 2018).

2.5.9 Transmission electron microscopy (TEM)

TEM is another imaging technique used in collagen fibrillogenesis studies to visualise the surface topography of a sample. TEM has advantages including a very high spatial resolution capability providing details of the characteristic D-banding of fibrils, fibril diameter, fibril volume fraction, mean fibril length and fibril cross-sectional features (Zhu et al., 2018). Drawbacks associated with TEM include high sample preparation costs, extensive sample preparation time, and failure to achieve real-time observation of collagen fibrillogenesis (Zhu et al., 2018). Figure 2.5 shows examples of imaging type I collagen using some of these techniques.

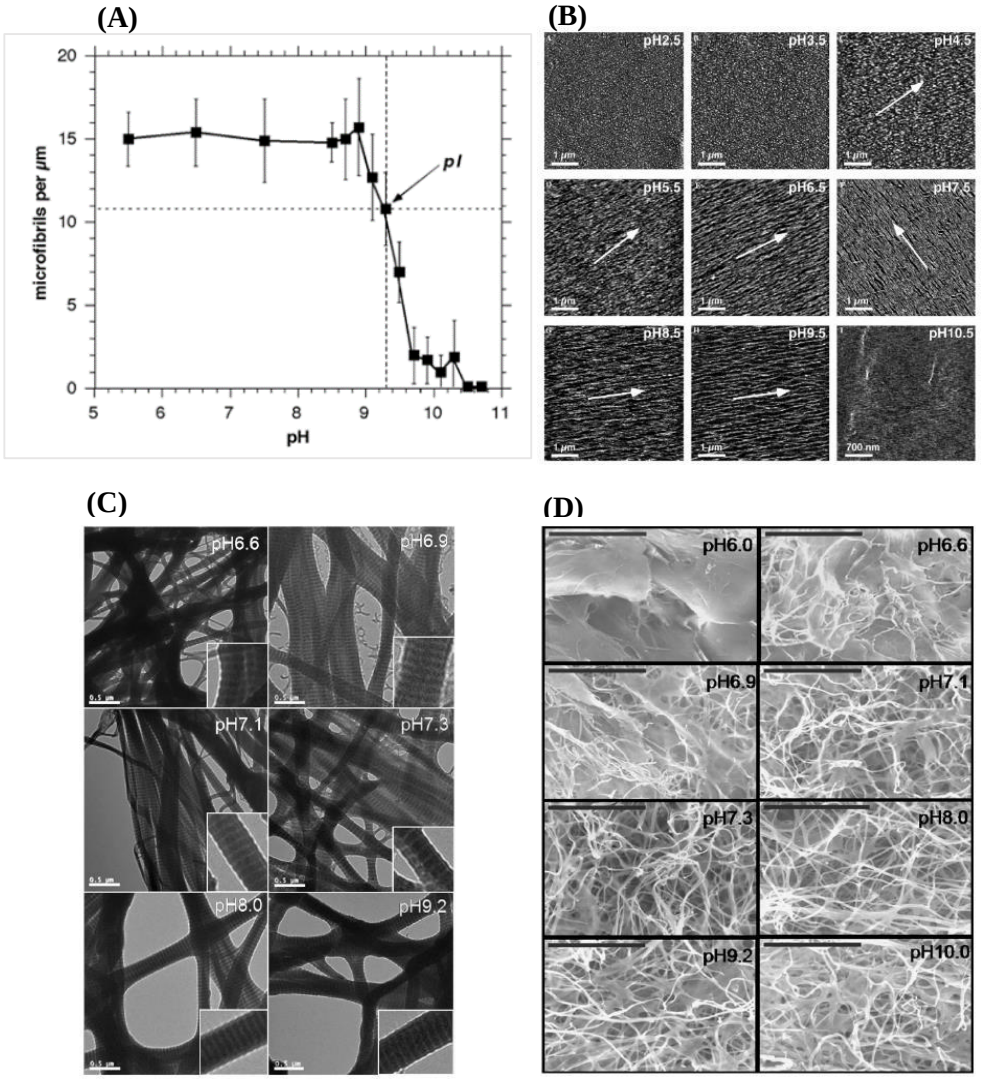

Figure 2.5 Self-assembly process of collagen type I showing the collagen fibril morphology and arrangement at different pH values during self-assembly process.
(A) Collagen fibrils per unit length of 1 µm. The pI value of collagen type I (9.3) is pointed out. (Jiang et al., 2004)
(B) AFM images (Jiang et al., 2004)
(C) TEM images (Li et al., 2009)
(D) SEM images (Li et al., 2009)

2.6 Conclusions

Characteristics of fish skin collagen are different from mammalian collagen. The required functionality of collagen depending on the biomedical application is possible with further treatment methods after extraction, such as physical or chemical cross-linking. In addition, fish skin collagen possesses favourable characteristics for biomedical applications such as high biodegradability, weak antigenicity, high cell adhesion, cell growth and cell proliferation potential than mammalian collagen. However, several gaps were evident in the existing knowledge on the use of fish as a source of collagen for biomedical applications.

Marine collagen processing for biomedical applications is only evident at the laboratory scale. Research has been done to extract and characterise collagen from different body parts of fish including the fish skin, however, it has not progressed beyond laboratory-level processing. These methods cannot be applied for industrial-level processing of collagen from fish skin due to their complexity and long processing times. Therefore, methods need to be modified and scaled-up for industrial level processing of fish skin collagen for biomedical applications.

Fish skin structure and composition vary due to different factors. Conditions in the collagen extraction process need to vary according to these factors. However, existing laboratory methods have not been focused on this important aspect. Therefore, the behaviour of fish skin structure and composition during the collagen extraction process from variable fish species need to be studied and the processing parameters need to be optimised.

The review of literature has demonstrated numerous detailed studies of how processing conditions and extraction protocols can be applied to fish skins to produce collagens. To facilitate commercial processing, this knowledge must be applied to adapt well established mammal-derived collagen processing methods to marine sources.

Chapter 3. Direct application of bovine collagen processing to fish skin

3.1 Introduction

While there are no industrially relevant fish collagen processes for biomedical applications reported in the literature, methods to produce biomedical collagen from bovine sources exist and these materials are commercially available. Several patents such as those by Li & Oakland (1997); Li et al. (1994, 1996); Nichols & Princeton (1991) form the basis of commercial processing systems. Collagen is generally derived from tendons which have a uniform structure and low fat content. Processing steps include the removal of fats using Sodium dodecyl sulphate (SDS), mechanical slicing, removal of non-collagenous proteins using Sodium sulphate (Na_2SO_4), extraction using mineral acids and fibrillogenesis using Sodium hydroxide (NaOH) (Figure 3.1). Conditions have been adapted to achieve high yield, high purity and good functionality that preserves the native triple-helix structure and native D-banding pattern while minimising the number of processing steps, the time required for each step and the amount of each solution used.

As shown in the literature review, fish skin processing methods at lab scale are long and complex with significant solvent use. As such, this work took the approach of taking a commercial bovine process and using this as the basis for the development of fish skin collagen processing. By demonstrating the problems that arise, adaptations could be proposed to overcome them. The literature review identified that key challenges in processing fish skins are likely to be due to greater structural heterogeneity, higher levels of non-collagenous components and reduced thermal stability of fish skins.

This chapter is focused on;

- Laboratory-scale implementation of a commercial process used for bovine collagen extraction from tendons and demonstrating the experimental techniques to characterise the composition and structure of the derived collagen.
- Direct application of this process to fish skins to identify the key areas where modifications of the process would be required to achieve high quality fish skin-derived collagen products.

This would form the basis for the adaptation of the process to improve performance.

3.2 Demonstrating a laboratory scale implementation of commercial bovine collagen processing

In this step, the laboratory scale application was demonstrated to become familiar with it, to set up key equipment and to demonstrate analysis methods. Figure 3.1 shows a process flow chart of the commercial process used which was based on the patents by Li & Oakland (1997); Li et al. (1994, 1996); Nichols & Princeton (1991).

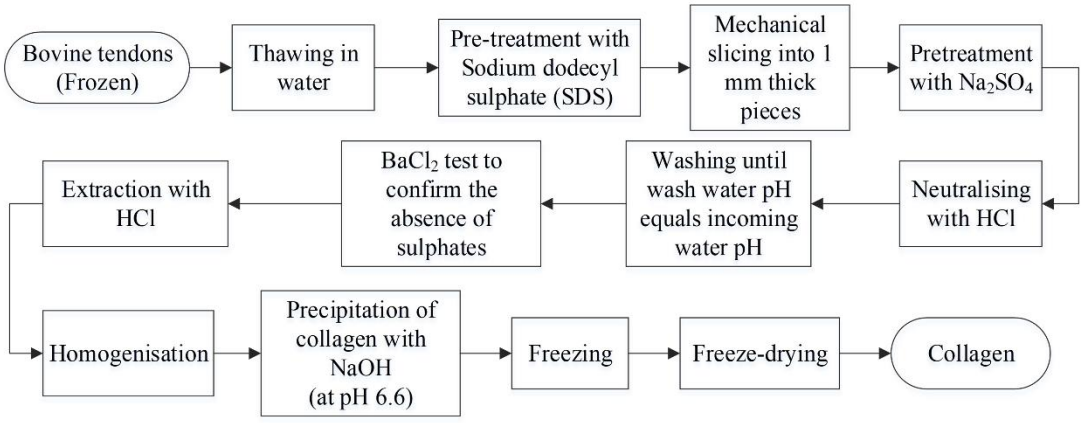

Figure 3.1 Process flow chart showing the key steps of the commercial bovine collagen process.

3.2.1 Materials and methods

3.2.1.1 Sample preparation

Bovine tendons were supplied in frozen condition from the Silver Fern Farms, New Zealand. These tendons were from animals between 24-30 months old. Whole samples were then thawed by soaking in distilled water at 1:5 (m/v) ratio for 6 h, and then drained for 2 min. Sample preparation and all the experiments were conducted at normal laboratory temperatures (19-20°C).

3.2.1.2 Pretreatment by SDS washing

Pretreatment with SDS was done to remove fats and other unwanted materials available on the surface of tendons. Tendons were added to a 2% SDS solution at 1:1 (m/v) ratio, stirred for 1 min, left undisturbed for 60 min and the solution was drained for 2 min. Then tendons were rinsed by adding distilled water at 1:1 (m/v) ratio, stirred for 1 min, left undisturbed for 30 min and drained for 2 min. This rinsing step was repeated 5 times.

3.2.1.3 Pretreatment with Sodium sulphate

Pretreatment with Na_2SO_4 was done to remove non-collagenous proteins from tendons. Tendons, after pretreatment with SDS were cut transversely into 1 mm thick pieces using a bacon slicer. The slices were then soaked in 0.25 M Na_2SO_4/ 0.1 M HCl at 1: 10 (m/v) ratio for 4 h with periodic gentle stirring every hour for 1-2 min during soaking, then were drained for 5 min. The samples were then soaked in 0.5 M Na_2SO_4 at 1: 5 (m/v) ratio for 30 min and drained for 5 min. After that, the samples were soaked in 0.75 M NaOH/ 1.0 M Na_2SO_4 at 1: 10 (m/v) ratio for 24 h with periodic gentle stirring every hour for 1-2 min during soaking. They were then neutralised with 1 M HCl and drained. The samples were then repeatedly washed with distilled water until the separated wash water pH became equal to the incoming wash water pH. A Barium chloride test was done to qualitatively confirm the absence of sulphate. A white colour precipitate (Barium sulphate) is formed if sulphate is present.

3.2.1.4 Extraction with hydrochloric acid

The pretreated samples were dispersed in 0.01 M HCl at 1: 30 (m/v) ratio for 1 h. By this time, the tendon pieces were swollen completely. The swollen pieces and the solution were

homogenised together for 3 bursts each for 15 s using a food processor (Nutrifusion 700 Series, Model XJ-15409). Samples were rested for 60 s in between bursts to avoid foaming and heating.

3.2.1.5 Fibrillogenesis with Sodium hydroxide

The homogenised solution was then precipitated with 0.01 M NaOH until pH 6.6, which is the isoelectric pH of bovine collagen. The precipitated collagen was separated from the rest of the solution by filtering through a stainless steel colander and packed in polythene bags. They were kept in the freezer for 24 h at -20°C and then freeze-dried at 0.5 mbar, 50°C for three days (BUCHI LyovaporTM L-300, BUCHI Labortechnik AG; Flawil, Switzerland).

3.2.1.6 Characterisation methods for extracted collagen

Freeze-dried bovine collagen was characterised by scanning electron microscopy (SEM), UV absorption spectroscopy, attenuated total reflectance-fourier transform infrared (ATR-FTIR) spectroscopy, differential scanning calorimetry (DSC) and circular dichroism (CD) spectroscopy.

3.2.1.6.1 Morphology and microstructure

Optical photographs were taken using a Samsung Galaxy Note9 phone to show the collagen morphology under the naked eye. The microstructure of collagens was analysed by the SEM. For the SEM, freeze-dried samples were mounted on aluminium stubs using double-sided tape to ensure high electrical conductivity between the specimen and the stub. Then, it was sputter-coated with approximately 100 nm of gold (Baltec SCD 050 sputter coater) and viewed in a FEI Quanta 200 Environmental Scanning Electron Microscope (Hillsboro, USA) at an accelerating voltage of 20 kV.

3.2.1.6.2 UV absorption spectroscopy

UV absorption spectroscopy was used to assess the effectiveness of pretreatment step to remove the non-collagenous proteins, and infer the purity of collagen. UV absorption spectra were obtained using the method of Zeng et al. (2009), which involved dissolving 0.04 mg of collagen in 100 mL of 0.02 M Sodium acetate buffer at pH 4.8 containing 2 M urea. The solution was then placed into a quartz cell with a path length of 1 mm. The UV spectrum was measured at wavelength 190-350 nm at a scan speed of 2 nm/s with an interval of 1 nm using a UV-visible spectrophotometer (Genesys 10S spectrophotometer, GENESYS 10S UV-VIS, Thermo Fisher Scientific; Madison, Wisconsin, USA). Pure type I collagen should give only one peak in the 220 nm to 240 nm wavelength range. If non-collagenous proteins are present as impurities, the spectrum provides an additional small peak at 280 nm corresponding to tryptophan and tyrosine amino acids which should be absent in pure collagen.

3.2.1.6.3 ATR-FTIR spectroscopy

The ATR-FTIR spectroscopy was used to assess the type of collagen and the native triple-helical conformation. The ATR-FTIR spectra were obtained using a Nicolet iS5FTIR spectrometer (Wisconsin, USA) equipped with a iD7 ATR diamond sampler accessory. A small piece of freeze-dried collagen was placed on the single reflection crystal cell. The signals were automatically collected for 32 scans over the 4000-400 cm^{-1} range using 2 cm^{-1}

resolution. Background spectra were collected from the clean empty crystal cell. The peak positions of the spectrum were analysed for collagen type, and triple-helical conformation as described in the §2.5.2.

3.2.2 Results and discussion

3.2.2.1 Morphology and microstructure

Collagen appeared as a white sponge with pores on its surface under the naked eye (Figure 3.2). SEM images were taken to analyse the morphology of extracted freeze-dried collagen. SEM images (Figure 3.3), at lower magnifications, showed the pore structure, and at higher magnifications the coil-like fibrils were seen as sheets interconnected to each other. Pores were found in the spaces between the interconnected sheets. This porous structure is an important characteristic in biomedical applications (Arumugam et al., 2018).

Figure 3.2 Optical photograph of the freeze-dried bovine tendon collagen as viewed by the naked eye.

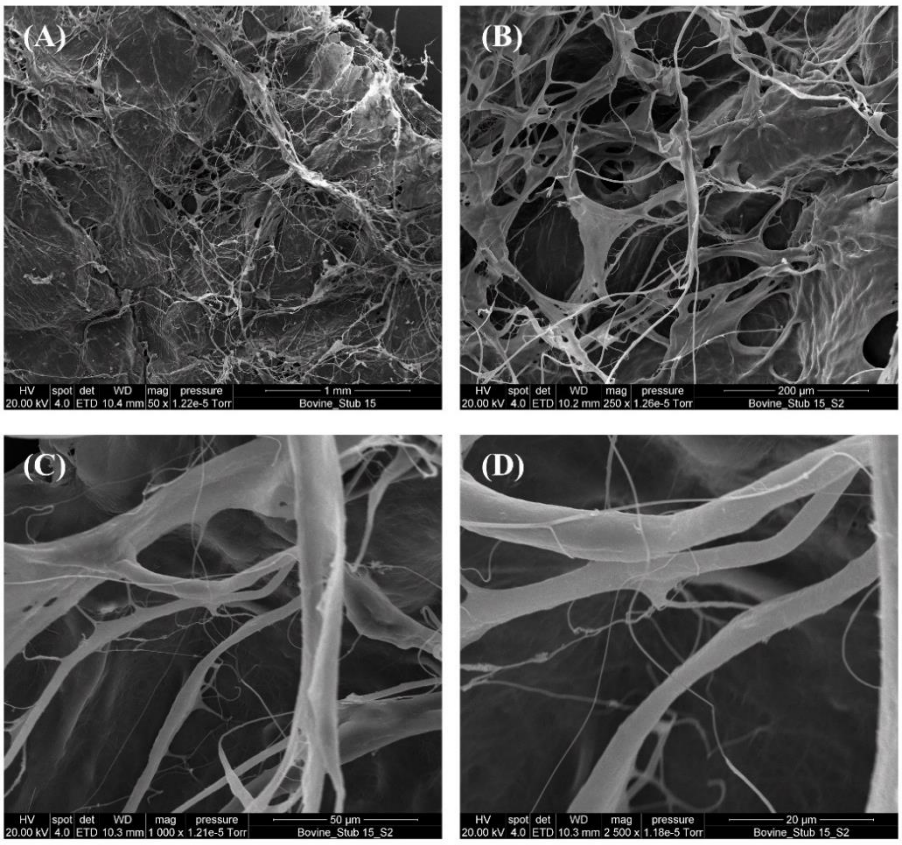

Figure 3.3 SEM images of freeze-dried collagen extracted from bovine tendons. A: (x50); B: (x250); C: (x1,000); D: (x2,500).

3.2.2.2 UV absorption spectroscopy

The UV absorption spectroscopy is a qualitative technique to analyse the purity of extracted collagen with respect to the absence of non-collagenous proteins. Pure type I collagen gives the maximum absorption peak in the 220 to 240 nm range (Nalinanon et al., 2011; Pal et al., 2015; Pal & Suresh 2017). This peak is associated with the -C=O, -COOH, -CONH2 groups in polypeptide chains of collagen molecules (Pal & Suresh 2017; Zeng et al., 2009). If non-collagenous proteins are present as impurities, it provides a small peak in the 250-280 nm range corresponding to tryptophan and tyrosine which are absent in collagen (Pal & Suresh 2017; Sionkowska 2000; Xu et al. 2017; Zeng et al. 2009). The spectra measured for bovine collagen showed a maximum absorption peak around 220 nm corresponding to collagen, without peaks for non-collagenous proteins in the 250-280 nm range (Figure 3.4). This is an indication of the effective removal of all non-collagenous proteins during the pretreatment.

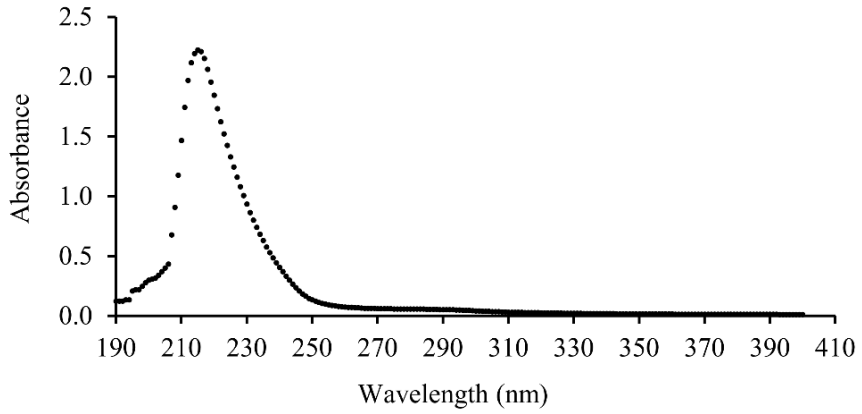

Figure 3.4 Measured UV absorption spectrum of bovine tendon collagen.

3.2.2.3 ATR-FTIR spectroscopy

The ATR-FTIR spectrum of bovine tendon collagen exhibited characteristic peaks of amide A, amide B, amide I, amide II, and amide III, typical of type I collagen (Figure 3.5). The peak analysis and interpretation of this spectrum are given in Table 3.1. These results confirm that extracted collagen from bovine tendons is type I collagen. The ratio of the absorbance of amide III and the peak near 1450 cm^{-1}, which is called the absorption ratio, is a critical parameter used to indicate the intactness of the triple-helical structure, comparing that obtained after collagen preparation to the native structure (Li et al., 2013; Sun et al. 2017; Wang et al. 2008). The absorption ratio calculated for bovine collagen was 0.89(±0.02) (close to 1) which indicates the triple-helical structure was intact and without any structural damage during the pretreatment, extraction or fibrillogenesis process steps.

Overall, these results demonstrate that the commercial process was successfully scaled down to the lab scale and could be used to produce collagen in the native structure with high purity.

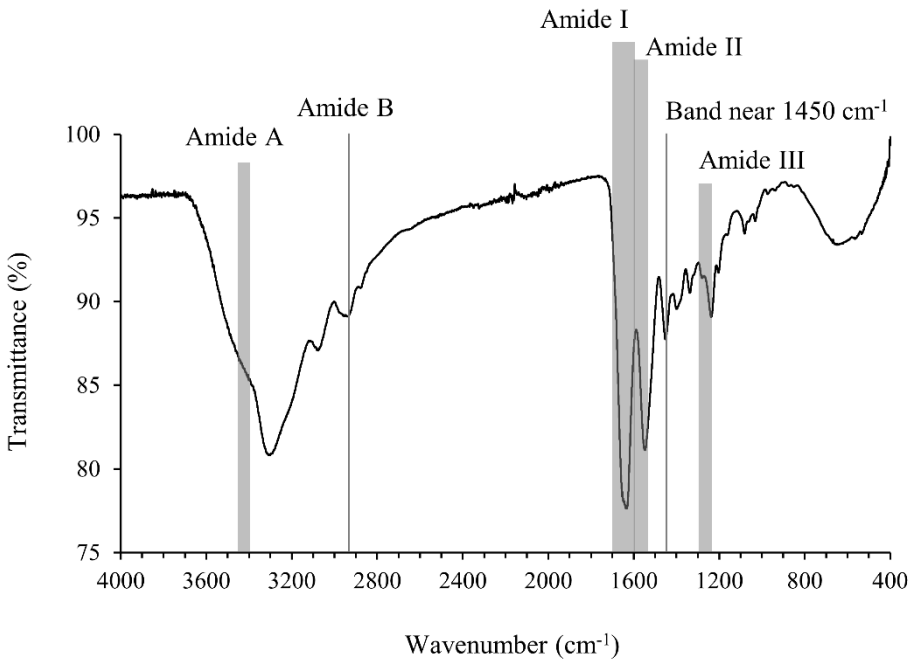

Figure 3.5 ATR-FTIR spectrum of collagen extracted from bovine tendons. The general peak areas relevant to amide A, B, I, II, III and the peak near 1450 cm^{-1} are shown as bands to compare with the peaks obtained for bovine collagen. Graph represents the mean of three replicates.

Table 3.1 FTIR peak locations, assignment and peak analysis for freeze-dried collagen extracted from bovine tendons. The mean (±SD) of three replicates are given.

Region	Reference peak wavenumber (cm^{-1})*	Sample peak wavenumber (cm^{-1})	Assignment	Peak analysis
Amide A	3400-3440	3300(±13)	N-H stretching	Shift to lower frequency due to N-H group involvement in H bonding.
Amide B	2920	2940(±19)	CH_2 asymmetrical stretching	
Amide I	1600-1700	1633(±3)	C=O stretching	Peptide secondary structure (Triple helical structure) is preserved.
Amide II	1550-1600	1546(±4)	N-H bending coupled with C-N stretching	Peptide secondary structure (Triple helical structure) is preserved. Shift to lower frequency due to more H bonds, indicating good activity of collagen and triple helical structure.
Amide III	1230-1300	1236(±2)	N-H bending coupled with C-N stretching	Peptide secondary structure (Triple helical structure) is preserved.

*****Data sources for reference peak wavenumbers and assignment: Li et al., 2013; Wang et al., 2008; Riaz et al., 2018.

3.3 Testing the direct application of the bovine collagen extraction process to fish skin

Almost all the collagen extraction methods used for fish skin available in the literature are laboratory-based protocols. Use of acetic acid to extract collagen is unsuitable when extracted collagen is used for biomedical applications because the presence of acetic acid residues in the end product can cause problems in desired applications. Further, these laboratory-based protocols involve centrifugation and dialysis steps which make the process more complicated and expensive at an industrial level. Therefore, this experiment aimed to see the applicability of the industrial method of collagen extraction from bovine tendons (outlined in §3.2), to fish skin. Knowledge gained by understanding the behaviour of fish skin during collagen extraction by this method will be useful for the development of a modified method suitable for fish skin.

3.3.1 Materials and methods

3.3.1.1 Materials

Skin samples of Tarakihi fish (*Nemadactylus macropterus*) were sourced from a local fish processor and retailer in Palmerston North, New Zealand. Tarakihi (Figure 3.6) belongs to the family Cheilodactylidae. Their average length is 30-40 cm and their average weight is 0.9-2.5 kg (www.seafood.co.nz). Their identification features include a darker collar behind the head. The lower pectoral fin extends approximately half-way the length of the fish (www.fishspecies.nz). They are commonly found on the South Island coasts and the lower part of the north island's east coast (www.fishspecies.nz). Adult fish inhabit over the open bottom at depths of 50-100 m in winter and 100-250 m in the rest of the year (www.seafood.co.nz). The commercial annual catch of this species was 4,034,946 kg in 2022 (fs. fish.govt.nz). Fishing season is from February to June, but they are caught throughout the year. Tarakihi is the New Zealand's second most important commercial catch (www.seafood.co.nz).

Figure 3.6 Tarakihi (*Nemadactylus macropterus*) (source: www.talleys.co.nz).

3.3.1.2 Sample preparation and processing

Scales and residual flesh on the skins were removed manually using a stainless steel knife. The skins were then washed thoroughly with distilled water to remove any extraneous matter. Thereafter, the cleaned skins were packed in polyethylene bags and kept frozen at -20 °C until use. Before the pretreatment step frozen skins were thawed overnight by keeping them in a cold room, and cut into small slices of 10 x 10 mm with a pair of scissors. Water was not used for thawing.

All the procedures of pretreatment by SDS and Na_2SO_4, HCl extraction and NaOH fibrillogenesis steps used for bovine tendons (described in §3.2.1.2-5) were directly adopted for the fish skin samples. The slicing of the skin was not done after pretreatment with SDS as they were already cut into pieces. Characterisation of the freeze-dried collagen samples was done using optical photographs, SEM, UV spectroscopy and ATR-FTIR as discussed in §3.2.1.6. Sample preparation and all the experiments were conducted at normal laboratory temperatures (19-20°C).

3.3.2 Results and discussion

3.3.2.1 Observations made during the collagen extraction process

The SDS pretreatment is used in the bovine collagen extraction method to remove fats from the bovine tendons. By applying the same method on fish skin complete removal of fats was expected. However, fat globules were observed even after the Na_2SO_4 pretreatment step. This result suggests that changes to the pretreatment steps are required to adequately separate fats due to the heterogenous structure of the fish skin and the higher lipid concentrations.

The solution after homogenisation for fish skins was not as thick as obtained for bovine tendons suggesting that solubilisation of the skin samples was not as complete as achieved with the bovine tendons. Modifications to the acidic conditions, the time requirement and or the initial particle size distribution are required to improve this behaviour.

Foam formation was also evident during the homogenisation step and remained during the precipitation step. The foam wasn't observed for the bovine collagen process, suggesting that either fats or non-collagenous proteins not removed in pre-processing steps may be causing and stabilising the foam. A sample of this foam was freeze-dried to see whether collagen was present in the foam.

During precipitation with 0.01 M NaOH, collagen was not precipitated from the homogenised solution. This is a key difference in the process where no fibrillogenesis was evident. This could have been due to reduced quantities of solubilised collagen or lower concentrations of solubilised collagen in the solution which affected aggregation and precipitation. A sample from the solution was freeze-dried to see whether the collagen was present in the acid extract. After freeze-drying, a thin and fragile layer of collagen was formed.

3.3.2.2 Characterisation of extracted fish skin collagen

3.3.2.2.1 Morphology and microstructure

Collagen freeze-dried from the solution appeared as a white, very thin fragile sheet under the naked eye (Figure 3.7). The SEM images were used to analyse the morphology of extracted freeze-dried collagen. SEM images (Figure 3.8), at lower magnifications, showed the pore structure, and at higher magnifications the coil-like fibrils were seen. However, both the porosity and fibrillar-like nature are low compared to that of bovine collagen (see Figure 3.3). The SEM images of collagen obtained by freeze-drying the foam showed a less uniform and highly fragile-like pore structure (Figure 3.9).

Figure 3.7 Optical photograph of the freeze-dried Tarakihi fish skin collagen from the solution phase.

Although collagen was not precipitated from fish skin as obtained from the bovine tendons, SEM images confirmed the presence of collagen extracted into the acid solution. The extractability of collagen into the acid solution and fibrillogenesis thereafter depends on the effectiveness of sample preparation, pretreatment, extraction conditions and fibrillogenesis conditions. Hence, the failure in collagen extraction could be due to any of these factors or a combination of them. Therefore, further experiments are needed to understand these factors in relation to the behaviour of fish skin during collagen extraction. The presence of collagen in the foam which was formed during the homogenisation step confirms the need of avoiding its formation, which would otherwise reduce the process yield.

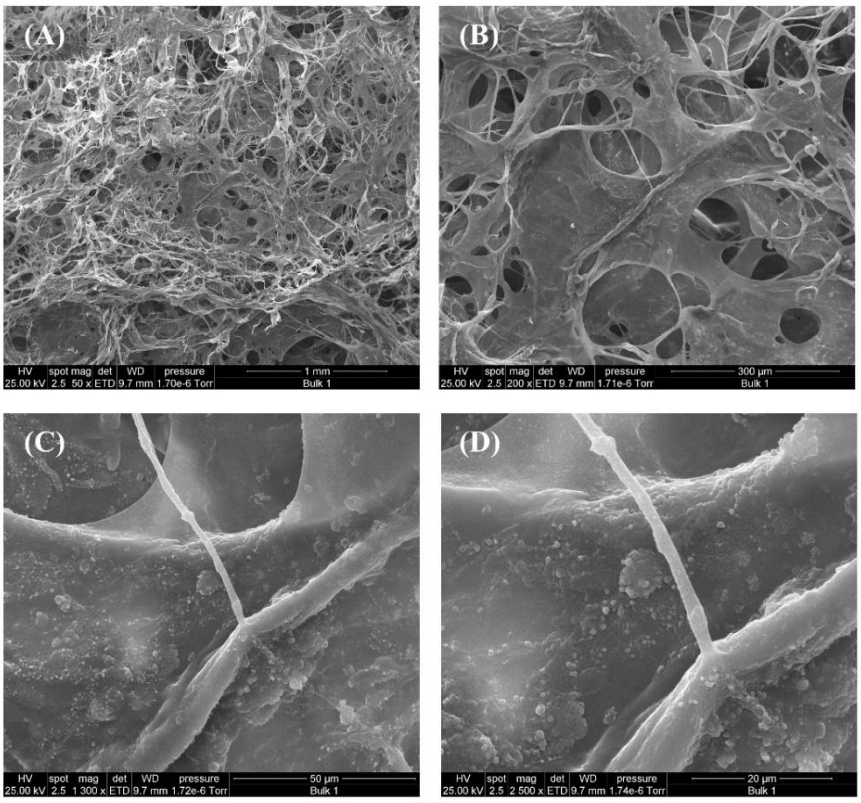

Figure 3.8 SEM images of Tarakihi fish skin collagen: freeze-dried from the solution. A: (x50); B: (x200); C: (x1,300); D: (x2,500)

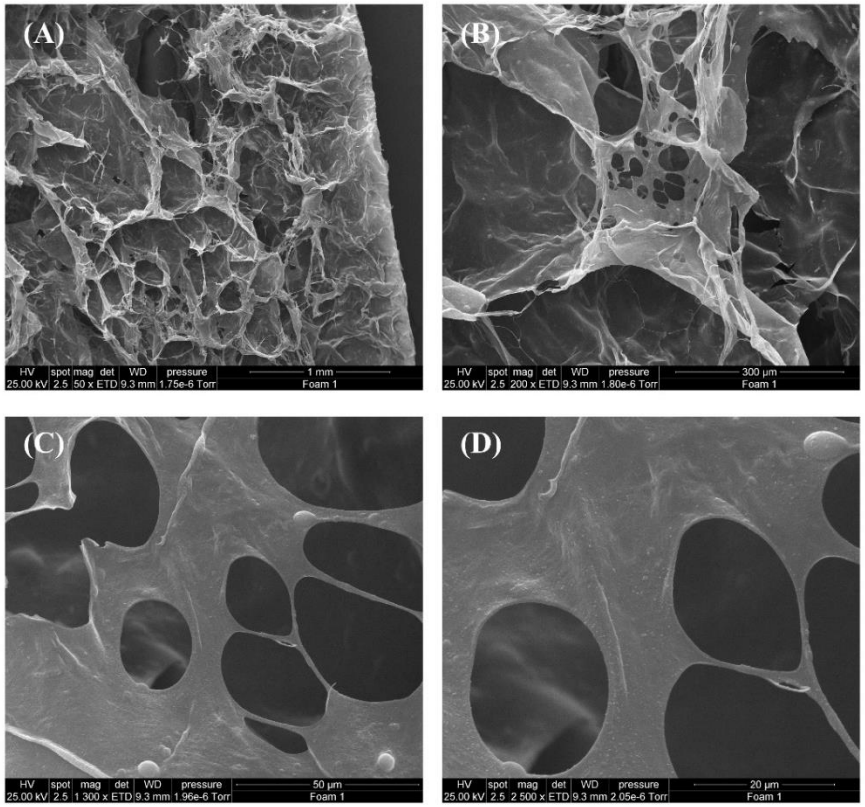

Figure 3.9 SEM images of fish skin collagen: freeze-dried from the foam. A: (x50); B: (x200); C: (x1,300); D: (x2,500)

3.3.2.2.2 UV absorption spectroscopy

The UV absorption spectrum obtained for Tarakihi skin collagen extracted by the commercial bovine collagen extraction method is shown in Figure 3.10. The spectrum reported a maximum absorption peak around 220 nm corresponding to collagen, and a small peak around 280 nm corresponding to the tryptophan and tyrosine amino acids which are generally absent in pure collagen (Pal & Suresh 2017; Sionkowska 2000; Xu et al. 2017; Zeng et al. 2009). This result indicates the inefficiency of the pretreatment method to remove all non-collagenous proteins from fish skin. Therefore, it highlights the need to study the pretreatment process in relation to the behaviour of fish skin.

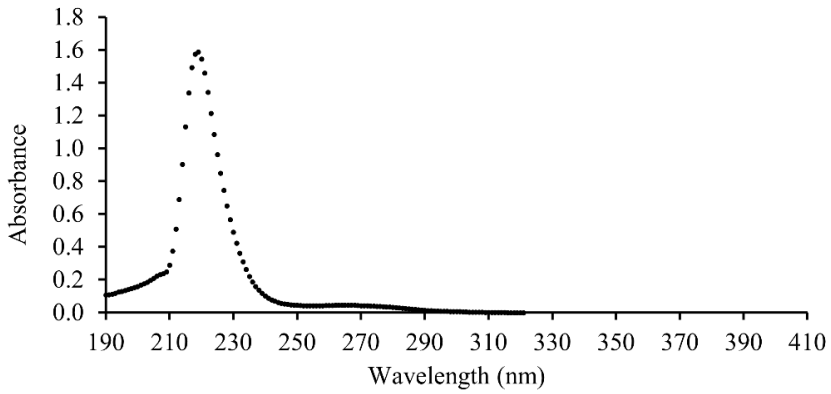

Figure 3.10 UV absorption spectrum of Tarakihi skin collagen extracted by the bovine collagen extraction method.

3.3.2.2.3 ATR-FTIR spectroscopy

The FTIR spectrum of collagen (Figure 3.11) confirmed the presence of type I collagen. The peak analysis and interpretation of this spectrum are given in Table 3.2. There is an indication of not preserving the triple-helical conformation in the collagen as the absorption ratio of 0.78 is not close to 1. This can be an effect of the pretreatment, extraction or fibrillogenesis conditions which need further study. Further, there is a peak present at 1744 cm^{-1} which corresponds to the presence of fats (Talari et al., 2017). This result indicates that the SDS treatment has not been effective in removing fats from the fish skin.

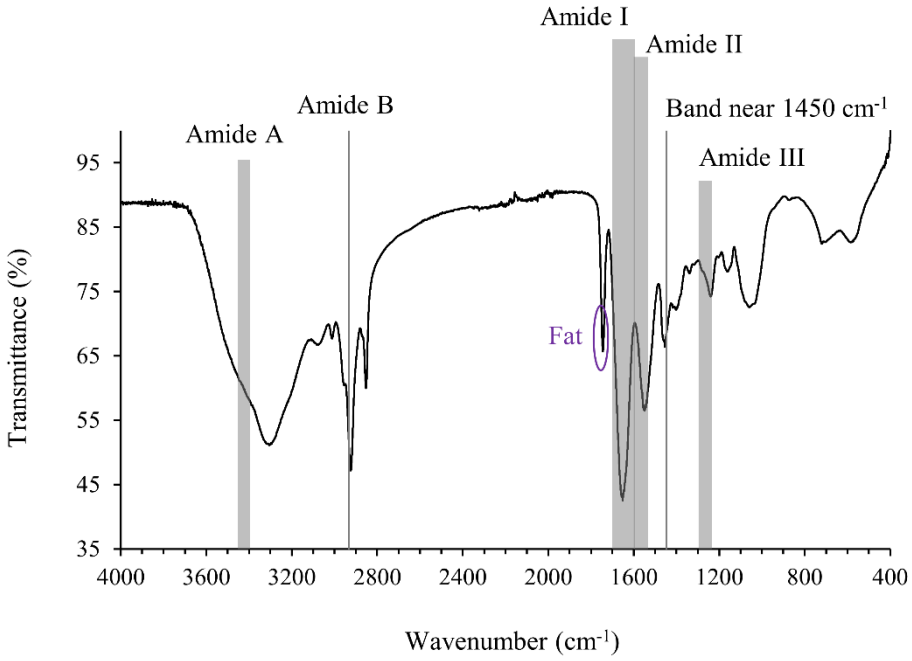

Figure 3.11 ATR-FTIR spectrum of collagen extracted from Tarakihi fish skin using the bovine collagen process. The general peak areas relevant to amide A, B, I, II, III and the peak near 1450 cm^{-1} are shown as bands to compare with the peaks obtained for Tarakihi fish collagen.

Table 3.2 FTIR peak locations, assignment and peak analysis for freeze-dried collagen extracted from Tarakihi fish skin.

Region	Reference peak wavenumber (cm^{-1})*	Sample peak wavenumber (cm^{-1})	Peak analysis
Amide A	3400-3440	3305	Shift to lower frequency due to N-H group involvement in H bonding.
Amide B	2920	2924	
Amide I	1600-1700	1652	Peptide secondary structure (Triple helical structure) is preserved.
Amide II	1550-1600	1549	Peptide secondary structure (Triple helical structure) is preserved. Shift to lower frequency due to more H bonds, indicating good activity of collagen and triple helical structure.
Amide III	1230-1300	1240	Peptide secondary structure (Triple helical structure) is preserved.

*Data sources for reference peak wavenumbers and assignment: Li et al., 2013; Wang et al., 2008; Riaz et al., 2018.

3.4 Conclusions

A lab-scale implementation of a commercial collagen extraction process for bovine tendons was achieved. Using this method extracted collagen with expected properties was produced and UV and FTIR analysis demonstrated the absence of fats and other non-collagenous components and that the native triple-helix structure was preserved.

Direct application of the process to Tarakihi fish skin was not as successful. A key problem was the incomplete pretreatment of the skin samples to remove non-collagen materials. This is likely to have compounded other problems that occurred in later processing steps. Acid hydrolysis to solubilise the skin structure was incomplete and foams were formed during homogenisation. On treating with NaOH, the solution did not exhibit fibrillogenesis and precipitation.

Overall, these results demonstrate the need for further research to overcome these issues.

Chapter 4. Testing potential process modifications to improve fish skin collagen recovery

4.1 Introduction

This chapter aimed to propose modifications to the bovine collagen extraction method and make it suitable to use for fish skin. Three fish species were used: Tarakihi fish (*Nemadactylus macropterus*) and Ling fish (*Genypterus blacodes*) from New Zealand, and Yellowfin tuna (*Thunnus albacares*) from Sri Lanka. The selection of fish species was based on the availability in the seafood industry, and to represent the different proximate compositions and different habitats.

Potential modifications were identified and evaluated by testing hypotheses which had been developed based on the available literature and the results of the preliminary experiments outlined in Chapter 3. Six hypotheses were formulated.

- Hypothesis 1: Swelling of fish skin by NaOH as a pretreatment agent facilitates the removal of non-collagenous materials
- Hypothesis 2: Collagen fibril formation and its size depend on the concentration of the collagen solution
- Hypothesis 3: Rapid increase of pH induces the formation of collagen fibres
- Hypothesis 4: Isoelectric pH of type I collagen from fish is different from mammalian collagen
- Hypothesis 5: Fibril aggregation in fish collagen is time-dependent
- Hypothesis 6: Collagen extractability depends on the temperature of the system which may have to be lower for fish skins than for bovine sources.

The proposed modifications to the reference method (bovine collagen extraction method) and the related hypothesis are shown in the flow chart (Figure 4.1). Modifications done to the industrial method of collagen extraction from bovine tendons when it was used for fish skin are marked by using dark-coloured boxes in the flow diagramme. These modifications are described in more detail in the methodology section. Alterations to some steps were required depending on the fish species as described in the methodology where relevant.

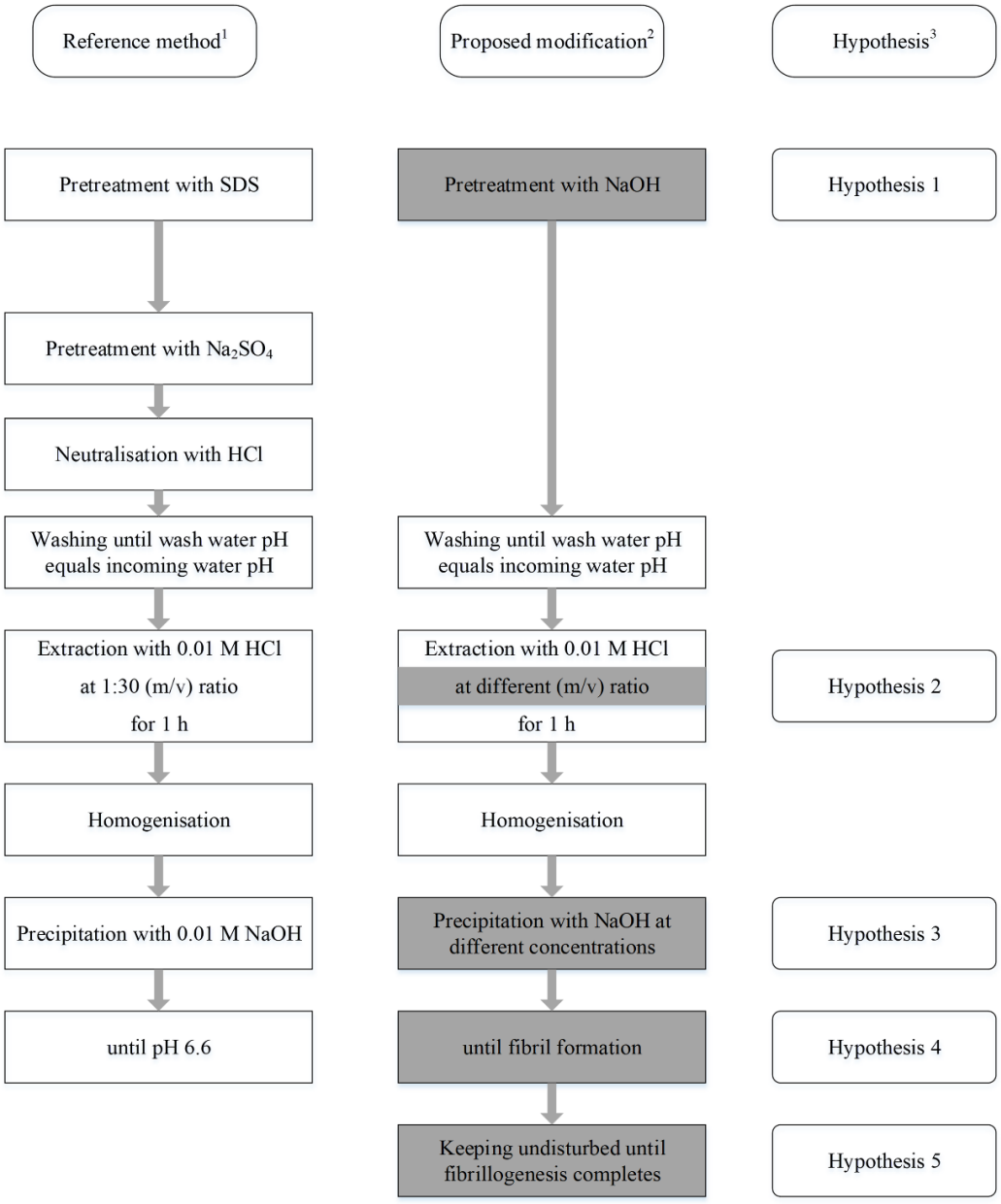

Figure 4.1 Flow diagramme showing the reference method of collagen extraction, proposed modifications and related hypothesis.
[1]Reference method is the industrial method of collagen extraction from bovine tendons carried out in Chapter 3.2;
[2]Proposed modifications to the reference method are highlighted using dark-coloured boxes;
[3]Hypothesis which the proposed modification is based on is shown next to the modification.

Hypothesis 6 was tested by experimenting with different temperatures for the Ling fish skin (4°C and 19°C). Ling skin was preferred for this temperature comparison because it has naturally low contents of fats and pigments, which are desirable to avoid interferences during extraction and fibrillogenesis.

4.2 Materials and methods

4.2.1 Materials

In this study, three fish species were selected, Tarakihi (*Nemadactylus macropterus*) (cold-water, 100-250 m deep), Ling (*Genypterus blacodes*) (cold-water, 300-500 m deep) from New Zealand and Yellowfin tuna (*Thunnus albacares*) (warm-water, pelagic) from Sri Lanka to represent different skin compositions and different habitat temperatures. Experiments on collagen extraction from Tarakihi and Ling were conducted in New Zealand, and Yellowfin tuna trials were carried out in Sri Lanka.

Ling (Figure 4.2) belongs to the family Ophidiidae. Their average length is 80-120 cm and their average weight is 4-10 kg (www.seafood.co.nz). Their identification features include pink colour elongated body with eel-like tail, barbel-like pelvic fins, and jaw extending behind the eye. They are commonly found off the southern south island coast (www.seafood.co.nz). They inhabit depths of 300-500 m (www.seafood.co.nz). The commercial annual catch of this species was 16,919,564 kg in 2022 (fs. fish.govt.nz). Fishing season is from October to November, but they are caught throughout the year. Ling is within the new Zealand's top ten export earners for seafood (www.seafood.co.nz).

Figure 4.2 Ling (*Genypterus blacodes*) (source: www.seafood.co.nz).

Yellowfin tuna (Figure 4.3) belongs to the family Scombridae. Their average length is about 150 cm (www.fishbase.se) and their average weight is 25-90 kg (www.srilankabusiness.com). Their identification features include torpedo-shaped body with dark metallic blue backs, yellow sides, and a silver belly (www.worldwildlife.org). They are highly migratory and found throughout the Pacific, Atlantic and Indian Oceans and found as schools (www.worldwildlife.org) in the temperature range of 15-31°C. They are pelagic-oceanic, and inhabit depths of 1-100 m (www.fishbase.se). The annual catch of this species was 44,760,000 kg in 2019 in Sri Lanka (Dept. of Census & Statistics, 2020). Yellowfin tuna fisheries plays a key role in export earnings of Sri Lanka.

Figure 4.3 Yellowfin tuna (*Thunnus albacares*) (source: fishider.org).

4.2.2 Sample preparation

Fish skins were collected from local fish markets and were transported to the laboratory in a chilled condition. Skins were cleaned by manually removing the scales from the outer surface and residual flesh left on the inner surface of the skin using a stainless steel knife. Skins were washed thoroughly with distilled water to remove any extraneous matter. The cleaned skins were packed in polyethylene bags and stored at -20°C until use. Before the experiments, the skin was thawed by keeping in a cold room, and cut into small slices of 10 x 10 mm in size. Water was not used for thawing. Samples of 50.00 g were taken for the experiments.

4.2.3 Moisture content and crude fat content in raw fish skin

Moisture content in raw fish skins was determined by oven-drying at 105°C (AOAC 930.15). Crude fat contents in raw fish skins were determined by the Soxhlet extraction method (AOAC 960.39) using petroleum ether as the solvent. Fish skins were analysed after first freeze-drying to facilitate fat extraction. Crude fat content was determined gravimetrically after evaporating off the solvent and reported as a percentage of the wet weight of the initial fish skin.

4.2.4 Pretreatment with Sodium hydroxide

The pretreatment process that was used in the experiments outlined in §3.2/3.3 was unable to effectively remove the non-collagenous material. It is understood from the previous literature (Arumugam et al., 2018) that Sodium hydroxide pretreatment swells the skin to facilitate the leaching out of non-collagenous material from the skin. Therefore, a Sodium hydroxide pretreatment was used in this experiment.

A sample of 50 g of fish skin was soaked in 0.3 M NaOH solution with continuous stirring at 1:10 (m/v) ratio for 4 h, changing the solution every 1 h. This modification was done to test the hypothesis 1. After a 4 h period, skin pieces were repeatedly washed with distilled water until the pH of the resulting wash water become equal to the incoming water.

4.2.5 Extraction with hydrochloric acid

Most fish collagen extraction methods available in the published literature have used acetic acid. However, due to the negative impacts associated with residues of acetic acid in producing collagen for biomedical applications, acetic acid was replaced by dilute hydrochloric acid. The concentration of 0.01 M ensures the pH remains above 2 to avoid the hydrolysis of collagen molecules, to retain the native triple-helix structure. The commercial bovine collagen extraction method (reference method) also used 0.01 M hydrochloric acid as the extraction medium. However, the 1:30 (m/v) ratio produced a very dilute collagen extract (§3.3), therefore that ratio was replaced by 1:10 (m/v). This was done to test the hypothesis 2.

Pretreated fish skin samples were soaked in 0.01 M HCl with a 1:10 (m/v) ratio for 1 h with continuous stirring. By this time, the skin pieces were expected to be swollen. The behaviour of Yellowfin tuna skin during the acid extraction step was different from the other two species. It formed a viscous solution by the end of 1 h with remaining skin pieces in it, indicating the insufficient volume of HCl solution to solubilise all the collagen from swollen skin. Therefore, a viscous solution containing swollen skin pieces was obtained at the end, however only the viscous solution without the skin pieces was taken for the next steps of the process.

4.2.6 Homogenisation of the acid extract

The homogenisation was used to achieve the most consistent solubility of collagen and produce an even particle size distribution of collagen fibres in the acid extract. For Tarakihi fish and Ling fish skin, after acid dispersion for 1 h, the suspension was homogenised as described in §3.2.1.4. For Tarakihi fish, a discolouration of the homogenised solution was observed due to the presence of pigments. Therefore, it was vacuum filtered using a Miracloth to separate dark colour pigment residues. The filtration step after homogenisation was not required for Ling fish skin as the discolouration of the extract was not present due to low pigment content and light colour of pigments compared to Tarakihi fish. Foam formation occurred during homogenisation in Tarakihi and Ling skins, but it was much less than in the preliminary fish skin trial that was described in §3.3. A homogenisation step was not required for Yellowfin tuna as it provided a viscous solution by the end of the extraction time. A small amount of pigments was present in the extract, but filtration was not possible due to the high viscosity of the solution.

4.2.7 Collagen fibrillogenesis

Fibrillogenesis was achieved by adding Sodium hydroxide to increase the pH to the isoelectric point, whereupon the collagen precipitates to its native fibrillar form, retaining its former structural properties. The concentration of NaOH was changed to suit each fish species, as explained later.

Precipitated collagen was separated from the solution manually using a stainless steel strainer, packed in polythene bags and frozen at -20°C. Frozen collagen was then freeze-dried at 0.5 mbar, 10°C for three days (BUCHI LyovaporTM L-300, BUCHI Labortechnik AG; Flawil, Switzerland) to obtain the final product of freeze-dried collagen.

4.2.8 Characterisation of collagen

All fish collagens were characterised by yield, scanning electron microscopy (SEM), UV absorption spectroscopy, attenuated total reflectance-fourier transform infrared (ATR-FTIR) spectroscopy, differential scanning calorimetry (DSC) and Circular Dichroism (CD) spectroscopy. They were then compared to the bovine tendon collagen extracted by the commercial method in §3.2.

The SEM images of freeze-dried collagens, UV absorption and ATR-FTIR spectra were obtained according to the methods described in §3.2.

4.2.8.1 Differential Scanning Calorimetry (DSC)

Small pieces of freeze-dried collagen between 3-4 mg were cut and accurately weighed. They were hydrated in a beaker by adding excess cold deionised distilled water. The samples were held underwater for 2-3 min with a clean spatula to speed up the hydration. The hydrated collagen was removed from the water and stuck to the side of the beaker where they were quickly blotted with filter paper to remove excess water until it no longer dripped. The hydrated samples were placed into aluminium pans and accurately weighed and hermetically sealed. Differential scanning calorimetry (DSC) was performed using a TA Systems Q2000 DSC (TA Instruments, Inc., New Castle, DE, USA). Temperature and enthalpy calibration was done using water and indium as standards. The samples were scanned in a nitrogen atmosphere from an initial temperature of 5°C held isothermally at this temperature for 1 min.

Two identical ramp profiles were subsequentially carried out consisting of a ramp up at 5°C/min to 85°C, then ramp down at 20°C/min to 5°C, then held isothermal at this temperature for 1 min, after which the cycle was repeated. Iced water was used as the cooling medium (TA systems refrigerated cooling system 40), and an empty sealed pan was used as the reference. The denaturation temperature was determined from the maximum transition point (the endothermic peak) of the thermal denaturation curve. The total denaturation enthalpy was estimated by measuring the peak area in the DSC thermogram based on the dry weight of the sample and expressing this as J/g sample. The onset temperature was also determined.

4.2.8.2 CD spectroscopy

CD spectroscopy was used to assess the native triple-helical conformation of collagen. The freeze-dried collagen samples were dissolved in 0.05 M acetic acid to a concentration of 0.1 mg/mL. Solutions were filtered through a 0.2 µm Millipore filter to remove any undissolved material and dust particles. Then the mixtures were equilibrated at 4°C for 48 h before testing. The same concentration of all the samples was verified by measuring the absorption at 192 nm using a UV-visible spectrophotometer (Genesys 10S spectrophotometer, GENESYS 10S UV-VIS, Thermo Fisher Scientific; Madison, Wisconsin, USA) (Bürck et al., 2013). The degree of ellipticity was recorded with a spectropolarimeter (Chirascan, Applied Photophysics, Leatherhead, UK) using a standard quartz cuvette of 1 mm pathlength (Hellma high-precision cells, Mullheim, Germany). Samples were scanned over a wavelength range from 260 to 180 nm at 0.5 nm intervals. Each sample was scanned five times at a scan rate of 40 nm/min, 0.5 s response time and 1 nm bandwidth. Acetic acid of 0.05 M concentration was used to record the baseline. The same cuvette was used for the baseline and samples. The temperature of the cell holder was maintained at 10°C using a temperature control unit (Quantum Northwest). The dynode voltage of all samples was checked to ensure they were below 600 V (Drzewiecki et al., 2016). Ellipticity measurements for replicates were averaged and the spectrum of 0.05 M acetic acid solution was subtracted from each sample spectrum. The degree of ellipticity values were converted to mean residue ellipticity (deg cm^2 $dmol^{-1}$) (Holmes et al. 2017) and were graphically presented as a function of wavelength.

$$[\theta] = \frac{\theta(MRW)}{10cd}$$

where $[\theta]$ is the mean residue ellipticity, θ is the degree of ellipticity (degrees), MRW is the average residue molecular weight, c is the concentration of the sample (mg/mL), d is the optical pathlength (cm). MRW was taken as 100 assuming the molecular weight of one collagen molecule is about 300,000 and the number of residues per molecule is 3000 (Akita et al., 2020).

The 'positive to negative peak ratio' (R_{pn}) was calculated (Perez-Puyana et al., 2019).

$$R_{pn} = \frac{\theta_p}{\theta_n}$$

where θ_p and θ_n are the molar ellipticity values of positive and negative peaks, respectively.

4.2.8.3 Yield of collagen

The dry matter content of the raw fish skin after initial cleaning and cutting was estimated using oven drying at 105°C for 24 h. The dry weight of the 50.00 g of sample taken for the collagen extraction was estimated accordingly. For collagen, the reference freeze-dried weight was taken as the dry weight. The yield was calculated as dry collagen (g) per dry weight of raw fish skin (g).

$$\text{Yield} = \left(\frac{M_{Freeze-dried\ collagen}}{M_{Dry\ matter\ in\ pretreated\ skin}} \right) \times 100\%$$

where M is the mass of the sample.

4.3 Results and discussion

4.3.1 Morphology and microstructure of collagen

All freeze-dried collagen samples appeared as white soft sponges to the naked eye, except for some discolouration due to the presence of skin pigments in Tarakihi and Yellowfin tuna samples. SEM images (Figure 4.4) show a pore structure that was produced as a result of the sublimation of water during freeze-drying. The freeze-drying conditions were kept constant for all samples, which means differences in pore structure are likely to reflect differences in the fibril structure of the collagen networks. For the bovine reference sample, pores could be seen with the naked eye. These are also clearly seen in the SEM images (Figure 4.4A), where the porous structure contains sheets of collagen interconnected by coil-like fibrils. The sheet-like layering with the porous structure is more clear at the lower magnification and the fibril structure is more clear at the higher magnification. This morphology is an important characteristic required for biomedical applications (Arumugam et al., 2018).

Similarly, the fish collagens appeared porous to the naked eye. The SEM images show some significant differences from the bovine reference sample. Fish collagens appeared less fibrillar, but more sheet-like than bovine collagen (Figures 4.4B-E). Nevertheless, all fish collagens exhibited an interconnected pore structure. The extent to which the porous characteristics are important will depend on the application.

4.3.2 UV absorption spectra

The UV absorption spectroscopy is a qualitative technique to analyse the purity of extracted collagen with respect to the absence of non-collagenous proteins. Pure type I collagen gives the maximum absorption peak in the 220-240 nm range (Nalinanon et al., 2011; Pal et al., 2015; Pal & Suresh 2017). This peak is associated with the -C=O, -COOH, -$CONH_2$ groups in polypeptide chains of collagen molecules (Pal & Suresh 2017; Zeng et al. 2009). If non-collagenous proteins are present as impurities it provides a small peak in the 250-280 nm range corresponding to tryptophan and tyrosine which are absent in collagen (Pal & Suresh 2017; Xu et al., 2017; Zeng et al., 2009; Sionkowska, 2000). In this study, all collagens samples showed maximum absorption peaks around 220 nm, corresponding to collagen without peaks for non-collagenous proteins (Figure 4.5). This is an indication of the effective removal of all non-collagenous proteins by the Sodium hydroxide pretreatment.

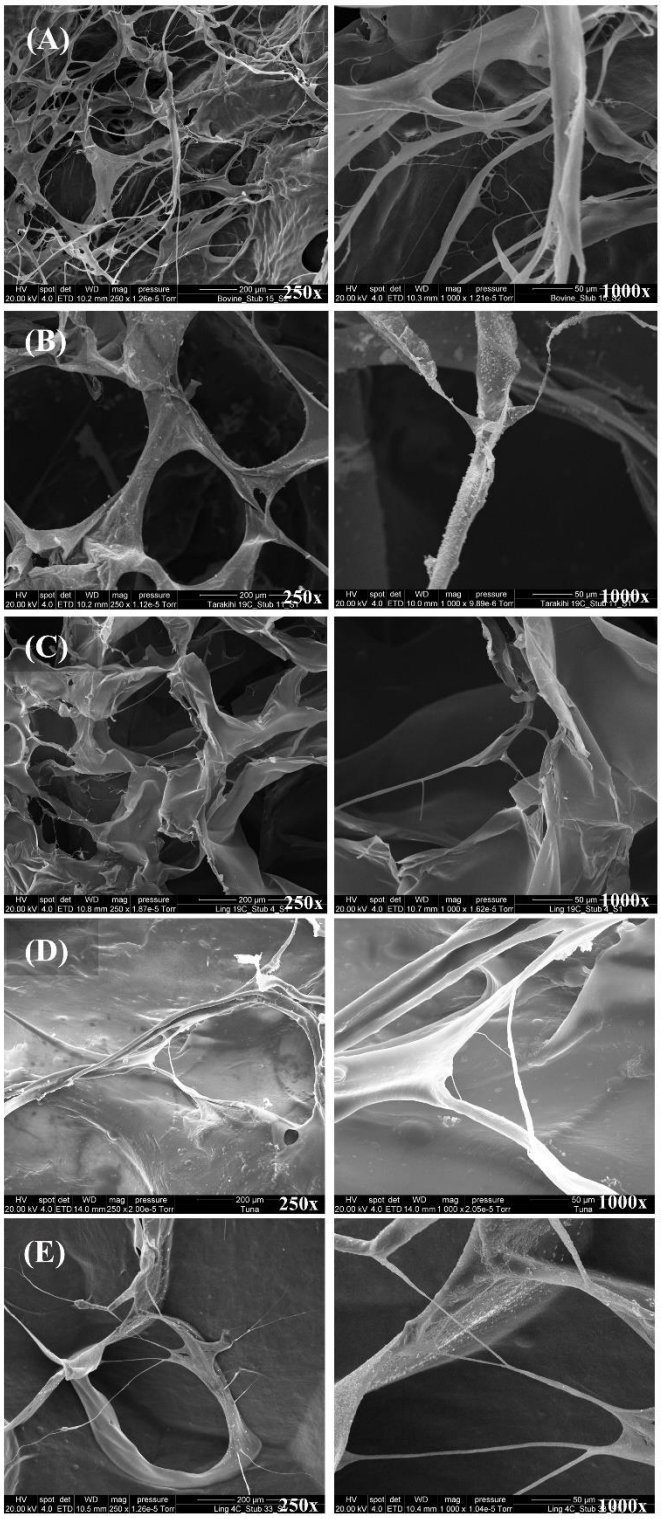

Figure 4.4 SEM images of extracted freeze-dried fish collagen and commercial bovine collagen.
A: Bovine collagen
B: Tarakihi fish skin collagen extracted by modified method at 19°C
C: Ling fish skin collagen extracted by modified method at 19°C
D: Yellowfin tuna fish skin collagen extracted by modified method at 19°C
E: Ling fish skin collagen extracted by modified method at 4°C

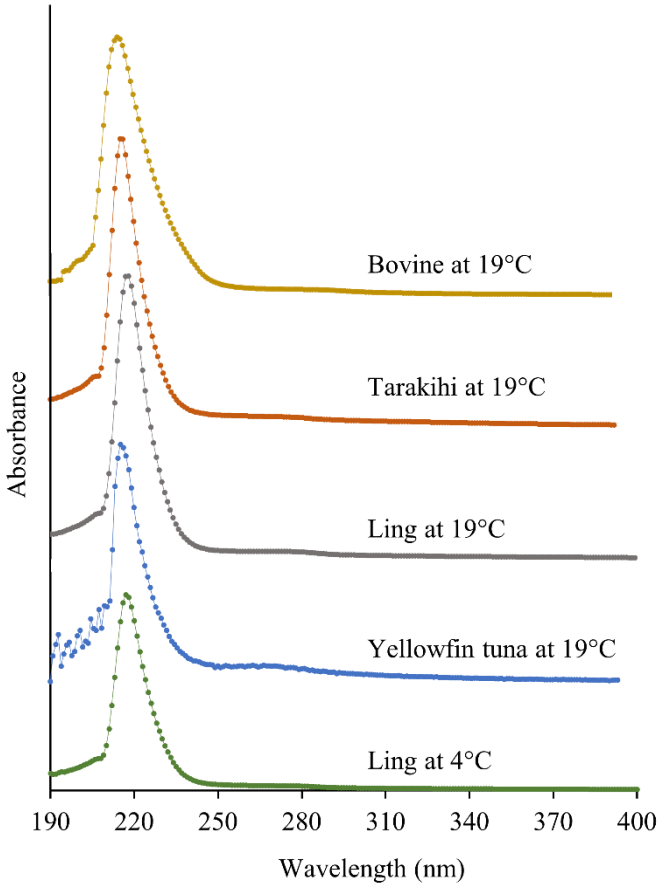

Figure 4.5 UV absorption spectra of collagens extracted from bovine tendons by the commercial method described in §3.2 and collagen extracted by three fishes using the modified method.

4.3.3 ATR-FTIR spectroscopy

The FTIR spectra and peak locations are shown in Figure 4.6 and Table 4.1. Examination of these peaks can identify sensitive changes in the secondary structure of protein (Harnkarnsujarit et al., 2015; Jeong et al., 2013; Wang et al., 2008). Peaks were present in all samples for amide A, B, I, II, and III, which are all typical of type I collagen (Riaz et al., 2018). However, the peak locations differed slightly from each other, indicating some differences in the protein secondary structure (Wang et al., 2008).

The amide A peak is associated with N-H stretching vibrations which occur generally in the 3440-3400 cm^{-1} range (Li et al., 2013; Jeong et al., 2013; Wang et al., 2008). The peak position shifts to a lower wavenumber when N-H groups of a peptide chain form hydrogen bonds (Jeong et al., 2013). This shift is seen in the results for the amide A peak, where bovine, Tarakihi and Yellowfin tuna skin prepared at 19°C, and Ling skin prepared at 4°C, have their peak at around 3300 cm^{-1}, whereas the peak for Ling prepared at 19°C occurred at 3284 cm^{-1}. These decreasing wavenumbers indicate that more hydrogen bonds are present. The amide B peaks are due to the asymmetrical stretching of CH_2 bonds (Chen et al., 2016), which occurred around 2924-2940 cm^{-1} for all collagens without any discernible differences.

The peak position of Amide I is the most useful measure of the secondary structure of proteins (Sai-Ut et al., 2012). The amide I band generally occurs in the 1600-1700 cm^{-1} range due to C=O stretching vibrations in the polypeptide backbone (Liu et al., 2012). Shifting of the peak to lower wavenumbers indicates more hydrogen bonding of C=O bonds with adjacent

α-chains (Li et al., 2013). All fish collagens recorded peaks at approximately similar wavenumbers in the middle region suggesting similar hydrogen bonding.

The amide II band generally occurs in the 1550-1600 cm^{-1} range due to N-H bending coupled with C-N stretching vibrations (Jeong et al., 2013). The peak position will shift to lower wavenumbers when hydrogen bonding between the N-H bond and adjacent α-chains occurs (Li et al., 2013). Here also, all collagens recorded peaks at lower wavenumbers near 1550 cm^{-1} indicating more hydrogen bonds.

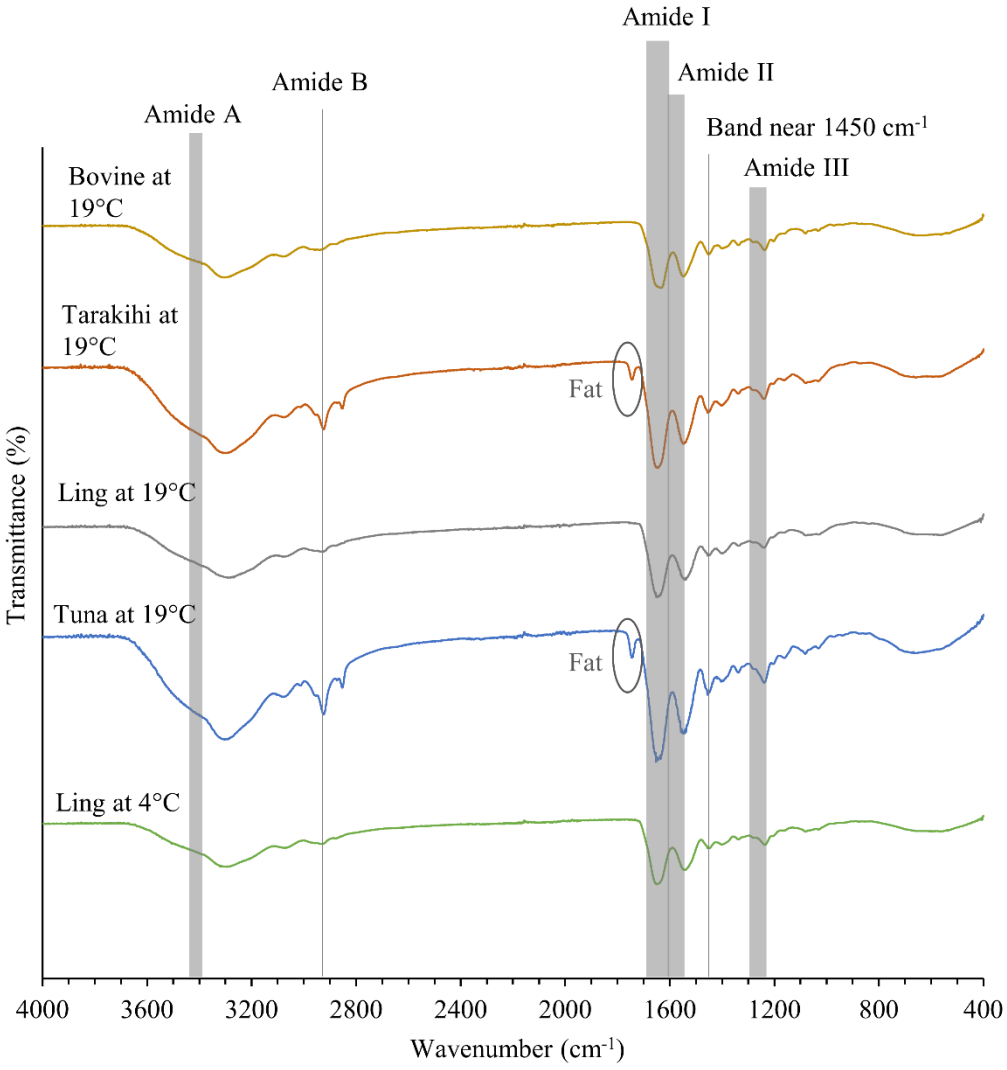

Figure 4.6 ATR-FTIR spectra of bovine collagen and fish collagens. General range of peak positions of amide A, B, I, II and III are shown vertical bars. Average of three values were used to draw the graphs. Sources for the general range of wavenumbers are from Jeong et al. 2013; Wang et al. 2008; Li et al. 2013.

There is another implication for the shift in peaks at the wavenumbers corresponding to amide I and II, which is that of crosslinking, where higher wavenumbers indicate a higher degree of intermolecular cross-links and molecular order (Li et al., 2013). This means the measured peak locations are subject to two opposing influences. Here, the net result is that hydrogen bonding dominates and so has shifted the peaks to smaller wavenumbers. The

consequence of more hydrogen bonding is that peptide chains are less likely to unwind (Li et al., 2013), and so preserve the secondary structure of proteins.

The amide III band occurs in the 1230-1300 cm^{-1} range due to N-H bending coupled with C-N stretching, and wagging vibrations from CH_2 groups on the glycine backbone and proline side-chains (Jeong et al., 2013; Li et al., 2013;). Additionally, a strong CH_2 bending occurs near 1450 cm^{-1} (Sun et al., 2017). The ratio of the absorbance of these two wavenumbers, which is called the absorption ratio, is a critical parameter used to indicate the intactness of the triple-helical structure, comparing that obtained after collagen preparation to the native structure (Li et al., 2013; Sun et al., 2017; Wang et al., 2008). The absorption ratios recorded by Tarakihi and Ling skin collagens at 19°C were lower which indicates some damage to the collagen structure. In contrast, the bovine prepared at 19°C and Ling collagen prepared at 4°C, recorded absorption ratios of 0.89 which indicates better preservation of the triple-helical structure. Yellowfin tuna collagen prepared at 19°C recorded an absorption ratio of 0.83. These differences are likely influenced by the processing temperature, which are well below the habitat temperature for Yellowfin tuna and cows, but processing Ling and Tarakihi at 19°C is much warmer than the habitat temperature for these species and hence samples prepared from these cold-water fish are more damaged.

Table 4.1 ATR-FTIR peak locations of bovine collagen and fish collagens. The mean (±SD) of three replicates are given.

Region	General range of wavenumber (cm^{-1})*	Processing temperature				
		at 19°C	at 19°C	at 19°C	at 19°C	at 4°C
		Bovine collagen	Tarakihi skin collagen	Ling skin collagen	Yellowfin tuna skin collagen	Ling skin collagen
Amide A	3400-3440	3300(±13)	3300(±7)	3284(±5)	3302(±1)	3295(±10)
Amide B	near 2920	2940(±19)	2925(±1)	2928(±9)	2924(±2)	2932(±8)
Amide I	1600-1700	1633(±3)	1650(±2)	1645(±0)	1647(±4)	1647(±5)
Amide II	1550-1600	1546(±4)	1547(±3)	1538(±0)	1549(±0)	1543(±6)
Amide III	1230-1300	1236(±2)	1239(±1)	1240(±1)	1239(±1)	1236(±2)
Absorption ratio		0.89(±0.02)	0.77(±0.00)	0.80(±0.03)	0.83(±0.02)	0.89(±0.01)

*Sources for the general range of wavenumbers: Jeong et al. 2013; Wang et al. 2008; Li et al. 2013

In addition, Tarakihi and Yellowfin tuna skin collagens had peaks near 1744 cm^{-1}, which is attributable to carbonyl compounds (Talari et al., 2017), which are present in fats. This result suggests the need for further pretreatment of Tarakihi and Yellowfin tuna skins to remove fats. Ling, which has a lower raw skin fat content, does not have a peak near 1744 cm^{-1} indicating the higher effectiveness of the Sodium hydroxide pretreatment.

4.3.4 Differential Scanning Calorimetry (DSC)

DSC is widely used to study the thermal behaviour of proteins. The triple-helix structure of collagens is stabilised by the restrictions imposed by the pyrrolidine rings of the imino acids (hydroxyproline and proline), and intramolecular hydrogen bonding by the hydroxyl group of hydroxyproline (Liao et al., 2018; Pal & Suresh, 2016). When hydrated collagen is heated, the denaturation starts with the breaking of these bonds, and with further heating, the three polypeptide chains of the triple-helix disintegrate into random coils. This temperature is called the denaturation temperature (Chen et al., 2021; Liu et al., 2016). The denaturation temperature is used as a measure to interpret the secondary structure conformation of collagen. The denaturation temperature (T_d), onset temperature and denaturation enthalpy (ΔH) of collagen samples are given in Figure 4.7. The denaturation temperature and the onset temperature are higher in bovine collagen than in fish collagens. The difference in these thermal properties between bovine and fish collagens can be attributed to the higher content of imino acids (proline and hydroxyproline) present in bovine collagen, which provides stability to the triple-helical collagen structure (Kittiphattanabawon et al., 2005; Liu et al. 2014).

The collagen extracted from Tarakihi skin and Ling skin at 19°C has not shown peaks indicating the sample was already denatured before testing. The denaturation temperature of fish collagen depends on the imino acid content (Chen et al., 2021; Nalinanon et al., 2011; Pal & Suresh, 2016; Xu et al., 2017), habitat temperature of the fish (Chen et al., 2021; Xu et al., 2017) and degree of cross-linking (Gauza-Włodarczyk et al., 2017). Yellowfin tuna is a warm-water fish with its collagen extracted at 19°C, and Ling is a cold-water fish with its collagen extracted at 4°C in these experiments. Generally, warm-water fishes have higher imino acid contents, hence their collagen can be expected to have higher denaturation temperature values (Kittiphattanabawon et al., 2005). However, this study gave unexpected results, where similar denaturation temperatures at around 43°C were obtained for collagen both from Yellowfin tuna and Ling. This is a high denaturation temperature value, which was not expected for two reasons; first, this is the first study reporting denaturation temperatures above 40°C for collagen from both warm and cold-water species; and second, the denaturation temperature was not expected to be the same for fish from these two distinctly different habitats. It is possible that the higher denaturation temperature obtained in this study may be due to the modified method used here, which used isoelectric precipitation during fibrillogenesis rather than salting out as used by other researchers (Li et al., 2013; Muralidharan et al., 2013; Woo et al., 2008), possibly causing more extensive cross-linking. Other researchers have found that cross-linking affects denaturation temperature. Singh et al. (2011) have also reported that higher denaturation temperatures around 39°C in collagen from striped catfish can be due to higher cross-linking. Pal & Suresh (2017) have reported that the low denaturation temperature in fish collagen can be improved to 40°C after fibril formation. The higher degree of cross-

linking provides stability to the collagen structure by binding the collagen molecules tightly together, thus reducing the space required for hydration which prevents hydrogen and electrostatic bond formation between molecules.

It is also known that denaturation temperature depends on the hydration level, where less hydration causes higher denaturation temperature (Miles et al., 2005; Zeugolis & Raghunath, 2010;). However, in this study, special attention was paid to fully hydrating the collagen samples to avoid this effect. Thus, the reason the denaturation temperature is high in this study can be attributed to the higher degree of cross-linking during fibrillogenesis.

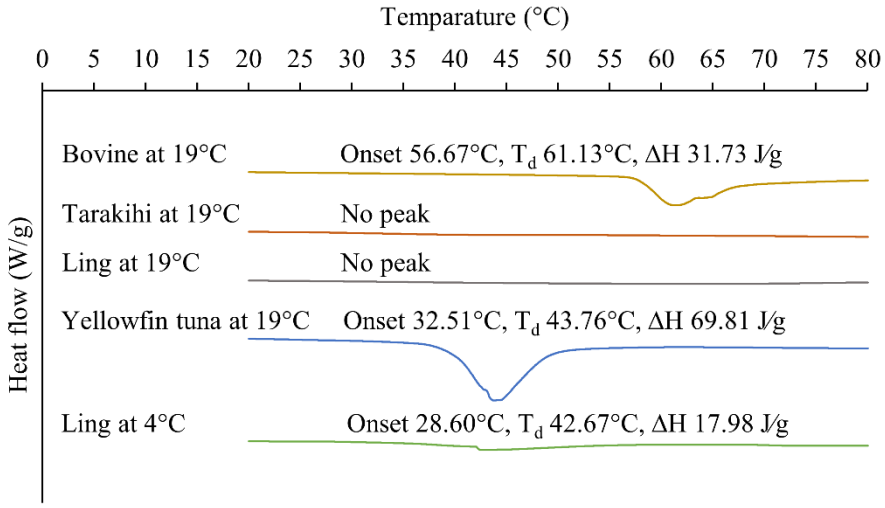

Figure 4.7 Differential scanning calorimetry thermogram of fish collagens and commercial bovine collagen.

Although the denaturation temperature was similar for these two collagens, Ling skin collagen extracted at 4°C has a comparatively lower enthalpy of denaturation (17.98 J/g) than that of tuna skin collagen extracted at 19°C (69.81 J/g). Kittiphattanabawon et al. (2005) have reported an indirect relationship between the enthalpy of denaturation and the denaturation temperature. Other workers have found that the enthalpy of denaturation depends on the content of Gly-Pro-Hyp sequence in the polypeptide chains, where a high content of this sequence is associated with a high enthalpy of denaturation (Ahmed et al., 2019; Bae et al., 2008). This is because hydrogen bonds between polypeptide chains of the collagen molecules with this Gly-Pro-Hyp sequence are more stable than with other sequences (Ahmed et al., 2019; Bae et al., 2008). So, while the reason tuna skin collagen has a higher enthalpy of denaturation is not known, it could be related to having a higher content of Gly-Pro-Hyp sequences, something which needs further investigation.

Another factor is the onset temperature of denaturation, obtained from the DSC curves. Here, the onset temperature of Ling skin collagen was 28.60°C, which is less than that of tuna skin collagen at 32.51°C. Given that both the enthalpy of denaturation and onset temperature are lower for Ling than tuna, this implies that Ling skin collagen has lower thermal stability. This means in processing, Ling skin collagen denaturation occurs at a lower temperature and requires less heat.

4.3.5 Circular dichroism (CD) spectra

Circular dichroism measures the differential absorption of left and right-handed polarised light by peptide bond chromophores in a protein to assess the secondary structure (Drzewiecki et al., 2016; Qi et al., 2015; Zhou et al., 2018;). The far UV range, generally from 250 to 190 nm is used for this quantitative estimation (Rodger & Marshall, 2021). The native secondary structure of the triple-helical structure of collagen in a solution is characterised by the presence of a negative peak at around 198 nm related to the content of the α-helix structure, a cross-over at 214 nm and a weak positive peak at around 220 nm due to the π-π* transition of peptide bonds (Liu et al., 2016; Zhou et al., 2018). The CD directly detects the triple-helical structure by the presence of the positive peak as it disappears upon denaturation (Drzewiecki et al., 2016). The degree of denaturation or the triple-helical content is estimated from the 'positive/negative ratio' (R_{pn}) from the CD spectra (Akita et al., 2020; Perez-Puyana et al., 2019;). Due to the easy identification of the native or denatured form of the protein, circular dichroism is considered the gold standard for estimating the secondary structure of proteins among other techniques such as FTIR or DSC (Gopinath et al., 2017).

The CD spectra obtained for fish collagens and commercial bovine collagen are shown in Figure 4.8. Collagen from Yellowfin tuna extracted at 19°C and Ling fish extracted at 4°C produced characteristic CD spectra with a negative peak at ~198 nm, a cross-over point at ~214 nm and a positive peak at ~220 nm. The positive peak almost disappeared for collagen from Tarakihi at 19°C and Ling at 19°C indicating a random conformation of the polypeptide chains (Zhou et al., 2018). The CD spectrum produced by bovine collagen also shows the characteristic pattern, but the peak positions are shifted relative to fish collagen, with a negative peak at ~200 nm, a cross-over point at ~218 nm and a positive peak at ~222 nm. These peak positions also lie within the acceptable range for the helical structure. The R_{pn} ratios, which is an indication of the integrity of the triple-helix structure, are shown in Table 4.2. The poorest results were obtained for collagens extracted from Tarakihi and Ling at 19°C, where it is evident that the triple-helical structure was not maintained as they both had a R_{pn} ratios of -0.03. The best results were obtained for Ling at 4°C which recorded the lowest R_{pn} ratio (-0.13) followed by Yellowfin tuna at 19°C (-0.11). Therefore, these processing temperatures and conditions were suitable for preserving the triple-helical structure. For comparison, the R_{pn} of bovine collagen was -0.08. Researchers have shown a higher R_{pn} ratio implies higher denaturation (Perez-Puyana et al., 2019). Native collagen has been reported at -0.10, -0.1075, and -0.123, by the following authors respectively (Gopinath et al., 2017; Nishad Fathima et al., 2009; Sun et al., 2020), with Gopinath et al. reporting a value of 0.05 for 100% denatured collagen. These results fall within these ranges.

Table 4.2 R_{pn} values of the extracted fish collagens and commercial bovine collagen.

	Bovine	**Tarakihi at 19°C**	**Ling at 19°C**	**Yellowfin tuna at 19°C**	**Ling at 4°C**
R_{pn} ratio from CD	-0.08	-0.03	-0.03	-0.11	-0.13

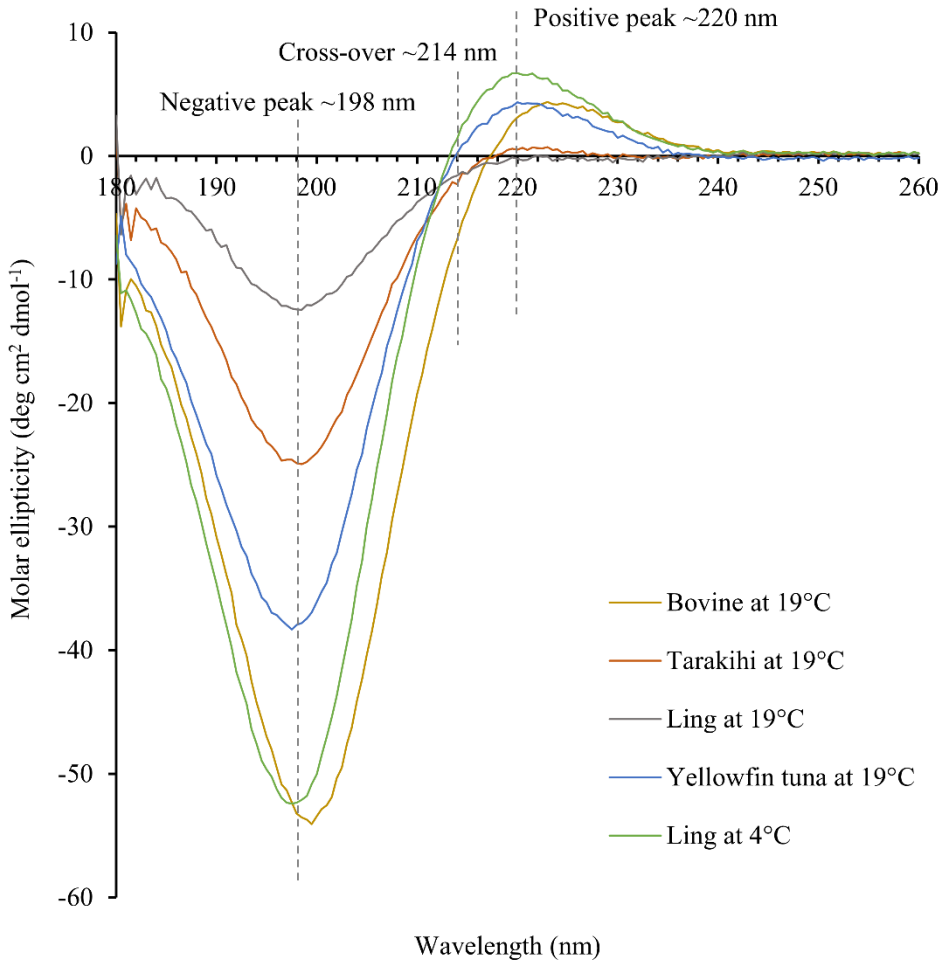

Figure 4.8 Circular dichroism spectra of fish collagens and commercial bovine collagen.

4.3.6 Yield

The yields of collagen are shown in Table 4.3.

Table 4.3 Yield of collagen.

Fish skin	Fish skin weight (g)	Dry matter content (%)	Collagen yield (Freez-dried weight) (g)	% (Freeze-dried weight/dry fish skin weight)
Bovine	50.00	23.79	8.21	69.02
Bovine	50.00	23.79	8.27	69.53
Bovine	50.00	23.79	8.42	70.79
Tarakihi 19°C	50.00	36.61	1.33	07.24
Tarakihi 19°C	50.00	36.61	1.25	06.83
Tarakihi 19°C	50.00	36.61	1.66	09.07
Ling 19°C	50.00	23.60	1.59	13.50
Ling 19°C	50.00	23.60	1.59	13.51
Ling 19°C	50.00	23.60	2.00	16.95
Tuna 19°C	50.00	43.55	6.51	29.90
Tuna 19°C	50.00	43.55	7.66	35.18
Tuna 19°C	50.00	43.55	6.53	29.99
Ling 4°C	50.00	23.60	3.37	28.56
Ling 4°C	50.00	23.60	3.01	25.51
Ling 4°C	50.00	23.60	3.45	29.24

The highest yield was for Yellowfin tuna processed at 19°C followed by Ling at 4°C, all with yields between 26-35% of the dry skin weight. It is important to note that in these samples the processing temperatures were well below their denaturation temperatures. On the other hand, Tarakihi processed at 19°C had the lowest, with a yield of 7-9%, followed by Ling processed at 19°C with a yield of 13-17%. These differences in yield are also reflected in the differences in R_{pn} ratio discussed above, suggesting that poor yield is caused by denaturation. Triple-helical collagen structure is lost or broken down in to individual polypeptide chains due to denaturation which loses its ability to form into fibrils during fibrillogenesis and therefore wastes in the solution.

4.4 Implications on collagen extraction process modification

Figure 4.9 shows the proposed modified treatment steps for the three selected fish species based on these findings. Step 1 is the Sodium hydroxide pretreatment, which is typically done at 0.1 M (for example, Muralidharan et al., 2013; Zhang et al., 2009; Duan et al., 2009). Here, the concentration of 0.3 M was used because it provided equivalent swelling to a 0.1 M NaOH solution but takes 3-4 h instead of 3 days. A shorter processing time is more practical. Furthermore, for effective impurity removal, four cycles of 1 h were used, with fresh NaOH solution added each hour. A significant swelling of fish skin in all three species was achieved when NaOH was used, compared to no swelling resulting from Na_2SO4 treatment used in the reference method (§3.3).

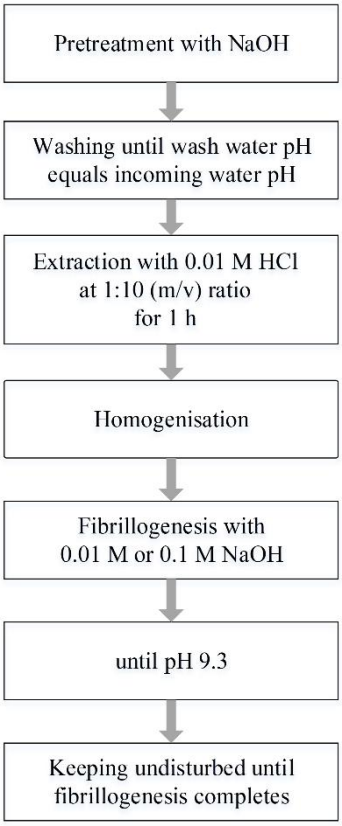

Figure 4.9 Proposed treatment steps for the production of collagen from three selected fish species. Note: Proposed processing temperature for cold-water fish (Tarakihi and Ling) is 4°C; warm-water fish (Yellowfin tuna) is 19°C.

The differences in swelling of Tarakihi skin between Sodium sulphate and Sodium hydroxide are shown in Figure 4.10. This swelling is required to expose and leach out the non-collagenous proteins, and to facilitate fats and pigments removal. The repeated washes remove the leached material. To further refine the time for the NaOH swelling process, it would be useful to determine the rate of swelling of the skin at different concentrations.

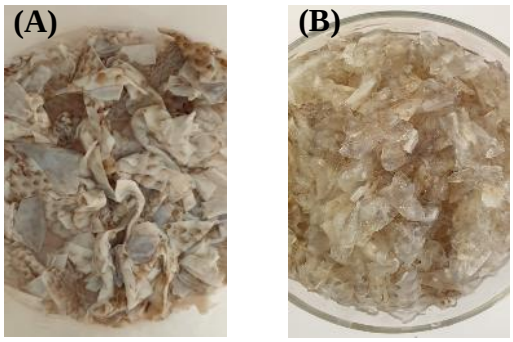

Figure 4.10 Photographs showing the differences between swelling of Tarakihi fish skin: (A) after Na_2SO_4 pretreatment; (B) after NaOH pretreatment.

Evidence of non-collagenous protein removal from Tarakihi, Ling and Yellowfin tuna fish skins is seen in the UV spectra by the absence of a peak in the 250-280 nm region (Figure 4.5). All lipid was removed in Ling, but not in Tarakihi or Yellowfin tuna fish skins. Evidence for the presence of residual fats was seen in the FTIR spectra with peaks at 1744.82 cm^{-1} for Tarakihi and 1741.11 cm^{-1} for Yellowfin tuna fish skins (Figure 4.6). This disparity in fat removal is likely to be due to the differing initial fat content in the fish skins; Tarakihi skin (7.5%), Yellowfin tuna (6.3%) and Ling skin (3.2%). These results confirm that the hypothesis 1 (Swelling of fish skin by NaOH as a pretreatment agent facilitates the removal of non-collagenous materials) is true. The results further confirm the need, as previously noted, of tuning the treatment conditions to the fish species to account for compositional differences.

Step 2 is the extraction of the collagen into an acid solution. A solution of 0.01 M HCl at 1:10 mass (of fish skin) to volume (of acid solution) ratio was used. Soaking occurred for 1 h, after which the mixture was homogenised. Fish collagen researchers typically use acetic acid in this step, (for example, Arumugam et al., 2018, Chen et al., 2016), but doing this requires many further processing steps including centrifugation and dialysis. Here, a process was sought with fewer steps more suited to a commercial operation. A HCl concentration of 0.01M was used because hydrolysis of collagen needs to occur between pH 2-4.

The mass to volume ratio was also adjusted for two reasons, concentration and viscosity. Both affect the later fibrillogenesis step (Zhu et al., 2018; Gobeaux et al., 2008; Mosser et al., 2006). Zhu et al. (2018) found a strong, but a non-linear relationship between the collagen fibril size and the concentration of the extraction solution. The proximity of collagen molecules is important to form the fibrils. Also important is the viscosity which, when it increases, reduces the molecular mobility for fibrillogenesis (Zhu et al., 2018). When the concentration of collagen solution is low, fibrillogenesis proceeds through a lag phase and more time is required to form fibrils. However, when the collagen concentration is increased the lag phase is shortened, which favours the growth of larger fibrils by increasing the electrostatic interactions among collagen triple-helices (Gobeaux et al., 2008). Countering this

is the processing challenge of viscous solutions which are difficult to mix well to achieve homogeneity.

Therefore, the 1:30 (m/v) ratio of the reference method was replaced by 1:10 (m/v) ratio. In contrast to the dilute solution of dissolved collagen produced by 1:30 ratio (in §3.2) which was too dilute for fibrillogenesis to occur, the 1:10 ratio produced a thick homogenised collagen solution which then allowed fibrillogenesis to occur easily in the next step. These results confirm that the hypothesis 2 (Collagen fibril formation and its size depend on the concentration of the collagen solution) is true. However, the optimum mass to volume ratio can only be confirmed by a further optimisation experiments.

Step 3 is fibrillogenesis where the collagen fibres are formed from the acid solution by the addition of NaOH solution to raise it to close to its isoelectric point. Generally, concentrated collagen solutions are transparent or translucent and become opaque upon reaching fibrillogenesis at the isoelectric point (Gobeaux et al., 2008). However, here the Tarakihi and Yellowfin tuna extract solutions were slightly discoloured due to the presence of pigments, as noted above, which can affect the isoelectric point (Zhu et al., 2018).

A rapid rate of pH increase is important for successful fibrillogenesis (Ramírez-Rodríguez et al., 2014), but achieving this is balanced by the ability to mix the NaOH solution into the collagen extract, where poor mixing can cause the localised pH to exceed the isoelectric point. Therefore, the NaOH solution concentration varied between fish species used, as some extracts were thicker than others. The viscosity depended on the collagen concentration, or yield, which was highest for Yellowfin tuna processed at 19°C and Ling at 4°C which meant their solutions were thicker. Consequently, to achieve good mixing without localised overshooting of the isoelectric point, more dilute NaOH solutions were used; 0.01 M for Ling processed at 4°C and 0.1 M for Yellowfin tuna at 19°C. The concentration difference is also related to temperature, with the Ling extract being colder and more viscous, needing a more dilute caustic solution to ensure good mixing without isoelectric point overshoot. For the low-yield solutions, Tarakihi and Ling were both processed at 19°C, and a 1 M NaOH solution was used. These results confirm that the hypothesis 3 (Rapid increase of pH induces the formation of collagen fibres) is correct.

The negative side of using a dilute caustic solution is that the rate of increase in pH is slower, and also it causes dilution of the collagen which makes fibrillogenesis more difficult. It is also important that any mixing be gentle because high-shear will prevent the collagen fibrils from coming together during fibrillogenesis. Even after fibrillogenesis, high shear can break up the collagen fibrils. Therefore, the fibrillogenesis step is a careful balance between the competing influences of extract conditions (step 2) and collagen concentration, caustic concentration, mixing rate, and the rate of pH increase. All of these can be argued to influence the results in different ways.

Tarakihi skin collagen fibril formation started at pH 11.2 and was completed in 18 h. The long time is a consequence of the extraction conditions at 19°C, and therefore only a low yield of collagen, (7-9%), was achieved, meaning the fibrils were relatively dilute in the extract solution. They were also partially denatured, identified by the 0.77 absorption ratio by FTIR noted above. In addition, the Tarakihi extract solution had residual pigment impurities and fats, which are likely to have affected fibrillogenesis. Ling skin collagen processed at

19°C also reached its isoelectric point at pH 11.2 but took 1.5 h to complete fibrillogenesis. The shorter time may well reflect the lack of impurities and the higher yields, (13-17%), meaning the collagen concentration was higher. Far faster fibrillogenesis occurred with Yellowfin tuna processed at 19°C, where it occurred at pH 9.3 and completed in 2-3 min, and for Ling processed at 4°C, where the isoelectric point was also pH 9.3 and fibrillogenesis completed very fast in less than 1 min. These results confirm that the hypothesis 4 (Isoelectric pH of type I collagen from fish is different from mammalian collagen) and hypothesis 5 (Fibril aggregation in fish collagen is time-dependent) are true. These short times reflect the processing temperature being well below the denaturation temperatures, resulting in higher collagen yields during extraction and better preservation of the native collagen. This produced higher yields, meaning more concentrated collagen extract solutions. The consequence was thicker extract solutions, but despite this, and therefore needing the addition of more dilute caustic solutions during the pH increase phase, they do, on balance, result in short fibrillogenesis times. These results really highlight the importance of the extraction conditions. Further, results on collagen yields imply that collagen extractability depends on the temperature of the system, confirming the hypothesis 6 is true.

Results from all three species depict a difference in fibrillogenesis pH conditions from bovine tendon collagens and between the three different fish species. Fibrillogenesis occurs at the isoelectric pH. Accordingly, the isoelectric pH of fish collagen (pH 9.3 as described for fish collagen in the literature, for example by Jiang et al., 2004) is different from that of bovine tendons (pH 6.6). Differences from pH 9.3 may occur due to species-wise differences in isoelectric pH. Isoelectric pH of collagen depends on the amino acid composition. Different fish species have different amino acid compositions; therefore, isoelectric pH may vary. The occurrence of fibrillogenesis at different pH values for three fish species is an indication of different isoelectric pH values, however it cannot be confirmed only by this experiment. For example, the presence of materials other than collagen in the extract has different effects on fibrillogenesis. Ions such as calcium can inhibit fibrillogenesis and conversely some macromolecules can induce fibrillogenesis.

The interplay of competing influences is also reflected in the SEM images (Figure 4.4). The two fish collagens processed well below their denaturation temperature, Ling at 4°C and Yellowfin tuna at 19°C, appeared to have a different pore and fibril structure than Ling and Tarakihi both processed at 19°C. However, all fish collagen images are different to the bovine (Figure 4.4A), which shows highly interconnected fibrils. The reasons for these differences are unknown but may well relate to the different amino acid structures of the fish collagens, the proximity of the processing conditions to the denaturation temperature, as well as the influence of pigment and fat impurities as fish skins, are more variable source of collagen than mammalian tendons.

4.5 Conclusions

These experiments show that further development of a commercial marine collagen process requires studies on how to optimise pretreatment steps to remove all non-collagenous materials, and determination of the best conditions for collagen solubilisation without damaging the underlying collagen structure and in fibril formation. Because each step depends

on the preceding step, these studies should be carried out in sequence. Key to the NaOH pretreatment step is the swelling rates and extents at different concentrations. This information will underpin efforts to optimise skin pretreatment.

Chapter 5. Swelling of fish skins in alkaline and acidic conditions

5.1 Introduction

Pretreatment steps are done to remove unwanted materials from fish skin such as non-collagenous proteins, fats and pigments before collagen extraction. Presence of these materials during extraction process negatively affects the efficiency of processing and the quality and purity of the end product. Therefore, the effective removal of unwanted materials is important in collagen processing. As shown in Chapters 3 and 4, swelling of fish skin can be achieved using Sodium hydroxide (NaOH), to expose the inner structure to solubilise these unwanted materials. Alkaline pretreatment mainly removes non-collagenous proteins and removes fats and pigments to some extent by solubilising them into solution. Swelling caused by the alkaline agent also facilitates access of degreasing and pigment removal agents that may be used to further improve processing.

Swelling of the pretreated fish skin is also needed during the extraction step to expose the inner structure to solubilise collagen molecules. However, prolonged exposure to the acid solution may cause deformation of collagen from its native structure which is undesirable.

How the fish skin behaves during pretreatment and extraction steps was investigated in this chapter. The degree of swelling of fish skin was used as the quantitative measurement and related to different processing conditions. The amount of protein removal during pretreatment and extraction was also measured. In addition to these quantitative measurements, observations made during these experiments provided a better understanding of the behaviour of fish skin.

5.2 Swelling of fish skin

5.2.1 Raw material preparation

The skins of Tarakihi fish were collected from a local fish retailer, scales and residual flesh were removed prior to being frozen as described in §3.3. Before swelling experiments, skins were defrosted overnight by keeping them in a cold room.

To test the behaviour of fish skin during alkaline pretreatment, the following parameters were measured; degree of swelling, and content of proteins removed. In addition to the above two measurements, colour changes in the solution and texture changes in the fish skin were used to support the results. The size of the fish skin slices (5 x 5 mm and 10 x 10 mm), NaOH concentration (0.1 M and 0.3 M), mass to volume ratio of skin: NaOH (1:10 and 1:100) were chosen as variables.

A 20 g of fish skin cut into adequate size was treated with NaOH as the alkaline pretreatment step, with gentle stirring to remove non-collagenous proteins. Experimental parameters, such as NaOH concentration, and size of skin slices varied depending on the experiment as stated. After treating the skin for the set time, skin slices were drained and washed with distilled water until the outgoing wash water pH equalled the incoming wash water pH. Samples were then tested by soaking in HCl and the degree of swelling was measured along with soluble protein. Sample preparation and all the experiments were conducted at normal laboratory temperatures (19-20°C).

5.2.2 Measurement of the degree of swelling

The experimental set-up is shown in Figure 5.1. Samples of skins were soaked in NaOH solutions over time and the weight change was recorded. To do this, an apparatus was constructed to periodically pull the skin samples from the solution, and allow a short time for the sample to drain prior to recording the weight.

For the experiments involving 10 x 10 mm skin pieces, 20 g of fish skin pieces were hung on fishhooks keeping adequate space between the slices for swelling, all hooks were attached together and hung from the bottom of a balance having the weigh-below feature. A NaOH solution was placed on a magnetic stirrer below the fish skin sample and a lab jack was used to move the NaOH solution up and down to alternate between submerging and separating the fish skin sample from the solution. In order to make a quick move of the skin into and out of the NaOH solution, a simple electric drill was connected to the lab jack. Up and down movements of the lab jack were made within 15 s keeping 1-min soaking time intervals between each measurement. Weight measurements were recorded in a computer using a data log software connected to the balance and at the same time, the change in pH in the NaOH solution was recorded continuously. The NaOH solution was stirred continuously throughout the experiment.

For the experiments involving 5 x 5 mm slices, fishhooks were replaced by a pouch made of a wire mesh as these small pieces couldn't be hung effectively on the hooks. All other set-up was kept similar.

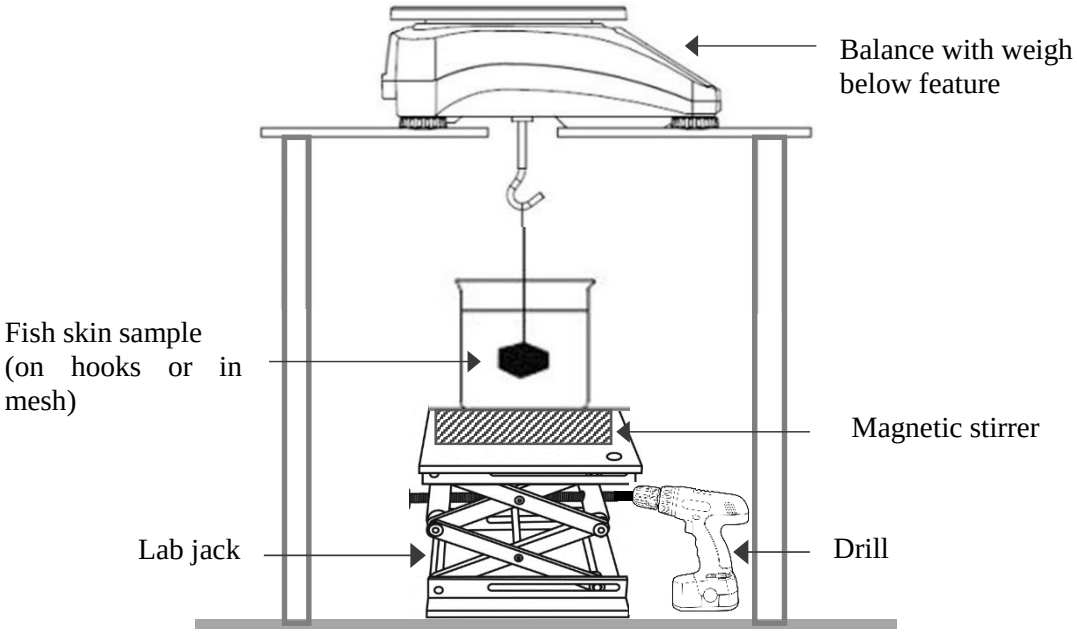

Figure 5.1 Experimental set-up for measuring degree of swelling.

The initial dry solids concentration of fish skin samples was determined according to the standard method of AOAC 930.15 using 20 g of fish skin in 4 replicates. Dry matter (g)/raw fish skin (g) of each sample was calculated according to the *Equation 5.1* and the average of these 4 values was taken as the dry matter content of fish skin for calculations in *Equation 5.2* to estimate the mass of dry solids in the skins used in the swelling experiments. The degree of swelling of fish skin samples in 1-min intervals was calculated according to

Equation 5.3. These experiments were conducted on the assumption that the amount of water absorbed to the skin is a measure of swelling. A similar method had been used by Bowes & Kenten (1950) and Bak et al. (2018).

Equation 5.1:

$$Dry\ matter\ (g)/raw\ fish\ skin\ (g)\ = \frac{Dry\ weight\ of\ fish\ skin\ (g)}{Mass\ of\ raw\ fish\ skin\ (g)}$$

Equation 5.2:

$$Dry\ matter\ content\ (g)\ = Weight\ of\ fish\ skin\ at\ the\ beginning\ of\ experiment\ (g)\ x\ Dry\ matter\ (g)/raw\ fish\ skin\ (g)$$

Equation 5.3:

$$Degree\ of\ swelling = \frac{(Weight\ of\ fish\ skin\ at\ the\ end\ of\ soaking\ (g) - Weight\ of\ fish\ skin\ at\ the\ beginning\ of\ soaking\ (g))}{Dry\ matter\ content\ of\ fish\ skin\ sample\ (g)}$$

5.2.3 Measurement of the protein removal from the fish skin

For the experiments involving a 1:100 (m/v) skin: solution ratio, 50 mL samples of solution were taken from the NaOH solution in every 5-min interval while performing the swelling experiments. The volume loss at each 50 mL sample taken out from the solution was neglected due to the comparatively large initial volume of 1 L. For the experiments involving 1:10 (m/v) ratio, samples after treatment with NaOH were used for analysis as continuous sampling was not practical due to the low volume. All the samples were preserved at -20°C for total nitrogen content analysis, using total carbon-nitrogen analyser (Shimadzu model TNM-L, Shimadzu corporation, Japan).

Total nitrogen content measurement was taken as a measure of non-collagenous proteins that could be removed during the NaOH pretreatment step. It was assumed that collagen is not lost during the treatments. The concentration of protein was the total nitrogen multiplied by universal conversion factor of 6.25 (Tylingo et al., 2016).

5.2.4 Effect of NaOH on swelling and non-collagenous protein removal

Figure 5.2 shows the dynamics of swelling measures for five replicate experiments at two different NaOH concentrations. There was no obvious difference found in swelling between the samples of two different concentrations (orange vs blue). However, samples with low dry matter content (0.276(±0.002) dry matter (g)/sample (g)) from both concentrations (0.1 M S1, 0.3 M S1, 0.3 M S2) reached a constant degree of swelling (plateau) at a comparatively higher degree of swelling (5-6) than the samples with high dry matter content (3.5-5) (0.319(±0.003) dry matter (g)/sample (g)). It is important to note that the experiment 1 of 0.1 M NaOH concentration and experiemnts 1 and 2 of 0.3 M concentrations were done on the day 1 and the rest of the samples were done on the following day. This may have caused the differences in dry matter content. There were some muscles attached to the skin pieces which could cause a variability due to the larger size (10 x 10 mm) of skin pieces. Therefore, the experiemnts starting from §5.3 used smaller size skin pieces (2 x 2 mm).

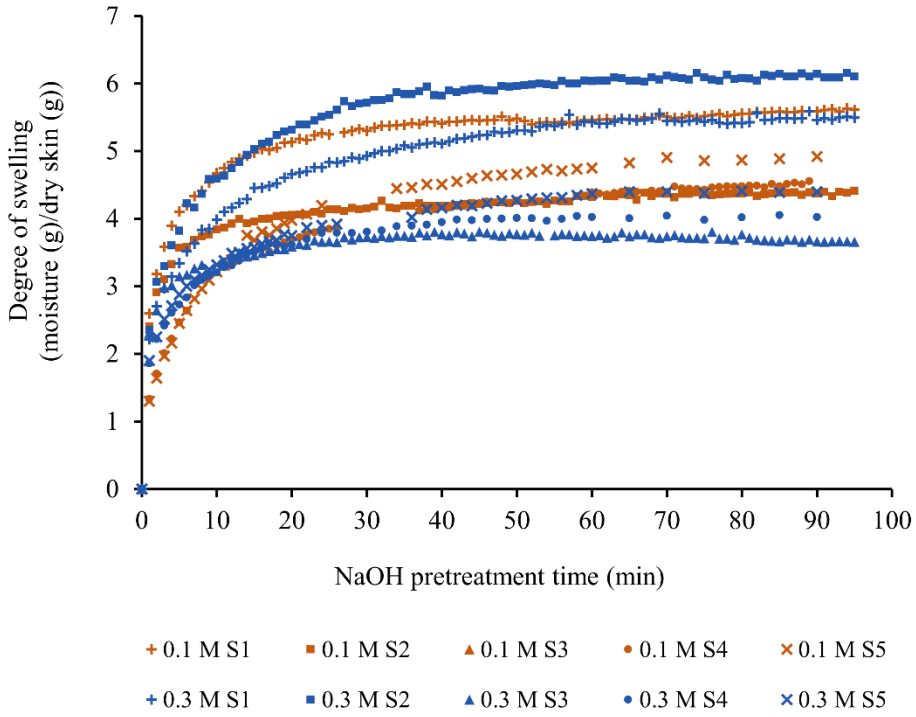

Figure 5.2 Degree of swelling of Tarakihi fish skin by two different concentrations of NaOH: 0.1 M and 0.3 M, as a function of pretreatment time. Size of skin slices (10 x 10 mm), m/v ratio (1:100), temperature (19°C) were kept constant. Five replicates under each concentration are marked as S1, S2, S3, S4, S5. Note that data are not shown for 0.1 S3 due to an error in data logging.

According to the pretreatment methods available in the literature, different NaOH concentrations have been used with different parameters, generally, 0.3 M NaOH concentration is used with 4 repeated treatments of 1 h duration at 1:10 (m/v) ratio (Arumugam et al., 2018), or 0.1 M concentration is used with 3 repeated treatments each of 8 h duration at 1:30 (m/v) ratio (Jongjareonrak et al., 2005). These kinetic measurements showed that all samples reached the maximum swelling before 1 h, indicating the possibility of reducing the soaking time.

Figure 5.3 shows there were very little pH changes over the course of the experiments. Figure 5.4 shows the dynamics of the removal of non-collagenous proteins from the skins during the swelling experiments. These results have similar kinetics to the swelling rates, supporting the hypothesis that swelling aids the access of the solution to hydrolyse myofibrillar proteins enhances the removal of these materials. In each case non-collagenous protein removal increases over time but approaches a plateau after approximately an hour (when swelling stops). Figure 5.5 shows the removal amount as a function of the degree of swelling.

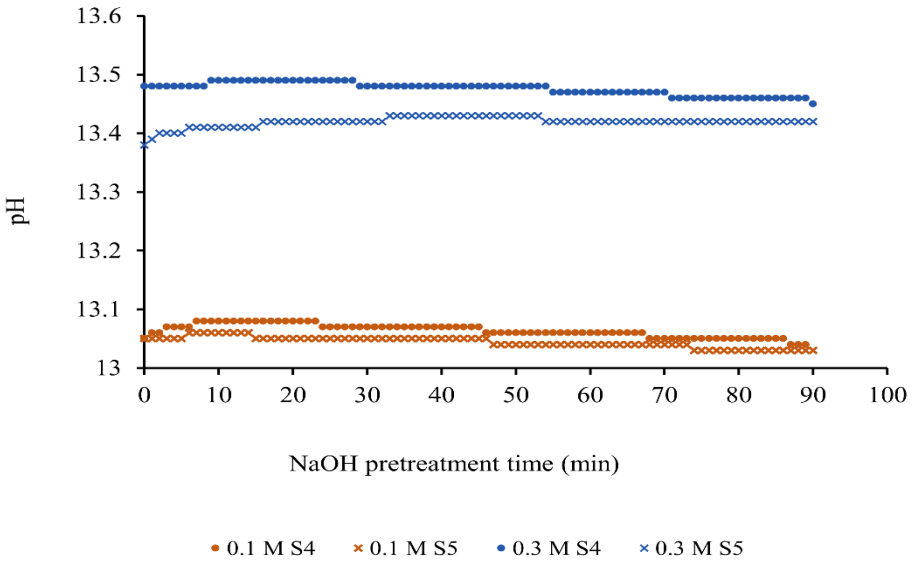

Figure 5.3 pH change in NaOH solutions at two different concentrations: 0.1 M and 0.3 M, as a function of pretreatment time. These measurements were from the same samples with swelling results shown in Figure 5.2.

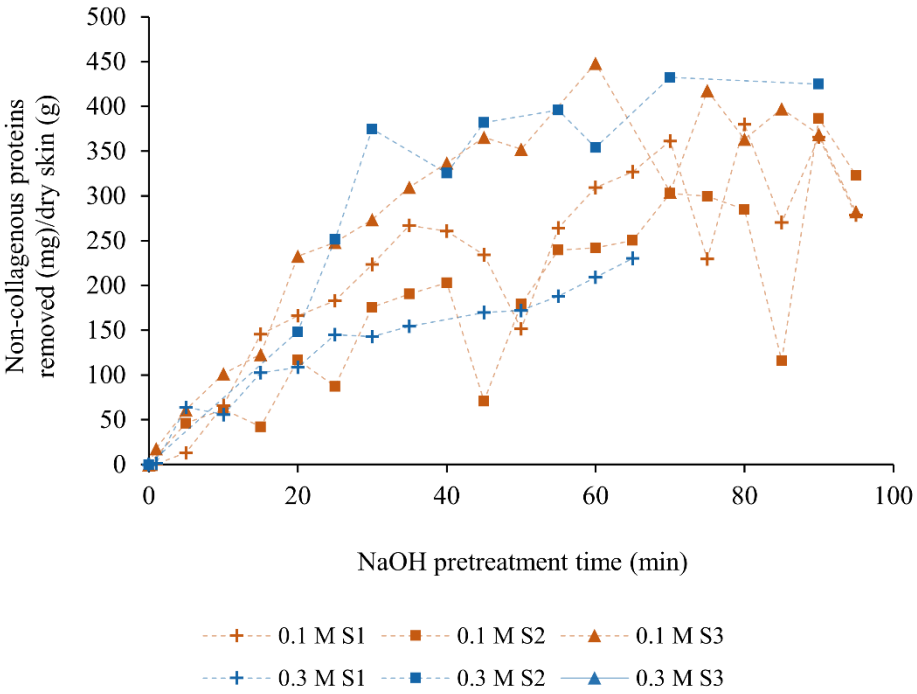

Figure 5.4 Total mass of non-collagenous proteins (per g dry skin) removed by the NaOH pretreatment solutions from Tarakihi fish skin at two different concentrations of NaOH: 0.1 M and 0.3 M as a function of pretreatment time. The size of skin slices (10 x 10 mm), m/v ratio (1:100), and temperature (19°C) were kept constant. Three replicates under each concentration were used. These measurements were from the same samples for the swelling results shown in Figure 5.2. Note that data are not shown for the 0.3 M S3 and 0-20 min time duration for 0.3 M S2 due to an error with the total carbon-nitrogen analyser. The data are shown by markers; the dash lines are only guides to the eye.

All curves in Figure 5.5 showed a similar trend: before reaching a constant degree of swelling the total amount of non-collagenous proteins remained at a lower level, thereafter a rapid increase in total non-collagenous proteins occurred. This is an indication of the extent of swelling required in the skin to achieve to allow the solvent access and to allow all non-collagenous proteins to be removed. In this work an assumption was made that only the non-collagenous proteins were removed during NaOH pretreatment (as detected by total nitrogen analysis) and that no collagen was solubilised.

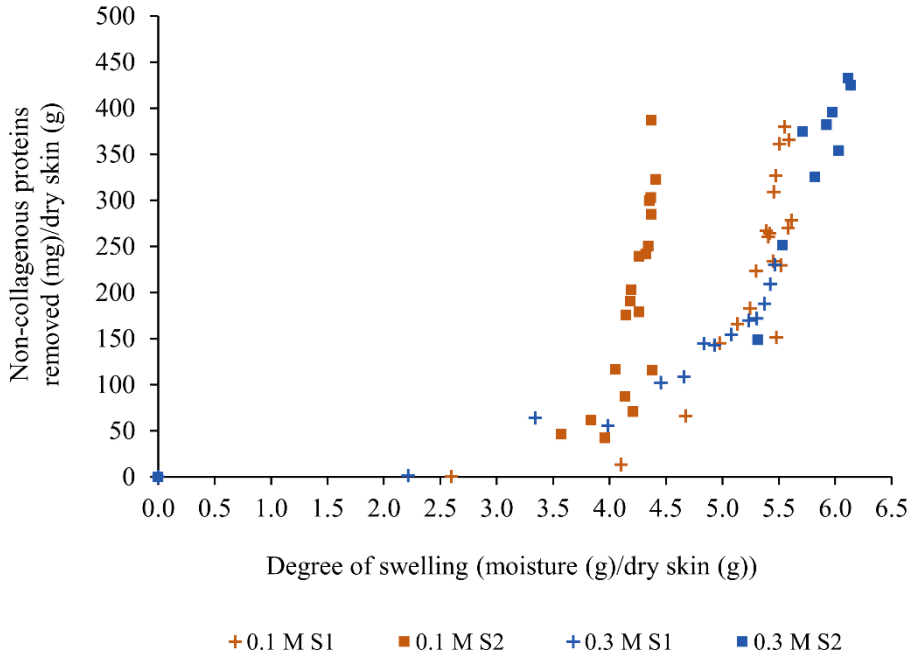

Figure 5.5 Total content of non-collagenous proteins removed by the NaOH pretreatment solutions from Tarakihi fish skin by two different concentrations of NaOH: 0.1 M and 0.3 M, as a function of the degree of swelling. This graph is drawn from the data from Figures 5.2 and 5.4. Note that initial data points are not shown for 0.3 M S2 as described for Figure 5.4 above.

Different swelling behaviour was observed between the skin and residual attached muscles (not removed in the skin preparation process). During soaking in NaOH, both muscle meat and skin swelled. By the end of the soaking time the muscle flesh had been detached from the skin and got into the NaOH solution leaving only the skin for further processing (Figure 5.6). This is useful in removing unwanted muscles from the skin which are tightly attached, and difficult to remove during the sample preparation step.

These differences in swelling behaviour between skin and muscles were analysed by the following experiment using similar conditions: 0.1 M and 0.3 M NaOH at 1:100 (m/v) ratio. For this experiment skin samples were prepared by removing all the attached muscles. For both 0.1 M and 0.3 M concentrations, swelling of the skin reached a plateau after 30 min (Figure 5.7A), in contrast to muscles which continued swelling even after 4-5 h of soaking at 0.1 M concentration, and reached a constant value after around 3 h at 0.3 M concentration (Figure 5.7B).

No obvious differences were observed between 1:10 and 1:100 mass to volume ratios after 60 min (see Figure 5.8), however, a conclusion cannot be made based on the results from one sample.

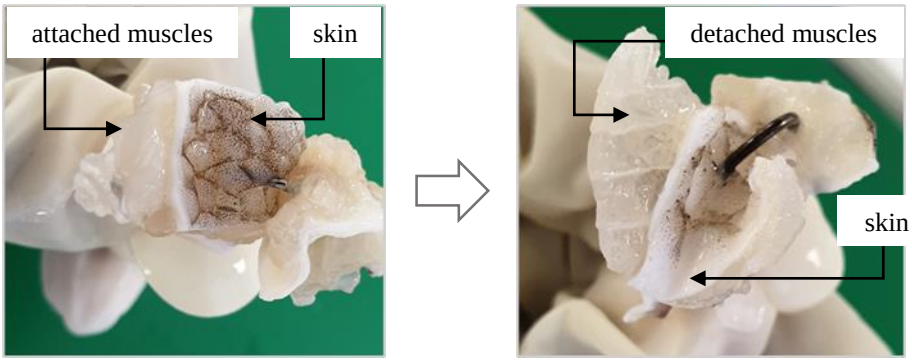

Figure 5.6 Photographs showing the differences in swelling behaviour between skin and muscles (A): after 20 min of NaOH treatment; (B): at the end of NaOH treatment.

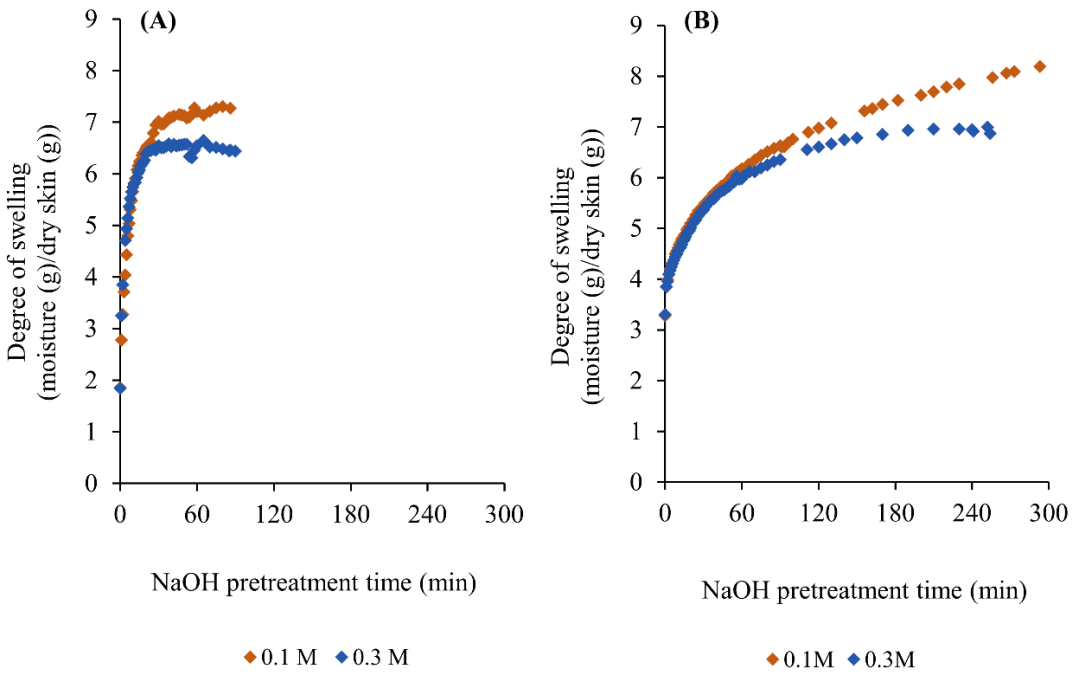

Figure 5.7 (A): degree of swelling of Tarakihi fish skin after removing all the attached muscles; (B): degree of swelling of Tarakihi fish muscles, using two different concentrations of NaOH: 0.1 M and 0.3 M, as a function of pretreatment time. The size of skin slices (10 x 10 mm), size of muscle pieces (10 x 10 x 10 mm), m/v ratio (1:100), temperature (19°C) were kept constant.

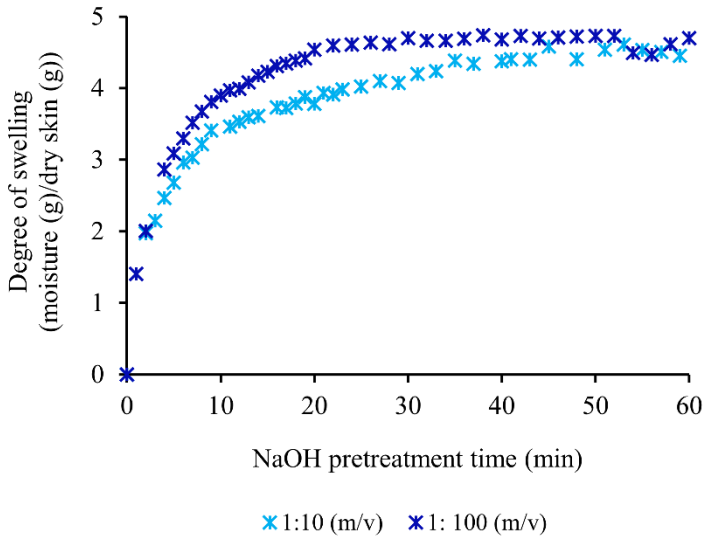

Figure 5.8 Degree of swelling of Tarakihi fish skin, using two different skin to solvent (m/v) ratios: 1:10 and 1:100, as a function of pretreatment time. The size of skin slices (10 x 10 mm), concentration (0.3 M NaOH) and temperature (19°C) were kept constant.

5.2.5 Effect of fish skin piece size on swelling and non-collagenous protein removal

This experiment was done by treating skin in 0.3 M NaOH for 4 h with a solution change every 1 h. As described earlier the mesh set-up was used for the 5 x 5 mm skin pieces, and the hook set-up was used for the 10 x 10 mm skin pieces. Throughout the process of non-collagenous protein removal, it was noticed that the colour of the solution got lighter until 3 h, and again increased in the final solution (Figure 5.9). This change to a darker colour at the final solution change may be associated with exposing the inner structures of the fish skin, and thus facilitating the removal of unwanted materials like pigments. A comparatively darker colour was expected from smaller pieces, but the reverse occurred. The same trend was observed in the swelling graphs (Figure 5.9 primary axis). This difference could be due to the mesh pouch used in this experiment. As the skin pieces inside the mesh were not well exposed to the NaOH solution due to the limited space inside compared to the set-up with hooks (Figure 5.10), it may have affected this result. However, a comparatively higher non-collagenous protein removal was observed from smaller pieces.

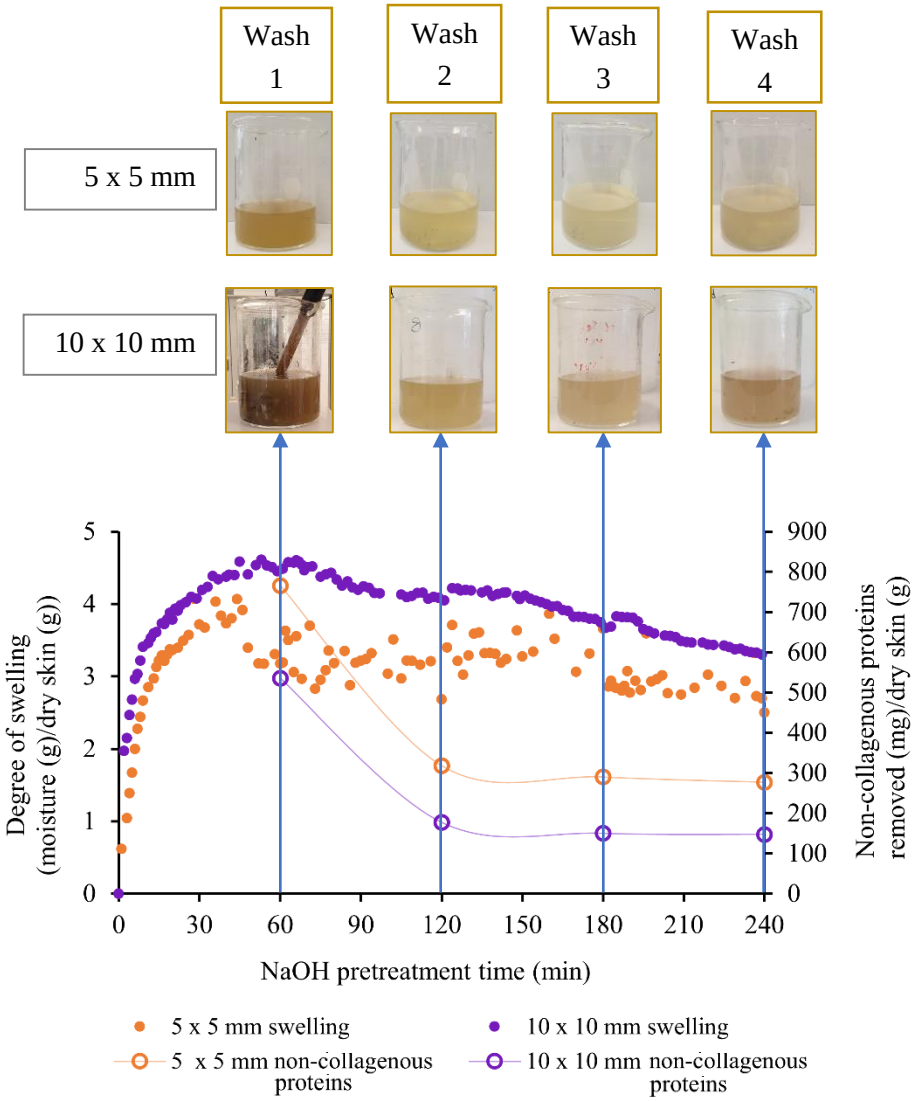

Figure 5.9 Degree of swelling of Tarakihi fish skin at two different sizes of skin pieces: 5 x 5 mm and 10 x 10 mm as a function of NaOH pretreatment time. Concentration (0.3 M NaOH), m/v ratio (1:10) and temperature (19°C) were kept constant. The amount of non-collagenous proteins leached into the NaOH solution at the end of each 1 h is shown using line graphs, showing the data points by markers and keeping lines only as guides to the eye. Colour changes of NaOH solutions at the end of each 1 h are shown using inset photographs. Dry matter content of skin samples was similar for both samples: 0.319(±0.003) dry matter (g)/sample (g).

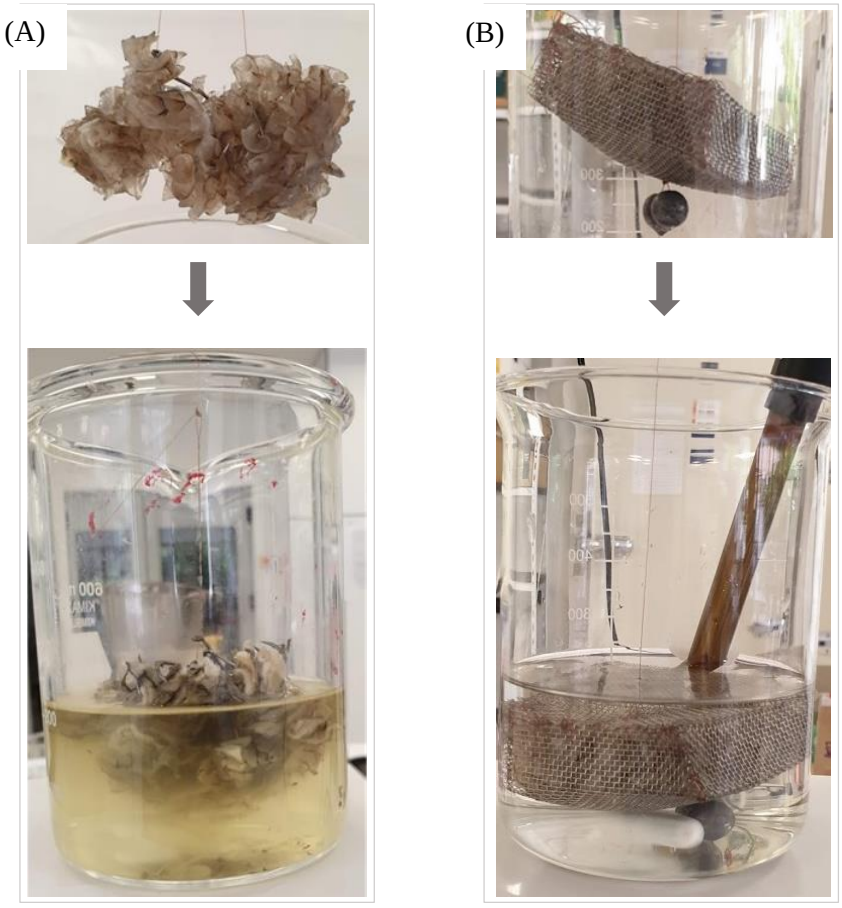

Figure 5.10 Photographs showing how fish skin pieces were exposed to the solution in (A) hooks set-up (for 10 x 10 mm pieces) and (B) mesh set-up (for 5 x 5 mm pieces).

5.2.6 Observations during soaking in distilled water to neutralise fish skin before HCl extraction

During soaking and washing in distilled water after the above NaOH pretreatment, shrinking of the skin was observed. When the pH reached neutral, absorbed water during NaOH pretreatment had been removed. In addition, all the swollen muscles had been washed off, leaving only the skin for the next step of processing (Figure 5.11; Figure 5.12).

Figure 5.11 Photographs showing the behaviour of fish skin during soaking in distilled water after NaOH pretreatment (A): before NaOH treatment; (B): after NaOH treatment; (C): after soaking in distilled water).

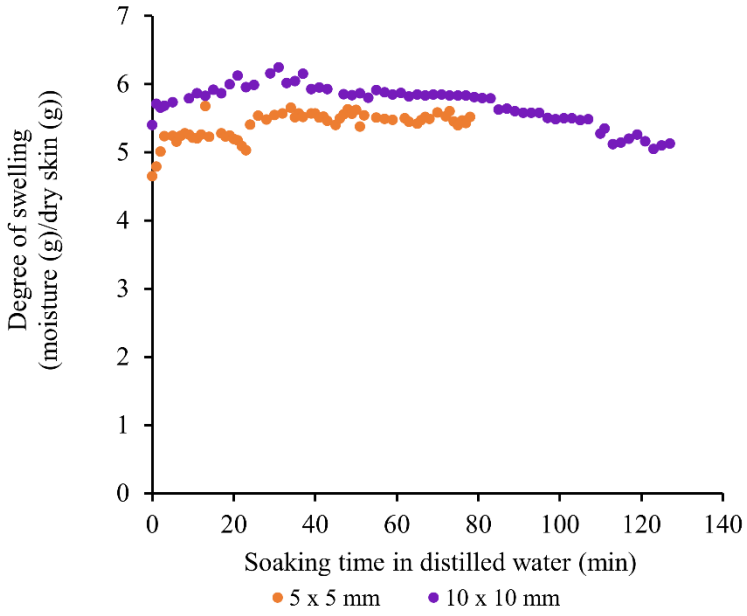

Figure 5.12 Degree of swelling of Tarakihi fish skin at two different sizes of skin pieces: 5 x 5 mm and 10 x 10 mm, as a function of soaking time in distilled water until neutral pH after NaOH pretreatment. Note these data are from the same samples shown in Figure 5.9.

5.2.7 The swelling behaviour of fish skin during acid extraction conditions

After alkaline washing and neutralisation, the skins are treated in acid conditions to breakdown the macro structure of the skin and facilitate extraction. Swelling of the skin is a key part of this process. This was investigated by treating the pretreated and neutralised skin pieces discussed in §5.2.5 and 5.2.6 above, in HCl solutions for an hour.

Figure 5.13 shows the HCl swelling behaviour of the skin samples swelled and reported previously in Figure 5.9 for two different sizes.

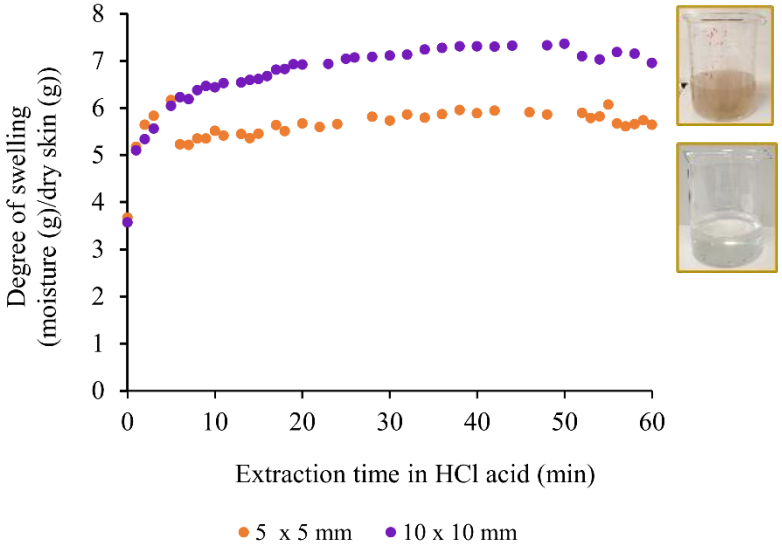

Figure 5.13 Degree of swelling of Tarakihi fish skin at two different sizes of skin pieces: 5 x 5 mm and 10 x 10 mm, as a function of extraction time in HCl acid. The colour of HCl solutions at the end of 1 h is shown using inset photographs. Note these data are from the same samples shown in Figure 5.9 after alkaline treatment.

This result was unexpected as by increasing the surface area using smaller pieces during the NaOH pretreatment step, it would be expected that swelling would be faster and more complete. The reason is likely to be as described above, where the samples on hooks had greater access to all the skin surfaces and the mesh samples caused diffusion limitations. For the 5 x 5 mm size samples, the total amount of protein in the HCl solution after 1 h extraction time was 27.11 mg/ dry matter (g). This can be related to the amount of collagen leached into the HCl solution assuming that all non-collagenous proteins have been removed during pretreatment with NaOH. This result showed that some collagen was leached into the acid solution during the 1 h extraction time. The swollen skin together with the solution should be taken for homogenisation prior to fibrillogenesis (as described in §4.2.6). According to these results it would result in a waste of collagen that will reduce the overall collagen yield if only the swollen skin is used for homogenisation.

There was a step change occurred after initial five data points in the graph related to 5 x 5 mm skin pieces. This was not due to a loss of skin piece as observations were made throughout the whole experiment. It's likely there was error with the function of the balance. Figure 5.13 shows very less extraction of protein using the mesh pouch. The mesh pouch was not effective at contacting the solution throughout the skin pieces, therefore the experiments using the mesh pouch were not continued.

5.3 Further experiments on swelling during neutralisation and extraction conditions

The methods available in published literature consist of a neutralisation step using water following the alkaline pretreatment, which consumes a large quantity of water and time. This neutralisation with water is important to remove NaOH salts which have been absorbed into the skin with water during pretreatment. This happens through shrinking or deswelling of the skin. In the methods available in published literature, this is done by washing the pretreated skin in running water or soaking the pretreated skin in a series of water until pH reaches 7. This neutral pH is important for the preceding extraction step with HCl where the skin again swells to solubilise the collagen molecules and dissolve them into the solution. This neutralisation and swelling depend on the solution pH, however, the studies done on understanding this aspect are lacking in the published literature. Therefore, this experiment was designed to understand the swelling behaviour of skin during neutralisation and extraction in relation to pH.

5.3.1 Sample preparation and pretreatment

Tarakihi fish skins were collected from a local fish store as soon the fish were processed and transported to the university laboratory (20-min drive) in chilled condition. Skins were then cleaned by removing both the scales from the outer surface and the residual flesh left on the inner surface of the skin. The device used for this was a food processor (Kenwood FPM910 Multi-Pro Excel Food Processor), where the skins become attached to the spinning blades and the scales and residual flesh are sheared off.

The skin was minced using a meat mincer (Kenwood PRO 2000 EXCEL MG700 Electric Mincer and Sausage Maker) with 3 mm mesh mince plate. A relatively small particle size is desirable for effective mass transfer. Ice was added to the mix which maintained a low

temperature while mincing, which was important to avoid denaturation of the collagen. The minced skin was then washed thoroughly using cold-water until the wash water ran clean. It was then drained on a strainer in a cold room at 4°C to remove as much free water as possible. To ensure uniformity, a random sampling method was used to collect 50 g samples which were individually packed in polyethylene bags and stored at -20°C until use. Sample preparation and all the experiments were conducted in a cold room at 4°C.

Before the experiments, samples were thawed at 4°C. The dry matter percentage of this prepared skin was determined using the oven drying method (AOAC 930.15).

Approximately 50 g (accurately weighed) samples were then pretreated with 0.3 M NaOH solution at a 1:10 (m/v) skin: solvent ratio for 90 min. The samples were soaked in this NaOH solution in a glass beaker and constantly stirred at 200 rpm using a magnetic stirrer. After that, the mixture of skin and solution was kept undisturbed without stirring for 1 min to settle the skin at the bottom of the beaker before decanting the solution phase into another beaker. Next, the treated skin was separated from the leftover solution by placing it on a stainless steel strainer of 2 x 2 mm mesh size and left for 10 min to ensure it was well-drained. This procedure was repeated for a second time and then the weight of the swollen skin was recorded.

5.3.2 Swelling experiments

Experiments to understand the swelling behaviour of skin were conducted according to the following design;

- Neutralisation with water followed by treatment with HCl
- Neutralisation with HCl followed by treatment with HCl

The pretreated skin was soaked in cold distilled water (4°C) at 1:10 (m/v) ratio in a glass beaker and constantly stirred at 200 rpm using a magnetic stirrer. The pH was continuously monitored using a digital pH meter. Once the pH became constant with time, the stirring was stopped. The pH and the time taken for the pH stabilisation were recorded. Next, the skin was separated from the leftover water solution by placing it on a stainless steel strainer of 2 x 2 mm mesh size and drained for 1 min. Then the weight of the washed skin was recorded. This procedure was repeated until the pH reached 7.

After neutralisation, this skin was soaked in 0.0025 M HCl (pH 2.6) at 1:10 (m/v) ratio in a glass beaker and constantly stirred at 200 rpm using a magnetic stirrer. The pH was continuously monitored using a digital pH meter. Once the pH became constant with time, the stirring was stopped. The pH and the time taken for the pH stabilisation were recorded. Next, the skin was separated from the leftover water solution by placing it on a stainless steel strainer of 2 x 2 mm mesh size and left to drain for 1 min before recording the weight of the washed skin. This procedure was repeated until the mass of the skin stopped increasing or started dropping. This experiment was conducted in three replicates.

To test acid neutralisation and acidification, the same procedure as described above was followed but replaced the cold distilled water with 0.0025 M HCl (pH 2.6). This experiment was also conducted in three replicates.

The measured variables in these experiments were the mass of the skin, pH and time. The calculations are described below.

5.3.3 Estimation of theoretical pH

As explained above, the pH value was recorded for each solution change. The reduction of pH occurred either by soaking in water or HCl in this experiment. The skin is soaked in a mass to volume ratio of 1:10, therefore theoretically the pH reduction can be calculated. However, in practice this can be different. The study of the difference between the theoretical and practical pH values are important in understanding the collagen extraction process in relation to swelling of the skin. The theoretical pH values were calculated based on the following equations.

The end pH value after each soaking was determined by the amount of OH^- or H^+ ions introduced by NaOH pretreatment, water wash or HCl treatment. Therefore, the theoretical end pH value was determined by the following equation.

$$End\ pH\ = \frac{(M_{initial\ water\ in\ skin} \times 10^{(-14-initial\ pH)})\ +\ (M_{soaked} \times 10^{(-14-solution\ pH)})}{(M_{initial\ water\ in\ skin} + M_{soaked})}$$

where $M_{initial\ water\ in\ skin}$ = mass of water present in skin at the beginning of each soaking, M_{soaked} = mass of water or HCl used for soaking, initial pH = pH value of the solution at the beginning of each soaking and, solution pH = pH value of water or HCl used for soaking.

5.3.4 Results and discussion

Figure 5.14 shows the swelling of skins versus solution pH. When neutralised with water, the swelling remained mostly unchanged until the pH decreased to around 11.5. The same result was observed with HCl. The amount of water that was removed from the skin was higher during neutralisation to pH 7 with water than for HCl. During neutralisation with HCl, OH^- ions from NaOH react with H^+ from HCl, producing H_2O. At the same time, the reaction between NaOH and HCl produces NaCl which would show up in the mass as it may not be washed out into the solution. These may be the reasons for showing comparatively less reduction in swelling by the samples neutralised with HCl. In contrast, neutralisation with water occurs by washing out NaOH salts from the swollen skin. This is likely to be the reason for consuming more water and taking more time for neutralisation when using water (Figure 5.15). When the time taken for both neutralisation and treatment with HCl is considered, the time taken to process using HCl neutralisation was much less than when using water (Figure 5.15).

The swelling of the skin during treatment with HCl was higher for the samples neutralised with HCl. The mass of the skin (swelling) increased until around 3.5, then started decreasing. On the other hand, the swelling with HCl was comparatively lower for the samples neutralised with water and the mass of skin (swelling) increased only until around pH 4 and then started decreasing. This mass reduction may be due to the dissolving of collagen in the HCl solution. Generally, the suitable pH range to dissolve collagen is below 4. Collagen is not generally soluble above pH 4 due to the closeness to the isoelectric pH value. Hydrophobic interactions among collagen molecules increase around the isoelectric pH, therefore collagen solubility decreases. On the other hand, in acidic pH values away from the isoelectric pH, the

net positive charge residues of collagen molecules increase, causing repulsive forces between collagen molecules, and therefore the collagen solubility increases (Li et al., 2013; Woo et al., 2008). It can be seen from Figure 5.15 that the solution pH should be maintained around 3.5-4 to solubilise collagen, and therefore the HCl concentration should be selected to achieve this.

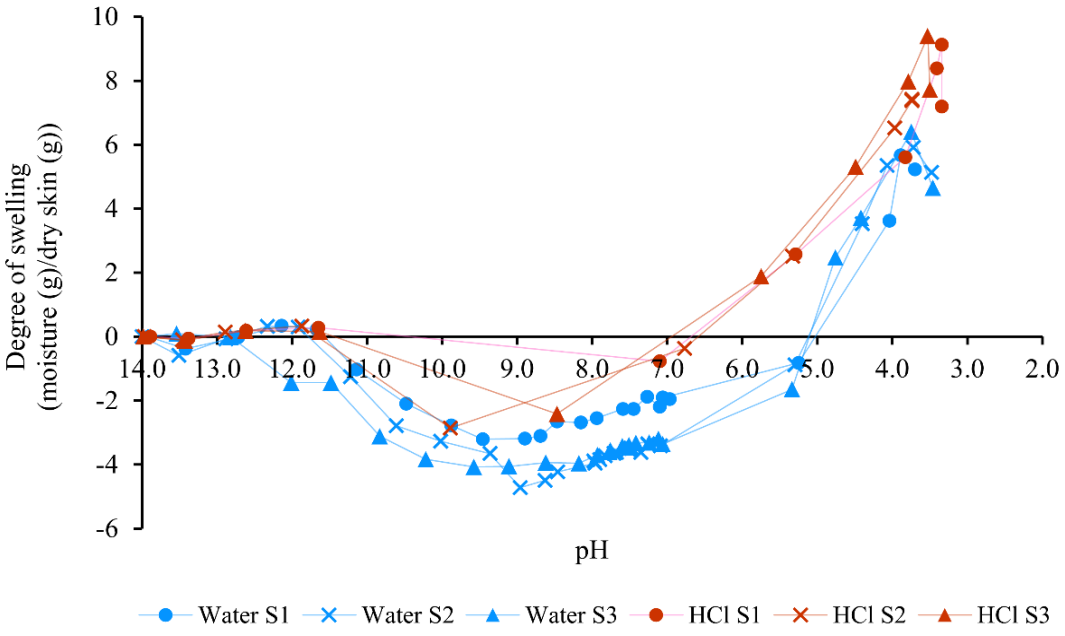

Figure 5.14 Swelling of skin during neutralisation and treating with HCl versus pH. The blue colour represents the samples neutralised with water and the brown colour represents the samples neutralised with HCl. Three replicates are marked as S1, S2, S3. Data points are shown by markers and the lines are used as guides to the eye.

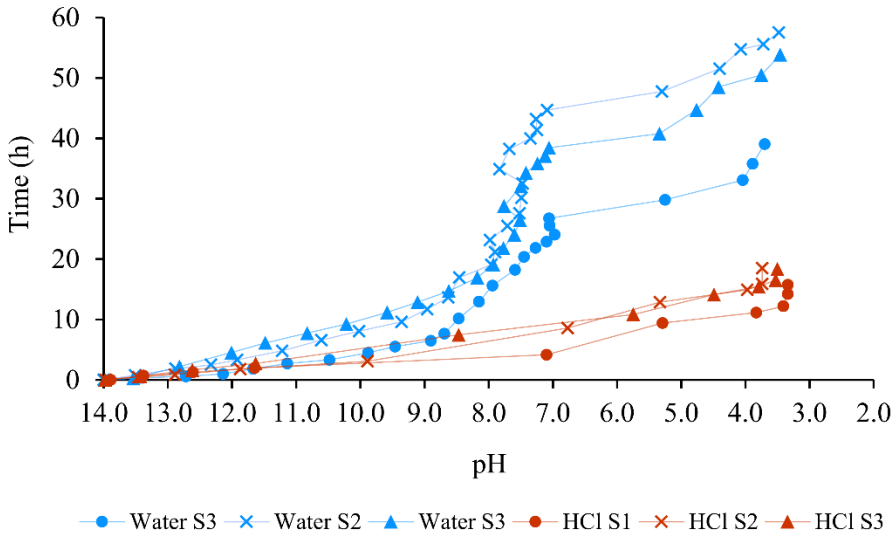

Figure 5.15 Cumulative time taken to stabilise the pH at each soaking. The blue colour represents the samples neutralised with water and the brown colour represents samples neutralised with HCl. Three replicates are marked as S1, S2, S3. Data points are shown by markers and the lines are used as guides to the eye.

Table 5.1 shows a comparison between experimental and theoretical pH obtained for each three replicates under two treatment conditions; (1) neutralisation with water followed by treatment with HCl and (2) neutralisation with HCl followed by treatment with HCl. Always the experimental pH value was higher than the theoretical pH value. This is likely to be due to some buffering capacity of the collagen itself. This should be considered in selecting the pH value of solutions to treat fish skin. For example, if the skins need to be treated at pH 4, the treatment solution should be prepared with a lower pH value.

Table 5.1 Comparison of experimental and theoretical pH at the end of each soaking.

1. Neutralisation with water followed by treatment with HCl						**2. Neutralisation with HCl followed by treatment with HCl**					
Water_rep 1		**Water_rep 2**		**Water_rep 3**		**HCl_rep 1**		**HCl_rep 2**		**HCl_rep 3**	
Exp. pH	Ther. pH	Exp. pH	Ther. pH	Exp. pH	Ther. pH	Exp. pH	Ther. pH	Exp. pH	Ther. pH	Exp. pH	Ther. pH
13.42	12.68	13.51	12.83	13.54	12.86	13.38	12.65	13.46	12.81	13.43	12.74
12.72	11.97	12.88	12.19	12.82	12.15	12.61	11.87	12.89	12.23	12.62	11.93
12.14	11.40	12.33	11.65	12.01	11.33	11.65	10.92	11.87	11.22	11.63	10.95
11.67	10.95	11.92	11.25	11.48	10.75	7.10	6.38	9.89	9.25	8.47	7.79
11.14	10.41	11.22	10.55	10.83	10.10	5.29	4.53	6.77	6.02	5.75	4.97
10.48	9.70	10.61	9.89	10.22	9.42	3.83	3.25	5.33	4.67	4.49	3.87
9.88	9.05	10.02	9.24	9.58	8.74	3.41	2.96	3.97	3.44	3.79	3.30
9.46	8.59	9.36	8.56	9.11	8.26	3.34	2.95	3.74	3.30	3.53	3.11
8.9	8.00	8.96	8.14	8.62	7.77	3.34	2.95	3.74	3.31	3.5	3.10
8.69	7.80	8.63	7.75	8.18	7.34						
8.47	7.59	8.46	7.60	7.93	7.09						
8.15	7.30	7.96	7.14	7.77	6.94						
7.94	7.10	7.9	7.10	7.6	6.78						
7.59	6.79	7.98	7.17	7.51	6.70						
7.45	6.69	7.71	6.93	7.76	6.95						
7.27	6.55	7.52	6.77	7.5	6.68						
7.1	6.44	7.49	6.75	7.42	6.60						
6.97	6.34	7.47	6.74	7.24	6.43						
7.05	6.40	7.83	7.05	7.12	6.31						
7.06	6.41	7.68	6.91	7.06	6.26						
5.25	4.43	7.35	6.64	5.34	4.53						
4.04	3.33	7.25	6.56	4.76	4.03						
3.89	3.32	7.26	6.58	4.42	3.81						
3.7	3.20	7.09	6.46	3.75	3.17						
		5.3	4.49	3.46	2.94						
		4.4	3.72								
		4.07	3.52								
		3.72	3.24								
		3.48	3.05								

5.4 Conclusions

This section shows the swelling behaviour of fish skins in alkaline and acidic conditions and the dynamics of neutralisation using water and HCl. The results show that at least one hour should be used to ensure the collagen matrix is fully swollen during NaOH pretreatment. This would allow greater access to the alkali for reaction and removal of non-collagenous components such as muscle proteins, fats and pigments. If residual flesh is present on the skin prior to pretreatment, then swelling can be used to separate it from the skin itself but this process takes up to 4 h.

Once pretreated, the skins need to be neutralised on the way towards acid extraction. This can be achieved using successive washes with fresh water, causing the skins to shrink (de-swell). This process is time-consuming and uses a lot of water as it relies on physically washing out residual NaOH in the skin. Neutralisation can be achieved much faster by direct neutralisation and swelling with HCl. This may leave behind residual NaCl in the skin which may have implications in later stages of the process.

Acid extraction should be carried out around pH 4 where there is maximum swelling and evidence of collagen solubilisation. This should provide ideal conditions for homogenisation prior to fibrillogenesis. There could be potential for excessive hydrolysis if the pH is dropped to low and damage to the native collagen triple-helix structure.

The dynamics and degree of swelling as a function of pH provided a sound basis for detailed investigation of the key steps involved in collagen processing.

Chapter 6. Physico-chemical methods for fish skin pretreatment

6.1 Introduction

Fish skin is generally removed from fish during commercial processing. Attached to the outer surface of the skin are scales and to the inner surface is some residue flesh. In collagen extraction, these scales and residue flesh must be removed during the initial cleaning. The remaining skin contains collagen protein as its main component, accounting for more than 70% on a dry weight basis (Liu et al., 2015). The other 30% consists of non-collagenous proteins, fats and pigments. Before collagen extraction, these non-collagenous components should be removed (in a pretreatment step) as they negatively affect the extraction efficiency and cause low purity and yield (Song et al., 2021).

The most important property of a fish skin pretreatment agent is the ability to swell the skin as shown in Chapter 5. This swelling loosens the fibres and allows the pretreatment solution to access and dissolve the non-collagenous components (Liu et al., 2015). The other function of a pretreatment agent is to remove only these non-collagenous components without significant loss or structural modification of the collagen molecules (Skierka & Sadowska, 2007; Xu et al., 2017). Alkaline solutions such as Sodium hydroxide (NaOH) and Calcium hydroxide ($Ca(OH)_2$) are capable of removing only the non-collagenous proteins. However, $Ca(OH)_2$ does not cause swelling (Liu et al., 2015) and therefore NaOH is commonly used as the pretreatment agent. As well as the non-collagenous proteins, the NaOH treatment also removes some fats and pigments. Further fat removal can be achieved with butyl alcohol or other degreasing agents, and hydrogen peroxide (H_2O_2) can be used to oxidise any remaining pigments.

Most literature is focused on the collagen extraction process rather than solely on the pretreatment. Of those publications that include pretreatment studies, most investigate the effect of pretreatment on the quality and purity of collagen after extraction. Very few studies have assessed the pretreatment conditions relative to the quality of pretreated material, (i.e., the extent to which the non-collagenous proteins, fats and pigments have been removed), and its impact on the quality of the collagen. Blanco et al. (2019) studied the effect of NaOH concentration, time and temperature using Small-spotted catshark (*Scyliorhinus canicula*) skin as the raw material, by analysing the collagen content in the pretreated skin and the pretreatment solution, however, they didn't consider the fat removal. Similarly, Liu et al. (2015) studied the effect of NaOH concentration, time and temperature using the skin of grass carp (*Ctenopharyngodon idella*) as the raw material. They analysed the solution separated after pretreatment for the total protein and collagen content, and the collagen content in the final collagen product after freeze-drying. However, the effect of NaOH pretreatment on fat removal has not been studied. None of the previous literature has studied the complete pretreatment process including the neutralisation step.

Due to the lack of information in the literature, this chapter investigates the effects of pretreatment conditions on the removal of undesirable components, providing a process optimised for fish skin processing. In developing this, there are some other important factors to be considered, which again are not well addressed in the published literature. First, residuals of pretreatment agents must be removed so that it does not become an impurity in the extracted

collagen. Second, some chemicals must be avoided, for example, butyl alcohol cannot be used to remove fats as the residues are not accepted in biomedical collagen. Third, the wastewater clean-up required for the discharge of pretreatment chemicals into the environment must be considered. Fourth, efficient use of chemicals is important because unnecessary chemicals are expensive and not cost-effective. And lastly, the pretreatment steps, (i.e., the processing unit operations), need to be few in number and with reasonable residence times to ensure the pretreatment is economically viable.

In this study, the pretreatment agents were selected considering the above aspects. Sodium hydroxide was selected as the pretreatment agent to remove the non-collagenous proteins. It has been used for pretreatment in fish and other collagen-rich raw materials and can swell the structure as shown in Chapter 5. Fats and pigments were expected to be removed to a greater extent by the same NaOH treatment. Sodium dodecyl sulphate (SDS), which is an anionic detergent, was tested as a degreasing agent to further remove fats. In the published literature, the pretreatment processes involve a washing step with distilled water at the end of the pretreatment to remove residual NaOH. This washing step consumes a large quantity of water and time. This was investigated in detail in §5.3. In this study, this washing step was replaced with a neutralisation step using hydrochloric acid (HCl) followed by washing with distilled water to remove the Sodium chloride (NaCl) salts. This required a much-reduced amount of water.

The experiments were designed in a way to understand the pretreatment process and the effect of removing non-collagenous components through a simple characterisation of the pretreated material. Treatment time, skin mass to solvent volume ratio and different treatment configurations were used as the process variables. The aims of this chapter were therefore to carry out experiments to understand the effect of treatment time, mass to volume ratio and different treatment configurations, and to develop a pretreatment process based on this understanding. The minimum use of chemicals, minimum wastage and time and cost-effectiveness were considered in developing this process.

The experiments were carried out under three main categories. The;

1. Effect of time
2. Effect of mass to volume (m/v) ratio of skin to NaOH solution
3. Different treatment configurations (involving NaOH)

6.2 Raw material preparation

Tarakihi fish skins (*ca*. 5 kg) were collected from a local fish store as soon the fish were processed and transported to the university laboratory (20-min drive) in chilled conditions to assure the freshness and to avoid contamination with extraneous matter. Skins were then cleaned by removing both the scales from the outer surface and the residual flesh left on the inner surface of the skin. This was done using a 1.6 L thermo-resist glass-bodied blender on a food processor (Kenwood FPM910 Multi-Pro Excel Food Processor), where the skins become attached to the spinning blades and the scales and residual flesh are sheared off. The skins were then manually cleaned by wiping-off, without using water.

Then the cleaned skins were minced using a meat mincer (Kenwood Pro 2000 EXCEL MG700 Electric Mincer and Sausage Maker) with 3 mm mincing plate, using speed number 1 rotary control in a single pass. This size reduction was done to facilitate maximum mass

transfer during NaOH soaking. Ice was added to the mix which maintained a low temperature while mincing, which was important to avoid denaturation of the collagen. The minced skin was then washed thoroughly using cold-water until the wash water ran clean. It was then drained on a strainer in a cold room at 4°C to remove as much free water as possible. To ensure uniformity, a random sampling method was used to take 50 g samples from the bulk mince, which were then individually packed in polyethylene bags and stored at -20°C until use. The proximate composition of one of these samples was analysed to obtain the moisture content by the oven drying method (AOAC 930.15), crude protein content by means of total nitrogen content according to the Kjeldahl method (AOAC 981.10), crude fat content by the Soxhlet method (AOAC 960.39) and, ash content by igniting in a muffle furnace (AOAC standard 920.153). All the analysis was done in triplicate. Prior to pretreatment experiments, the samples were thawed at 4°C overnight. This sample preparation procedure was followed for all three categories of experiments mentioned in this chapter.

6.3 The effect of time on pretreatment

6.3.1 Experimental protocol

Treatment times of 30, 40, 50, 60, 70, 80 and 90 min were selected to determine the non-collagenous material removal. The 30 min time duration was selected as the minimum requirement based on the preliminary experiments (Chapter 5) which indicated that at least 30 min is required to start swelling of the fish skin in 0.3 M NaOH solution. The 90 min was selected as the maximum time duration to avoid hydrolysis of collagen and to save time. A 0.3 M NaOH concentration was selected based on the preliminary experiments outlined in Chapter 4 and the swelling experiments carried out in Chapter 5. Experiments were done in a cold room at 4°C to assure that the processing conditions are maintained below the denaturation temperature. According to the results of Chapter 4, Td of cold-water fish collagen was found at 42°C which implies that the collagen is not denatured above 4°C. A sample of nominally 50 g was taken, and the exact mass was recorded. The mass to volume ratio of skin to NaOH solution was kept constant at 1:10. The exact weight (approximately 500 mL) of NaOH solution was recorded. Fish skin samples were soaked in this NaOH solution in a 1 L glass beaker and constantly stirred at 200 rpm using a magnetic stirrer (40 mm long stirring bar) for the particular time duration. After that, this mixture of skin and solution was kept undisturbed without stirring for 1 min to settle the skin at the bottom of the beaker. Then the solution was decanted into another beaker.

The treated skin was separated from any residual solution by filtering through a stainless steel strainer of 2 x 2 mm mesh size. The skin was left on the strainer for 10 min; by this time solution had stopped filtering through. The volume and weight of the filtrate was measured and stored for the later determination of dissolved non-collagenous protein content by means of total nitrogen content according to the Kjeldahl method using the same methods described above. The pretreated skin was weighed. It was frozen at -20°C and freeze-dried at 0.5 mbar pressure, 10°C temperature for 3 days (BUCHI LyovaporTM L-300, BUCHI Labortechnik AG; Flawil, Switzerland). The freeze-dried weight was recorded and stored for the determination of collagen protein content, fat content and ash content as previously described. All analysis was done in triplicate. The dependant variables were non-collagenous

proteins in the pretreated skin, non-collagenous proteins in the washed solution, fats in the pretreated skin and fats in the washed solution. Experiment was performed in a cold room at 4°C.

6.3.2 Calculations

6.3.2.1 Calculation of composition

By the end of pretreatment, all non-collagenous proteins should have been leached into the treatment solution. The collagen is retained in the skin. As explained above, each solution and the skin are then subjected to the Kjeldahl method to determine total nitrogen, where the conversion factors are N x (100/18) for collagen and N x (100/16) for non-collagenous proteins. The conversion factors are according to Mariotti et al. (2008). Therefore, the following balance equations apply.

$$M_{collagen,pretreated\ skin} = [\mathrm{N} \times (100/18)] M_{pretreated\ skin,dry\ basis}$$

$$M_{NCP,pretrmt\ soln} = [\mathrm{N} \times (100/16)] M_{pretrmt\ soln}$$

$$Percentage\ collagen\ in\ raw\ fish\ skin = \frac{M_{collagen,pretreated\ skin}}{M_{collagen,pretreated\ skin} + M_{NCP,pretrmt\ soln}} \times 100$$

where $M_{collagen,pretreated\ skin}$= mass of collagen protein in the skin after pretreatment [g], $M_{NCP,pretrmt\ soln}$ = mass of non-collagenous proteins in the filtrate after pretreatment [g], $M_{pretreated\ skin,dry\ basis}$ = mass of freeze-dried pretreated skin [g], $M_{pretrmt\ soln}$ = mass of filtrate after pretreatment, and N = percentage of nitrogen obtained from the Kjeldahl method [%].

Nearly 90% of all proteins was found to be present as collagen for all experiments regardless of experiment time. Therefore, the crude protein mass balance can be simplified to the skin containing 90% of the crude protein as collagen and 10% of the crude protein as non-collagenous proteins. In equation form this is

$$M_{CP,raw\ skin} = \left[N \times \left(0.9\left(\frac{100}{18}\right) + 0.1\left(\frac{100}{16}\right)\right)\right] M_{raw\ skin,dry\ basis}$$

where $M_{CP,raw\ skin}$ = grams of crude protein in raw skin [g], N = percentage of nitrogen obtained using the Kjeldahl method [%] and $M_{raw\ skin,dry\ basis}$ = mass of freeze-dried raw skin $[g]$

6.3.2.2 Corrections for the pretreated skin mass

After treating with NaOH solution, NaOH salts are retained in the pretreated skin, which adds to the recorded mass of the skin, and so must be removed to obtain an accurate skin-only mass. If not removed, the NaOH salts elevate the ash content.

Assuming that the ash minerals (other than NaOH) are not removed during pretreatment, but are instead retained within the skin, the NaOH content can be accounted for. For a starting sample of 50 g (wet basis) of raw skin, the NaOH mass balance is given as

$$\frac{M_{NaOH,pretreated\ skin}}{50\ g\ raw\ skin\ sample} = \frac{M_{ash,pretreated\ skin}}{50\ g\ raw\ skin\ sample} - \frac{M_{ash,raw\ skin}}{50\ g\ raw\ skin\ sample}$$

where $M_{ash,pretreated\ skin} = M_{NaOH,pretreated\ skin} + M_{ash,raw\ skin}$

This then allows the mass of pretreated skin to be expressed on a NaOH-free basis.

$$\frac{M_{pretreated\ skin,dry\ basis,NaOH-free\ basis}}{50\ g\ raw\ skin\ sample} = \frac{M_{pretreated\ skin,dry\ basis,with\ NaOH}}{50\ g\ raw\ skin\ sample} - \frac{M_{NaOH,pretreated\ skin}}{50\ g\ raw\ skin\ sample}$$

As explained in the methods section, the ash measurements were done on freeze-dried skin samples before and after pretreatment. The results for crude protein, fat and ash contents were then adjusted from a total basis to a NaOH-free basis.

6.3.2.3 Removal of non-collagenous proteins and fats with time

Pretreatment aims to remove the non-collagenous proteins and fats, however, some remain in the skin. The extent to which these are removed is compared across the range of 30-90 min, of pretreatment times. To calculate the amount of proteins and fats remaining in the skin, it is necessary to assume that some of the solubilised non-collagenous proteins remain with the liquid phase retained in the skin and that their concentration (relative to the amount of water in the skin) is equal to that washed into the pretreatment solution. Therefore, the following balance equations apply (Table 6.1).

Table 6.1 Mass balances determined in the experimental method.

Category	Balance equation
Raw skin	$M_{total,raw\ skin} = M_{water,raw\ skin} + M_{NCP,raw\ skin} + M_{collagen,raw\ skin} + M_{fat,raw\ skin} + M_{ash,raw\ skin}$
Raw skin crude protein	$M(CP, raw\ skin) = [N \times (0.9(100/18) + 0.1(100/16))]\ M(raw\ skin, dry\ basis)$ where $M_{collagen,raw\ skin} = \left[N \times 0.9\left(\frac{100}{18}\right)\right]$ $M_{raw\ skin,dry\ basis}$ and $M_{NCP,raw\ skin} = \left[N \times 0.1\left(\frac{100}{16}\right)\right] M_{raw\ skin,dry\ basis}$
Initial solution	$M_{initial\ soln} = M_{water,initial\ soln} + M_{NaOH,initial\ soln}$
Pretreated skin	$M_{total,pretreated\ skin} = M_{water,pretreated\ skin} + M_{NCP,pretreated\ skin} + M_{collagen,pretreated\ skin} + M_{fat,pretreated\ skin} + M_{ash,raw\ skin} + M_{NaOH,pretreated\ skin}$

Category	Balance equation
Solution after pretreatment	$M_{pretrmt\ soln} = M_{water,pretrmt\ soln} + M_{NaOH,pretrmt\ soln} + M_{NCP,pretrmt\ soln} + M_{fat,pretrmt\ soln}$
Crude protein balance	$M_{CP,raw\ skin} = M_{collagen,raw\ skin} + M_{NCP,raw\ skin} = M_{collagen,pretreated\ skin} + M_{NCP,ptretreated\ skin} + M_{NCP,pretrmt\ soln}$
Water balance	$M_{water,initial\ soln} = M_{water,pretreated\ skin} + M_{water,pretrmt\ soln}$
NaOH balance	$M_{NaOH,initial\ soln} = M_{NaOH,pretreated\ skin} + M_{NaOH,pretrmt\ soln}$
Fat balance	$M_{fat,raw\ skin} = M_{fat,pretreated\ skin} + M_{fat,pretrmt\ soln}$

The concentrations used in the results section are determined from the above masses, where;

$$C_{NCP,pretrmt\ soln} = direct\ measurement\ from\ Kjeldahl\ method$$

$$C_{NCP,pretreated\ skin} = \frac{M_{water,pretreated\ skin} C_{NCP,pretrmt\ soln}}{M_{pretreated\ skin,dry\ basis,NaOH-free\ basis}}$$

$$C_{fat,pretreated\ \ skin} = \frac{M_{pretreated\ skin,dry\ basis,with\ NaOH} C_{fat,pretreated\ skin,dry\ basis}}{M_{pretreated\ skin,dry\ basis,NaOH-free\ basis}}$$

$$C_{fat,pretrmt\ soln} = \frac{M_{fat,raw\ skin} - M_{fat,pretreated\ skin}}{M_{pretrmt\ soln}}$$

$$M_{pretrmt\ soln} = Mass\ of\ pretreatment\ solution\ after\ separating\ skin\ [g]$$

$$C_{NCP} = Concentration\ of\ noncollagenous\ protein\ in\ the\ pretreatment\ solution\ \left[\frac{g}{g}\right]$$

The best treatment time was selected based on the efficiency of removing non-collagenous proteins and fats.

6.3.3 Results and discussion

An initial series of experiments were conducted to determine the best treatment time, before investigating the other variables. The results are shown in Figure 6.2. In Figures 6.2(A) and (B), the non-collagenous protein concentration values varied within a very narrow range across the selected time durations of 30-90 min, with the 30-50 minute results showing the

best removal and also being very similar to each other. The 60-80 minute results had slightly poorer removal and were also similar to each other, with the 90 min result being in between. Analysis of Variances (ANOVA) showed that the differences are significant with treatment time ($p<0.05$). However, according to the Tukey pairwise comparison, the 90 min treatment time was not different to either the 30-50 min or the 60-80 min treatment times. When the removal of fats is considered in Figures 6.3(A) and (B), the results are all similar except at 90 min which shows better removal. However, ANOVA showed a significant difference with treatment time ($p<0.05$), due to the weighting of the 90 min result. This is confirmed by the Tukey pairwise comparison, which shows that the 90 min treatment is significantly better to each of the other treatment times ($p<0.05$).

Overall, considering both non-collagenous protein and fat removal, the 90 min pretreatment time was selected for all the following experiments. The dynamics found in this experiment are consistent with the kinetics of swelling found and reported in Chapter 5. This makes sense as swelling, provides access into the skin for the NaOH to hydrolyse non-collagenous proteins and wash out fats.

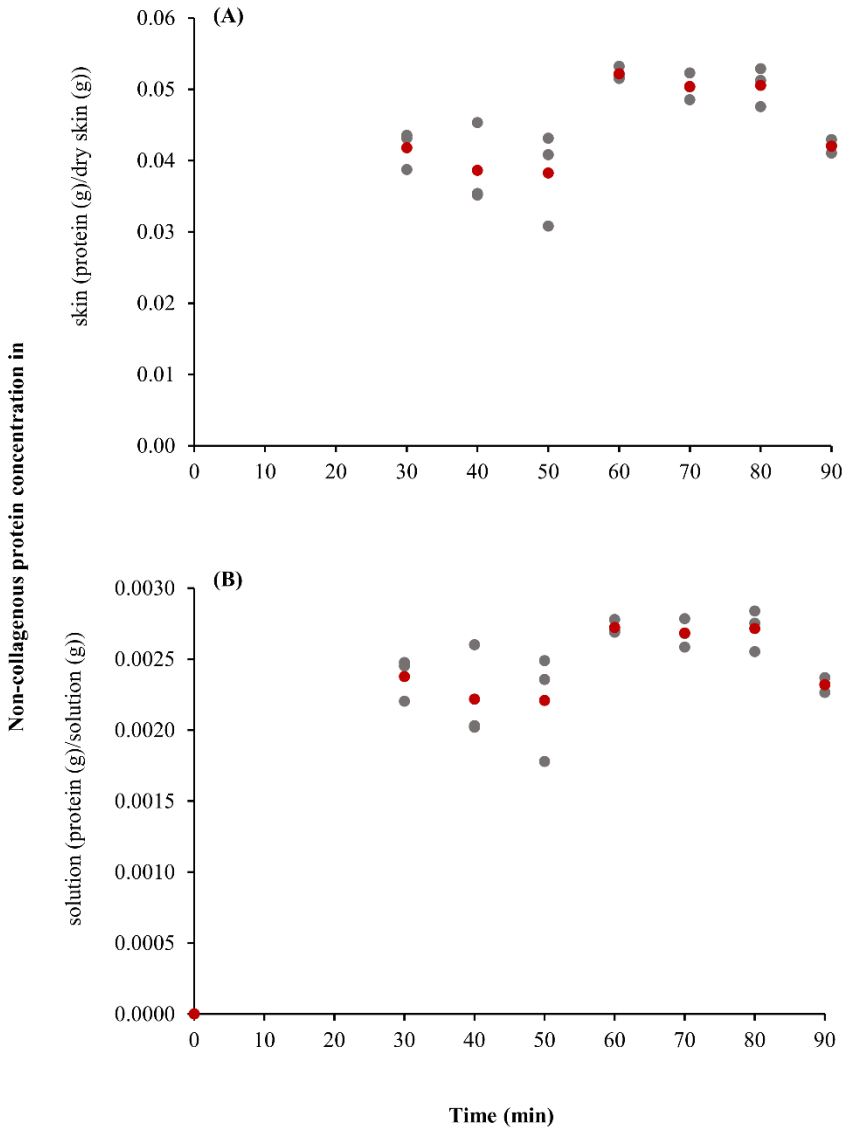

Figure 6.1 Removal of non-collagenous proteins from fish skin as a function of the time, varied from 30 to 90 min. Sub-figures show; (A), the non-collagenous protein remaining in the skin; (B), the non-collagenous protein in the pretreatment solution. Grey colour dots represent individual values and red colour dots represent average values.

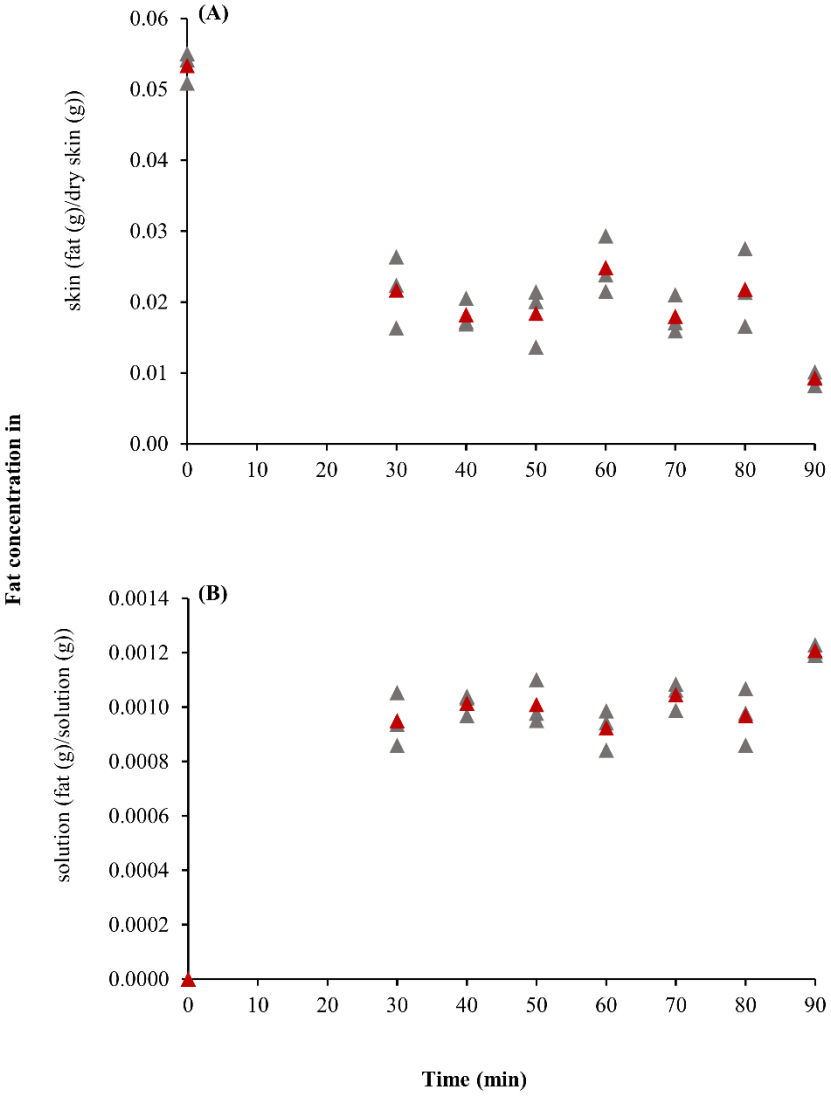

Figure 6.2 Removal of fats from fish skin as a function of the time, varied from 30 to 90 min. Sub-figures show; (A) the fat remaining in the skin; and (B), the fat in the pretreatment solution. Grey colour triangles represent individual values and red colour triangles represent average values.

6.4 Effect of skin mass to NaOH volume ratio

6.4.1 Experimental protocol

Ratios of 1:5, 1:10, 1:20 and 1:30 were selected for the mass of skin to the volume of NaOH solution. In industrial applications using the least amount of solution is desirable, but where the removal of non-collagenous proteins and fats is still achieved. This requires smaller vessels and results in more concentrated waste solutions that are easier to treat. A concentration of 0.3 M NaOH was used, as in the previous experiments.

For each treatment, a sample of *ca*. 50 g of fish skin was taken and its exact mass was recorded. Similarly, the exact volume and mass of NaOH solution were recorded. Fish skin samples were soaked in NaOH solution in a glass beaker (1 L for 1:5 and 1:10 ratios; 2 L for 1:20 ratio; 5 L for 1:30 ratio) and constantly stirred at 200 rpm using a magnetic stirrer (40

mm long stirring bar) for 90 min. The rest of the procedure was the same as the previous experiment where measurements were taken accordingly, and all calculations were the same. The best mass to volume ratio was defined to be that which removed the most grams of non-collagenous proteins and fats per gram of fish skin.

6.4.2 Results and discussion

Visual observations of the results (see Figures 6.4 and 6.5) were confirmed by ANOVA, where the mass to volume ratio had a significant effect on non-collagenous protein removal ($p<0.05$); however, it did not affect fat removal, although it does appear that fat removal in 1:10, 1:20 and 1:30 ratio solutions were higher than the 1:5 ratio solution. Therefore, considering both the non-collagenous protein and fat removal, and the need to choose the lowest effective ratio for industrial application, the 1:10 ratio was selected for all following experiments.

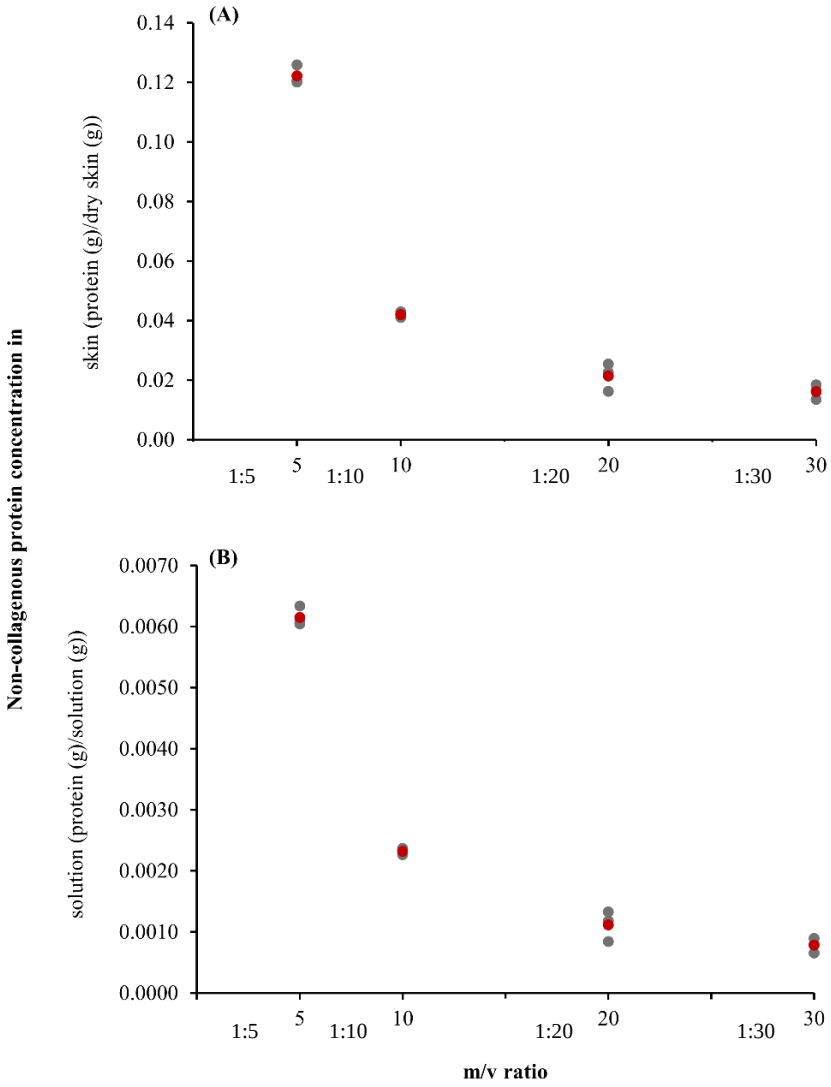

Figure 6.3 Removal of non-collagenous proteins from fish skin as a function of the mass of fish skin to volume of pretreatment solution ratio, varied from 1:5 to 1:30, for a soak time of 90 min. Sub-figures show; (A), the non-collagenous protein remaining in the skin; (B), the non-collagenous protein in the pretreatment solution. Grey colour dots represent individual values and red colour dots represent average values.

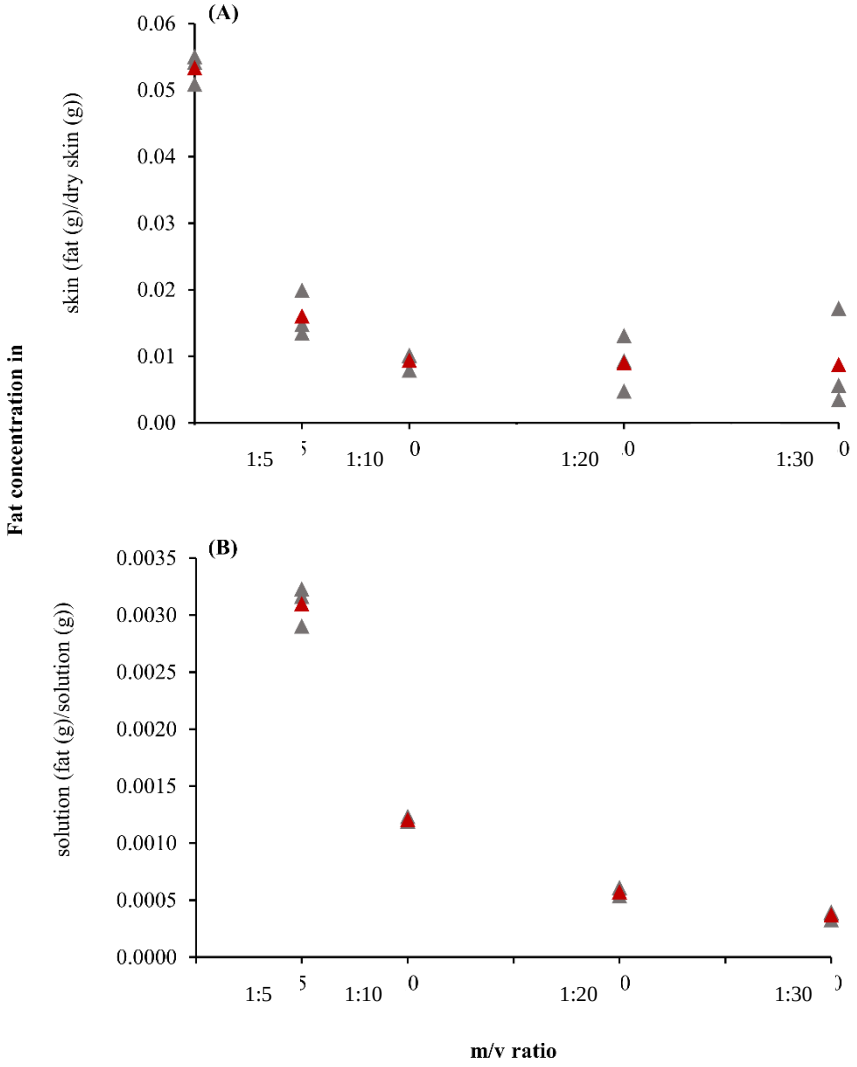

Figure 6.4 Removal of fats from fish skin as a function of the mass of fish skin to volume of pretreatment solution ratio, varied from 1:5 to 1:30, for a soak time of 90 min. Sub-figures show; (A) the fat remaining in the skin; and (B), the fat in the pretreatment solution. Grey colour triangles represent individual values and red colour triangles represent average values.

6.5 Effect of different treatment configurations

After fish skin has been soaked for 90 min and removed from the solution, it still contains residual non-collagenous proteins and fats, as shown in the above results. These need to be washed out. A series of wash treatments was then trialled to determine the most effective treatment. Two of these also altered the pretreatment step with the addition of a surfactant (SDS), targeting improved removal of fats.

6.5.1 Experimental protocol

The different subsequent wash treatment configurations were as shown in Table 6.2.

Table 6.2 Summary of alternative pretreatmnt configurations.

	Pretreatment step	Subsequent wash step
1	NaOH wash (1:10 m/v for 90 min)	None
2	NaOH wash (1:10 m/v for 90 min)	NaOH wash (1:10 m/v for 90 min)
3	NaOH wash (1:10 m/v for 90 min)	water wash (1:10 m/v for 90 min)
4	2% SDS in NaOH wash (1:10 m/v for 90 min)	None
5	2% SDS in NaOH wash (1:10 m/v for 90 min)	2% SDS in NaOH wash (1:10 m/v for 90 min)
6	NaOH wash (1:10 m/v for 90 min)	HCl wash (until pH 7)

In each experiment, a sample of *ca*. 50 g of fish skin was taken and its exact weight was recorded. As explained above, the mass of skin: volume ratio of pretreatment solution was kept constant at 1:10, and its exact volume and mass (*ca*. 500 mL) were recorded. Also, as described above, each fish skin sample was soaked in NaOH solution in a glass beaker (1 L) and constantly stirred at 200 rpm using a magnetic stirrer (40 mm long stirring bar) for 90 min. However, in trials 4 and 5 the pretreatment solution also had the addition of 2% SDS. Between the pretreatment and the subsequent wash step, the treated skin was separated using a stainless steel strainer of 2 x 2 mm mesh size until no further dripping occurred. Then it was soaked in the subsequent wash solution in a glass beaker (1 L), also at a 1:10 (m/v) ratio and stirred again at 200 rpm using a magnetic stirrer (40 mm long stirring bar) for 90 min.

After the sixth pretreatment and separation of the fish skin with a stainless steel strainer, the subsequent wash step is better described as a neutralisation step. Here, a solution of 0.1 M HCl was added little-by-by little with continuous mixing until the residue liquid achieved pH 7. The addition of this acid solution had the effect of shrinking the swollen skin, exuding liquid. The rest of the procedure, for these trials 1-6, was the same as the previous experiment, with measurements and calculations conducted in the same way. The best combination of pretreatment step and subsequent wash step was then selected to be that which removed the most grams of non-collagenous proteins and fats per gram of fish skin.

6.5.2 Results and discussion

The results (see Figures 6.6 and 6.7) show clear differences; first, that the subsequent washing with NaOH solution improves the removal of both proteins and fats; second, that subsequent washing with water does not improve the removal of fats; third, that the addition of 2% SDS only improved fat removal; and fourth, that subsequent neutralisation with HCl has a negative effect on the removal of fat.

The first observation was expected because replacing the solution and stirring for an additional 90 min will remove any remaining soluble proteins and fats. The second observation. that washing with water does not affect fat removal, is explained later with

respect to the fat chemistry, which also explains the fourth observation. For the third observation, there is a drawback in using SDS to treat fish skin in cold temperatures. SDS is not dissolvable in cold temperatures such as at 4°C used in these experiments. As maintaining cold temperatures is critical to avoid the denaturation of collagen in cold-water fish, this rules out SDS solutions as a treatment option. Here, it was also found that precipitated SDS powder was found deposited in the treated fish skin, which means that the SDS had not dissolved but rather was in suspension, and therefore not acting as a surfactant.

The statistical analysis supports the general observations. Non-collagenous protein removal from the skin was significantly different between trials 1-6 (ANOVA, $p<0.05$). According to the Tukey pairwise comparison, trials 1 and 4 showed the same effect, but all other pairwise comparisons were significantly different from each other (i.e., 2:3, 2:5, 2:6, 3:5, 3:6 and 5:6). Fat removal from the skin was also significantly different between trials 1-6 (ANOVA, $p<0.05$). According to Tukey pairwise comparison, trials 2, 4 and 5 showed the same effect, but all the other pairwise comparisons were significantly different from each other (1:3, 1:6 and 3:6).

The variability in the amount of fats present in the pretreated skin after different treatment configurations can be explained as follows. The crude fat content in the pretreated freeze-dried skin was analysed by the Soxhlet method. Crude fat includes phospholipids, sterols, free fatty acids, carotenoids, chlorophyll, and some other minor compounds, in addition to the fats. In trials 1 and 2, fat reacts with NaOH and produces sodium salts of fatty acids and glycerol as shown in Figure 6.8. These sodium salts of fatty acids are dissolved in water and therefore do not contribute to the crude fat. When water is added to these sodium salts of fatty acids as done in trial 3, it forms free fatty acids which contribute to the crude fat. When HCl is added to the sodium salts of fatty acids as done in trial 6, it forms free fatty acids which contribute to the crude fat content. This is likely to be the cause that trials 3 and 6 show higher amounts of fat compared to trial 1. This implies that the actual fat content in the form of triglycerides in trials 1, 3 and 6 are almost similar despite the different recorded concentrations.

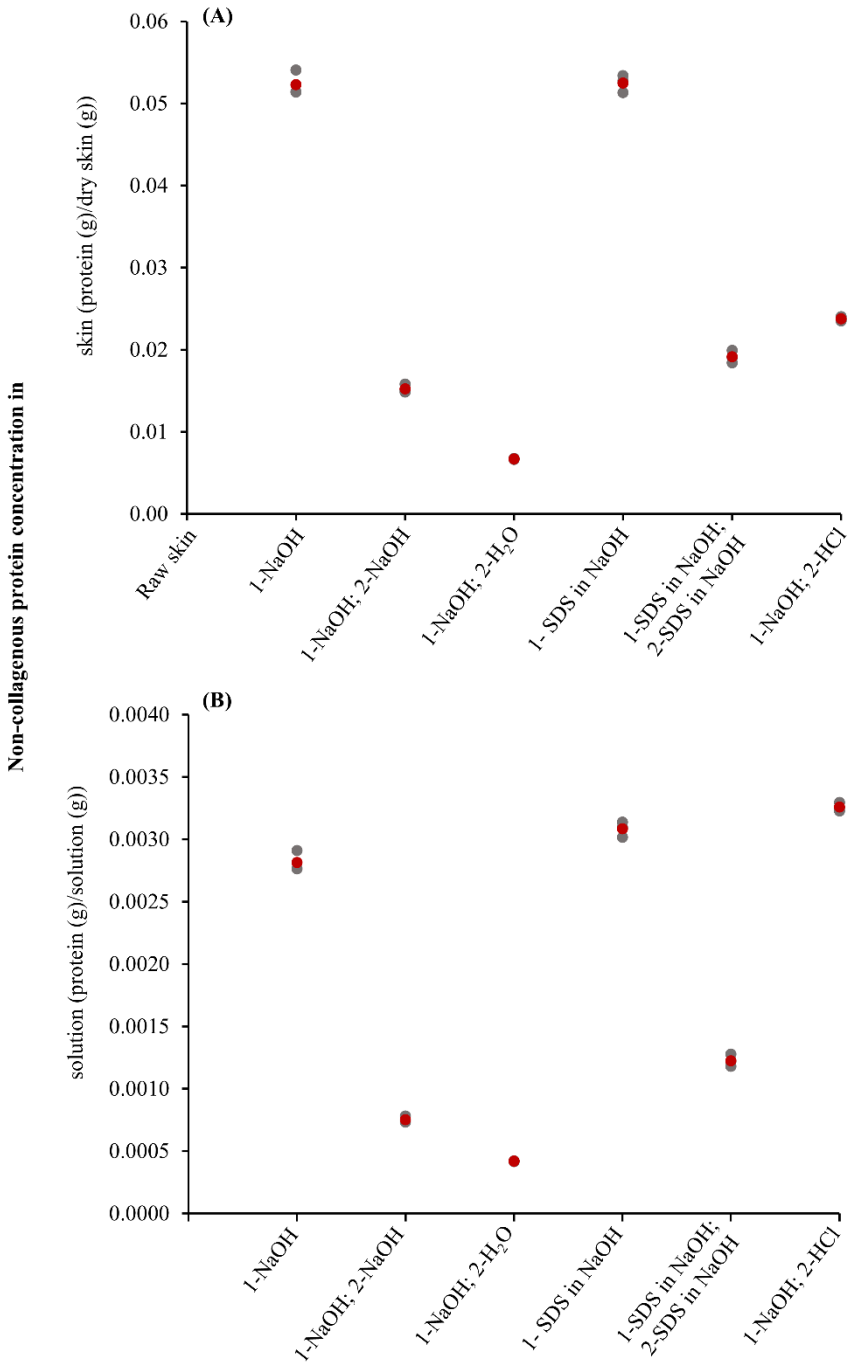

Figure 6.5 Removal of non-collagenous proteins from fish skin for the combinations of pretreatment and subsequent wash steps. Each uses a 1:10 ratio for both the mass of fish skin to volume of pretreatment solution, and to the subsequent wash solution. Soaks times are 90 min. Sub-figures show; (A), the non-collagenous protein remaining in the skin; (B), the non-collagenous protein in the pretreatment solution. Grey colour dots represent individual values and red colour dots represent average values.

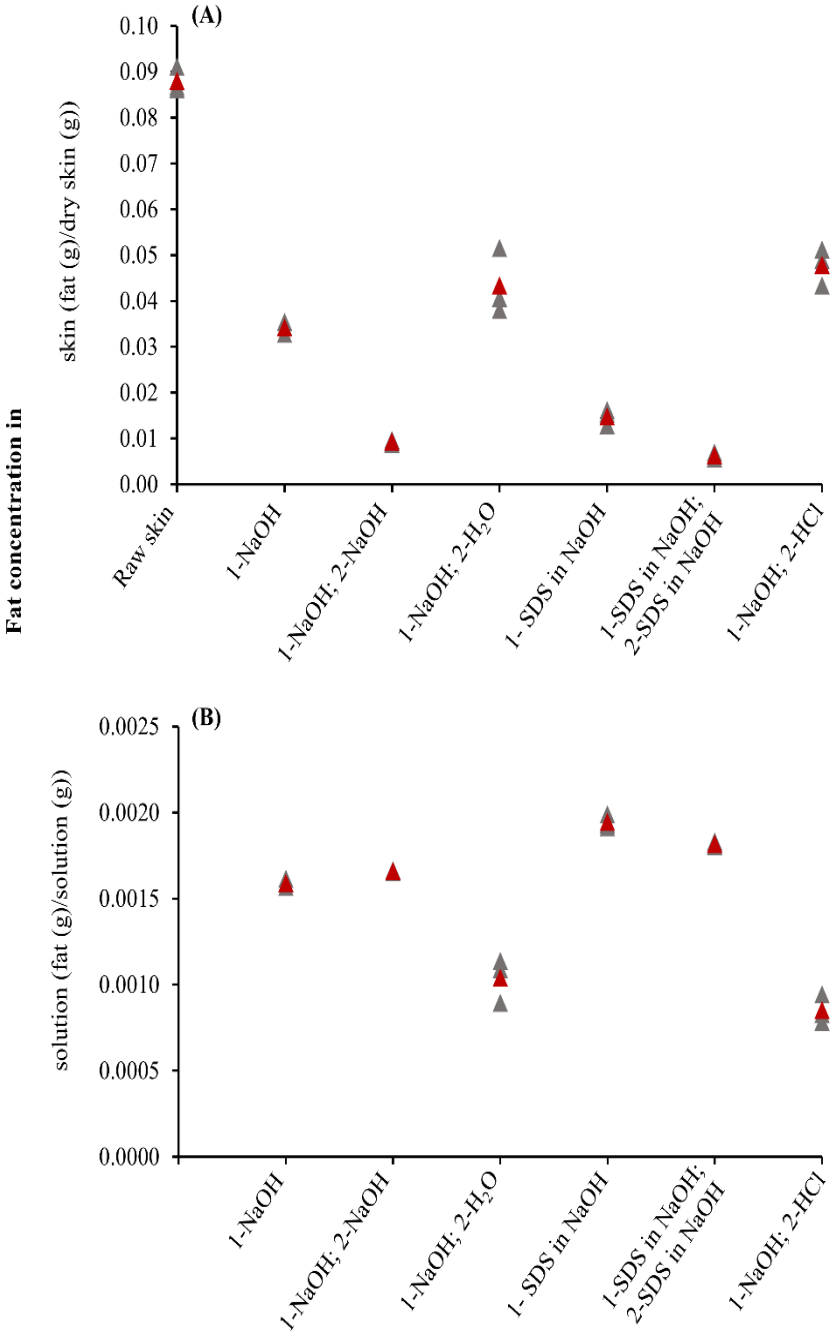

Figure 6.6 Removal of fats from fish skin for the combinations of pretreatment and subsequent wash steps. Each uses a 1:10 ratio for both the mass of fish skin to volume of pretreatment solution, and to the subsequent wash solution. Soaks times are 90 min. Sub-figures show; (A), the fat remaining in the skin; (B), the fat in the pretreatment solution. Grey colour triangles represent individual values and red colour triangles represent average values.

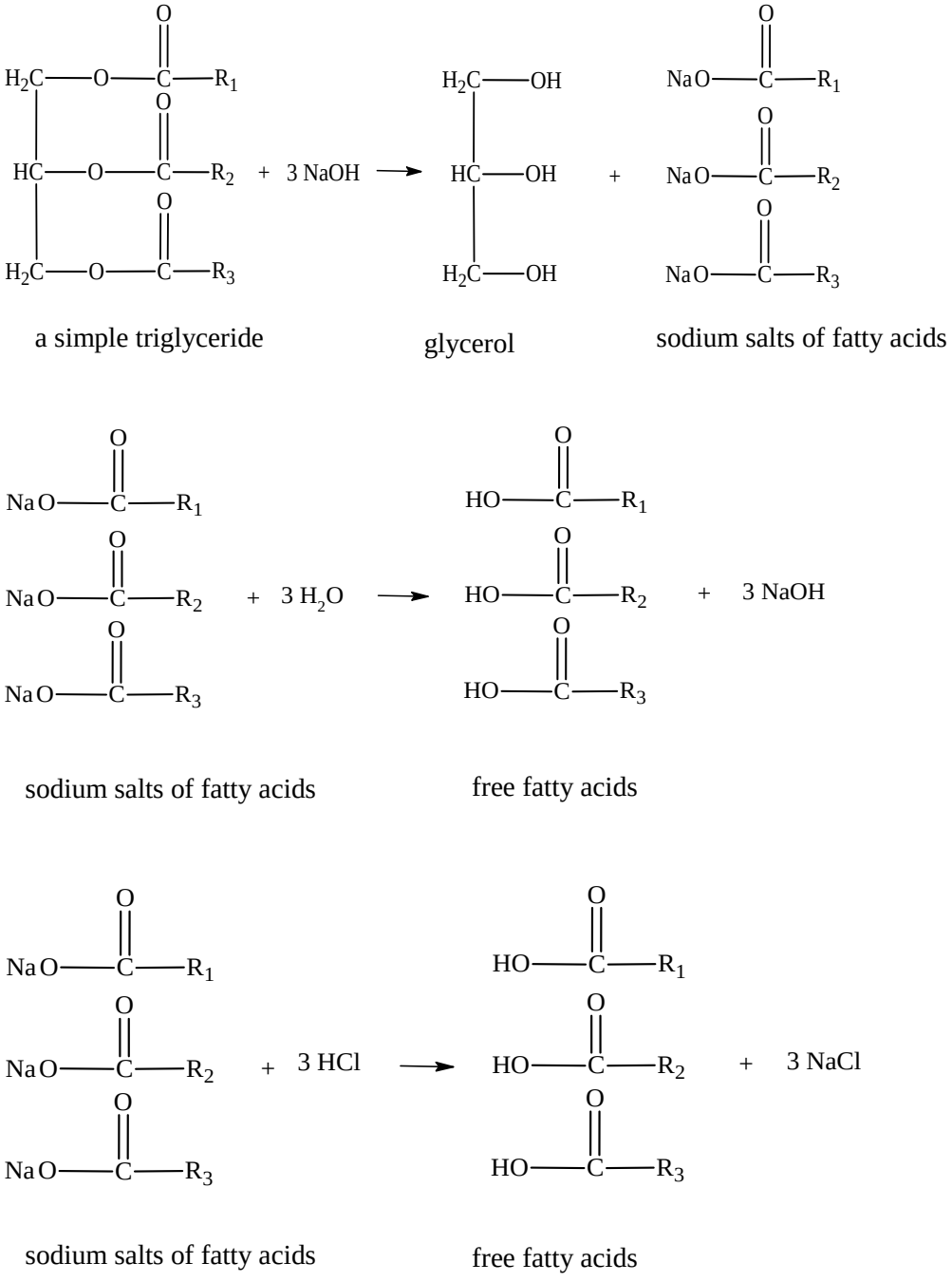

Figure 6.7 Reactions of fatty acids with NaOH, H_2O and HCl.

Based on the necessity to remove both non-collagenous proteins and fats, the method given in trial 2, i.e., a pretreatment and subsequent wash with NaOH, was selected to incorporate into the overall pretreatment process, making it now a two-step process. However, this still needs to be developed into a complete process, because the NaOH salts remain within the skin. Literature studies achieve this by washing with distilled water until neutral pH is achieved, which involves high consumption of water and time, generally overnight (Chapter 4). In this study, our focus on developing an industrially relevant process means minimising water wastage, cost and time. Therefore, a third step, neutralisation with HCl was assessed as an alternative to water washing. Trial 6 above, explored this after a single NaOH pretreatment

step, and showed benefit in removing additional non-collagenous proteins. Here, a HCl neutralisation was trialled after two NaOH washes, which was expected to enhance this effect. However, the reaction of HCl with the sodium salts of fatty acids produces NaCl salts which are then present as residues in the skin. These residues need to be washed from the skin before the later collagen extraction process. Therefore, a fourth step, a water wash, was incorporated. The effect of this final water wash and the frequency of washing were assessed in the next experiment.

6.6 Washing off the salts

As explained above, the determined pretreatment process consists of two NaOH washes followed by neutralisation with HCl. Here, because residual salt, NaCl, remains in the skin, this stage of the process development explores a washing step to remove the salt solution. Two different procedures were experimented as follows:

Procedure A

1. 0.3 M NaOH wash at 1:10 m/v ratio for 90 min
2. 0.3 M NaOH wash at 1:10 m/v ratio for 90 min
3. Neutralise with 0.1 M HCl
4. Water wash at 1:10 m/v ratio for 90 min

Procedure B

1. 0.3 M NaOH wash at 1:10 m/v ratio for 90 min
2. 0.3 M NaOH wash at 1:10 m/v ratio for 90 min
3. Neutralise with 0.1 M HCl
4. Water wash at 1:10 m/v ratio for 90 min
5. Water wash at 1:10 m/v ratio for 90 min

6.6.1 Methodology

A sample of about 50 g was taken and the exact weight was recorded. The sample was treated according to the above procedure in a glass beaker with constant stirring at 200 rpm using a magnetic stirrer for each of a series of steps. Once each treatment time was reached, the mixture of skin and solution was kept undisturbed without stirring for 1 min to settle the skin at the bottom of the beaker. Then, the solution was removed as much as possible by decanting it into another beaker. Then the treated skin was separated from the leftover solution by filtering through a stainless steel strainer of 2 x 2 mm mesh size. The skin was left on the strainer for 10 min, by which time the solution stopped filtering. It was then added to the next treatment solution and the same procedure was repeated until the end.

The volume and weight of the filtrate were measured and stored for the determination of dissolved non-collagenous protein content using total nitrogen content according to the Kjeldahl method. The pretreated skin was weighed. It was frozen at -20°C and freeze-dried. The freeze-dried weight was recorded and stored for the determination of collagen protein content, fat content and ash content as previously described. The dependent variables were collagen protein in the pretreated skin, non-collagenous proteins in the filtrate, fat in the pretreated skin and fat in the filtrate. The calculations were done as explained earlier. All the

experiments were done in triplicate. The best pretreatment process was selected based on the efficiency of removing non-collagenous proteins and fats.

6.6.2 Results and discussion

The concentration of non-collagenous proteins for both procedures were found below the lower detection limit of Kjeldahl protein analysis (0.1 mgN) indicating the successful removal of non-collagenous proteins from both procedures. Fat removal was not significantly different between the two procedures (ANOVA, $p<0.05$) (Figure 6.8). Process A was selected as the final treatment because, with four steps instead of five, it is the simpler of the two procedures.

However, the results show there is still some fats present in the pretreated skin, which ideally would be removed. This may be due to the same reason associated with crude fat determination by the Soxhlet method as explained earlier, caused by the neutralisation, in step 3, where HCl helps form free fatty acids which contribute to the measured crude fat content.

In addition to non-collagenous protein and fat removal, pigment removal was also expected from the pretreatment step. The presence of pigments in the final collagen product gives an undesirable colour which is not acceptable. In this study, pigment removal by the pretreatment process was not successful, as shown by the remaining slight discouloration after step four of Procedure A in Figure 6.9. However, complete pigment removal was achieved by a filtration step at the end of the collagen fibrillogenesis process described in Chapter 8.

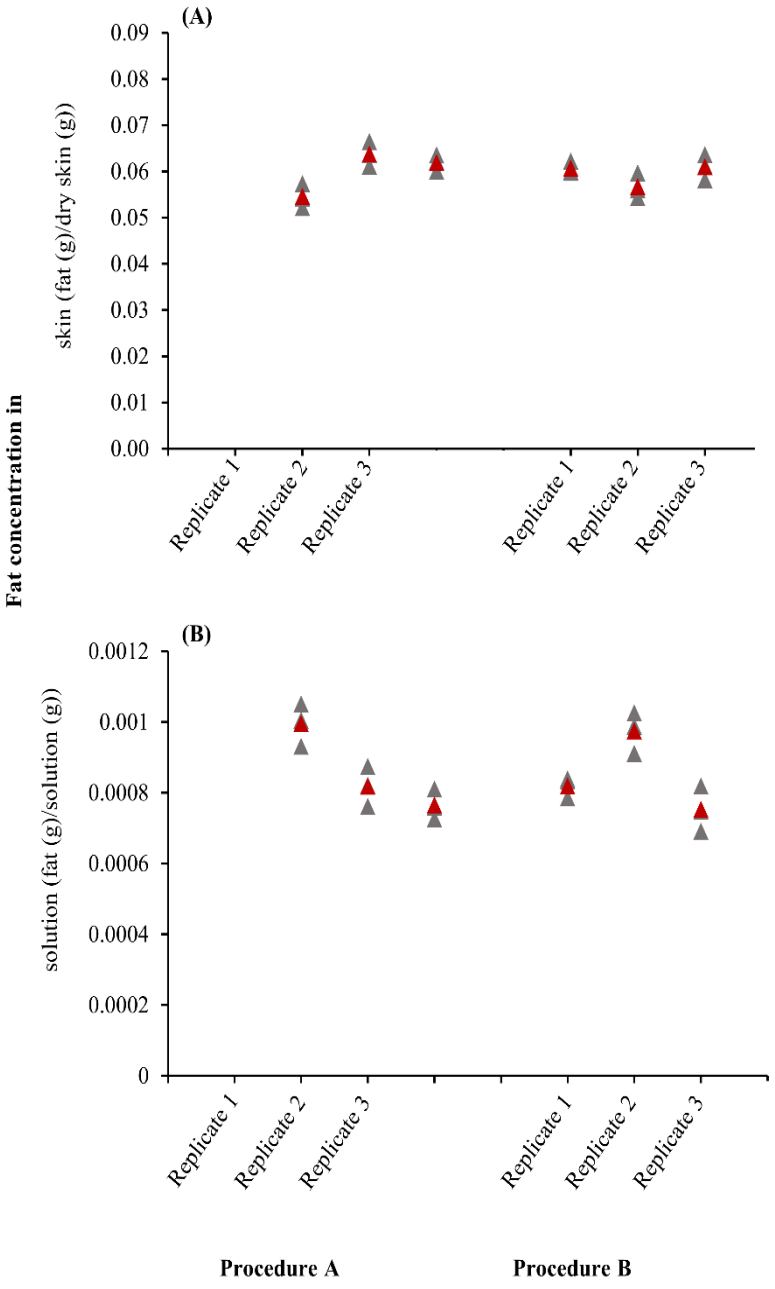

Figure 6.8 Removal of fats from fish skin for the two pretreatment procedures; Procedure A and Procedure B. Sub-figures show; (A), the fat remaining in the skin; (B), the fat in the pretreatment solution. Grey colour triangles represent individual values and red colour triangles represent average values.

Figure 6.9 Photographs of the fish skin after steps 1-4 of procedure A. Step 1: 0.3 M NaOH wash at 1:10 (m/v) ratio for 90 min; Step 2: 0.3 M NaOH wash at 1:10 (m/v) ratio for 90 min; Step 3: Neutralise with 0.1 M HCl; Step 4: Water wash at 1:10 (m/v) ratio for 90 min.

6.7 Conclusions

This chapter has developed a rigorous procedure for pretreatment of fish skin to remove non-collagenous proteins, fats and pigment, prior to the later steps of extraction and fibrillogenesis. The procedure developed here is mindful of the commercial imperative for a cost-effective process, minimising water wastage and minimising the number of processing steps. This work, therefore, presents a guideline for scale-up to the industrial level, and for use on other fish as a starting methodology, whether or not they have similar or different protein and fat contents. The outcome of the pretreatment procedure described here is that non-collagenous proteins are removed below the lower detection limit of Kjeldahl method, some fat remains, which is expected to be related to the effect of free fatty acid formation in procedure A - step 3, and not all pigments are removed as shown by the discolouration. However, this pretreatment procedure is effective, because the later steps of extraction and fibrillogenesis, result in further purification. The next two chapters discuss the optimisation of the extraction and fibrillogenisis steps.

Chapter 7. The effect of process conditions on collagen extraction

7.1 Introduction

Type I collagen is a right-handed supercoiled triple-helix molecule composed of three left-handed α-helices (Bhuimbar et al., 2019; Brown et al., 2000). The stability of this super helical structure is maintained by two main forces: the steric hindrance or the conformational restrictions imposed by the pyrrolidine rings of the imino acids (proline and hydroxyproline) (Nagai et al., 2008; Jenkins & Raines, 2002), and the intramolecular hydrogen bonds formed through the hydroxyl groups between glycine and hydroxyproline (Zeugolis et al., 2008; Nagai et al., 2008; Jenkins and Raines, 2002). When these collagen molecules are arranged into fibres, lysine-derived covalent cross-links occur between the non-helical end of one collagen molecule and the helical region of another collagen molecule (Hofman et al., 2012). During collagen extraction it is important to preserve the intramolecular hydrogen bonds but break the intermolecular covalent cross-links.

Collagen extraction begins by the hydration and swelling of collagen fibres which facilitates the exposure of collagen to the extraction medium (Skierka & Sadowska, 2007). As the swelling occurs, the inter-molecular cross-links are cleaved and collagen molecules become soluble in the medium, but retain their triple-helical structure (Schmidt et al., 2016). This dissolution step is necessary because these collagen molecules self-assemble back into fibres during the subsequent fibrillogenesis step. The most important factor is that the solubilised collagen remains in its native triple-helical conformation (Qi et al., 2015). If this structure is broken or the collagen molecules are hydrolysed, they cannot self-assemble into fibres with the required D-spacing which is essential for biomedical applications (Zhu et al., 2018). The effectiveness at each step of the extraction is determined by the fish-type and processing conditions. Variables include the type and concentration of the acid (or pH), mass to volume ratio of the skin and acid, duration of extraction, and temperature of processing. These effects have been described in detail in Chapter 2.

Many researchers have described the importance of a mild chemical treatment, mainly using acetic acid for this purpose. The higher efficiency of acetic acid over hydrochloric acid (Skierka and Sadowska, 2007; Wang et al., 2008; Schmidt et al., 2016; Liu et al., 2015) in relation to breaking cross-links, solubility of collagen and higher extractability (Liu et al., 2015) have been mentioned without proper explanation of the reasons. However, acetic acid has drawbacks for biomedical collagen extraction. Due to the incomplete ionisation nature of acetic acid, it can be adsorbed onto collagen molecules and can remain as residues in the final freeze-dried collagen product (Qi et al., 2015). Bak et al. (2018) prepared porous scaffolds using porcine skin collagen by dissolving in acetic acid and water separately while keeping all other conditions similar. They reported that acetic acid residues are not suitable to maintain a stable environment for cells in cell therapy-related applications. Furthermore, they reported that acetic acid residues make larger pores with weaker pore walls during freeze-drying which cause inferior structural modifications. A denaturation temperature of 225°C in the dehydrated state was recorded for collagen scaffolds made with water while reporting the denaturation of collagen scaffolds made with acetic acid. These facts are described in detail in Chapter 2 (§2.4.3). Therefore, traditional extraction methods using acetic acid, (for example,

Muralidharan et al., 2013; Li et al., 2013; Wang et al., 2008; Xu et al., 2017) require dialysis steps to remove the acetic acid residues, which introduces additional costs for industrial application. In addition, extraction of collagen with acetic acid involves longer extraction times, usually for 72 h (Ahmed et al., 2019; Muralidharan et al., 2013; Pal & Suresh, 2015), which is another drawback at the industrial-scale.

An alternative is to use HCl solution. In solution, HCl ionises to H^+ and Cl^- ions, where only the H^+ ions adsorb to collagen molecules (Zhou et al., 2018). The Cl^- ions adsorb only in highly acidic conditions (below pH 2) which can lead to decreased hydration and low solubility (Skierka & Sadowska, 2007). However, conditions below pH 2 are not used due to the denaturing effect (Skierka & Sadowska, 2007), therefore, the use of HCl acid above pH 2 avoids the drawback of having acid residues in the collagen product. For these reasons, HCl acid was selected as the extraction medium in this research. The preliminary experiments (Chapter 4-5) demonstrated marine collagen could be derived using HCl. Secondly, the HCl concentration of 0.01 M (pH 2) was selected based on the understanding from the swelling experiments with HCl (Chapter 5).

In the collagen extraction processes, the raw material is soaked in extraction medium with agitation until collagen molecules are completely solubilised. Longer extraction times can denature the collagen molecules and shorter extraction times can cause incomplete solubilisation of collagen due to incomplete cleavage of the cross-links (Skierka & Sadowska, 2007). In addition, longer extraction times are not cost and time effective at industrial-scale. Therefore, homogenisation was used in this study to first break down the swollen skin to small pieces, and so speed up the collagen solubilisation. Homogenisation is a high-shear activity which causes heating and can cause denaturation of collagen. Therefore, care should be taken to pulse homogenisation to avoid unduly increasing the temperature of the extraction medium.

Homogenisation has been applied in collagen extraction processes by previous researchers, but in different ways to this study. Sadowska et al. (2003) and Hwang et al. (2007) used homogenisation for pretreatment of the skin, but details about their methods or purpose were not reported. There are no references in the literature on homogenisation during extraction. Homogenisation promotes solubilisation, and so improves the extraction efficiency. Nevertheless, incomplete solubilisation can leave skin pieces which are visible to the naked eye. This was used as a measure of the homogenisation-solubilisation efficiency. The homogenisation and solubilisation produces a viscous solution in which the viscosity varies with the extraction conditions, such as mass to volume ratio, extraction time and temperature. The viscosity is important for the fibril formation during fibrillogenesis, which is the final step of collagen processing. The effect of swelling, pH, solubility of collagen, and viscosity should be studied together for a proper understanding of the collagen extraction process, which is generally lacking in published literature. This knowledge is important to understand the behaviour of fish skin in the extraction medium, and design efficient extraction processes. Most importantly, the method of extraction should be capable of extracting the collagen in its native triple-helical form for biomedical applications (Sun et al., 2020). Therefore, a more detailed characterisation of collagen using different techniques was done in this study to determine the effect of a range of extraction conditions on the triple-helical structure.

The experiments in this chapter were designed to study the different sub-steps (Figure 7.1) of the extraction process in relation to the behaviour of fish skin. Extraction time, and mass to volume ratio of fish skin to HCl acid solution were used as the process variables. The aims of this chapter were therefore to develop the understanding of the effect of these processing variables in relation to the changes in skin and extraction medium and to develop an extraction process. The quality of collagen, the time and cost- effectiveness, minimum use of chemicals, water, and energy were considered in selecting the processing conditions for the extraction process.

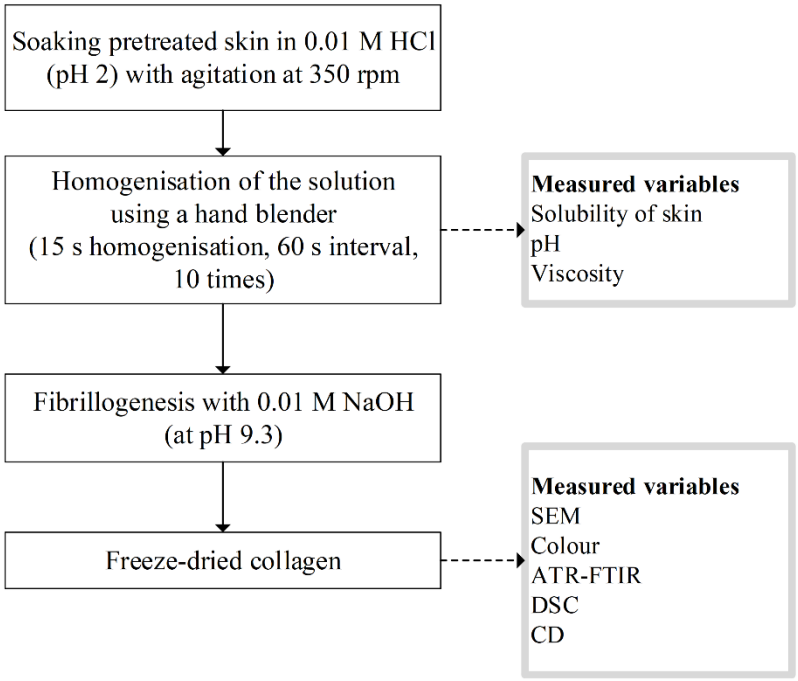

Figure 7.1 Flow diagramme of collagen extraction and subsequent fibrillogenesis showing the measured variables.

7.2 Materials and methods

The extraction time in 0.01 M HCl solution and the mass to volume ratio of skin to HCl solution were selected as the independent variables. There were 20 treatments experimented, by selecting the combinations of five extraction times; (0.5 h, 1 h, 2 h, 5 h, and 8 h) and four mass to volume ratios; (1:10, 1:15, 1:20, and 1:25).

7.2.1 Sample preparation

Tarakihi fish skin was used as the raw material. The fish skin was minced and 50.00 g samples were selected according to the method in §6.2. The samples were then pretreated according to the method developed in Chapter 6 where, to recall, each sample was soaked in 0.3 M NaOH solution at 1:10 weight to volume ratio for 90 min with continuous stirring at 200 rpm using a magnetic stirrer. After 90 min, the skin was separated from the solution using a strainer of 2 x 2 mm mesh. Then, this skin was added into a fresh 0.3 M NaOH solution and the procedure was repeated, after which the skin was neutralised with 0.1 M HCl, and similarly filtered through the strainer. Distilled water was then added at 1:10 mass to volume ratio and soaked

for 90 min with the same continuous stirring, and again filtered through the strainer. The skin was then left on the strainer until the solution stopped dripping. The weight of the skin was recorded. The dry matter content of a representative sample was determined by oven drying.

7.2.2 Experimental protocol

The mass to volume ratio was based on the 50.00 g of raw skin mass taken after mincing as described above. HCl solutions of 0.01 M concentration were prepared separately for each of the 20 treatments. The initial pH of these HCl solutions were recorded. For each treatment, pretreated fish skin samples were soaked in HCl solutions in 2.5 L plastic containers and constantly stirred at 350 rpm using a magnetic stirrer (40 mm long stirring bar). After the particular extraction time, the weight of swollen skins and the pH of the solutions were recorded. Then, they were recombined and homogenised using a hand blender (Kenwood Triblade Systempro, 1000 W) at high speed for 15 s followed by a 60 s rest interval to avoid overheating, and repeated 10 times. A preliminary experiment (data not shown) was performed which showed that 10 x 15 second homogenisation pulses achieved adequate structural breakdown. By keeping each pulse short and by resting the samples for 60 s between pulses, avoided the samples from overheating. The temperature of the solution was monitored during homogenisation to keep it below 10°C. At the completion of homogenisation, a 1.5 mL vial of the homogenised solution was taken from the top middle region to analyse the solubility of the skin as described below. The pH and the weight of the homogenised solution were measured, after which the solution viscosity was measured, using the procedure described below, and the pH was again recorded just before fibrillogenesis. For all the samples, homogenisation and viscosity measurements were completed within 40 min.

Collagen fibres were then formed in each homogenised solution by slowly adding NaOH solution of 0.01 M concentration until pH 9.3 was reached. This precipitated collagen fibres leaving a colourless solution. Then, the solutions were kept undisturbed for 10 min before separation from the fibres by filtering through a strainer of 2 x 2 mm mesh size. These fibres were then packed in polythene bags, frozen at -20 °C and freeze-dried at 0.5 mbar, 10 °C. The weight of the freeze-dried collagen was recorded. The freeze-dried collagen was characterised for colour, morphology, and native structure. All the experiments were done in a cold room at 4°C.

7.2.2.1 pH of the solutions

The pH of the solutions was measured using a portable pH meter (Thermoscientific, Orion Star A326 pH/RDO/DO meter). It was calibrated every time according to the manual (Thermo Scientific 2015).

7.2.2.2 Solubility of the skin after homogenisation

The 1.5 mL vial sample taken from the homogenised solution as described above was put into a glass petri dish of 14.32 mm diameter. A 7.5 mL volume of distilled water and 1.0 mL of Coomassie blue staining solution were added to the same petri dish and mixed well using a glass rod. The petri dish was put in a flat-bed scanner with a dark background and scanned at 2400 dpi resolution and saved as a colour *.jpg image. These images clearly differentiate the undissolved skin pieces from the dissolved skin in the solution. The estimation of the homogenisation efficiency was based on the amount of undissolved skin pieces in the 1.5 mL

sample. The areas of these undissolved skin pieces were measured using the ImageJ software version 1.53t. The areas similar or higher than 2 mm^2 were taken as undissolved skin pieces and compared between different treatments.

7.2.2.3 Viscosity of the solutions after homogenisation

Viscosity was used as a measure of dynamics of solutions over time. Characterisation of the rheology of the system was not considered in this experiment as it needs sophisticated instruments like rheometers. The well-mixed homogenised collagen sample was poured to the 500 mL mark of a 600 mL glass beaker and the viscosity was measured using spindle number 4 at 10 rpm in a Brookfield viscometer (Brookfield viscometer DV2T extra, Brookfield Engineering Laboratories, Middleboro, USA). Spindle 5 was used to measure the viscosity above 20,000 cP. Ideally, the temperature was maintained between 9-10 °C. The viscosity was measured three times. Brookfield viscometer is useful in the industry due to its simple operation.

7.2.2.4 Yield of collagen

The dry matter content of the pretreated skin was estimated using oven drying at 105°C for 24 h (AOAC 930.15). For collagen, the reference freeze-dried weight was taken as the dry weight. Yield was calculated as dry collagen (g) per dry weight of pretreated fish skin (g).

$$\text{Yield} = \left(\frac{M_{Freeze-dried\ collagen}}{M_{Dry\ matter\ in\ pre-treated\ skin}}\right) \times 100\%$$

7.2.2.5 Morphology and microstructure of collagen

Optical photographs were taken to show the visual differences of collagen under the naked eye. Microstructure of collagens was analysed by scanning electron spectroscopy (SEM). For SEM, the freeze-dried collagen samples were mounted onto aluminium stubs using double-sided tape to ensure high electrical conductivity between the specimen and the stub. Then, it was sputter-coated with approximately 100 nm of gold (Baltec SCD 050 sputter coater) and viewed in the FEI Quanta 200 Environmental Scanning Electron Microscope (Hillsboro, USA) at an accelerating voltage of 20 kV.

7.2.2.6 Colour

The colour of freeze-dried collagen samples was measured using a spectrophotometer (Minolta CR-400). The instrument was calibrated using the white standard (L*=83.86, a*=0.72, b*=5.91). The L* (lightness), a* (redness⁄greenness) and b* (yellowness⁄blueness) colour coordinates were recorded from five places in each sample, and the total difference of colour (ΔE*) was calculated according to the following equation (Pal and Suresh 2015):

$$\Delta E* = [(\Delta L*)^2 + (\Delta a*)^2 + (\Delta b*)^2]^{1/2}$$

where ΔL^*, Δa^* and Δb^* are the differences between each five place of a sample and the white standard.

7.2.2.7 Characterisation techniques to determine the native triple-helical structure

The collagen samples prepared in this experiment were characterised using the methods outlined in §Chapter 4.2.8 (ATR-FTIR, DSC and CD). A summary of each method is given below for convenience.

The ATR-FTIR spectra were used to assess the type of collagen and the native triple-helical conformation. The ATR-FTIR spectra were obtained using a Nicolet iS5FTIR spectrometer (Wisconsin, USA) equipped with an iD7 ATR diamond sampler accessory. A small piece of freeze-dried collagen was placed on the single reflection crystal cell. The signals were automatically collected for 32 scans over the 4000-400 cm^{-1} range using 2 cm^{-1} resolution. Background spectra were collected from the clean empty crystal cell.

Differential Scanning Calorimetry (DSC) was used to determine the thermal properties of collagen. Small pieces of freeze-dried collagen between 3-4 mg were cut and accurately weighed. They were hydrated in a beaker by adding excess cold deionised distilled water. The samples were held underwater for 2-3 min with a clean spatula to speed up the hydration. The hydrated collagen was removed from the water and stuck to the side of the beaker where they were quickly blotted with filter paper to remove excess water until water was no longer dripping. The hydrated samples were placed into aluminium pans and accurately weighed and hermetically sealed. Differential scanning calorimetry was performed using a TA Systems Q2000 DSC (TA Instruments, Inc., New Castle, DE, USA). Temperature and enthalpy calibration was done using water and indium as standards. The samples were scanned in a nitrogen atmosphere from an initial temperature of 5°C held isothermal at this temperature for 1 min. Two identical ramp profiles were subsequentially carried out consisting of a ramp up at 5°C/min to 85°C, then ramp down at 20°C/min to 5°C, then held isothermal at this temperature for 1 min, after which the cycle was repeated. Iced water was used as the cooling medium (TA systems refrigerated cooling system 40), and an empty sealed pan was used as the reference. The denaturation temperature was determined from the maximum transition point (the endothermic peak) of the thermal denaturation curve. The total denaturation enthalpy was estimated by measuring the peak area in the DSC thermogram based on the dry weight of the sample and expressing this as J/g sample. The onset temperature was also determined.

Circular Dichroism (CD) spectroscopy was used to assess the native triple-helical conformation of collagen. The freeze-dried collagen samples were dissolved in 0.05 M acetic acid to a concentration of 0.1 mg/mL. Solutions were filtered through a Whatman grade 1 filter paper to remove any undissolved material. Then, the mixtures were equilibrated at 4°C for 48 h before testing. The concentrations of the samples, which should all be the same, were verified by measuring the absorption at 192 nm (Bürck et al., 2012). The degree of ellipticity was recorded with a spectropolarimeter (Chirascan, Applied Photophysics, Leatherhead, UK) using a standard quartz cuvette of 1 mm pathlength (Hellma high-precision cells, Mullheim, Germany). Samples were scanned with a wavelength range from 260 to 180 nm at 0.5 nm intervals. Each sample was scanned five times at a scan rate of 40 nm/min, 0.5 s response time and 1 nm bandwidth. The same acetic acid of 0.05 M concentration which was used to prepare the samples was used to record the baseline. The same cuvette was used for baseline and samples. The temperature of the cell holder was maintained at 10°C using a temperature control unit (Quantum Northwest). The dynode voltage of all samples was checked to ensure

they were below 600 V (Drzewiecki et al., 2016). The ellipticity measurements were averaged and the spectrum of 0.05 M acetic acid solution was subtracted from each sample spectrum. The degree of ellipticity values were converted to mean residue ellipticity or molar ellipticity (deg cm^2 $dmol^{-1}$) (Holmes et al., 2017) and graphically presented as a function of wavelength.

$$[\theta] = \frac{\theta(MRW)}{10cd}$$

where $[\theta]$ is the mean residue ellipticity or molar ellipticity, θ is the degree of ellipticity (degrees), *MRW* is the average residue molecular weight, is the c concentration of the sample (mg/mL), *d* is the optical pathlength (cm). *MRW* was taken as 100 assuming the molecular weight of one collagen molecule is about 300,000 and the number of residues per molecule is 3000 (Akita et al., 2020).

The 'positive to negative peak ratio' (R_{pn}) was calculated (Perez-Puyana et al., 2019).

$$R_{pn} = \frac{\theta_p}{\theta_n}$$

where θ_p and θ_n are the molar ellipticity values of positive and negative peaks, respectively.

7.3 Results and discussion

7.3.1 pH, solubility and viscosity during extraction

Table 7.1 shows the pH values of collagen extracts at different stages of extraction. A 0.01 M HCl solution was used as the extraction medium which has a theoretical pH of 2.00. The initial pH values of the HCl solutions, and the pH values at three different stages of extraction (by the end of each extraction time, by the end of homogenisation, and before starting the fibrillogenesis), as measured by the pH meter are given in the table.

Table 7.1 clearly shows an increase of pH throughout the extraction process irrespective of the treatment conditions. Further, different extraction conditions have led to different pH levels at different stages of extraction. In most literature, the initial pH or the concentration of the chosen acid has been mentioned, however the changes of pH during extraction has not been discussed with respect to its effect on collagen dispersion. This is addressed here. The collagen extraction process starts by swelling the skin thus facilitating the exposure of collagen fibres to the extraction medium. This allows the acid to promote the dispersion of collagen fibres to colloidal particles by breaking the intermolecular cross-links between collagen molecules. Complete ionisation of HCl provides H^+ and Cl^- into the extraction medium. Some of these H^+ ions adsorb onto the alkaline side chain radicals ($-NH_2$) of collagen molecules and the rest are free in the solution. This adsorption of H^+ decreases the concentration of H^+ in the solution, therefore increasing the solution pH. The H^+ adsorption also increases the net positive charge which increases the electrostatic repulsion between different parts of the collagen molecules bound within colloidal particles (Qi et al., 2015; Li et al., 2013; Woo et al., 2008; Rodrı´guez et al., 2017; Pal and Suresh, 2016). This repulsion drives further breakdown into even smaller particles and into collagen molecules. This exposes more alkaline side chains and consequently more H^+ adsorption, thus further increasing the solution pH (Qi et al., 2015).

Table 7.1 The pH values of collagen extracts at different stages of extraction for 20 different treatments.

Extraction time (h)	Skin: HCl (m/v) ratio	HCl pH (initial)	pH by the end of extraction time	pH by the end of homogenisation	pH before starting the fibrillogenesis
0.5	1:10	2.04	3.24	3.99	4.20
	1:15	2.04	3.21	3.30	3.46
	1:20	2.04	3.02	2.95	3.06
	1:25	2.04	2.83	2.70	2.71
1	1:10	2.04	4.12	4.57	4.60
	1:15	2.04	3.57	3.87	3.91
	1:20	2.04	3.29	3.15	3.29
	1:25	2.05	2.92	2.83	2.83
2	1:10	1.99	3.95	4.02	4.23
	1:15	2.00	3.42	3.56	3.60
	1:20	2.00	3.34	3.42	3.48
	1:25	2.00	3.04	2.97	3.00
5	1:10	2.04	4.51	4.58	4.61
	1:15	2.00	3.92	4.11	4.21
	1:20	2.01	3.66	3.75	3.82
	1:25	2.01	3.07	3.18	3.22
8	1:10	2.00	4.82	4.90	4.93
	1:15	2.02	4.14	4.17	4.29
	1:20	2.01	3.64	3.77	3.77
	1:25	1.99	3.16	3.25	3.28

There was a time gap between the end of homogenisation, due to the time required to do the viscosity measurements reported later, and the start of fibrillogenesis, and so pH was recorded again because further dissolving of collagen molecules into the solution had occurred. As the pH approaches the isoelectric point of collagen, it decreases the net positive charges and so decreases the repulsive forces between molecules thus decreasing the solubility, and forming collagen aggregates (Rodrı´guez et al., 2017; Woo et al., 2008). Therefore, pH conditions close to the isoelectric pH of collagen are not suitable for collagen extraction. Previous studies have reported less solubility of collagen above pH 4 due to the approach to the isoelectric pH of collagen. For example, Song et al. (2021) reported a remarkable decrease in the solubility of Nile tilapia skin collagen from pH 4 to 7; and Rodrı´guez et al. (2017) reported maximum solubility between pH 2-4, and a decrease in solubility between pH 4-8 for mussel byssus collagen. In the experiments reported in Table 7.1 and marked in red, the 1:10 mass to volume ratio for all five extraction times, and the 1:15 mass to volume ratio for both 5 and 8 h extraction times, exceeded pH 4 during extraction. This will be discussed alongside the other results later in this chapter.

As noted earlier, although solubility increases with increasing acidity, this also has a limit. Very high acidic conditions are not suitable due to their denaturing effect, as reported by Qi et al. (2015) for pH 3 and Ahmed et al. (2019) for pH 2. In this study, the 1:25 mass to volume ratio for 0.5, 1 and 2 h extraction times have reported pH below 3, which should be avoided in selecting the extraction conditions. It is well understood from the results of this experiment that the pH during extraction is more important in deciding extraction conditions

than the initial pH of acid. In these experiments the initial pH was 2, which is on the borderline of causing denaturation according to these authors; however, here, the pH quickly increases due to the removal of the H+ ions from the solution as alkaline side chain radicals become exposed. Therefore, it can be assumed that it is the pH during extraction that is important rather than the initial pH. Nevertheless, it is possible that there is an initial pH that is too acidic and initiates denaturation rather than adsorption. If so, this work shows that it is not pH 2, but must be some lower but undetermined value.

Because the pH has a relationship with the solubility of collagen, it is important to discuss them together. As described above, previous studies have reported the effect of pH on the solubility of collagen, however no studies were found describing the effect of pH on collagen dispersion from fish skin. Therefore, experiments were done to measure this aspect, as explained in §7.2.2.2 above. This simple method was introduced in this study to qualitatively measure the solubility of the skin by measuring the number of undissolved skin pieces and their surface areas after homogenisation. For the analysis, seven categories of surface area were selected; 2-5, 5-10, 10-20, 20-30, 30-40, 40-50 and 50-60 mm^2 and the number of skin pieces in each category were counted and presented as a frequency distribution (Figure 7.2). The results can be anticipated from the expected chemistry. More skin should dissolve in the extraction medium with increasing extraction time (from 0.5 to 8 h) and with increasing solution (from 1:10 to 1:25 skin mass to solution volume ratio). Homogenisation then mechanically breaks down remaining undissolved skin pieces, reducing large skin pieces to form smaller pieces. The particle area analysis indicates the efficacy of dissolution and homogenisation in reducing skin piece size.

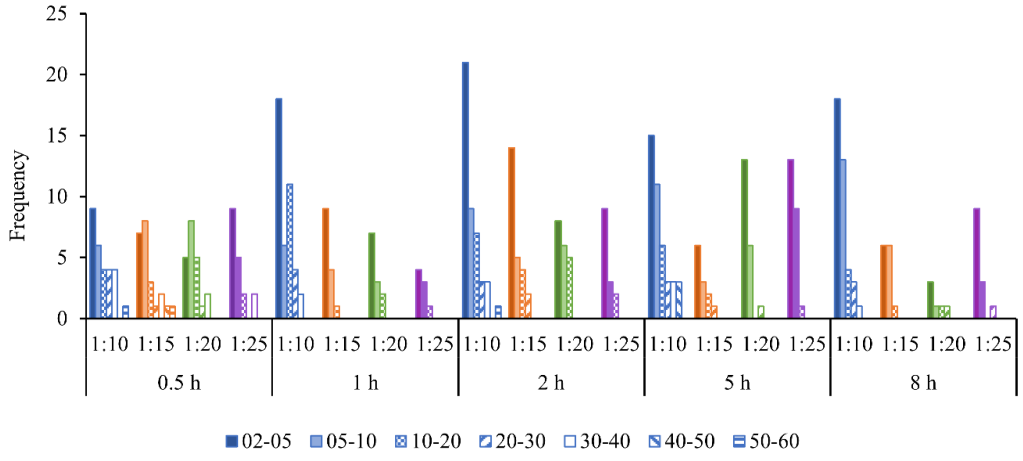

Figure 7.2 Frequency distribution of undissolved skin pieces after homogenisation for all treatments of the combination of extraction time (0.5 to 8 h) and skin mass to solution volume ratio (1:10 to 1:25). Skin surface area categories are 2-5, 5-10, 10-20, 20-30, 30-40, 40-50 and 50-60 (mm^2). The legend shows the shading for the 1:10 ratio in blue colour. The other ratios follow the same shading with different colours as orange for 1:15, green for 1:20, and purple for 1:25.

The results in Figure 7.2 approximately follow this expectation where there are more small-area skin pieces than large-area ones. In addition, there are three trends; (i), at 0.5 h extraction time, the count distribution is unaffected by the skin mass to solution volume ratio which suggests an insufficient time for solubilisation of skin pieces; (ii), at 1 h extraction time, the overall count reduces as the ratio decreases, which suggests that there is sufficient time for solubilisation so that the effect of the amount of solution becomes important; and (iii), for all results across extraction times from 1 to 8 h there are many more skin pieces at a skin to solution ratio of 1:10 than at 1:25, which suggests that the 1:10 ratio provides insufficient hydrogen ions for the required adsorption, and which is also supported by the finding that the pH of these solution rises above 4, indicating depletion in the availability of H^+ ions. Interestingly, trend (ii) does not carry through to the longer extraction times of 2, 5 and 8 h, but this could be statistical as the total number of measured skin pieces was not high.

These solubility results can be further interpreted with respect to the viscosities of the homogenised solutions, which are shown in Figure 7.3. Viscosity of the homogenised collagen solutions were measured by spindle 4 at 10 rpm. Spindle 5 was used to measure the viscosity above 20,000 cP. As shown in Figure 7.3, viscosity values recorded for 2 h, 1:20 (m/v) treatment by both spindles number 4 and 5 were very similar as shown by green colour triangles. Similarly, viscosity values recorded for 5 h, 1:20 (m/v) treatment by both spindles were also very similar. This may be due to the very small differences found in shear rates between these two spindles because of their very similar diameters. Therefore, it is reasonable to use spindle 5 to measure viscosities which are not possible with spindle 4. Viscosity affects two aspects; the molecular mobility and the ease of mixing, which are both important in the next step, fibrillogenesis, where the collagen fibres are formed from the acid solution by the addition of NaOH solution to raise it to close to its isoelectric point. When the viscosity of the solutions is too high, it both reduces the ease of mixing and therefore mixture uniformity during the fibrillogenesis, and the molecular mobility for self-assembly (Gobeaux et al., 2008; Mosser et al., 2006; Zhu et al., 2018).

Solution viscosity is also expected to affect the swelling of the skin, and solubilisation of collagen molecules. Swelling of the skin occurs by absorbing the solution, which is easier when the solution has low viscosity. As described before, swelling enables breaking down the inter-molecular cross-links and dispersion of collagen molecules into the extraction medium. Low viscosity will provide good molecular mobility for diffusion of the H+ ions to the adsorption sites and the movement of the dissolved collagen molecules back into the solution. However, the gradual increase in dissolved collagen content in the solution is expected to increase the solution viscosity over time. This is supported by the results, which show that the 1:15, 1:20 and 1:25 ratios have progressively lower viscosity at all extraction times because the dissolved collagen is more dilute in the solution. However, of great interest is the peak in viscosity, which occurs at 2 h extraction time, and thereafter decreases, which suggests that even in solution the collagen is undergoing further cleavage of crosslinks. The 1:10 ratio, as noted before, appears to not have enough H^+ ions for the adsorption phase of the dissolution, and so the development of viscosity is limited.

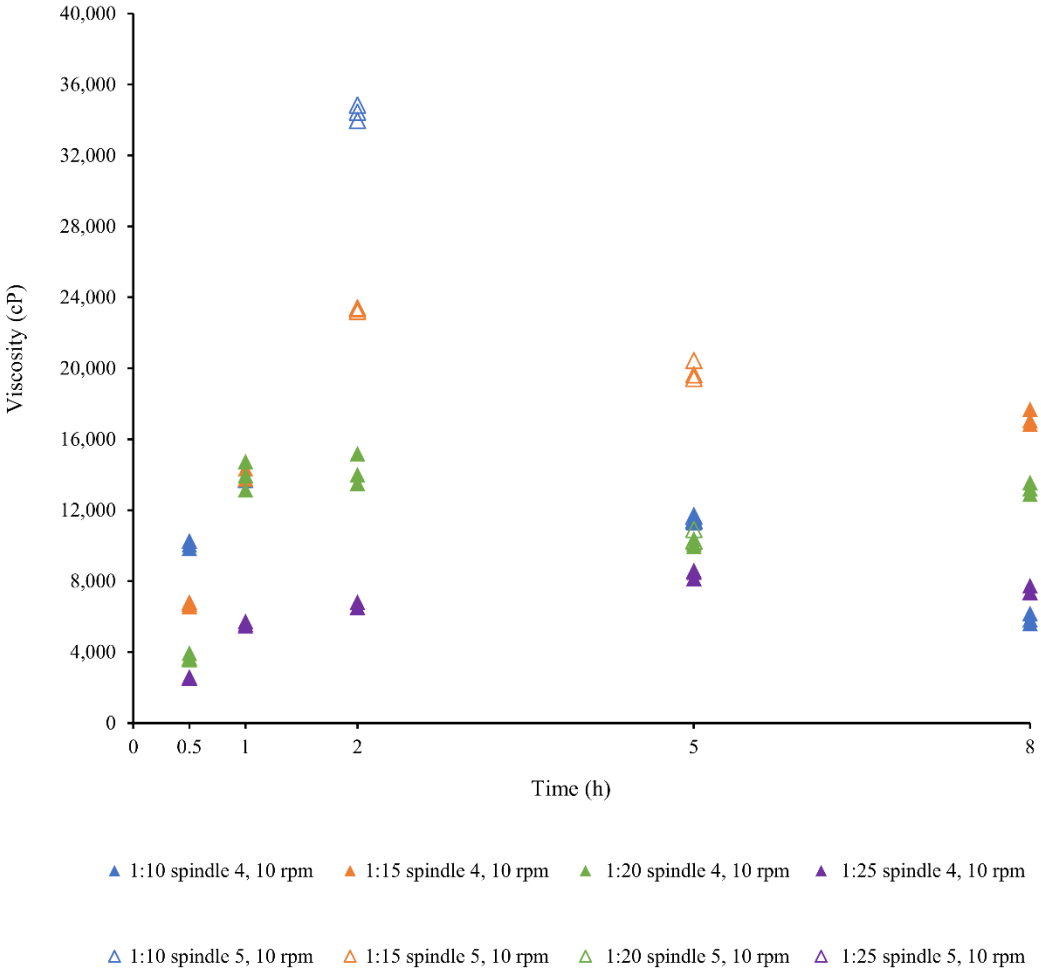

Figure 7.3 Viscosity of homogenised collagen solutions measured by spindle 4 at 10 rpm. Spindle 5 was used to measure the viscosity above 20,000 cP. Note: Direct comparison of spindle 4 and 5 are not theoretically same. So, there will be small differences in shear rates. The 2 h and 5 h treatment times at 1:20 (m/v) rato show they are comparable.

These two adjustable parameters, extraction time and skin mass to solution volume ratio, also influence the swelling, measured here by the total weight of extracted skin just prior to homogenisation, as shown in Figure 7.4. The treated skin contains the absorbed solution plus the initial mass of 50 g of fresh skin. The 0.5 h extraction time has the least swelling and, as noted previously, the lowest solution viscosity and least solubility, which all support the hypothesis that the process is time constrained. For the 1 and 2 h extraction times, swelling, solution viscosity and solubility all increase, because the process is increasingly less time constrained. However, here the effect of the skin mass to solution volume ratio becomes apparent, with the 1:10 ratio being constrained by the available H+ ions, and the 1:15, 1:20 and 1:25 less so, but which also have the progressive advantage of lower solution viscosity and so appear to achieve slightly more swelling in the given extraction time. The most perplexing result is the dip in the swelling of the skin at 5 h, but which is restored at 8 h to the same swelling as observed at 2 h. The reason for this is unknown. The results show that measurements made at higher spindle speeds (circles) generally have lower viscosity than those made at low RPM. This suggests that the solutions exhibit shear thinning behaviour where the viscosity decreases with increasing shear rate.

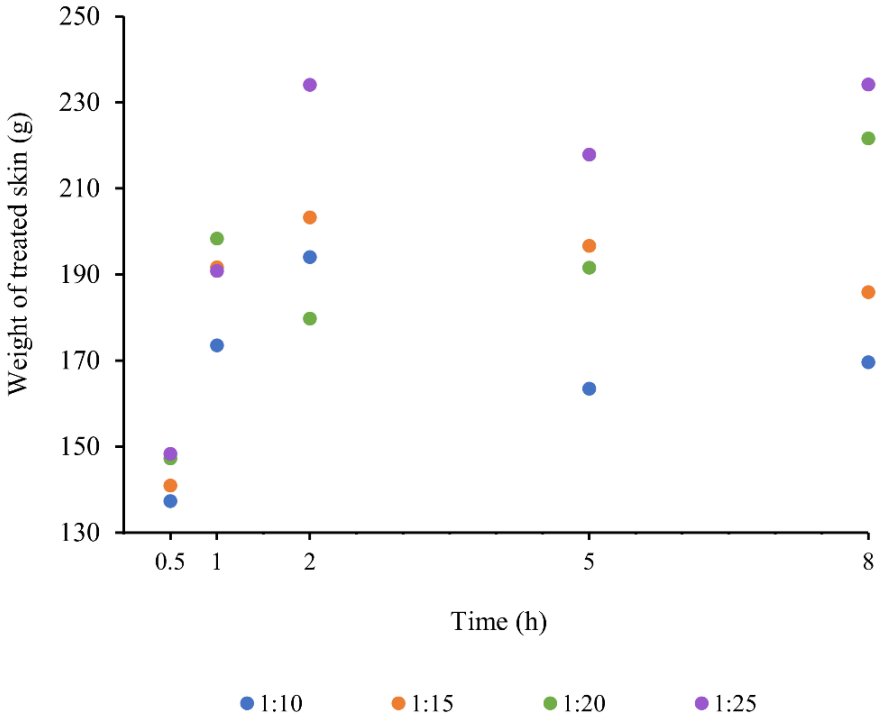

Figure 7.4 Weight of swollen skin after treating with HCl. Before swelling, the fresh skin mass was nominally 50.0 g.

These results provide important information about the influence of the process conditions on the efficacy of collagen extraction, with a particular focus on the solution. The processing objectives are to have; (i), an upper limit of pH 4 for the extraction solution; (ii), maximum swelling; (iii), a manageable viscosity of the extraction solution; and (iv) as few undissolved pieces of skin as possible. Considering all these factors, the 5 h extraction time at 1:20 mass to volume ratio was provisionally selected as the optimal treatment condition. The next section moves from analysing measurements of the solution to measurements of the collagen produced.

7.3.2 Yield of collagen

The freeze-dried yield of collagen extracted from the skin lied between 80-87%, but are inconclusive with respect to trends; because here the yield includes undissolved skin pieces if still present. This yield is the total yield after fibrillogenesis and so is also affected by the conditions during fibrillogenesis, however the fibrillogenesis conditions were kept the same for all treatments to allow comparison.

7.3.3 Morphology and microstructure of collagen

Optical photographs of the collagen are shown in Figure 7.5. Undissolved skin pieces are clearly seen in the top row for the 1:10 ratio solution, but a few or absent in the 1:20 and 1:25 ratios of 5 and 8 h extraction times. These observations align with the counting of the undissolved skin pieces in the solution after homogenisation as shown in Figure 7.2.

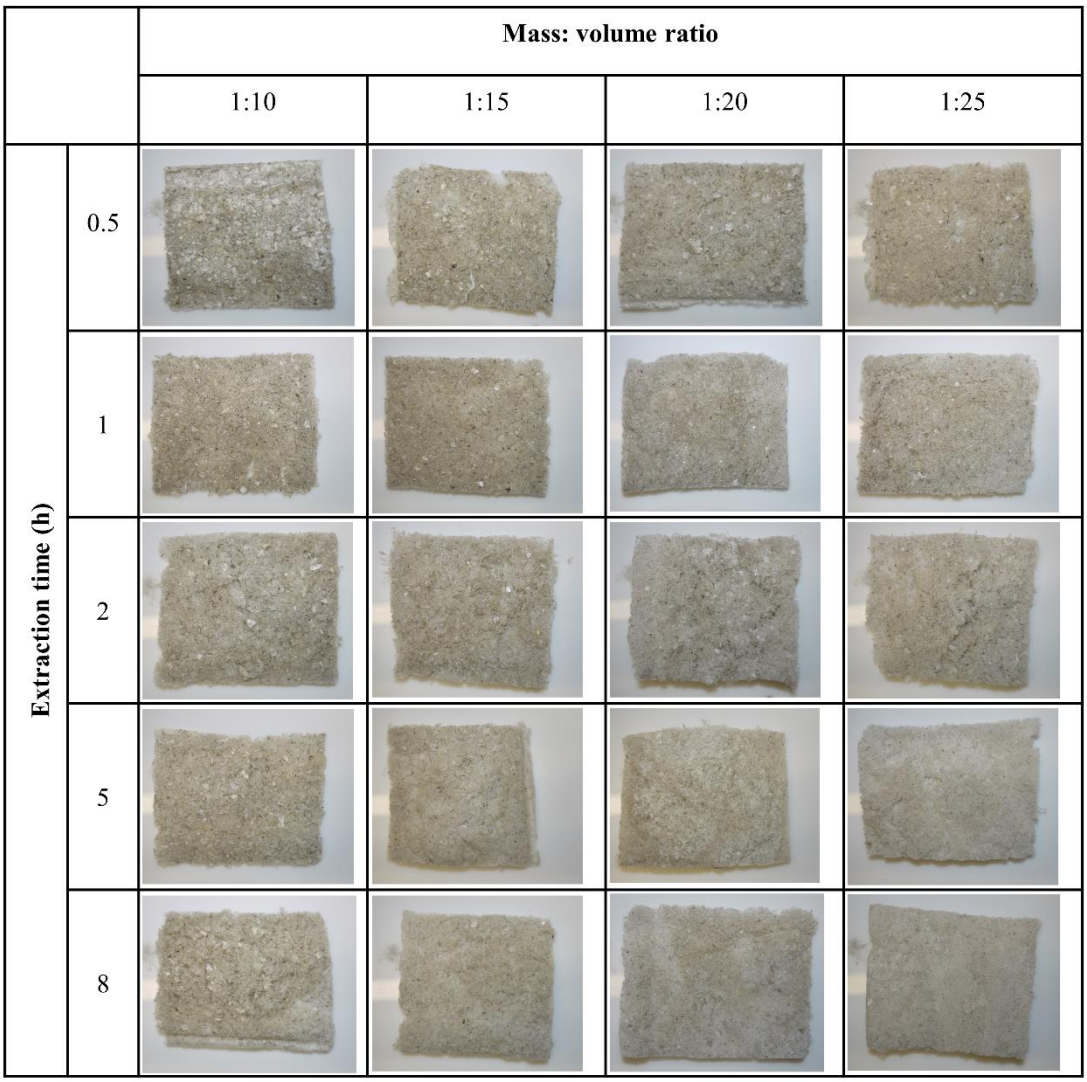

Figure 7.5 The optical photographs of freeze-dried collagen after fibrillogensis with respect to extraction time and the fish skin mass to solution volume ratio. The solution is 0.3 M NaOH.

Figure 7.5 also shows colour. Fish skin contains pigments in different amounts depending on the species, gender, habitat, season, therefore it is difficult to obtain collagen which is completely devoid of colour. Generally, in fish collagen extraction methods, a pretreatment agent such as H_2O_2 is used to oxidise pigments and provide a white colour. In this study, pigment removal was expected from the NaOH pretreatment which was used for non-collagenous protein and fat removal (Chapter 6). However, Figure 7.5 shows that pigments were not totally removed, yielding a brown colour to the freeze-dried collagen, although there is a transition to a lighter colour with increasing extraction time and decreasing solids to solution ratio. While the colour of collagen gives an aesthetic value depending on the intended application and does not influence the functional properties (Pal & Suresh, 2015), it is nevertheless preferred to be white and so the colour was explored in more detail.

The colour was characterised using L*a*b* colour space compared to a white colour standard. In this method, L* indicates lightness, a* indicates redness or greenness, and b* indicates yellowness or blueness. In the analysis, these parameters were not analysed separately, but the total colour difference between the samples and the standard is graphically presented in Figure 7.6. The total colour difference should be close to zero if the collagen is devoid of pigments and white in colour. No samples had a value close to zero, where the minimum difference was recorded by 1:25 ratio of 8 h extraction time, followed by the 1:20 ratio of 5 h extraction times. This outcome supports the earlier decision that the 1:20 ratio and 5 h extraction time was the best case selection of operating parameters according to the solubility, viscosity, and pH.

To achieve a whiter product, further pigment removal is needed for this collagen, which can be achieved by incorporating an H_2O_2 treatment during the pretreatment as reported in previous literature. It can be done in different ways; with combination of NaOH (Xu et al., 2017) or NaCl (Sadowska et al., 2003), at different concentrations, mass to volume ratios and time durations at different levels of effectiveness. Structural changes in gelatin due to H_2O_2 treatment have been reported by Nagarajan et al. (2013). No such information for collagen has been found. Some others, for example, Sadowska et al. (2003) have used centrifugation to successfully remove pigments. In this study, further removal of pigments was achieved by a second extraction of collagen to achieve a total colour difference close to zero. These results will be discussed in §7.4.

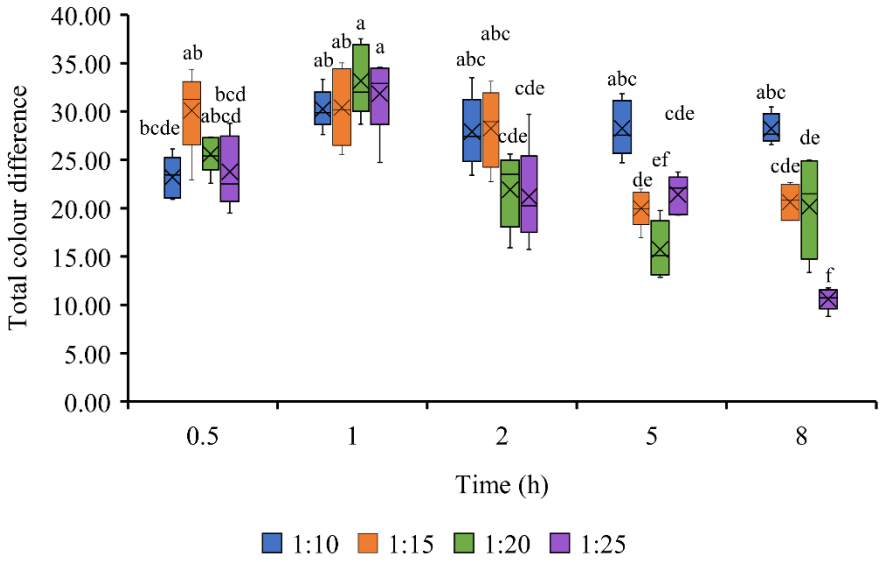

Figure 7.6 Total colour difference of collagens as measured from L*a*b* colour method as a function of the extraction time. The legend gives the ratio of dry skin mass to solution volume. Treatments with no significant differences (Two-way ANOVA, $p<0.05$) are shown by similar letters.

The surface microstructures of freeze-dried collagens were visualised using SEM images at low magnification (Figure 7.7). All images show a sheet-like layering with a porous structure produced as a result of the sublimation of water during freeze-drying. The freeze-drying conditions were kept constant for all samples, which means differences in pore structure are likely to reflect differences in the collagen networks. However, no differences can be seen in these images to conclude any effect from extraction time or mass to volume ratio.

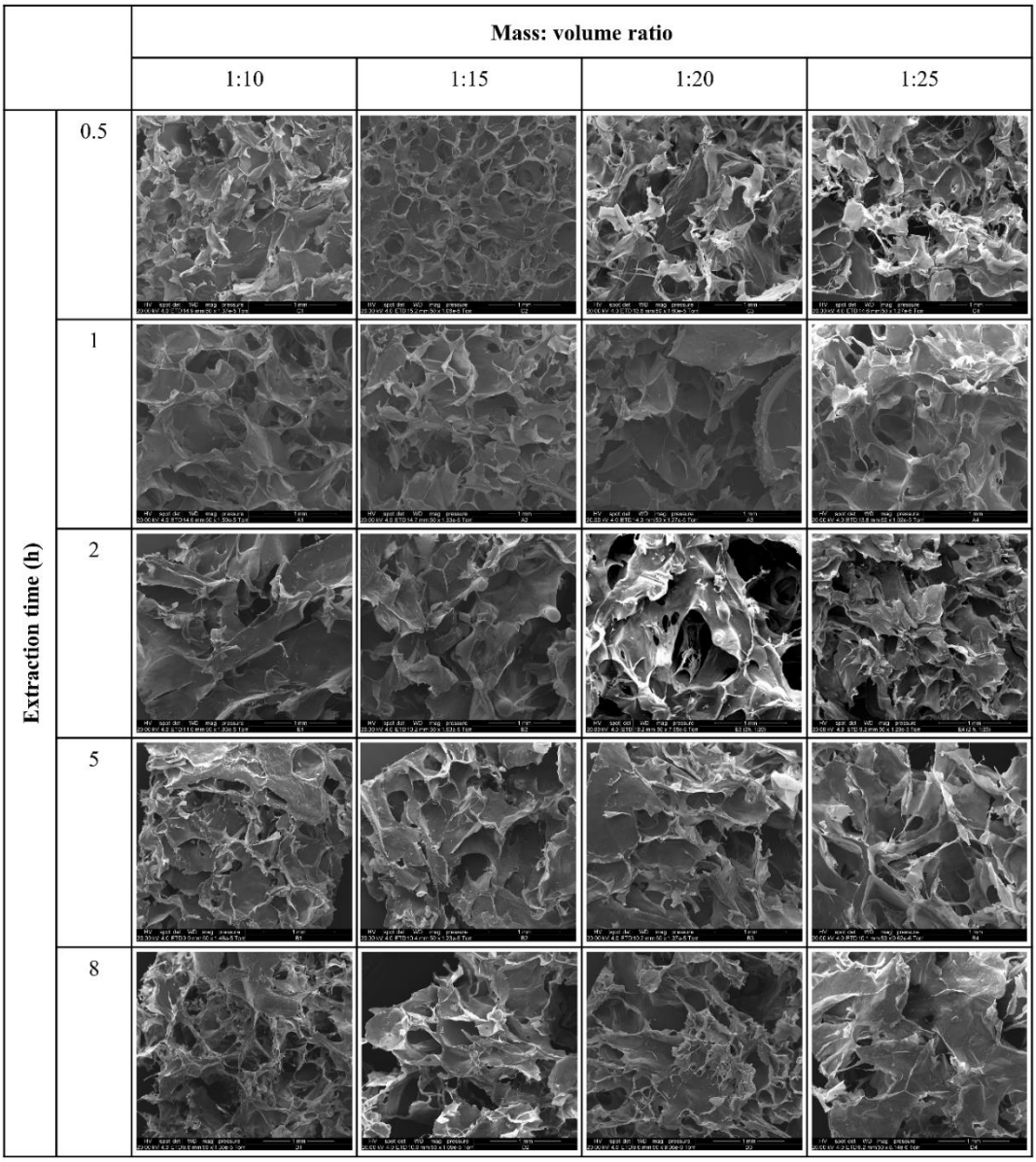

Figure 7.7 SEM images (x50) of freeze-dried collagen after fibrillogensis with respect to extraction time and the fish skin mass to solution volume ratio.

7.3.4 Analysis of the native collagen structure

The secondary structure of collagen was analysed by the ATR-FTIR spectroscopy, DSC and CD spectroscopy techniques.

7.3.4.1 ATR-FTIR spectroscopy

FTIR is used to determine the type of collagen (Riaz et al., 2018) and the changes in the secondary structure of collagen based on the chemical bonding state (Harnkarnsujarit et al., 2015; Jeong et al., 2013; Wang et al., 2008). The peak locations of all 20 collagen samples are given in Table 7.2 and Figure 7.8. Amide A, B, I, II, and III peaks were present for all samples which are typical of Type I collagen. However, peak positions showed slight differences indicating some differences in the secondary structure (Wang et al., 2008).

Amide A peak is due to the stretching vibration of the N-H bond in the 3400-3440 cm^{-1} region (Jeong et al., 2013; Li et al., 2013; Wang et al., 2008). This peak shifts to a lower wavenumber when the N-H group is involved in hydrogen bonding with a carbonyl group of a peptide bond from another polypeptide chain (Jeong et al., 2013; Riaz et al., 2018). All collagens have shown decreased wavenumbers towards 3300 cm^{-1} indicating more hydrogen bonds which is a good indication of the triple-helical collagen structure. All collagens have shown a strong peak around 2925 cm^{-1} due to the asymmetrical stretching of CH_2 bonds, which is responsible for amide B (Chen et al., 2016).

The amide I peak is found in the 1600-1700 cm^{-1} region due to C=O stretching vibration (Liu et al., 2012). The formation of H bonds between N-H (X position) and C=O (Gly) of the fourth residue is responsible for the triple-helical conformation and is shown by the shifting of peak position to a lower frequency (Li et al., 2013). The amide I peak position is the most useful measure which allows a better differentiation of the secondary structures (Sai-Ut et al., 2012; Woo et al., 2008): 1620-1640 cm^{-1} (β sheet or extended structure); 1640-1644 cm^{-1} (irregular structure); 1645-1659 cm^{-1} (α-helix); 1660-1700 cm^{-1} (β turn) (Farrell et al., 2001 in Li et al., 2013). The wavenumbers for all twenty collagens were found in the 1645-1659 cm^{-1} region suggesting the α-helix structure. There are some peaks found which are related to β sheet and irregular structures, but this is negligible compared to the content of α-helix structure.

The N-H in-plane bending coupled with C-N stretching vibrations is responsible for amide II peak in the 1550-1600 cm^{-1} region (Jeong et al., 2013). Here also, the peak position shifts to a lower wavenumber if more hydrogen bonds are present between adjacent α-chains (Li et al., 2013). All collagen samples have recorded peak positions around or below 1550 cm^{-1} indicating more hydrogen bonds.

There is another implication for the shift in wavenumber for amide I and II peaks, which is that of crosslinking, where higher wavenumbers indicate a higher degree of intermolecular cross-links and molecular order (Li et al., 2013). This means the measured wavenumbers are subject to two opposing influences. Here, the net result is that hydrogen bonding dominates and so has decreased the wavenumbers. The consequence of more hydrogen bonding is that peptide chains are less likely to unwind (Li et al., 2013), and so preserve the secondary structure of proteins.

The amide III band occurs in the 1230-1300 cm^{-1} region mainly due to N-H bending coupled with C-N stretching, and wagging vibrations from CH_2 groups of the glycine backbone and proline side-chains (Ahmed et al., 2019; Jeong et al., 2013; Li et al., 2013; Xu et a; 2017). All collagens have recorded peaks in the 1230-1238 cm^{-1} region. Another strong peak occurs near 1450 cm^{-1} due to pyrrolidine ring vibrations of proline and hydroxyproline (Liu et al., 2012). A useful parameter which is called the absorption ratio is calculated from the ratio of the amide III and 1450 cm^{-1} absorbances to determine the intactness of the triple-helical structure (Li et al., 2013; Sun et al., 2017; Wang et al., 2008). This ratio is close to 1 for triple-helical structure (Chen et al., 2016; Liu et al., 2015; Song et al., 2021; Xu et al., 2017); and close to 0.5 if the structure is denatured (Goissis et al., 1998). The absorption ratios calculated for twenty samples are shown in Table 7.2 which are around 0.85 confirming the triple-helical structure (Barzideh et al., 2014). These results confirm that the extraction

conditions used in this study were able to maintain the native triple-helical conformation of collagen up to 8 h.

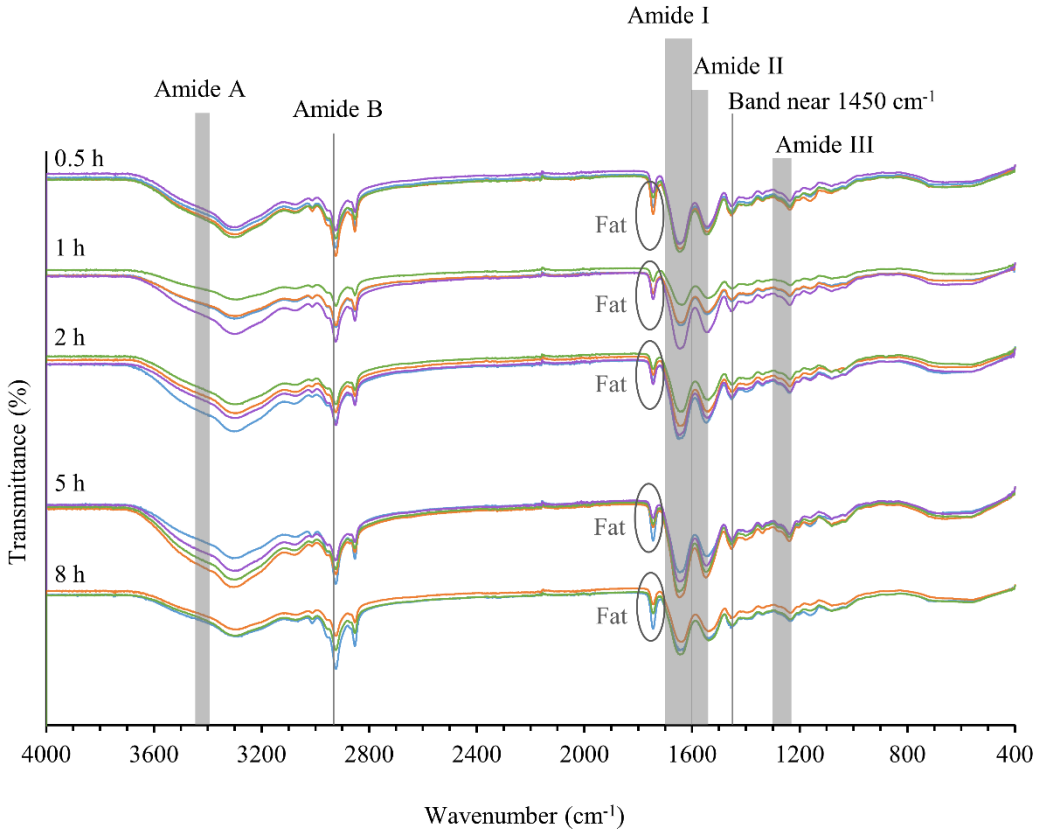

Figure 7.8 FTIR spectra of freeze-dried collagen extracted at five extraction times and four mass to volume ratios. Graphs represent the mean of five replicates. Blue colour represents 1:10, orange colour represents 1:15, green colour represents 1: 20, and purple colour represents 1:25.

The triple-helical structure of collagens is stabilised by the restrictions imposed by the pyrrolidine rings of the proline and hydroxyproline, and intramolecular hydrogen bonding between the hydroxyl group of hydroxyproline in one polypeptide chain and the amide carboxyl group of another chain, mediated by water molecules (Ahmed et al., 2019; Liao et al., 2018; Pal & Suresh, 2016). The thermal denaturation process of collagen starts by first breaking these intramolecular bonds upon heating which unravels the tightly-bound triple-helix into looser polypeptide chains, followed by disintegrating into random coils at a particular temperature which is defined as the denaturation temperature (Chen et al., 2021; Liu et al., 2016;). This thermal denaturation results in irreversible damage in physico-chemical and biological properties of collagen (Usha & Ramasami, 2004).

Table 7.2 ATR-FTIR peak locations of freeze-dried collagen extracted at five extraction times and four mass to volume ratios. The mean (±SD) of five replicates are given.

Region	General range of wavenumber (cm^{-1})*	m/v ratio	Extraction time				
			0.5 h	**1 h**	**2 h**	**5 h**	**8 h**
Amide A	3400-3440	1: 10	3303(±5)	3300(±5)	3298(±11)	3298(±9)	3289(±4)
		1: 15	3298(±5)	3298(±6)	3299(±4)	3301(±3)	3294(±7)
		1: 20	3303(±4)	3296(±4)	3297(±10)	3301(±7)	3298(±5)
		1: 25	3298(±6)	3300(±3)	3298(±8)	3297(±5)	3293(±10)
Amide B	near 2920	1: 10	2924(±1)	2923(±1)	2924(±1)	2924(±1)	2924(±1)
		1: 15	2924(±1)	2923(±1)	2924(±1)	2924(±1)	2923(±0)
		1: 20	2924(±1)	2923(±1)	2924(±2)	2924(±0)	2924(±0)
		1: 25	2923(±1)	2924(±1)	2924(±0)	2924(±1)	2923(±1)
Amide I	1600-1700	1: 10	1649(±5)	1641(±6)	1646(±9)	1644(±7)	1651(±3)
		1: 15	1645(±5)	1644(±9)	1642(±6)	1647(±6)	1639(±4)
		1: 20	1647(±8)	1636(±3)	1642(±7)	1647(±7)	1641(±5)
		1: 25	1650(±2)	1649(±3)	1649(±2)	1649(±2)	1645(±5)
Amide II	1550-1600	1: 10	1541(±4)	1540(±5)	1545(±6)	1541(±7)	1538(±1)
		1: 15	1542(±5)	1542(±6)	1540(±3)	1546(±5)	1538(±2)
		1: 20	1543(±3)	1540(±3)	1540(±5)	1547(±3)	1536(±3)
		1: 25	1542(±3)	1540(±3)	1542(±5)	1548(±2)	1536(±4)
Amide III	1230-1300	1: 10	1236(±1)	1235(±2)	1237(±1)	1236(±2)	1235(±1)
		1: 15	1236(±1)	1235(±2)	1236(±1)	1238(±1)	1234(±1)
		1: 20	1237(±1)	1235(±2)	1236(±1)	1238(±1)	1233(±1)
		1: 25	1236(±0)	1237(±1)	1236(±1)	1237(±1)	1233(±2)
Absorption ratio		1: 10	0.85 (±0.01)	0.86 (±0.02)	0.86 (±0.02)	0.85 (±0.02)	0.82 (±0.02)
		1: 15	0.87 (±0.01)	0.87 (±0.01)	0.86 (±0.02)	0.86 (±0.01)	0.84 (±0.03)
		1: 20	0.85 (±0.02)	0.86 (±0.02)	0.84 (±0.01)	0.86 (±0.01)	0.84 (±0.01)
		1: 25	0.86 (±0.02)	0.85 (±0.01)	0.88 (±0.03)	0.87 (±0.01)	0.85 (±0.02)

*Sources for the general range of wavenumbers: Jeong et al., 2013; Wang et al., 2008; Li et al., 2013.

7.3.4.2 Differential scanning calorimetry

These thermal properties are measured in DSC by direct measurement of heat to interpret the secondary structure conformation of collagen (Gauza-Włodarczyk et al., 2017). There are two characteristic temperatures measured in DSC: denaturation temperature which corresponds to the temperature of maximum power absorption during denaturation providing a sharp peak in the thermogram, and the onset temperature which is the temperature at which the tangent to the initial power versus temperature line crosses the baseline (Zeugolis & Raghunath, 2010). In addition, the denaturation enthalpy which is calculated from the area under peak corresponding to the total heat involved in the transition is also used (Zeugolis & Raghunath, 2010).

The denaturation temperature (T_d), onset temperature and denaturation enthalpy (ΔH) of collagen samples are given in Table 7.3 and Figure 7.9. The 1:10 and 1:15 mass to volume ratios have higher T_d values which may be due to the presence of undissolved skin pieces. Other ratios have values around 34-38°C. Previous studies have reported T_d values for warm-water fish collagen around 30°C (Kittiphattanabawon et al., 2005; Nalinanon et al., 2011), and cold-water fish collagen mostly below 20°C (Kittiphattanabawon et al., 2005; Li et al., 2013). Therefore, the T_d values reported in this study is higher than previously reported values for cold-water fish collagen. Denaturation temperature depends on the fish species (Chen et al., 2021), proline and hydroxyproline contents (Chen et al., 2021; Xu et al., 2017; Pal and Suresh 2016; Nalinanon et al., 2011), the degree of cross-linking (Gauza-Włodarczyk et al. 2017), and habitat temperature of the fish (Chen et al., 2021; Gauza-Włodarczyk et al., 2017; Xu et al., 2017;). The higher denaturation temperatures in warm-water fish collagen are due to higher contents of proline and hydroxyproline which provide stability to the collagen structure (Kittiphattanabawon et al., 2005; Liu et al., 2014).

There are several factors affecting the DSC results which should be considered in sample preparation and choice of method, such as pH and concentration of the medium, heating mode (Chen et al., 2021), the water content in the sample, and presence of admixtures (Gauza-Włodarczyk et al., 2017). Considering these factors, it can be argued that the higher T_d values reported in this study were not due to any of these, as the source of collagen, sample preparation and analysis method were the same. It is possible that the higher T_d may be due to the higher degree of cross-links formed during the fibrillogenesis step which used isoelectric precipitation rather than salting out as used by other researchers such as Li et al. (2013), Muralidharan et al. (2013), and Woo et al. (2008). More cross-links can bind the collagen molecules tightly together, reducing the space required for hydration, whereas less hydration causes higher denaturation temperatures (Miles et al., 2005; Zeugolis & Raghunath, 2010). Pal & Suresh, (2017) have reported increased denaturation temperature to 40°C in fish collagen after fibril formation. Singh et al. (2011) have reported that T_d around 39°C in collagen from striped catfish can be due to a higher degree of cross-linking.

The onset temperatures were comparatively lower and varied for extraction durations up to 2 h, while much more consistent and higher values (25-30°C) were observed for 5 and 8 h. This may be due to the presence of more homogenous solutions consisting of collagen molecules after 5 and 8 h extractions compared to the mix of skin and collagen molecules in the extracts up to 2 h as explained in §7.3.1. These results imply the possibility of using processing temperatures up to 25°C without any thermal degradation effect on collagen. This

is important in practical handling and further processing into biomedical materials since the physico-chemical, mechanical and biological properties are destroyed by thermal denaturation (Liu et al., 2014; Sugiura et al., 2009; Sun et al., 2010).

There was no relationship found between T_d and denaturation enthalpy. Previous studies have reported that a higher denaturation enthalpy is associated with a higher content of Gly-Pro-Hyp sequence in the polypeptide chains (Bae et al., 2008; Ahmed et al., 2019; Burjanadze, 1999 in Ahmad and Benjakul, 2010). This is due to the higher stability of hydrogen bonds between polypeptide chains of this Gly-Pro-Hyp sequence compared to other sequences (Bae et al., 2008; Ahmed et al., 2019). However, the different denaturation enthalpy values reported in this study cannot support this argument, hence further studies are needed.

Table 7.3 Thermal properties of collagen measured by differential scanning calorimetry.

Time (h)	m/v ratio	Onset temperature (°C)	Denaturation temperature (°C)	Enthalpy of denaturation (J/g)
0.5	1:10	26.13	40.13	24.90
	1:15	22.82	41.49	21.83
	1:20	25.78	37.41	52.52
	1:25	21.46	39.44	36.07
1	1:10	21.04	41.43	40.50
	1:15	20.89	42.34	26.51
	1:20	25.89	36.03	49.15
	1:25	21.34	36.79	46.66
2	1:10	20.85	34.23	78.45
	1:15	21.76	34.66	44.59
	1:20	27.00	34.50	49.09
	1:25	21.30	34.98	40.90
5	1:10	25.82	42.12	24.06
	1:15	28.14	35.20	42.89
	1:20	26.15	35.05	54.01
	1:25	27.34	33.98	33.22
8	1:10	26.34	42.59	69.36
	1:15	30.55	42.85	36.40
	1:20	27.51	33.59	34.15
	1:25	28.35	37.70	39.79

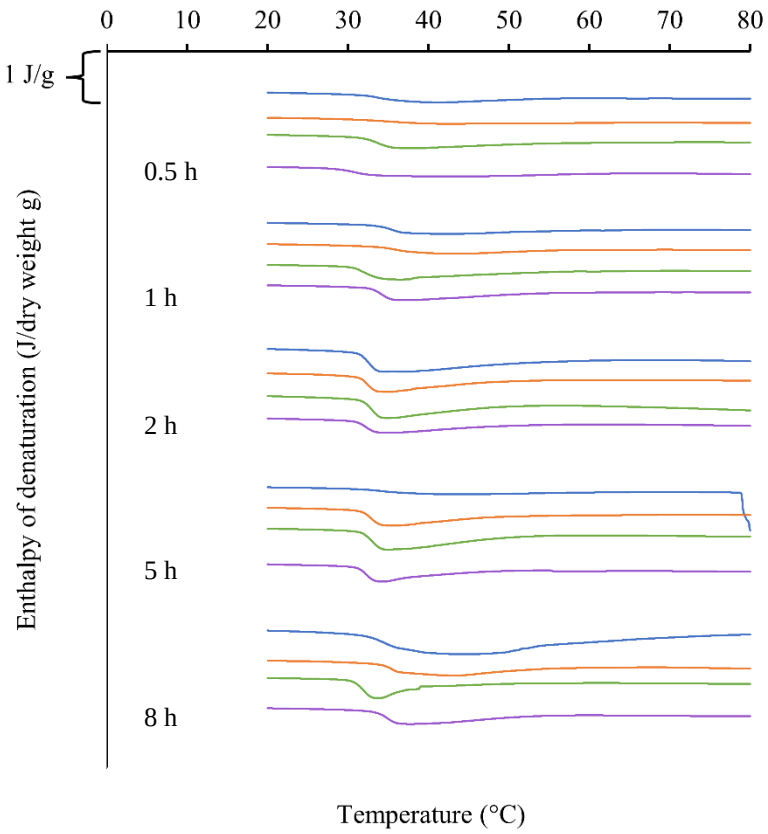

Figure 7.9 Differential scanning calorimetry thermograms of collagens. Blue colour represents 1:10, orange colour represents 1:15, green colour represents 1: 20, and purple colour represents 1:25.

7.3.4.3 Circular dichroism spectroscopy

Circular dichroism spectroscopy is considered the gold standard for estimating the secondary structure of proteins among other techniques like FTIR and DSC due to the easy identification of the native and denatured conformations (Gopinath et al., 2017). The secondary structure determination by this technique is based on the measurement of differential absorption of left and right-handed polarised light by peptide bond chromophores in a protein (Drzewiecki et al., 2016; Zhou et al., 2018; Qi et al., 2015), in the far UV range, generally from 250 to 190 nm (Rodger and Marshall 2021). The native triple-helical structure of collagen in a solution is characterised by the presence of a negative peak at around 198 nm related to the content of the α-helix structure, a cross-over at 214 nm and a weak positive peak at around 220 nm due to the π-π* transition of peptide bonds (Zhou et al., 2018; Liu et al., 2016). The easy identification of the native structure from the denatured structure is based on the presence or absence of the positive peak as it disappears upon denaturation (Drzewiecki et al., 2016). The calculated value of the 'positive/negative ratio' (R_{pn}) from the CD spectra is used as a measure to estimate the degree of denaturation or the triple-helical content (Perez-Puyana et al., 2019; Akita et al., 2020).

The CD spectra obtained for twenty different treatment combinations are shown in Figure 7.10. All collagens have produced characteristic CD spectra with a negative peak at ~198 nm, a cross-over point at ~214 nm and a positive peak at ~220 nm. The R_{pn} ratios of 20 samples are shown in Table 7.4. If the collagen is denatured the R_{pn} ratio is a positive value

and increases with an increasing degree of denaturation (Perez-Puyana et al., 2019). For example, Gopinath et al. (2017) reported a R_{pn} ratio of 0.05 for 100% denatured collagen. The R_{pn} ratios reported in previous studies for native collagens were -0.12, -0.1075, and -0.123, by Gopinath et al. (2017), Nishad Fathima et al. (2009); and Sun et al. (2020), respectively. The values reported in this study were almost similar for all samples and found in the range from -0.11 to -0.13 which falls within the values of previous studies. Therefore, these results indicate that the extraction durations and mass to volume ratios used in this study were suitable for preserving the triple-helical structure.

Considering all of the above results, and the time and cost-effectiveness, the treatment time of 5 h at 1:20 mass to volume ratio can be selected as the best treatment time to extract collagen in native triple-helical conformation.

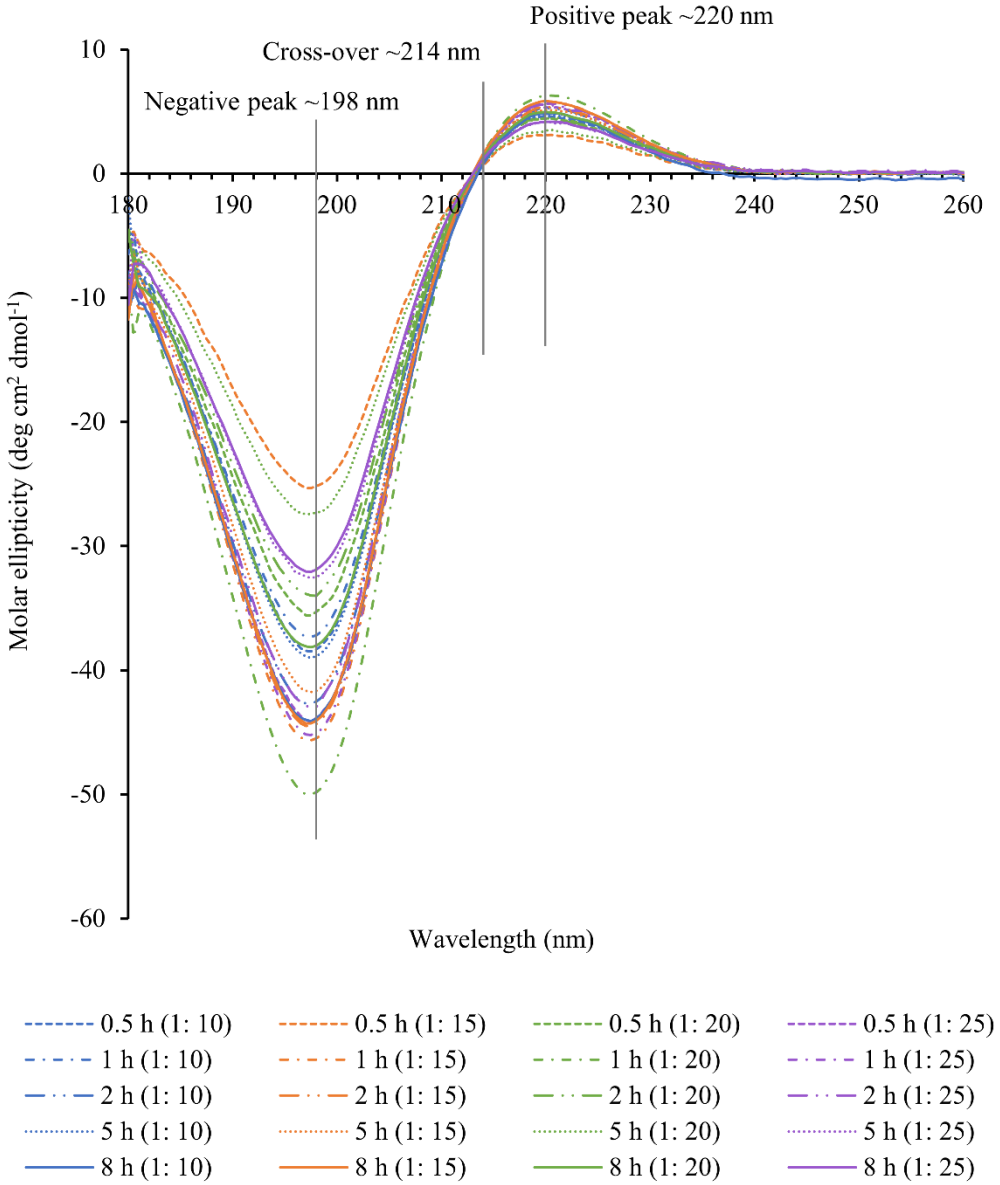

Figure 7.10 Circular dichroism spectra of collagens.

Table 7.4 R_{pn} values of the extracted collagens.

	Extraction time (h)				
m/v ratio	**0.5**	**1**	**2**	**5**	**8**
1:10	- 0.12	-0.13	- 0.12	- 0.12	- 0.11
1:15	- 0.12	-0.13	- 0.12	- 0.12	- 0.13
1:20	- 0.12	-0.13	- 0.13	- 0.12	- 0.13
1:25	- 0.12	- 0.12	- 0.13	- 0.13	- 0.13

7.4 A second extraction to increase the purity and colour of collagen

The collagens extracted under the twenty different treatments presented in the last section, showed discolouration due to the presence of skin pigments. These were the remaining pigments which had not been removed by the Sodium hydroxide pretreatment. Functional properties are not affected by the colour of collagen, however it gives an aesthetic value depending on the intended application (Pal and Suresh, 2015). The presence of pigments affects the purity of collagen as well. Therefore, it is advantageous to remove pigments at some point during the processing.

There are already available methods to get rid of this discolouration, for example, H_2O_2 treatment to bleach the colour pigments (Xu et al., 2017; Sadowska et al., 2003) or centrifugation to remove them (Sadowska et al., 2003). In this research, the H_2O_2 treatment was not used as it is only a bleaching technique in which the pigments will remain in the final product. The centrifugation was not used mostly due to the need of high cost refrigerated centrifugation to avoid heat denaturation of collagen. Therefore, a different approach was taken in this study to remove the pigments – i.e. repeating the extraction procedure.

The extent to which the second extraction was capable of removing pigments was measured by comparing the colour of the freeze-dried collagen. Also, the integrity of the native triple-helical conformation was again measured as it is the key factor to be considered in any application.

7.4.1 Materials and methods

Tarakihi fish skin was used as the raw material and preprocessed using the method developed in Chapter 6. The first extraction was performed using the best of the 20 treatments investigated in the previous section, that being the 5 h extraction time using a skin solid mass to solution volume ratio of 1:20. A second identical extraction was performed on the collagen extracted from the fibrillogenesis of the first. The freeze-dried collagen from the second extraction was then subjected to the tests detailed below.

Optical photographs were used to show the colour of freeze-dried collagen as seen by the naked eye. In addition, the colour was measured using L*a*b* colour method compared to a white colour standard as described earlier in this chapter. The freeze-dried collagen was characterised to determine the presence of native triple-helical conformation by the ATR-

FTIR spectroscopy, DSC and CD spectroscopy techniques in the same way as described for the single-step extraction process. These characteristics were compared to that of collagen obtained by 5 h extraction time at 1:20 mass to volume ratio as this was selected as the best treatment condition to extract collagen in native triple-helical conformation.

7.4.2 Results and discussion

7.4.2.1 Colour of collagen

Figure 7.11 shows optical photographs of the collagen formed after one and two extractions, each of 5 h extraction time at 1:20 mass of skin to solution volume ratio. Clearly, the second extraction removes more pigments. It is whiter in appearance and when assessed using the colour difference to the white standard, the score goes from 15.74 (±2.91) to 0.57 (±0.25) which is close to zero.

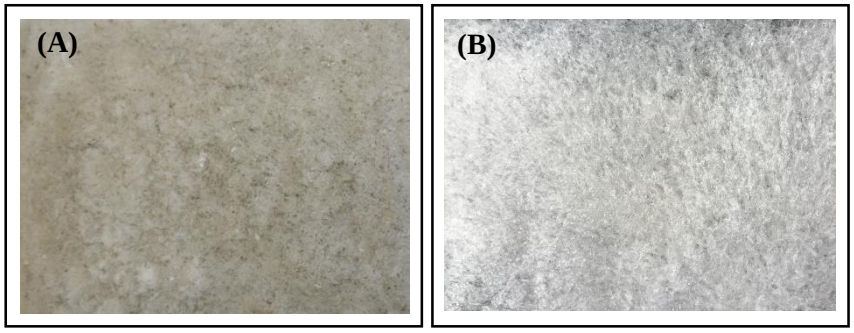

Figure 7.11 The optical photographs of freeze-dried collagen after fibrillogensis: (A) 5 h extraction time at 1:20 mass fish skin mass to NaOH solution volume ratio; (B) second extraction using the same conditions of 5 h extraction time at 1:20 mass to volume ratio.

7.4.2.2 ATR-FTIR spectroscopy

As previously done, the FTIR was used to determine the changes in the secondary structure of collagen based on the chemical bonding state. After the second cycle of extraction, the peak locations for five replicates (Table 7.5) corresponding to Amide A, B, I, II, and III were present for all samples. The amide A and amide II peak positions shifted to lower frequencies indicating more hydrogen bonds between polypeptide chains (Riaz et al., 2018; Jeong et al., 2013; Li et al., 2013), which are good indications of the stability of the triple-helical collagen structure. The position of amide I peak provides information on the different secondary structures present in collagen (Sai-Ut et al., 2012; Woo et al., 2008): 1620-1640 cm^{-1} (β sheet or extended structure); 1640-1644 cm^{-1} (irregular structure); 1645-1659 cm^{-1} (α-helix); 1660-1700 cm^{-1} (β turn) (Farrell et al., 2001 in Li et al., 2013). The wavenumbers for all five replicates were found at 1652 cm^{-1} suggesting the α-helix structure is present to form the triple-helix. The absorption ratio is calculated from the ratio of the amide III and 1450 cm^{-1} absorbances to determine the intactness of the triple-helical structure (Li et al., 2013; Sun et al., 2017; Wang et al., 2008). This ratio increased slightly from an average of 0.86 for the first extraction to 0.88, which also reflects positively on the stability of triple-helical conformation. These results confirm that the second extraction, which was used to increase the purity of collagen was also able to maintain the native triple-helical conformation.

Table 7.5 ATR-FTIR peak locations of freeze-dried collagen extracted by two repeated extractions. The mean (±SD) of five replicates are given.

Region	General range of wavenumber (cm^{-1})*	Peak position
Amide A	3400-3440	3310(±6)
Amide B	near 2920	2924(±2)
Amide I	1600-1700	1652(±0)
Amide II	1550-1600	1554(±2)
Amide III	1230-1300	1240(±0)
Absorption ratio	0.88(±0.01)	

*Sources for the general range of wavenumbers: Jeong et al., 2013; Wang et al., 2008; Li et al., 2013

7.4.2.3 Differential scanning calorimetry (DSC)

As described above, the thermal properties of collagen: denaturation temperature, onset temperature and denaturation enthalpy measured by DSC can be used to interpret the secondary structure conformation of collagen. Collagen from the second extraction had a denaturation temperature of 34.85°C, an onset temperature of 25.72°C, and a denaturation enthalpy of 40.36 J/g. These were similar to the first extraction values of 35.05°C, 26.15°C and 54.01 J/g respectively. The temperature values show that the second extraction has not altered the structure of the collagen, and so the assumption still holds that processing temperatures are possible up to 25°C without thermal degradation. The denaturation enthalpy was somewhat lower. The reason for this is unknown, but was still within the range found for the 20 treatments (Table 7.3).

7.4.2.4 Circular dichroism spectroscopy (CD)

The collagen produced a characteristic CD spectrum with a negative peak at ~198 nm, a cross-over point at ~214 nm and a positive peak at ~220 nm (Figure 7.12). The R_{pn} ratio was -0.11 which is close to -0.12 found for the first extraction and in agreement with the published literature (Gopinath et al., 2017; Nishad Fathima et al., 2009; Sun et al., 2020) for collagens with native triple-helical structure.

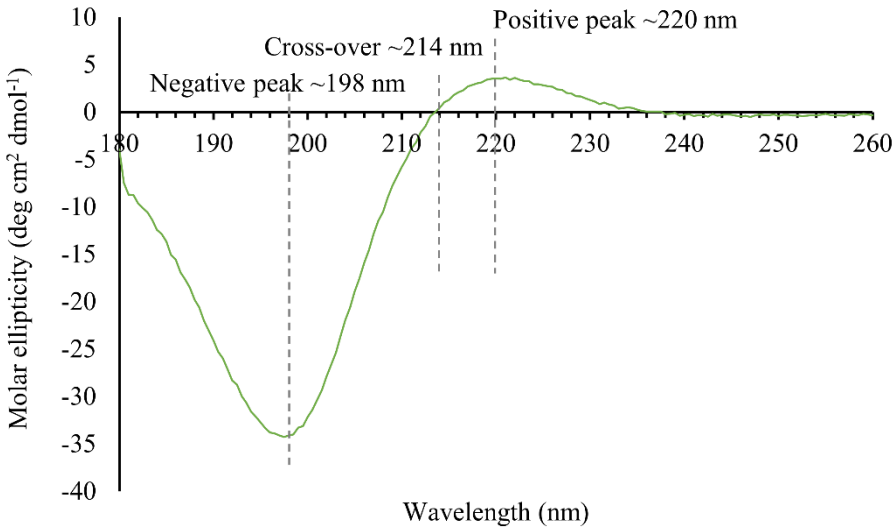

Figure 7.12 Circular dichroism spectra of collagen after the second extraction.

These results indicate that the repeated extraction of collagen for 5 h at 1:20 mass to volume ratio produced successful results of removing skin pigments and improving the colour. Moreover, these conditions have not caused any deterioration to the native triple-helical collagen structure. Therefore, it can be used as a successful method to increase collagen purity and colour by removing pigments without using any chemicals or expensive methods like refrigerated centrifugation. The down side is that it adds significant extra time to the overall process as it requires two extractions and two fibrillogenesis steps.

7.5 Conclusions

This chapter developed an effective extraction method to solubilise collagen in its native triple-helical conformation, with a particular focus on the behaviour of fish skin and changes in the extraction medium. It further provides guidelines for the application of this knowledge on any fish species of interest by providing four processing objectives: (i) an upper limit of pH 4 for the extraction solution; (ii) maximum swelling; (iii) a manageable viscosity of the extraction solution; and (iv) as few undissolved pieces of skin as possible; and two quality objectives; (v) preserving the native helical structure of the collagen; and (vi), minimising pigment discolouration. The 5 h extraction time at 1:20 mass of skin to volume of solution ratio was selected as the best treatment conditions to achieve these objectives. This chapter further introduced a pigment removal step to improve the purity and colour of collagen by using a second extraction, while still preserving the collagen native structure. While fibrillogenesis conditions were standardised in this chapter, there are several variables that could be manipulated to control the macrostructure of the precipitated collagen. This is the focus of the next chapter.

Chapter 8. The effect of process conditions on fibrillogenesis

8.1 Introduction

In vivo fibrillogenesis is an entropy-driven self-assembly process that is regulated by the cell (Silver et al., 2003). During this process, triple-helical collagen molecules assemble in parallel into fibrils having a characteristic banding pattern with a distinct periodicity of about 67 nm (the D-period) (Gelse et al., 2003; Lee et al., 2001; Li and Douglas, 2013). Fibril diameters are between 25 and 400 nm (Gelse et al., 2003), and their length is less than 1 cm (Shoulders and Raines, 2009). Similar structural properties can be recreated *in vitro* by manipulating the fibrillogenesis conditions such as pH (Li and Douglas., 2013; Zhu and Kaufman, 2014); rate of pH change (Pawelec et al., 2016; Zhu et al., 2018); temperature (Christiansen et al., 2000; Zhu and Kaufman, 2014), ion species (Li et al., 2009), ionic strength (Zhu and Kaufman, 2014), and buffer conditions (Christiansen et al., 2000).

In collagen processing, fibrillogenesis is the third and final step following the pretreatment and extraction. Pretreatment involves the removal of non-collagenous components such as non-collagenous proteins, fats and pigments which is essential for the purity of collagen. The extraction involves the solubilisation of collagen molecules into the extraction medium in the native triple-helical conformation. If the triple-helical conformation is not preserved during extraction, it will form fibres without a native D-banding pattern during the fibrillogenesis step and so will lose its application as a biomedical material (Qi et al., 2015; Sun et al., 2020), because cellular responses such as cell proliferation, cell migration, cell differentiation, and cell adhesion (Zhu et al., 2018), and mineralisation of the collagen matrix (Li et al., 2009) depend on this D-banding pattern. Chapters Six and Seven studied the first two processing steps in detail and developed pretreatment and extraction processes suitable for fish skin.

Fibrillogenesis has been well-studied by previous researchers. The self-assembly process of fibrillogenesis is an entropy-driven process that is favoured by a large positive entropy contribution due to the release of structured water around collagen molecules (Li and Douglas 2013; Pawelec et al., 2016; Li et al., 2009). Three main intermolecular interactions have been described to affect this process and to form the D-periodicity: the hydrophobic interactions between non-polar regions of adjacent collagen molecules, hydrogen bonding between polar residues, and the electrostatic interactions due to the charges on ionisable groups (Li et al., 2009). The highest hydrophobic and polar interactions are achieved when the collagen molecules are set by a distance of 234 amino acid residues, forming the native D-banding pattern (Li et al., 2009).

In almost all the fish collagen extraction studies, (for example, Nagai & Suzuki, 2000; Zeng et al., 2009; Li et al., 2013; Arumugam et al., 2018), Sodium chloride was used to achieve fibrillogenesis, which involves a salting-out mechanism. Salting-out can leave salt residues and requires a number of complex and time-consuming dialysis treatments with intermediate centrifugation to remove the salts. Therefore, the isoelectric precipitation method was used in this study to induce the fibril formation by raising the pH to the isoelectric point. Different factors can shift the isoelectric point, which include: fish species differences, processing temperature, collagen concentration, and rate of fibrillogenesis.

A better understanding of the *in vitro* fibrillogenesis process is required to develop a fish collagen extraction method. Therefore, the experiments reported in this chapter were designed to assess the effect of three processing variables on the morphology of fibrils: initial collagen concentration, end pH of fibrillogenesis and mixing speed.

8.2 Research strategy

Two variables, the concentration of initial collagen solution and the end pH of the fibrillogenesis were studied first, as step 1, in a matrix of experiments. The speed of mixing to achieve the end pH was studied later, as step 2, on a selected pairing of the initial concentration and end pH.

In step one, 12 fibrillogenesis conditions were experimented as: two collagen concentrations; 0.15% (1.5 mg/mL) and 0.30% (3.0 mg/mL) and six pH levels; 6.0, 7.0, 8.0, 9.0, 9.3, and 10.0. These collagen concentrations and pH levels were selected based on the understanding of the previous literature. The pH 9.3 condition was included as previous literature has described it as the isoelectric pH of type I collagen (Jiang et al., 2004). It was observed during the experiments under Chapter Four that the mixing speed has an effect on fibril morphology, however it was not a focus of that chapter. Previous lietrature has explained the effect of rate of pH change on the fibril morphology, for example, by Pawelec et al. (2016); Zhu et al. (2018), however no studies were found regarding the effect of different mixing speeds. Therefore, in step two, to test the effect of speed of mixing, three speeds were tested at 0.30% collagen concentration and pH 9.3.

8.3 Materials and methods

8.3.1 Sample preparation

Tarakihi fish skin was used as the raw material. The fish skin was minced and a 50.0 g sample was taken according to the method in §6.2. The samples were then pretreated according to the method developed in §6.6. Then the collagen from this pretreated skin was extracted into HCl acid medium according to the method developed in Chapter 7 where, to recap, the pretreated skin sample was soaked in 0.01 M HCl solution at 1:20 mass to volume ratio for 5 h with continuous stirring at 350 rpm using a magnetic stirrer. After 5 h, the skin and the solution were homogenised together using a hand blender. Then, the pH of the medium was raised to pH 9.3 by adding 0.01 M NaOH to form fibrils. These collagen fibrils in a hydrated state were then separated using a strainer of 2 x 2 mm mesh. They were then added to a fresh 0.01 M HCl solution in a second extraction step and the pH of the medium was raised to pH 9.3 by adding 0.01 M NaOH to form fibrils. Afterwards, these collagen fibrils in a hydrated state were separated using a strainer of 2 x 2 mm mesh, and packed into polythene bags, frozen at -20 °C, then freeze-dried at 0.5 mbar, 10 °C. The collagen needed for all the experiments in this chapter was extracted in the same batch to avoid variability in fibrillogenesis experiments due to differences that might occur between batches.

8.3.2 Experimental protocol

8.3.2.1 Effect of initial collagen concentration and end pH on fibrillogenesis

Collagen solutions of 0.15% and 0.30% concentrations were prepared by dissolving freeze-dried collagen obtained according to §8.3.1, in 100 mL of 0.01 M HCl (pH 2.0) for 1 h in a cold room at 4°C. The pH of each solution was adjusted by adding 0.1 M NaOH and mixing at a constant speed to reach the desired pH according to the following procedure. A 0.5 mL of NaOH solution was first added into the 100 mL collagen solution (in a 250 mL glass beaker) and mixed with a stainless steel plate attached to a stirrer (Phipps & Bird stirrer, Model 7790-402, Unit of General Medical Corp., Richmond, VA) at a speed of 18 revolutions per minute and NaOH addition and mixing were repeated four times. After that NaOH was added dropwise while mixing at the same speed until the desired pH was reached. This was done on ice to maintain the sample temperature at 4°C. Then the turbidity of this sample was measured according to the method described below in §8.3.4.

The collagen fibrils which were precipitated in the glass beaker were kept undisturbed for 24 h and were separated by filtering through a strainer of 2 x 2 mm mesh size. The fibrils were then packed in polythene bags, frozen at -20 °C and freeze-dried at 0.5 mbar, 10 °C. The weight of the freeze-dried collagen was recorded.

The freeze-dried collagen samples were characterised for surface morphology, fibril diameter, and D-space using the methods described below.

8.3.2.2 Effect of mixing speed on fibrillogenesis

Three mixing speeds were tested as 9 revolutions per minute (low speed), 18 rpm (medium speed), and 36 rpm (high speed) by using the 0.30% initial collagen concentration and end pH of 9.3. Otherwise, the experiment followed the same procedure as §.8.3.2.1 above.

8.3.3 pH Measurement

The pH of the solutions were measured using a portable pH meter (Thermoscientific, Orion Star A326 pH/RDO/DO meter).

8.3.4 Turbidity measurement

The fibril-forming ability was determined by measuring the absorbance at 310 nm based on the turbidity change during fibril formation. As described in the §8.3.2 above, soon after reaching the desired pH, a sample was taken from the top middle area of the beaker to a 1.5 mL quartz cuvette of 1 cm path length and the absorbance was measured at 310 nm using a UV-visible spectrophotometer (Genesys 10S spectrophotometer, Wisconsin, USA), conditioned at 6°C in a cold room. The 0.01 M HCl solution was used as the blank. The absorbance measurement was continued every minute until 10 min; then every 10 min until 60 min; and hourly until 24 h.

8.3.5 Yield of collagen

The yield of collagen was calculated as dry collagen (g) per dry weight of collagen taken for the experiment (g).

$$\text{Yield} = \left(\frac{M_{Freeze-dried\ collagen\ after\ each\ fibrillogenesis}}{M_{Freeze-dried\ collagen\ taken\ for\ the\ experiment}} \right) \times 100\%$$

8.3.6 Surface morphology of collagen

The surface morphology of collagen samples was analysed by scanning electron spectroscopy (SEM) according to the method described in §3.2.1.6.1.

8.3.7 Fibril characteristics

Transmission electron microscopy (TEM) was used to analyse the D-periodicity and the fibril diameters. Small pieces of approximately 5x5 mm size were cut from freeze-dried collagens and fixed in a modified Karnovsky fixative and kept refrigerated until further processing. When the samples were ready for processing they were washed with buffer and fixed successively in glutaraldehyde and osmium in cacodylate buffer. Then the samples were progressively dehydrated in an acetone series (25%, 50%, 75%, 95%, 100%) before embedding in resin. The resin-embedded samples were sectioned at 100 nm Leica UC6 Ultramicrotome (Leica Microsystems GmbH Ernst-Leitz-Straße 17–37 Wetzlar, 35578 Germany) and imaged in a Philips CM100 BioTWIN transmission electron microscope with LaB6 emitter (Philips/FEI Corporation, Eindhoven, Holland) fitted with MegaView lll digital camera (Olympus Soft Imaging Solutions GmbH, Münster, Germany) using an accelerating voltage of 100 kV. The D-periodicity and the fibril diameters were measured from these images using ImageJ software version 1.53t.

8.3.8 Zeta potential measurement of collagen solutions

The surface charge of collagen molecules was measured as the zeta potential. A collagen solution of 0.5 mg/mL in 12 mM HCl with MilliQ water was prepared at 4°C by dissolving freeze-dried collagen using a magnetic stirrer at 200 rpm until collagen was completely solubilised. A series of solutions were prepared from this solution in the pH range from 3.0 to 11.0 in 0.5 intervals by adding 0.1 M NaOH. The zeta potential of each solution was carried out at 4°C using a zeta potential analyser (Malvern Zetasizer Pro).

8.4 Results and discussion

8.4.1 Fibril-forming ability

In this research, the fibrillogenesis was induced by the addition of NaOH solution to raise the pH of the acidic collagen solution to close to the desired pH. Generally, concentrated collagen solutions are transparent or translucent and become opaque upon forming fibrils. These fibrils can scatter light depending on the amount of fibrils, where the higher intensity of scattered light means higher turbidity or a higher degree of fibril formation (Gobeaux et al., 2008). The fibrillogenesis mechanism has been described as progressing through three phases: a lag phase, the growth phase, and the plateau phase resulting in absorbance following a sigmoidal curve over time (Li & Douglas, 2013). The lag phase occurs before the onset of fibrillogenesis, therefore no change in turbidity occurs. The growth phase is observed by a rapid increase in turbidity due to fibril formation, and the plateau phase marks the completion of fibrillogenesis by no further turbidity increase (Li et al., 2009).

The turbidity vs. time curves of collagen fibrillogenesis under the effect of initial collagen concentration and end pH is shown in Figure 8.1. The highest turbidity was seen at pH 8.0 for both 0.15% and 0.30% concentrations over the 24 h. Interestingly, both graphs did not show a lag phase and had reached the plateau by eight minutes. The lowest turbidity was

seen at pH 10.0 for both collagen concentrations. The turbidity values remained unchanged until around 12 h without evidence of any growth, but then slightly decreased. The fibrillogenesis at pH 6.0 and pH 7.0 for both concentrations progressed through a lag phase, growth phase and plateau phase, but the turbidity remained in the middle range. Fibrillogenesis at both pH 9.0 and pH 9.3 at 0.30% concentration followed the typical sigmoidal curve, having almost similar turbidity and reaching a plateau by 10 minutes. Similarly, fibrillogenesis at pH 9.0 and pH 9.3 at the lower 0.15% concentration have followed the sigmoidal curve, but the turbidity remained at comparatively lower values and showed an increase again after around 16 h.

The results obtained on the fibril-forming ability are quite different from that of previous literature. Liao et al., (2018) reported the highest turbidity at pH 7.0 for collagen extracted from the skin of barramundi (*Lates calcarifer*) fish, and Li et al. (2009) reported the highest turbidity at pH 9.2 for collagen extracted from cattle hide, which are different from this study. These differences can be due to the collagen extraction method, the solvent used for dissolving collagen, and the initiation conditions of fibril formation (Zhang et al., 2014). In addition, in these studies, fibril formation ability had been assessed in the buffer solutions at different pH levels to maintain the pH unchanged, however, in the present study buffer solutions were not used because the experiments were conducted without any deviations from the method intended to develop in the research. Therefore, in this work, the solution passed through a range of pH until it reached the intended pH. These facts have been considered in discussing the results later in this chapter.

The surface charge of collagen solutions over a pH range from 3.0 to 11.0 was measured as zeta potential and correlated with the fibrillogenesis process (Figure 8.2). The isoelectric pH (pI) of the collagen measured at 4°C in this experiment was pH 7.5. The pI of type I collagen reported in the literature is pH 9.3, however, it can be shifted to lower values around pH 7.0 due to electrostatic interactions between some ions and the amino or carboxyl groups of collagen molecules (Li et al., 2009; Li & Douglas 2013). For example, Li et al. (2009) reported the pI at pH 9.2 at a lower ionic strength compared to pH 7.4 at a higher ionic strength, indicating the net dependence of the surface charge of collagen molecules by the medium pH and the added salts. In the current research no ions were added to induce fibrillogenesis. However, it is possible that there are still some salts remaining from neutalising the NaOH with HCl during the pretreatment which can shift the pI to pH 7.5. It should be noted that the comparisons are more valid when the processing conditions are more similar. However, the highest turbidity at both collagen concentrations were recorded at pH 8.0 which is close to the pI obtained in this study. In addition, these graphs clearly show that the turbidity values of 0.30% collagen concentration were always higher than that of 0.15% concentration. These results are described below in relation to intermolecular interactions where possible.

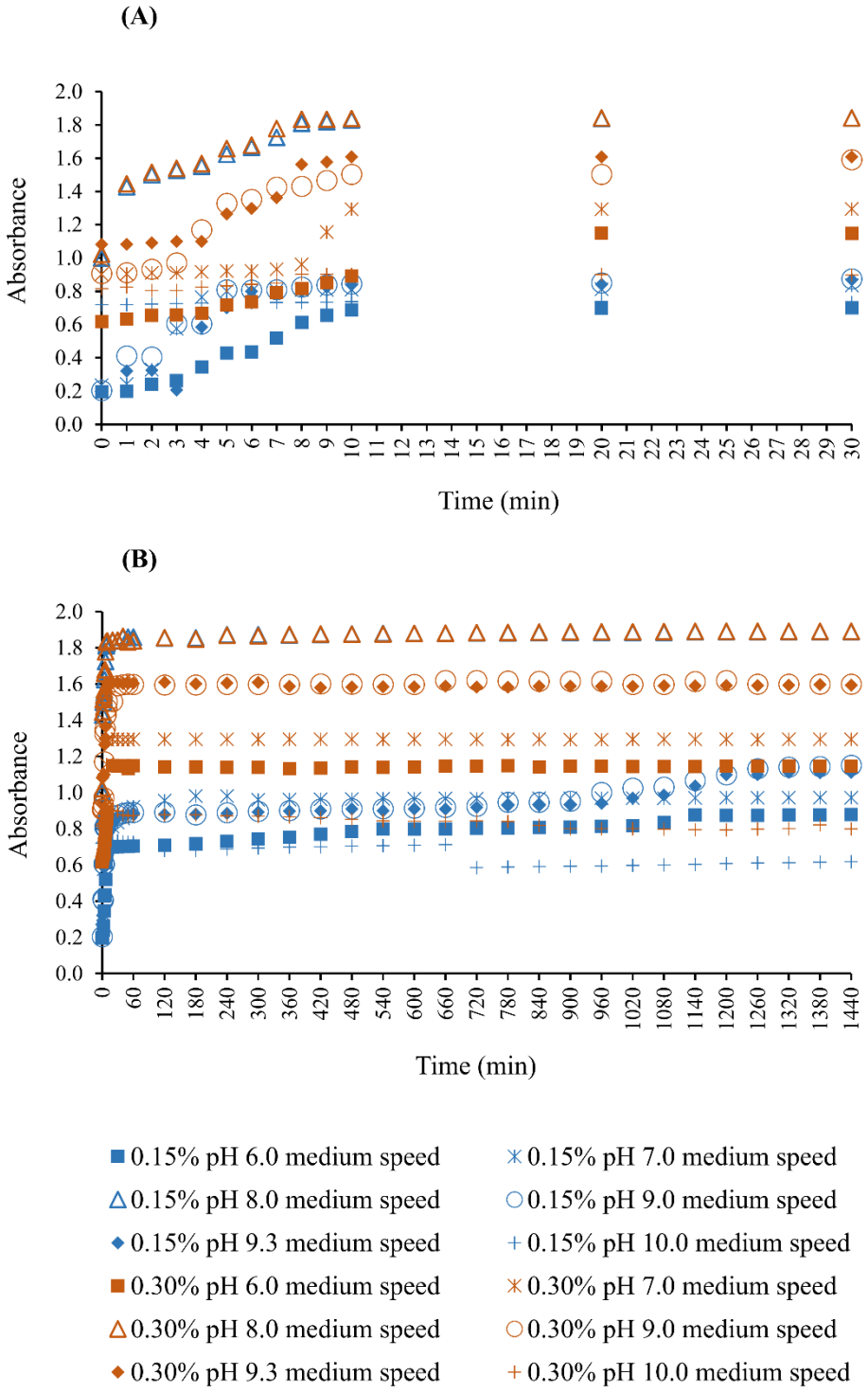

Figure 8.1 Progress of fibril formation under the effect of initial collagen concentration and end pH. (A) From 0 min to 30 min showing the short-term turbidity changes; (B) From 0 min to 1440 min (24 h) showing the long-term turbidity changes.

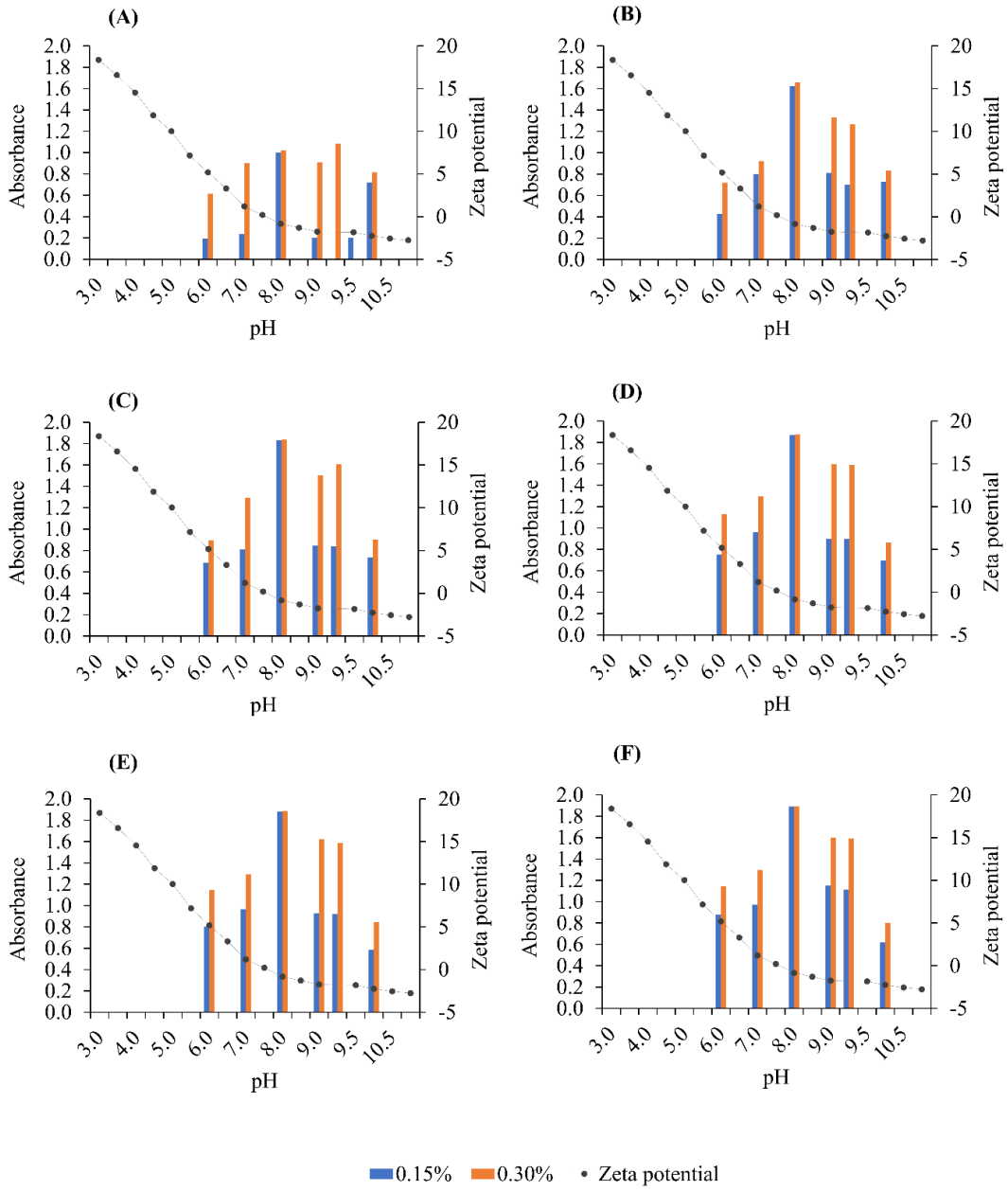

Figure 8.2 Fibril formation as a measure of change in turbidity at particular time durations, under the effect of initial collagen concentration and end pH: (A) 0 min; (B) 5 min; (C) 10 min; (D) 6 h; (E) 12 h; (F) 24 h. The measured zeta potentials in the pH range from 3 to 11 are shown in the second y axis of the same graph. Broken lines of the zeta potential graphs are guides to the eye.

The turbidity vs. time curves of collagen fibrillogenesis under the effect of different mixing speeds are shown in Figure 8.3. The time taken to reach the end pH of 9.3 was different at the three different speeds; 5 min at high speed (36 rounds per min), 20 min at medium speed (18 rounds per min), and 40 minutes at low speed (9 rounds per min). The highest turbidity over the whole 24-h period was recorded at the high mixing speed. It progressed through a growth and a plateau phase. The medium speed (the same graph in Figure 8.1) followed the typical sigmoidal curve. The initial turbidity shown by the low speed was higher than that of the medium speed. The low mixing speed provided the fibrils time to change through the

different pH values, including the isoelectric pH (pH 7.5) until the medium eventually reached pH 9.3. It can be argued that fibrils had been aggregated at the isoelectric point and had come to the top by the time the solution reached pH 9.3. This may be the reason for showing higher turbidity from the beginning without continuing through a lag or growth phase. These results can be explained with the fibril characteristics described below in §8.4.2.

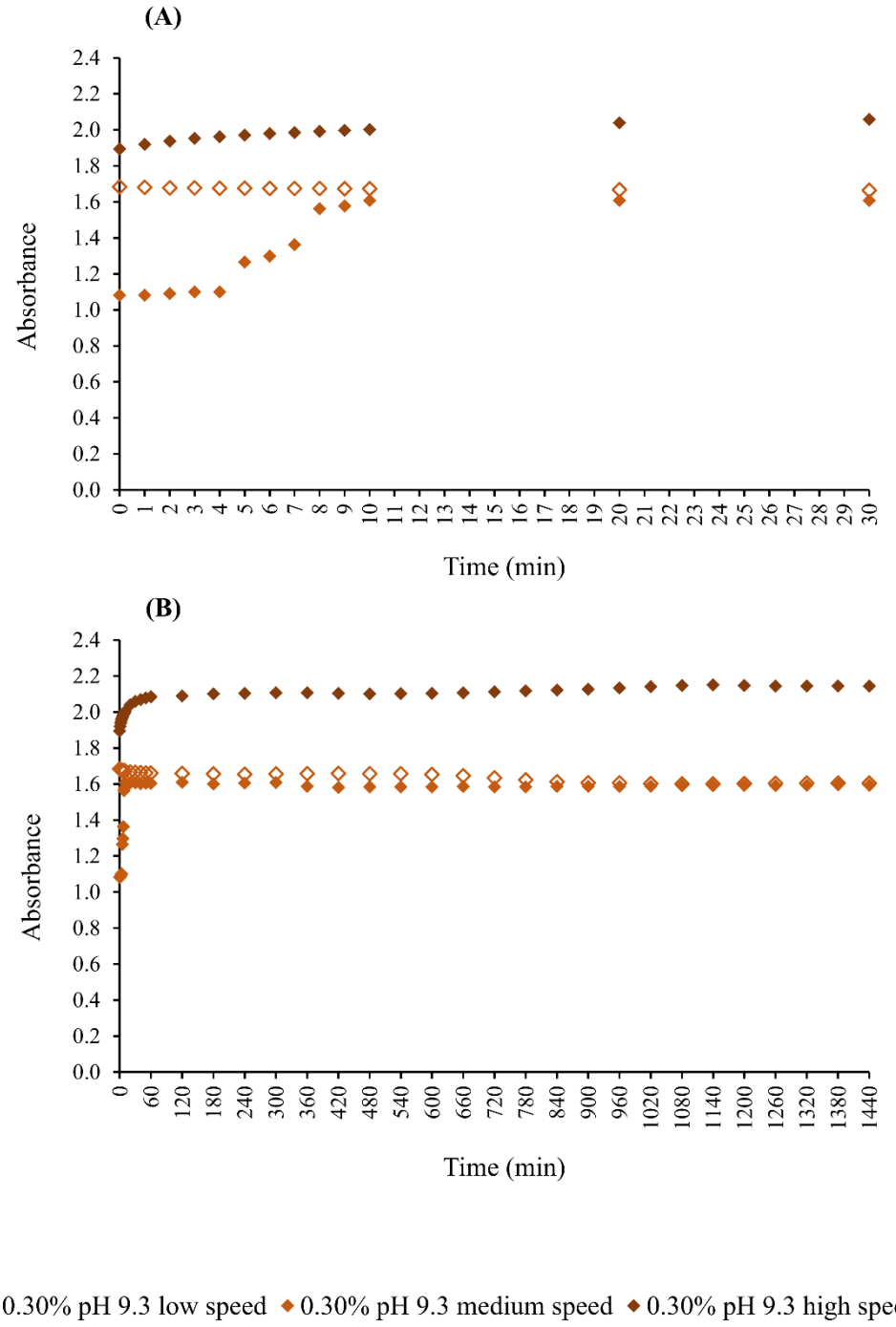

Figure 8.3 Progress of fibril formation under the effect of mixing speed. (a) From 0 min to 1440 min (24 h); (b) From 0 min to 30 min.

8.4.2 Fibril characteristics

The transmission electron micrographs of the self-assembled collagen fibrils after 24 h, under the effect of initial collagen concentration and the end pH, are shown in Figure 8.4. Out of the six end pH values at 0.15% concentration, the fibril structure with a banding pattern was visible only for pH 10.0 (Figure 8.4 (F)). The banding periodicity was 50-56 nm and the fibril diameters ranged from 170-410 nm and appeared as loose bundles of fibrils. From Figure 8.4 (A-E), disordered small nanofibrils were visible all over the field of view. There were only one or two fibril-like structures visible with some unclear banding pattern. These results indicate that the fibril formation has been started, however, it has not produced fibrils of native D-banding of 62-67 nm. Previous studies have reported native D-periodicity of 65-67 nm for wet tissues and 62-64 nm for air-dried samples (Li et al., 2009). The banding pattern around 50-60 nm has been reported in previous studies as an unusual alignment of collagen molecules in the early stage of fibrillogenesis (Li et al., 2009).

For the 0.30% collagen concentration, small fibrils which are more densely packed than that of 0.15% are seen in the images from figure 8.4 (G-J). Periodic arced patterns suggestive of a helical structure are seen for pH 7.0, 8.0 and 9.0 (Figure 8.4 (H-J)). Similar results have been reported by Gobeaux et al. (2008) for higher collagen concentrations. This pattern was more prominent at pH 9.0, and interestingly it has progressed to form collagen fibrils with a banding pattern of 65-69 nm similar to the native D-banding pattern at pH 9.3. The fibril diameters ranged from 155-275 nm with a higher frequency above 200 nm. Ramı´rez-Rodrı´guez et al. (2014) reported that the formation of the D-banding pattern is a pH-dependent process which starts after the fibril formation becomes steady, and a D-periodicity close to native collagen (62-67 nm) is an indication that the fibril formation has reached the final most stable state. Therefore, pH 9.3 at a 0.30% initial collagen concentration and medium mixing speed can be taken as the most suitable fibrillogenesis condition to form fibrils with native D-banding pattern. The fibril structures have been disappeared again if fibrillogenesis was ended at pH 10.3.

The fibril characteristics at different mixing speeds are shown in Figure 8.5. There were only small nanofibrils visible at low speed (Figure 8.5 (K1)). The low mixing speed may have caused the fibrils to stay at unnecessary long residence time durations at the different transient pH levels and destroy fibril structures as explained above in §8.4.1. Figure 8.5 (K2) is the same as Figure 8.4 (K) which shows the fibril characteristics at medium speed (a D-banding of 65-69 nm, and fibril diameter of 155-275 nm). The high-speed fibrillogenesis produced tightly-packed collagen fibrils with a banding pattern of 55-65 nm, and fibril diameters of 90-148 nm (Figure 8.5 (K3)). This difference in fibril diameter with the medium speed can be related to the rate of fibrillogenesis. A gradual increase of pH during fibrillogenesis can slow down the fibril formation length-wise due to unnecessary time the solution spends at undesirable fibrillogenesis conditions. Instead, it favours the lateral aggregation forming broader fibrils. In contrast, a rapid increase in pH favours the formation of thinner fibrils (Ramı´rez-Rodrı´guez et al., 2014). This is the reason for the smaller diameter of fibrils at high mixing speed compared to that of medium speed. However, at high speed a heterogeneity in the D-periodicity between 55-65 nm was seen and may be due to the existence of a few localised areas of different pH values in the collagen solution resulted from improper

mixing at high speed. Although previous studies have reported similar unusual D-periodicities, the literature is still limited on this aspect which needs further investigation.

The mechanism of fibrillogenesis in relation to the isoelectric point has been well-explained in the previous literature. At the isoelectric pH, the surface charges on collagen molecules become zero thus decreasing the electrostatic repulsion, and the hydrophobic interactions increase, leading to collagen aggregation and precipitation (Kittiphattanabawon et al., 2005; Li & Douglas 2013; Pawelec et al., 2016; Li et al., 2009;). When the pH of the medium is above or below the isoelectric pH, a net negative or positive charge exists on collagen molecules, leading to interaction with water and solubilisation due to charge repulsions (Kittiphattanabawon et al., 2005). These mechanisms have been described in detail in §2.4.4.1. In the current study, although higher turbidity was observed at a pH very close to the pI, the desired D-periodicity occurred at a pH higher than pI.

The results of this study didn't indicate a relationship between turbidity and D-periodicity. The highest turbidity was reported at pH 8.0 for both concentrations, however, the fibril structures with banding patterns were visible only at pH 10.0 for 0.15% concentration and at pH 9.3 for 0.30% concentration. The highest turbidity at pH 8.0 means higher aggregation of collagen molecules, however, the collagen molecules are still present as non-fibrillar collagen as shown in Figure 8.4 (C and I). This can be a reason of higher viscoelasticity once the collagen molecules are aggregated to the top of the beaker, hence reducing the molecular mobility. Gobeaux et al. (2008) reported that high viscoelasticity can obstruct the fibril formation process, and only a limited fraction of collagen molecules is aggregated into fibrils. This is evident from the results of this study as well where only one or two fibril structures are seen in a majority fraction consisting of non-fibrillar collagen. However, further experiments are suggested to analyse the effect of the viscosity of collagen solutions on the formation of collagen fibrils with D-periodicity using rheology. Previous studies on this aspect is limited, with different arguments reported in relation to D-banding and pI.

Ramı´rez-Rodrı´guez et al. (2014) reported that a higher number of fibres having native D-periodicity were observed at a pH higher than the pI. According to Zhu et al. (2018) and Pawelec et al. (2016), at pH values far away from the isoelectric point, fibrillogenesis was slow or incomplete where fibrils gathered to form sub-fibrils without the D-banding pattern. However, the findings of Gobeaux et al. (2008) were different, where they reported the formation and stability of native fibrils in a wide pH range from 6.2 to 12.2, and the fibrils without banding structure were formed only at pH 13. The stability of fibrils above the pI can be due to non-ionic forces such as hydrophobic or van der Waals forces (Gobeaux et al., 2008). However, a comparison of the fibril characteristics of previous studies with that of the current study is not easy when the extraction medium, fibrillogenesis method and fibrillogenesis conditions are different.

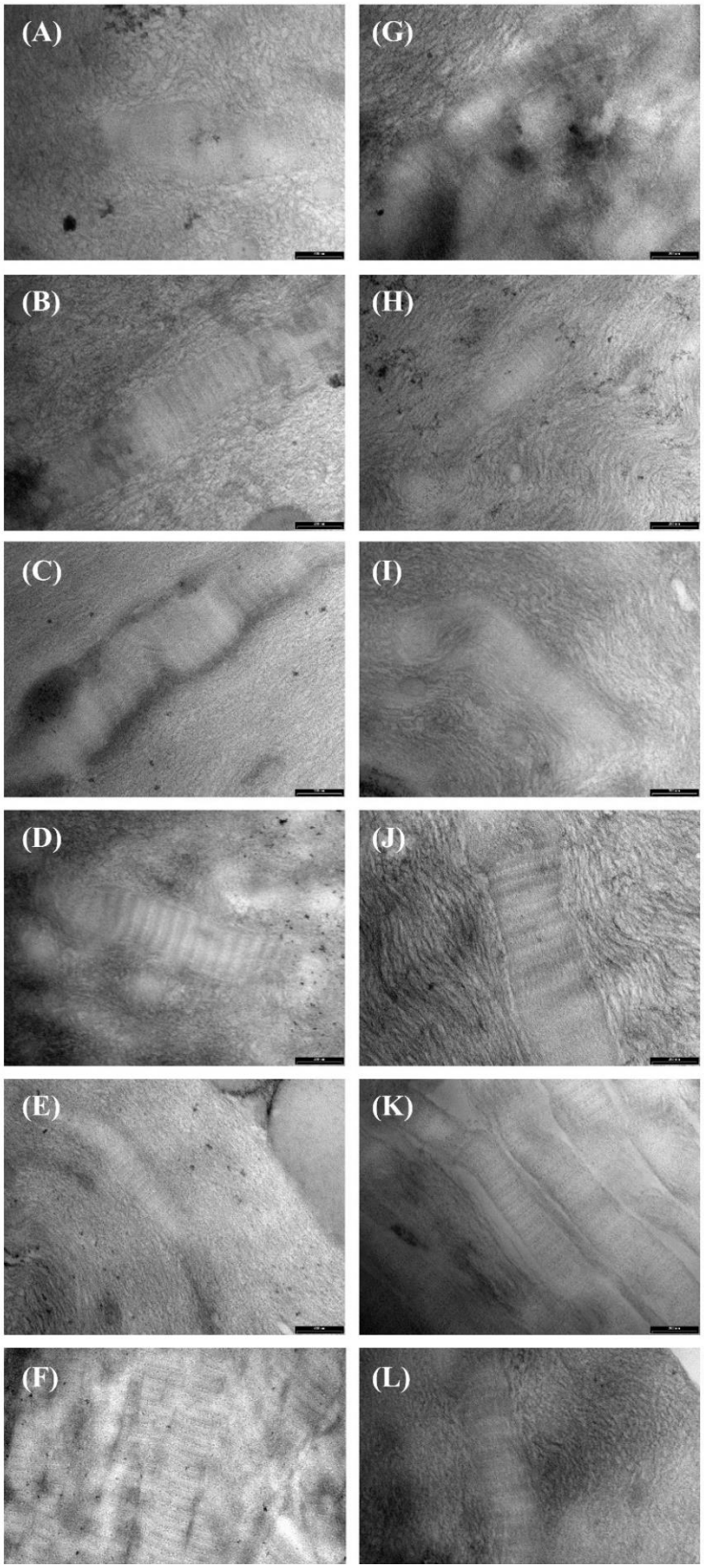

Figure 8.4 TEM images of the self-assembled collagen fibrils after 24-h of fibrillogenesis: (A) 0.15% pH 6.0; (B) 0.15% pH 7.0; (C) 0.15% pH 8.0; (D) 0.15% pH 9.0; (E) 0.15% pH 9.3; (F) 0.15% pH 10.0; (G) 0.30% pH 6.0; (H) 0.30% pH 7.0; (I) 0.30% pH 8.0; (J) 0.30% pH 9.0; (K) 0.30% pH 9.3; (L) 0.30% pH 10.0. The mixing was done at medium speed. The scale bar represents 200 nm.

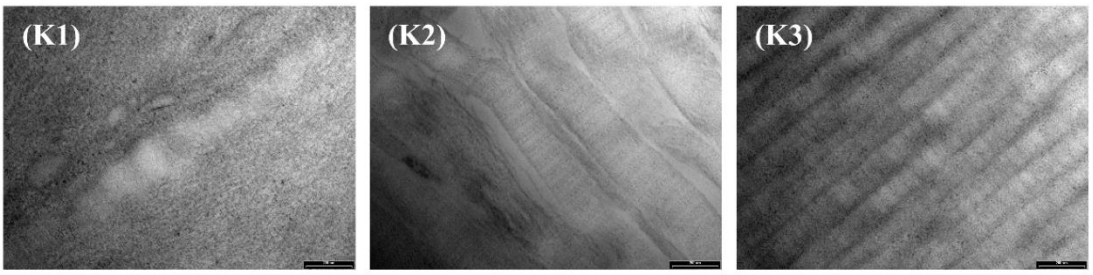

Figure 8.5 TEM images of the self-assembled collagen fibrils after 24 h of fibrillogenesis: (K1) low speed; (K2) medium speed; (K3) high speed. The initial collagen concentration was 0.3% and the end pH of fibrillogenesis was pH 9.3. The scale bar represents 200 nm.

8.4.3 Surface morphology of collagen

Scanning electron micrographs were used to analyse the surface morphology of freeze-dried collagens. The effect of initial collagen concentration and the end pH of fibrillogenesis is shown in Figure 8.6 and the effect of mixing speed is shown in Figure 8.7. All collagens appeared as sheet-like structures with irregular porosity with no obvious differences between samples.

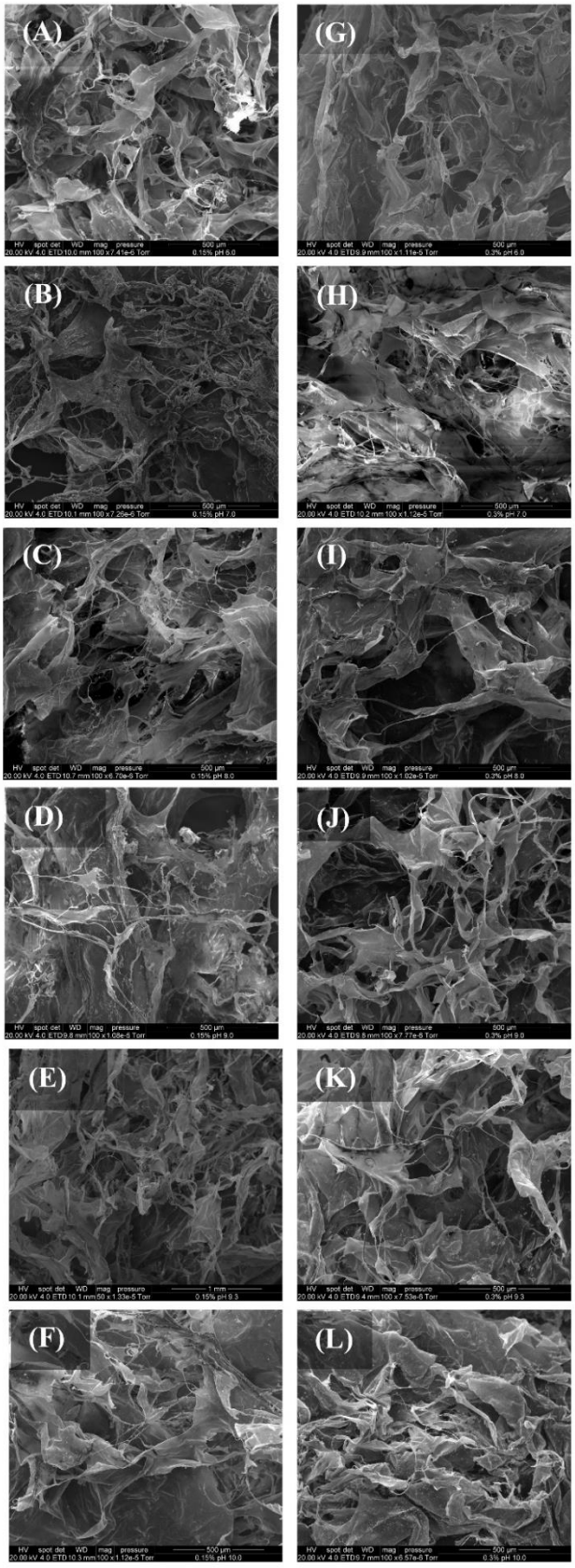

Figure 8.6 SEM images of freeze-dried collagens at x100 magnification: (A) 0.15% pH 6.0; (B) 0.15% pH 7.0; (C) 0.15% pH 8.0; (D) 0.15% pH 9.0; (E) 0.15% pH 9.3; (F) 0.15% pH 10.0; (G) 0.3% pH 6.0; (H) 0.3% pH 7.0; (I) 0.3% pH 8.0; (J) 0.3% pH 9.0; (K) 0.3% pH 9.3; (L) 0.3% pH 10.0. The mixing was done at medium speed. The scale bar represents 500 µm.

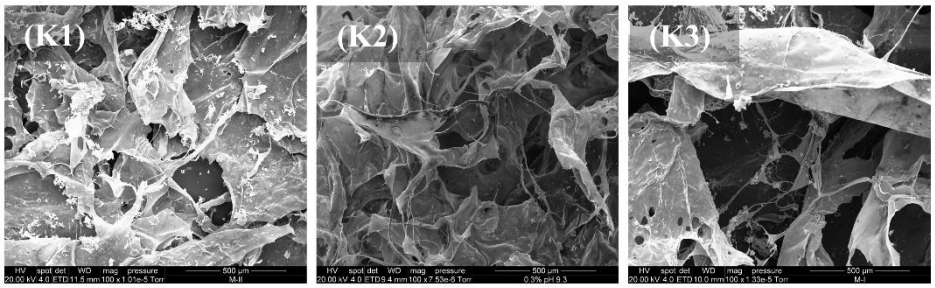

Figure 8.7 SEM images of freeze-dried collagens: (K1) low speed; (K2) medium speed; (K3) high speed. The initial collagen concentration was 0.30% and the end pH of fibrillogenesis was pH 9.3. The scale bar represents 500 µm.

8.4.4 Yield of collagen

The yield of collagen obtained at combinations of six different end pH values and two different collagen concentrations are given in Table 8.1. The lowest yields were recorded at pH 10.0 for both concentrations. The lowest turbidity has also been recorded at pH 10.0 as discussed above. The lower yield of collagen at pH 10.0 may be due to the increased solubility of collagen by the increased repulsive forces between collagen molecules at a pH so far away from the isoelectric point. The yields obtained at pH 6.0 were also less. According to the results of turbidity and TEM images, the fibril formation has been started when the solution reaches pH 6.0 however it is only at its initial stage. This may be the reason for the lower yield at pH 6.0. When the different mixing speeds at pH 9.3 for 0.30% collagen concentration are concerned the highest yield (84.40%) was recorded at high speed, and the lowest (79.27%) at low speed. The reason can be the increased amount of fibrils formed at high speed and the destruction of fibrils at low speed as discussed under §8.4.1.

Table 8.1 The yield of collagen expressed as dry collagen (g) per dry weight of freeze-dried collagen taken for the experiment (g).

Initial collagen concentration	End pH of fibrillogenesis					
	6.0	7.0	8.0	9.0	9.3	10.0
0.15%	78.27	80.67	83.93	80.93	81.27	74.60
0.30%	79.07	81.67	84.03	83.27	82.37	75.30

8.5 Conclusions

This chapter developed a method to form collagen fibrils with D-banding pattern which is an important requisite for biomedical applications. A possible explanation from the results of these experiments is that self-assembly process of *in vitro* fibrillogenesis depends to a greater extent on the initial collagen concentration and the mixing speed. There should be a

proper balance between the initial collagen concentration and the mixing speed where concentration is important for the molecular availability and the mixing speed is important for the molecular mobility. The end pH is also important, which has been shown to be of greater influence than the concentration and the mixing speed. These results indicated that although the fibril aggregation is highest at or near the isoelectric pH, the formation of D-banding requires a higher pH. However, more experiments are needed to properly describe this factor in relation to molecular interactions.

Chapter 9. Conclusions and opportunities for future research

9.1 Conclusions

The work presented in this thesis was based on building mechanistic knowledge on how the fish skin structure and composition relate to the physico-chemical processes of collagen extraction. A method was developed to extract biomedical collagen from fish skin based on this understanding while presenting guidelines to use this method for variable fish species at the industrial level.

The application of a commercial bovine biomedical collagen extraction method to fish skin at laboratory scale and discovering the reasons for failure was the key to developing a fish skin collagen extraction method in this work. The heterogenous structure of the fish skin was identified as the reason for non-applicability and changes were proposed based on this understanding. The method development for fish skin was carried out in a sequence of steps because each step depends on the preceding step: pretreatment, collagen extraction, and fibrillogenesis.

Although this biomedical collagen extraction method developed in on the laboratory scale has not been scaled-up to the industrial level in the present study, it shows the potential industrial application. The process flow diagramme of the developed process is presented in Figure 9.1. The process was developed in a way to be simple, cost and time effective, having a small number of processing steps, and minimising the water and chemical use. Due to the simplicity and non-requirement of high-tech equipment, it is likely that this method can be used at small or large-scale processing. Most importantly, the mechanistic knowledge developed through the whole study forms the basis on how the processing conditions should be adjusted to the fish species of interest.

One key process condition is the need to carry out processing well below the thermal denaturation temperature. For cold-water fish such as Tarakihi and Ling, this should be around 4℃. Note that low temperatures are also likely to be needed to avoid microbial growth during processing.

The need for swelling of the fish skin during pretreatment was identified as the driving force for a successful removal of non-collagenous proteins and fats. This swelling was achieved by using Sodium hydroxide as the pretreatment agent. The developed pretreatment process uses only two washes with a Sodium hydroxide solution followed by neutralisation with hydrochloride acid, and removal of residual salts by a water wash. This procedure is efficient in water use, chemicals, and time as well.

The mechanistic approach taken to study the collagen solubilisation process from fish skin formed the knowledge of the relationship between the behaviour of fish skin and changes in the extraction medium during the collagen solubilisation. Maintaining an upper limit of pH 4 during extraction, obtaining maximum swelling of skin, attaining a manageable viscosity after homogenisation to achieve maximum dissolution of skin were all found to be important processing objectives. The use of a hydrochloric acid solution with an initial pH 2 was shown to be successful to achieve this while maintaining the native triple-helical collagen structure.

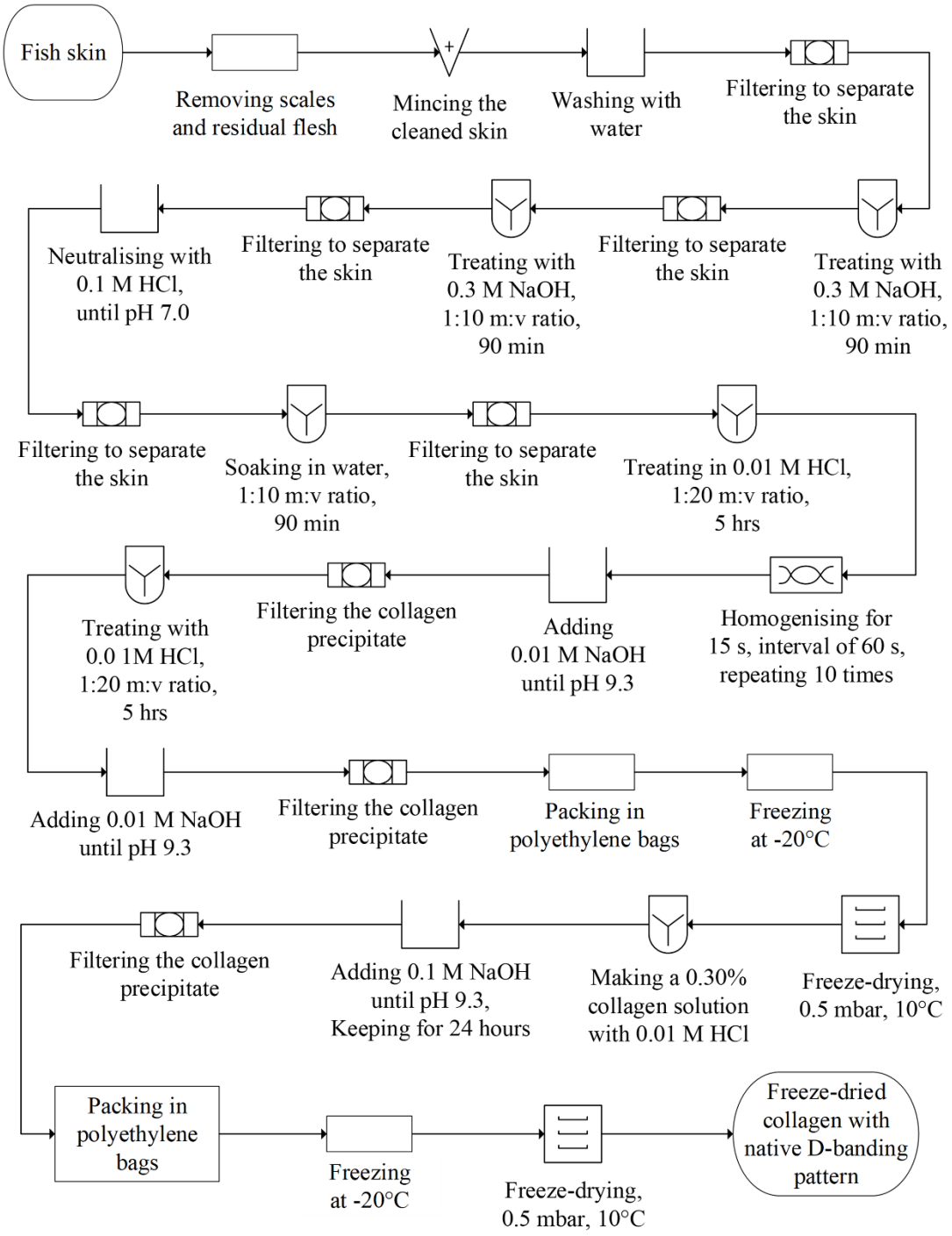

Figure 9.1 The process flow diagramme of the fish skin collagen extraction process developed in this study.

It is expected that the swelling will be different for other fish species, causing differences in skin solubility, pH during extraction and viscosity. Therefore, it is likely that the process conditions will need to be adjusted for different fish species of interest. It is likely that the above processing objectives can be achieved by using a hydrochloric acid solution with initial pH 2 and checking that the solution pH during extraction does not exceed pH 4. This is an easy way of adjusting this method for any fish species even without knowledge about the behaviour of its skin in the extraction medium.

The pigment removal was not successful by the pretreatment process developed in this study, causing a discolouration in the collagen fibrils after first fibrillogenesis. However, it opened a pathway to re-think the need for pigment removal, whether to improve only the colour or, both purity and colour. With this understanding, a second extraction was introduced to remove pigments to achieve improvement in both colour and purity. This was successful while still maintaining the triple-helical conformation. This result showed the opportunity for processing fish skins having a high amount of skin pigments if sufficient pigment removal was not achieved during the pretreatment step.

The native D-banding pattern of collagen fibrils which is essential for biomedical applications so was the ultimate focus. This was achieved through studying the underlying mechanisms governing the fibril morphology. A proper balance between the initial collagen concentration and mixing speed was found to be an important determinant of molecular availability for fibrillogenesis. Interestingly, the native D-banding occurred at a higher pH, far away from the isoelectric pH, and was influenced by the initial collagen concentration and mixing speed. It is likely that different molecular interactions play a role in forming D-banding at a pH higher than the isoelectric pH. Although some efforts were made in this study to describe the underlying mechanisms of forming D-bands, more experiments are needed to properly describe this factor in relation to molecular interactions.

The best conditions for forming collagen fibrils with native D-banding pattern according to those found in this study were: an initial collagen concentration of 0.30% in 0.01M hydrochloric solution, adding 0.1 M Sodium hydroxide until pH 9.3 with a gentle mixing and keeping for 24 h at 4°C. Collagen with native D-banding can be obtained from the skin of any fish species of interest once these processing conditions are used. However, it cannot be predicted from this study how the fibril structure would be changed when these conditions are altered.

It is important to mention some issues that should be considered in using this method at small or large-scale processing. One important aspect is the filtering mechanism of the skin after each pretreatment step. In the present study, the skin was separated from the pretreatment solution by keeping the solution undisturbed until the skin pieces settle in the bottom, decanting the solution as much as possible, and then sieving the skin through a stainless steel filter. This approach was taken to avoid the trapping of fat back onto the skin after it been removed into the solution. This method was not that successful to avoid re-trapping the fat, therefore it is proposed to investigate a possible alternative to separate the skin.

Another aspect is the homogenisation method. In the present study this was done using a hand blender, but at the industrial-scale it can be replaced with a homogeniser. Foams can

form during homogenisation due to void space. Therefore, it is recommended to consider this aspect as well.

Mixing the collagen solution during fibrillogenesis is another important aspect. A turbulent flow should be avoided as it can break the fibrils. There should be a method to have a laminar flow with a gentle forward and backward mixing. Therefore, designing a rocking mixer considering these aspects is proposed for industrial-scale.

The term 'biomedical collagen' lies in a spectrum of structure, toxicology, biocompatibility and cell viability. The method developed in the present study was focused on confirming the native D-banding pattern, and it was successful. However, it is suggested to test the other aspects before confirming this collagen as 'biomedical-grade collagen'.

9.2 Opportunities for future research

While this work has contributed to an improved understanding of the collagen extraction process from fish skin for potential biomedical applications, it also highlights some areas which need further research for a more complete understanding and to develop a more complete industrial process. They are listed below.

- The initial water washing of the minced skin was done until the washed water ran clean to remove any remaining scales or attached muscles. It was observed that some fat is removed while washing, however, this washing process was not studied in the present study in relation to the amount of fat and non-collagenous proteins that can be washed off. It is likely that a proper optimisation study can be done on initial water washing with the objective of minimising water use for cleaning.
- The viscosity of the collagen solutions were found to be important in the fibrillogenesis process to form fibrils with a D-banding pattern, however, it was not studied (except in terms of initial concentration) in the present study. Therefore, rheology experiments while combining the effect of mixing speed are suggested for a better understanding of the effect of viscosity of collagen solutions on the fibril morphology. This study can also look into different collagen concentrations, shear rates, and the dependence of Sodium hydroxide concentration on these factors to increase the medium pH.
- It was evident from the present study that the fibril morphology, particularly the D-banding pattern has not shown a relationship with the turbidity. There may be an effect of time, but the evidence from this study is insufficient to prove it. There is an opportunity to study this effect and relate it to possible molecular interactions.
- The process temperature used in this study was 4°C, and it was not allowed to increase the medium temperature above 10°C, for example, during homogenisation. It is suggested to test the effect of temperature, especially on the fibril morphology as fibrillogenesis is an entropy-driven process. And also, it will be important at the industrial-scale to minimise energy use. However, it is recommended to maintain the temperature below the onset temperature of thermal denaturation.
- It is suggested to do a scaling-up study of this method for pilot scale and industrial-scale.

- Although the method developed in this study is particularly intended for biomedical collagen extraction, there is likely to be a greater opportunity of using this method as a reference for marine collagen processing for other applications such as cosmetics.
- There were some innovative low-cost techniques introduced in this study such as measurement of swelling and measurement of skin solubility which may be useful techniques for similar or different types of research.

References

Achilli, M., & Mantovani, D. (2010). Tailoring mechanical properties of collagen-based scaffolds for vascular tissue engineering: the effects of pH, temperature and ionic strength on gelation. *Polymers*, *2*(4), 664-680.

Addad, S., Exposito, J. Y., Faye, C., Ricard-Blum, S., & Lethias, C. (2011). Isolation, characterization and biological evaluation of jellyfish collagen for use in biomedical applications. *Marine drugs*, *9*(6), 967-983.

Ahmed, R., Haq, M., & Chun, B. S. (2019). Characterization of marine derived collagen extracted from the by-products of bigeye tuna (Thunnus obesus). International Journal of Biological Macromolecules, 135, 668-676.

Akita, M., Nishikawa, Y., Shigenobu, Y., Ambe, D., Morita, T., Morioka, K., & Adachi, K. (2020). Correlation of proline, hydroxyproline and serine content, denaturation temperature and circular dichroism analysis of type I collagen with the physiological temperature of marine teleosts. Food chemistry, 329, 126775.

Anon. (1978). In Li, Z. R., Wang, B., Chi, C. F., Zhang, Q. H., Gong, Y. D., Tang, J. J., Luo, H. & Ding, G. F. (2013). Isolation and characterization of acid soluble collagens and pepsin soluble collagens from the skin and bone of Spanish mackerel (Scomberomorous niphonius). *Food hydrocolloids*, *31*(1), 103-113.

AOAC International. (1990). Official methods of analysis of the association of official analytical chemists. AOAC Method 960.39. 15 ed. Helrich K, editor. Virginia, USA.

Arumugam, G. K. S., Sharma, D., Balakrishnan, R. M., & Ettiyappan, J. B. P. (2018). Extraction, optimization and characterization of collagen from sole fish skin. *Sustainable Chemistry and Pharmacy*, *9*, 19-26.

Bae, I., Osatomi, K., Yoshida, A., Osako, K., Yamaguchi, A., & Hara, K. (2008). Biochemical properties of acid-soluble collagens extracted from the skins of underutilised fishes. Food chemistry, 108(1), 49-54.

Bak, S. Y., Lee, S. W., Choi, C. H., & Kim, H. W. (2018). Assessment of the Influence of Acetic Acid Residue on Type I Collagen during Isolation and Characterization. *Materials*, *11*(12), 2518.

Barzideh, Z., Latiff, A. A., Gan, C. Y., Benjakul, S., & Karim, A. A. (2014). Isolation and characterisation of collagen from the ribbon jellyfish (C hrysaora sp.). International journal of food science & technology, 49(6), 1490-1499.

Bateman, J. F., Lamande, S. R., & Ramshaw, J. A. (1996). Collagen superfamily. Extracellular matrix, 2, 22-67.

Bhuimbar, M. V., Bhagwat, P. K., & Dandge, P. B. (2019). Extraction and characterization of acid soluble collagen from fish waste: Development of collagen-chitosan blend as food packaging film. *Journal of Environmental Chemical Engineering*, *7*(2), 102983.

Bligh, E. G., & Dyer, W. J. (1959). A rapid method of total lipid extraction and purification. *Canadian journal of biochemistry and physiology*, *37*(8), 911-917.

Bloomfield, S. E., Miyata, T., Dunn, M. W., Bueser, N., Stenzel, K. H., & Rubin, A. L. (1978). Soluble gentamicin ophthalmic inserts as a drug delivery system. Archives of Ophthalmology, 96(5), 885-887.

Bowes, J. H., & Kenten, R. H. (1950). The swelling of collagen in alkaline solutions. 1. Swelling in solutions of sodium hydroxide. Biochemical Journal, 46(1), 1.

Box, G. E. P., & Wilson, K. B. (1951). On the experimental attainment of optimum conditions. Journal of the Royal Statistical Society (Series B), 13, 1–45. In Woo, J. W., Yu, S. J., Cho, S. M., Lee, Y. B., & Kim, S. B. (2008). Extraction optimization and properties of collagen from yellowfin tuna (Thunnus albacares) dorsal skin. *Food Hydrocolloids*, *22*(5), 879-887.

Brodsky, B., & Persikov, A. V. (2005). Molecular structure of the collagen triple helix. In *Advances in protein chemistry* (Vol. 70, pp. 301-339). Academic Press.

Brown, E. M., Farrell, H. M., & Wildermuth, R. J. (2000). Influence of neutral salts on the hydrothermal stability of acid-soluble collagen. Journal of Protein Chemistry, 19, 85-92.

Bürck, J., Heissler, S., Geckle, U., Ardakani, M. F., Schneider, R., Ulrich, A. S., & Kazanci, M. (2013). Resemblance of electrospun collagen nanofibers to their native structure. Langmuir, 29(5), 1562-1572.

Chen, J., Li, L., Yi, R., Xu, N., Gao, R., & Hong, B. (2016). Extraction and characterization of acid-soluble collagen from scales and skin of tilapia (Oreochromis niloticus). *LWT-Food Science and Technology*, *66*, 453-459.

Chen, X., Guo, Z., Zhang, J., Li, Y., & Duan, R. (2021). A new method for determining the denaturation temperature of collagen. Food Chemistry, 343, 128393.

Cheng, X., Gurkan, U. A., Dehen, C. J., Tate, M. P., Hillhouse, H. W., Simpson, G. J., & Akkus, O. (2008). An electrochemical fabrication process for the assembly of anisotropically oriented collagen bundles. *Biomaterials*, *29*(22), 3278-3288.

Chi, C. F., Wang, B., Li, Z. R., Luo, H. Y., Ding, G. F., & Wu, C. W. (2014). Characterization of Acid-soluble Collagen from the Skin of Hammerhead Shark (S phyrna lewini). *Journal of food biochemistry*, *38*(2), 236-247.

Cho, J. K., Jin, Y. G., Rha, S. J., Kim, S. J., & Hwang, J. H. (2014). Biochemical characteristics of four marine fish skins in Korea. *Food chemistry*, *159*, 200-207.

Christiansen, D. L., Huang, E. K., & Silver, F. H. (2000). Assembly of type I collagen: fusion of fibril subunits and the influence of fibril diameter on mechanical properties. Matrix Biology, 19(5), 409-420.

Ciarlo, A. S., Paredi, M. E., & Fraga, A. N. (1997). Isolation of soluble collagen from hake skin (Merluccius hubbsi). *Journal of Aquatic Food Product Technology*, *6*(1), 65-77.

Coelho, R. C., Marques, A. L., Oliveira, S. M., Diogo, G. S., Pirraco, R. P., Moreira-Silva, J., ... & Mano, J. F. (2017). Extraction and characterization of collagen from Antarctic and Sub-Antarctic squid and its potential application in hybrid scaffolds for tissue engineering. *Materials Science and Engineering: C*, *78*, 787-795.

Coppola, D., Oliviero, M., Vitale, G. A., Lauritano, C., D'Ambra, I., Iannace, S., & de Pascale, D. (2020). Marine collagen from alternative and sustainable sources: Extraction, processing and applications. Marine drugs, 18(4), 214.

Department of Census & Statistics (2020). Fisheries statistics. Statistics Unit, Ministry of Fisheries. Retrieved January 3, 2023. www.fisheriesdept.gov.lk/

Drzewiecki, K. E., Grisham, D. R., Parmar, A. S., Nanda, V., & Shreiber, D. I. (2016). Circular dichroism spectroscopy of collagen fibrillogenesis: A new use for an old technique. Biophysical journal, 111(11), 2377-2386.

Duan, R., Zhang, J., Du, X., Yao, X., & Konno, K. (2009). Properties of collagen from skin, scale and bone of carp (Cyprinus carpio). *Food chemistry*, *112*(3), 702-706.

Englert, C., Blunk, T., Müller, R., von Glasser, S. S., Baumer, J., Fierlbeck, J., ... & Hammer, J. (2007). Bonding of articular cartilage using a combination of biochemical degradation and surface cross-linking. *Arthritis research & therapy*, *9*(3), R47.

FAOSTAT, 2001 in Kim, S. K., & Mendis, E. (2006). Bioactive compounds from marine processing byproducts–a review. *Food Research International*, *39*(4), 383-393.

Foegeding, E. A. (1996). Characteristics of edible muscle tissues. *Food chemistry*. In Nalinanon, S., Benjakul, S., Kishimura, H., & Osako, K. (2011). Type I collagen from the skin of ornate threadfin bream (Nemipterus hexodon): Characteristics and effect of pepsin hydrolysis. *Food chemistry*, *125*(2), 500-507.

Freudenberg, U., Behrens, S. H., Welzel, P. B., Müller, M., Grimmer, M., Salchert, K., ... & Werner, C. (2007). Electrostatic interactions modulate the conformation of collagen I. Biophysical journal, 92(6), 2108-2119.

Gara, S. K., Grumati, P., Urciuolo, A., Bonaldo, P., Kobbe, B., Koch, M., ... & Wagener, R. (2008). Three novel collagen VI chains with high homology to the α3 chain. *Journal of Biological Chemistry*, *283*(16), 10658-10670.

Gauza-Włodarczyk, M., Kubisz, L., Mielcarek, S., & Włodarczyk, D. (2017). Comparison of thermal properties of fish collagen and bovine collagen in the temperature range 298–670 K. *Materials Science and Engineering: C*, *80*, 468-471.

Geesin, J. C., Brown, L. J., Liu, Z., & Berg, R. A. (1996). Development of a skin model based on insoluble fibrillar collagen. Journal of biomedical materials research, 33(1), 1-8.

Gelse, K., Pöschl, E., & Aigner, T. (2003). Collagens—structure, function, and biosynthesis. *Advanced drug delivery reviews*, *55*(12), 1531-1546.

Gobeaux, F., Mosser, G., Anglo, A., Panine, P., Davidson, P., Giraud-Guille, M. M., & Belamie, E. (2008). Fibrillogenesis in dense collagen solutions: a physicochemical study. *Journal of molecular biology*, *376*(5), 1509-1522.

Goissis, G., Piccirili, L., Goes, J. C., De Guzzi Plepis, A. M., & Das-Gupta, D. K. (1998). Anionic collagen: polymer composites with improved dielectric and rheological properties. Artificial Organs, 22(3), 203-209.

Gómez-Guillén, M. C., Giménez, B., López-Caballero, M. A., & Montero, M. P. (2011). Functional and bioactive properties of collagen and gelatin from alternative sources: A review. *Food hydrocolloids*, *25*(8), 1813-1827.

Gopinath, A., Shanmugam, G., Madhan, B., & Rao, J. R. (2017). Differential behavior of native and denatured collagen in the presence of alcoholic solvents: a gateway to instant structural analysis. International journal of biological macromolecules, 102, 1156-1165.

Green, J. J., & Elisseeff, J. H. (2016). Mimicking biological functionality with polymers for biomedical applications. *Nature*, *540*(7633), 386-394.

Harnkarnsujarit, N., Kawai, K., & Suzuki, T. (2015). Effects of freezing temperature and water activity on microstructure, color, and protein conformation of freeze-dried bluefin tuna (Thunnus orientalis). Food and Bioprocess Technology, 8(4), 916-925.

Harris, J. R., Soliakov, A., & Lewis, R. J. (2013). In vitro fibrillogenesis of collagen type I in varying ionic and pH conditions. Micron, 49, 60-68.

Hinderer, S., Layland, S. L., & Schenke-Layland, K. (2016). ECM and ECM-like materials—biomaterials for applications in regenerative medicine and cancer therapy. *Advanced drug delivery reviews*, *97*, 260-269.

Hofman, K., Tucker, N., Stanger, J., Staiger, M., Marshall, S., & Hall, B. (2012). Effects of the molecular format of collagen on characteristics of electrospun fibres. Journal of Materials Science, 47(3), 1148-1155.

Holmes, R., Kirk, S., Tronci, G., Yang, X., & Wood, D. (2017). Influence of telopeptides on the structural and physical properties of polymeric and monomeric acid-soluble type I collagen. Materials Science and Engineering: C, 77, 823-827.

Hoyer, B., Bernhardt, A., Lode, A., Heinemann, S., Sewing, J., Klinger, M., ... & Gelinsky, M. (2014). Jellyfish collagen scaffolds for cartilage tissue engineering. *Acta biomaterialia*, *10*(2), 883-892.

Hulmes, D. J. (2002). Building collagen molecules, fibrils, and suprafibrillar structures. *Journal of structural biology*, *137*(1-2), 2-10.

Hwang, J. H., Mizuta, S., Yokoyama, Y., & Yoshinaka, R. (2007). Purification and characterization of molecular species of collagen in the skin of skate (Raja kenojei). *Food Chemistry*, *100*(3), 921-925.

Ikoma, T., Kobayashi, H., Tanaka, J., Walsh, D., & Mann, S. (2003). Physical properties of type I collagen extracted from fish scales of Pagrus major and Oreochromis niloticas. *International journal of biological macromolecules*, *32*(3-5), 199-204.

Ito, S., Wakamatsu, K., & Ozeki, H. (1993). Spectrophotometric assay of eumelanin in tissue samples. *Analytical biochemistry*, *215*(2), 273-277.

Jenkins, C. L., & Raines, R. T. (2002). Insights on the conformational stability of collagen. Natural product reports, 19(1), 49-59.

Jafari, H., Lista, A., Siekapen, M. M., Ghaffari-Bohlouli, P., Nie, L., Alimoradi, H., & Shavandi, A. (2020). Fish collagen: Extraction, characterization, and applications for biomaterials engineering. Polymers, 12(10), 2230.

Jeong, H. S., Venkatesan, J., & Kim, S. K. (2013). Isolation and characterization of collagen from marine fish (Thunnus obesus). Biotechnology and bioprocess engineering, 18(6), 1185-1191.

Jiang, F., Hörber, H., Howard, J., & Müller, D. J. (2004). Assembly of collagen into microribbons: effects of pH and electrolytes. *Journal of structural biology*, *148*(3), 268-278.

Jongjareonrak, A., Benjakul, S., Visessanguan, W., Nagai, T., & Tanaka, M. (2005). Isolation and characterisation of acid and pepsin-solubilised collagens from the skin of Brownstripe red snapper (Lutjanus vitta). *Food Chemistry*, *93*(3), 475-484.

Kadler, K. E., Holmes, D. F., Trotter, J. A., & Chapman, J. A. (1996). Collagen fibril formation. *Biochemical Journal*, *316*(1), 1-11.

Karunarathna, K. A. A. U., & Attygalle, M. V. E. (2010). Nutritional evaluation in five species of tuna.

Kelly, S. M., Jess, T. J., & Price, N. C. (2005). How to study proteins by circular dichroism. Biochimica et Biophysica Acta (BBA)-Proteins and Proteomics, 1751(2), 119-139.

Khong, N. M., Yusoff, F. M., Jamilah, B., Basri, M., Maznah, I., Chan, K. W., Armania, N. & Nishikawa, J. (2018). Improved collagen extraction from jellyfish (Acromitus hardenbergi) with increased physical-induced solubilization processes. *Food chemistry*, *251*, 41-50.

Kim, J. S., & Park, J. W. (2004). Characterization of acid-soluble collagen from Pacific whiting surimi processing byproducts. Journal of food science, 69(8), C637-C642.

Kim, S. K., & Mendis, E. (2006). Bioactive compounds from marine processing byproducts–a review. *Food Research International*, *39*(4), 383-393.

Kittiphattanabawon, P., Benjakul, S., Visessanguan, W., Nagai, T., & Tanaka, M. (2005). Characterisation of acid-soluble collagen from skin and bone of bigeye snapper (Priacanthus tayenus). *Food chemistry*, *89*(3), 363-372.

Kittiphattanabawon, P., Benjakul, S., Visessanguan, W., & Shahidi, F. (2010a). Isolation and properties of acid-and pepsin-soluble collagen from the skin of blacktip shark (Carcharhinus limbatus). *European Food Research and Technology*, *230*(3), 475.

Kittiphattanabawon, P., Benjakul, S., Visessanguan, W., & Shahidi, F. (2010b). Isolation and characterization of collagen from the cartilages of brownbanded bamboo shark (Chiloscyllium punctatum) and blacktip shark (Carcharhinus limbatus). *LWT-Food Science and Technology*, *43*(5), 792-800.

Kittiphattanabawon, P., Benjakul, S., Visessanguan, W., Kishimura, H., & Shahidi, F. (2010c). Isolation and characterisation of collagen from the skin of brownbanded bamboo shark (Chiloscyllium punctatum). Food Chemistry, 119(4), 1519-1526.

Kittiphattanabawon, P., Nalinanon, S., Benjakul, S., & Kishimura, H. (2015). Characteristics of pepsin-solubilised collagen from the skin of splendid squid (Loligo formosana). *Journal of Chemistry*, *2015*.

Kołodziejska, I., Sikorski, Z. E., & Niecikowska, C. (1999). Parameters affecting the isolation of collagen from squid (Illex argentinus) skins. *Food Chemistry*, *66*(2), 153-157.

Kong, J., & Yu, S. (2007). Fourier transform infrared spectroscopic analysis of protein secondary structures. *Acta biochimica et biophysica Sinica*, *39*(8), 549-559.

Krishnamoorthi, J., Ramasamy, P., Shanmugam, V., & Shanmugam, A. (2017). Isolation and partial characterization of collagen from outer skin of Sepia pharaonis (Ehrenberg, 1831) from Puducherry coast. *Biochemistry and biophysics reports*, *10*, 39-45.

Lee, C. H., Singla, A., & Lee, Y. (2001). Biomedical applications of collagen. *International journal of pharmaceutics*, *221*(1-2), 1-22.

Li S., & Oakland N. J. (1997). Charged collagen particle-based delivery matrix. U.S. Patent No. 5,677,284. Washington, DC: U.S. Patent and Trademark Office.

Li, S., Ter K., & Oakland N. J. (1994). Resorbable vascular wound dressings. U.S. Patent No. 5,376,376. Washington, DC: U.S. Patent and Trademark Office.

Li, S., Ter K., & Oakland N. J. (1996). Method of making resorbable vascular wound dressing. U.S. Patent No. 5,512,291. Washington, DC: U.S. Patent and Trademark Office.

Li, D., Yang, W., & Li, G. Y. (2008). Extraction of native collagen from limed bovine split wastes through improved pretreatment methods. Journal of Chemical Technology & Biotechnology: International Research in Process, Environmental & Clean Technology, 83(7), 1041-1048.

Li, Y., Asadi, A., Monroe, M. R., & Douglas, E. P. (2009). pH effects on collagen fibrillogenesis in vitro: Electrostatic interactions and phosphate binding. *Materials Science and Engineering: C*, *29*(5), 1643-1649.

Li, Y., & Douglas, E. P. (2013). Effects of various salts on structural polymorphism of reconstituted type I collagen fibrils. *Colloids and Surfaces B: Biointerfaces*, *112*, 42-50.

Li, Z. R., Wang, B., Chi, C. F., Zhang, Q. H., Gong, Y. D., Tang, J. J., .Luo, H. & Ding, G. F. (2013). Isolation and characterization of acid soluble collagens and pepsin soluble collagens from the skin and bone of Spanish mackerel (Scomberomorous niphonius). *Food hydrocolloids*, *31*(1), 103-113.

Liao, W., Guanghua, X., Li, Y., Shen, X. R., & Li, C. (2018). Comparison of characteristics and fibril-forming ability of skin collagen from barramundi (Lates calcarifer) and tilapia (Oreochromis niloticus). International journal of biological macromolecules, 107, 549-559.

Liu, D., Liang, L., Regenstein, J. M., & Zhou, P. (2012). Extraction and characterisation of pepsin-solubilised collagen from fins, scales, skins, bones and swim bladders of bighead carp (Hypophthalmichthys nobilis). *Food Chemistry*, *133*(4), 1441-1448.

Liu, D., Wei, G., Li, T., Hu, J., Lu, N., Regenstein, J. M., & Zhou, P. (2015). Effects of alkaline pretreatments and acid extraction conditions on the acid-soluble collagen from grass carp (Ctenopharyngodon idella) skin. *Food Chemistry*, *172*, 836-843.

Liu, H., Li, D., & Guo, S. (2007). Studies on collagen from the skin of channel catfish (Ictalurus punctaus). Food Chemistry, 101(2), 621-625.

Liu, W., Tian, Z., Li, C., & Li, G. (2014). Thermal denaturation of fish collagen in solution: a calorimetric and kinetic analysis. *Thermochimica Acta*, *581*, 32-40.

Liu, X., Dan, N., & Dan, W. (2016). Preparation and characterization of an advanced collagen aggregate from porcine acellular dermal matrix. International journal of biological macromolecules, 88, 179-188.

Makareeva, E., & Leikin, S. (2007). Procollagen triple helix assembly: an unconventional chaperone-assisted folding paradigm. *PloS one*, *2*(10).

Maroušek, J., Maroušková, A., Myšková, K., Váchal, J., Vochozka, M., & Žák, J. (2015). Techno-economic assessment of collagen casings waste management. *International Journal of Environmental Science and Technology*, *12*(10), 3385-3390.

Miles, C. A., Avery, N. C., Rodin, V. V., & Bailey, A. J. (2005). The increase in denaturation temperature following cross-linking of collagen is caused by dehydration of the fibres. Journal of molecular biology, 346(2), 551-556.

Mosser, G., Anglo, A., Helary, C., Bouligand, Y., & Giraud-Guille, M. M. (2006). Dense tissue-like collagen matrices formed in cell-free conditions. Matrix Biology, 25(1), 3-13.

Muralidharan, N., Shakila, R. J., Sukumar, D., & Jeyasekaran, G. (2013). Skin, bone and muscle collagen extraction from the trash fish, leather jacket (Odonus niger) and their characterization. *Journal of Food Science and Technology*, *50*(6), 1106-1113.

Muyonga, J. H., Cole, C. G. B., & Duodu, K. G. (2004). Characterisation of acid soluble collagen from skins of young and adult Nile perch (Lates niloticus). *Food Chemistry*, *85*(1), 81-89.

Myllyharju, J., & Kivirikko, K. I. (2004). Collagens, modifying enzymes and their mutations in humans, flies and worms. *TRENDS in Genetics*, *20*(1), 33-43.

Nagai, T., Araki, Y., & Suzuki, N. (2002). Collagen of the skin of ocellate puffer fish (Takifugu rubripes). *Food chemistry*, *78*(2), 173-177.

Nagai, T., Ogawa, T., Nakamura, T., Ito, T., Nakagawa, H., Fujiki, K., ... & Yano, T. (1999). Collagen of edible jellyfish exumbrella. *Journal of the Science of Food and Agriculture*, *79*(6), 855-858.

Nagai, T., & Suzuki, N. (2000). Isolation of collagen from fish waste material—skin, bone and fins. *Food Chemistry*, *68*(3), 277-281.

Nagai, T., Suzuki, N., & Nagashima, T. (2008). Collagen from common minke whale (Balaenoptera acutorostrata) unesu. Food chemistry, 111(2), 296-301.

Nagai, T., Yamashita, E., Taniguchi, K., Kanamori, N., & Suzuki, N. (2001). Isolation and characterisation of collagen from the outer skin waste material of cuttlefish (Sepia lycidas). *Food Chemistry*, *72*(4), 425-429.

Nagarajan, M., Benjakul, S., Prodpran, T., & Songtipya, P. (2013). Effects of bleaching on characteristics and gelling property of gelatin from splendid squid (Loligo formosana) skin. Food Hydrocolloids, 32(2), 447-452.

Nalinanon, S., Benjakul, S., & Kishimura, H. (2010). Collagens from the skin of arabesque greenling (Pleurogrammus azonus) solubilized with the aid of acetic acid and pepsin from albacore tuna (Thunnus alalunga) stomach. Journal of the Science of Food and Agriculture, 90(9), 1492-1500.

Nalinanon, S., Benjakul, S., Kishimura, H., & Osako, K. (2011). Type I collagen from the skin of ornate threadfin bream (Nemipterus hexodon): Characteristics and effect of pepsin hydrolysis. *Food chemistry*, *125*(2), 500-507.

Nalinanon, S., Benjakul, S., Visessanguan, W., & Kishimura, H. (2007). Use of pepsin for collagen extraction from the skin of bigeye snapper (Priacanthus tayenus). Food Chemistry, 104(2), 593-601.

Nichols, J. & Princeton, N. J. (1991). Nerve regeneration conduit. U.S. Patent No. 5,019,087. Washington, DC: U.S. Patent and Trademark Office.

Nishad Fathima, N., Saranya Devi, R., Rekha, K. B., & Dhathathreyan, A. (2009). Collagen-curcumin interaction—A physico-chemical study. Journal of chemical sciences, 121, 509-514.

Nurilmala, M., Pertiwi, R. M., Nurhayati, T., Fauzi, S., Batubara, I., & Ochiai, Y. (2019 a). Characterization of collagen and its hydrolysate from yellowfin tuna Thunnus albacares skin and their potencies as antioxidant and antiglycation agents. Fisheries science, 85(3), 591-599.

Ogawa, M., Moody, M. W., Portier, R. J., Bell, J., Schexnayder, M. A., & Losso, J. N. (2003). Biochemical properties of black drum and sheepshead seabream skin collagen. *Journal of Agricultural and food Chemistry*, *51*(27), 8088-8092.

Ogawa, M., Portier, R. J., Moody, M. W., Bell, J., Schexnayder, M. A., & Losso, J. N. (2004). Biochemical properties of bone and scale collagens isolated from the subtropical fish black drum (Pogonia cromis) and sheepshead seabream (Archosargus probatocephalus). *Food chemistry*, *88*(4), 495-501.

Orgel, J. P., Miller, A., Irving, T. C., Fischetti, R. F., Hammersley, A. P., & Wess, T. J. (2001). The in situ supermolecular structure of type I collagen. *Structure*, *9*(11), 1061-1069.

O'Sullivan, A., Shaw, N. B., Murphy, S. C., Van de Vis, J. W., Van Pelt-Heerschap, H., & Kerry, J. P. (2006). Extraction of collagen from fish skins and its use in the manufacture of biopolymer films. *Journal of aquatic food product technology*, *15*(3), 21-32.

Pal, G. K., Nidheesh, T., & Suresh, P. V. (2015). Comparative study on characteristics and in vitro fibril formation ability of acid and pepsin soluble collagen from the skin of catla (Catla catla) and rohu (Labeo rohita). *Food Research International*, *76*, 804-812.

Pal, G. K., & Suresh, P. V. (2016). Sustainable valorisation of seafood by-products: Recovery of collagen and development of collagen-based novel functional food ingredients. Innovative food science & emerging technologies, 37, 201-215.

Pal, G. K., & Suresh, P. V. (2017). Comparative assessment of physico-chemical characteristics and fibril formation capacity of thermostable carp scales collagen. *Materials Science and Engineering: C*, *70*, 32-40.

Park, J. C., Hwang, Y. S., Lee, J. E., Park, K. D., Matsumura, K., Hyon, S. H., & Suh, H. (2000). Type I atelocollagen grafting onto ozone-treated polyurethane films: Cell attachment, proliferation, and collagen synthesis. *Journal of biomedical materials research*, *52*(4), 669-677.

Paterson, S. (Ed.). (2008). *Skin diseases of exotic pets*. John Wiley & Sons.

Pati, F., Datta, P., Adhikari, B., Dhara, S., Ghosh, K., & Mohapatra, P. K. D. (2012). Collagen scaffolds derived from fresh water fish origin and their biocompatibility. *Journal of Biomedical Materials Research Part A*, *100*(4), 1068-1079.

Pawelec, K. M., Best, S. M., & Cameron, R. E. (2016). Collagen: a network for regenerative medicine. *Journal of Materials Chemistry B*, *4*(40), 6484-6496.

Perez-Puyana, V., Ostos, F. J., López-Cornejo, P., Romero, A., & Guerrero, A. (2019). Assessment of the denaturation of collagen protein concentrates using different techniques. Biological Chemistry, 400(12), 1583-1591.

Potaros, T., Raksakulthai, N., Runglerdkreangkrai, J., & Worawattanamateekul, W. (2009). Characteristics of collagen from nile tilapia (Oreochromis niloticus) skin isolated by two different methods. *Nat Sci*, *43*, 584-593.

Qi, P., Zhou, Y., Wang, D., He, Z., & Li, Z. (2015). A new collagen solution with high concentration and collagen native structure perfectly preserved. RSC advances, 5(106), 87180-87186.

Ramírez-Rodríguez, G. B., Iafisco, M., Tampieri, A., Gómez-Morales, J., & Delgado-López, J. M. (2014). pH-responsive collagen fibrillogenesis in confined droplets induced by vapour diffusion. Journal of Materials Science: Materials in Medicine, 25(10), 2305-2312.

Riaz, T., Zeeshan, R., Zarif, F., Ilyas, K., Muhammad, N., Safi, S. Z., ... & Rehman, I. U. (2018). FTIR analysis of natural and synthetic collagen. *Applied Spectroscopy Reviews*, *53*(9), 703-746.

Ricard-Blum, S., & Ballut, L. (2011). Matricryptins derived from collagens and proteoglycans. *Front Biosci*, *16*, 674-697.

Ricard-Blum, S., Dublet, B., & van der Rest, M. (2000). *Unconventional Collagens: Types 6, 7, 8, 9, 10, 12, 14, 16, and 19*. Oxford University Press on Demand. In Ricard-Blum,

S., & Ballut, L. (2011). Matricryptins derived from collagens and proteoglycans. *Front Biosci*, *16*, 674-697.

Rodger, A., & Marshall, D. (2021). Beginners guide to circular dichroism. Biochemist, 43(2), 58-64.

Rodhouse, P., Dawe, E. G., & O'Dor, R. K. (Eds.). (1998). *Squid recruitment dynamics: the genus Illex as a model, the commercial Illex species and influence on variability* (Vol. 376). Food & Agriculture Org.

Rodríguez, F., Moran, L., González, G., Troncoso, E., & Zúñiga, R. N. (2017). Collagen extraction from mussel byssus: a new marine collagen source with physicochemical properties of industrial interest. Journal of food science and technology, 54, 1228-1238.

Rubin, A. L., Stenzel, K. H., Miyata, T., White, M. J., & Dunn, M. (1973). Collagen as a vehicle for drug delivery: preliminary report. The Journal of Clinical Pharmacology and New Drugs, 13(8-9), 309-312.

Sadowska, M., Kołodziejska, I., & Niecikowska, C. (2003). Isolation of collagen from the skins of Baltic cod (Gadus morhua). *Food Chemistry*, *81*(2), 257-262.

Sai-Ut, S., Jongjareonrak, A., & Rawdkuen, S. (2012). Re-extraction, recovery, and characteristics of skin gelatin from farmed giant catfish. Food and Bioprocess Technology, 5(4), 1197-1205.

Sankar, S., Sekar, S., Mohan, R., Rani, S., Sundaraseelan, J., & Sastry, T. P. (2008). Preparation and partial characterization of collagen sheet from fish (Lates calcarifer) scales. *International Journal of Biological Macromolecules*, *42*(1), 6-9.

Schmidt, M. M., Dornelles, R. C. P., Mello, R. O., Kubota, E. H., Mazutti, M. A., Kempka, A. P., & Demiate, I. M. (2016). Collagen extraction process. *International Food Research Journal*, *23*(3).

Shoulders, M. D., & Raines, R. T. (2009). Collagen structure and stability. *Annual review of biochemistry*, *78*, 929-958.

Silver, F. H., Freeman, J. W., & Seehra, G. P. (2003). Collagen self-assembly and the development of tendon mechanical properties. Journal of biomechanics, 36(10), 1529-1553.

Silvipriya, K. S., Kumar, K. K., Bhat, A. R., Kumar, B. D., John, A., & Lakshmanan, P. (2015). Collagen: Animal sources and biomedical application. *J. Appl. Pharm. Sci*, *5*(3), 123-127.

Singh, P., Benjakul, S., Maqsood, S., & Kishimura, H. (2011). Isolation and characterisation of collagen extracted from the skin of striped catfish (Pangasianodon hypophthalmus). *Food chemistry*, *124*(1), 97-105.

Sionkowska, A. (2000). Modification of collagen films by ultraviolet irradiation. Polymer Degradation and Stability, 68(2), 147-151.

Skehel, J. M. (2004). Preparation of extracts from animal tissues. In *Protein Purification Protocols* (pp. 15-20). Humana Press.

Skierka, E., & Sadowska, M. (2007). The influence of different acids and pepsin on the extractability of collagen from the skin of Baltic cod (Gadus morhua). *Food Chemistry*, *105*(3), 1302-1306.

Song, Z., Liu, H., Chen, L., Chen, L., Zhou, C., Hong, P., & Deng, C. (2021). Characterization and comparison of collagen extracted from the skin of the Nile tilapia by fermentation and chemical pretreatment. Food chemistry, 340, 128139.

Stamov, D. R., & Pompe, T. (2012). Structure and function of ECM-inspired composite collagen type I scaffolds. *Soft Matter*, *8*(40), 10200-10212.

Subhan, F., Ikram, M., Shehzad, A., & Ghafoor, A. (2015). Marine collagen: an emerging player in biomedical applications. *Journal of food science and technology*, *52*(8), 4703-4707.

Sugiura, H., Yunoki, S., Kondo, E., Ikoma, T., Tanaka, J., & Yasuda, K. (2009). In vivo biological responses and bioresorption of tilapia scale collagen as a potential biomaterial. Journal of Biomaterials Science, Polymer Edition, 20(10), 1353-1368.

Sun, L., Li, B., Song, W., Si, L., & Hou, H. (2017). Characterization of Pacific cod (Gadus macrocephalus) skin collagen and fabrication of collagen sponge as a good biocompatible biomedical material. *Process Biochemistry*, *63*, 229-235.

Talari, A. C. S., Martinez, M. A. G., Movasaghi, Z., Rehman, S., & Rehman, I. U. (2017). Advances in Fourier transform infrared (FTIR) spectroscopy of biological tissues. *Applied Spectroscopy Reviews*, *52*(5), 456-506.

Thermo Scientific (2015). Thermo Scientific Orion Star A320 series Electrochemistry portable meters. https://assets.thermofisher.com/TFS-Assets/LED/manuals/Orion-Star-A320-Series-Portable-Meter-User-Manual-EN.PDF

Tylingo, R., Mania, S., Panek, A., Piątek, R., & Pawłowicz, R. (2016). Isolation and characterization of acid soluble collagen from the skin of african catfish (Clarias gariepinus), salmon (Salmo salar) and baltic cod (Gadus morhua). *J Biotechnol Biomater*, *6*(234), 2.

Usha, R., & Ramasami, T. (2004). The effects of urea and n-propanol on collagen denaturation: using DSC, circular dicroism and viscosity. Thermochimica Acta, 409(2), 201-206.

Veeruraj, A., Arumugam, M., & Balasubramanian, T. (2013). Isolation and characterization of thermostable collagen from the marine eel-fish (Evenchelys macrura). *Process Biochemistry*, *48*(10), 1592-1602.

Von der Mark, K. (2006). Structure, biosynthesis and gene regulation of collagens in cartilage and bone. In *Dynamics of Bone and Cartilage Metabolism. Principles and Clinical Applications* (pp. 3-40). Academic Press/Elsevier Burlington, MA. In Gelse, K., Pöschl, E., & Aigner, T. (2003). Collagens—structure, function, and biosynthesis. *Advanced drug delivery reviews*, *55*(12), 1531-1546.

Wang, L., An, X., Xin, Z., Zhao, L., & Hu, Q. (2007). Isolation and characterization of collagen from the skin of deep-sea redfish (Sebastes mentella). *Journal of food science*, *72*(8), E450-E455.

Wang, L., An, X., Yang, F., Xin, Z., Zhao, L., & Hu, Q. (2008). Isolation and characterisation of collagens from the skin, scale and bone of deep-sea redfish (Sebastes mentella). *Food Chemistry*, *108*(2), 616-623.

Weiner, A. L., Carpenter-Green, S. S., Soehngen, E. C., Lenk, R. P., & Popescu, M. C. (1985). Liposome–collagen gel matrix: A novel sustained drug delivery system. Journal of pharmaceutical sciences, 74(9), 922-925.

Wasswa, J., Tang, J., & Gu, X. (2007). Utilization of fish processing by-products in the gelatin industry. Food Reviews International, 23(2), 159-174.

Wong, D. W. (1989). Mechanism and theory in food chemistry (Vol. 115). New York: Van Nostrand Reinhold.

Woo, J. W., Yu, S. J., Cho, S. M., Lee, Y. B., & Kim, S. B. (2008). Extraction optimization and properties of collagen from yellowfin tuna (Thunnus albacares) dorsal skin. *Food Hydrocolloids*, *22*(5), 879-887.

Wu, H., Wu, C., He, Q., Liao, X., & Shi, B. (2010). Collagen fiber with surface-grafted polyphenol as a novel support for Pd (0) nanoparticles: Synthesis, characterization and catalytic application. Materials Science and Engineering: C, 30(5), 770-776.

Xu, S., Yang, H., Shen, L., & Li, G. (2017). Purity and yield of collagen extracted from southern catfish (Silurus meridionalis Chen) skin through improved pretreatment methods. *International journal of food properties*, *20*(sup1), S141-S153.

Yamamoto, K., Yoshizawa, Y., Yanagiguchi, K., Ikeda, T., Yamada, S., & Hayashi, Y. (2015). The characterization of fish (tilapia) collagen sponge as a biomaterial. *International Journal of Polymer Science*, *2015*.

Yang, Y. J., Jung, D., Yang, B., Hwang, B. H., & Cha, H. J. (2014). Aquatic proteins with repetitive motifs provide insights to bioengineering of novel biomaterials. *Biotechnology journal*, *9*(12), 1493-1502.

Zeng, S. K., Zhang, C. H., Lin, H., Yang, P., Hong, P. Z., & Jiang, Z. (2009). Isolation and characterisation of acid-solubilised collagen from the skin of Nile tilapia (Oreochromis niloticus). *Food Chemistry*, *116*(4), 879-883.

Zeugolis, D. I., & Raghunath, M. (2010). The physiological relevance of wet versus dry differential scanning calorimetry for biomaterial evaluation: a technical note. Polymer International, 59(10), 1403-1407.

Zhang, M., Liu, W., & Li, G. (2009). Isolation and characterisation of collagens from the skin of largefin longbarbel catfish (Mystus macropterus). *Food Chemistry*, *115*(3), 826-831.

Zhang, X., Ookawa, M., Tan, Y., Ura, K., Adachi, S., & Takagi, Y. (2014). Biochemical characterisation and assessment of fibril-forming ability of collagens extracted from Bester sturgeon Huso huso× Acipenser ruthenus. Food Chemistry, 160, 305-312.

Zhang, Y., Liu, W., Li, G., Shi, B., Miao, Y., & Wu, X. (2007). Isolation and partial characterization of pepsin-soluble collagen from the skin of grass carp (Ctenopharyngodon idella). *Food chemistry*, *103*(3), 906-912.

Zhou Y, Li S, Wang D, Zhao Y, Lei X. (2018). Estimation of type i collagen structure dissolved in inorganical acids from circular dichroism spectra. Biosci. J. 34(3):778-789.

Zhu, S., Yuan, Q., Yin, T., You, J., Gu, Z., Xiong, S., & Hu, Y. (2018). Self-assembly of collagen-based biomaterials: preparation, characterizations and biomedical applications. *Journal of Materials Chemistry B*, *6*(18), 2650-2676.

https://www.fao.org (Proximate composition of 5 parts and whole fish (g/100 g wet weight; mean and range))

https://www.fishbase.se/summary/thunnus-albacares.html. Retrieved February 2, 2023.

https://fishider.org/en/guide/osteichthyes/scombridae/thunnus/thunnus-albacares. Retrieved February 2, 2023.

https://www.fishspecies.nz/tarakihi. Retrieved February 3, 2023.

https://fs.fish.govt.nz/Page.aspx?pk=7&tk=100&ey=2022. Retrieved February 2, 2023.
https://www.seafood.co.nz/species/tarakihi. Retrieved February 3, 2023.
https://www.slideshare.net/SoniaBajaj10/fish-skin. Retrieved January 23, 2023.
https://www.srilankabusiness.com/sea-food/sri-lankan-sea-food-products.html#finfish. Retrieved February 2, 2023.
https://www.talleys.co.nz/seafood/species/tarakihi. Retrieved February 3, 2023. Retrieved February 3, 2023.

Copyright permissions

Copyright permission for Figure 2.1

ELSEVIER LICENSE TERMS AND CONDITIONS

Feb 05, 2023

This Agreement between Massey University -- Suchima Gonapinuwala ("You") and Elsevier("Elsevier") consists of your license details and the terms and conditions provided byElsevier and Copyright Clearance Center.

License Number	5482790958258
License date	Feb 05, 2023
Licensed Content Publisher	Elsevier
Licensed Content Publication	Advanced Drug Delivery Reviews
Licensed Content Title	Collagens—structure, function, andbiosynthesis
Licensed Content Author	K. Gelse,E. Pöschl,T. Aigner
Licensed Content Date	Nov 28, 2003
Licensed Content Volume	55
Licensed Content Issue	12
Licensed Content Pages	16
Start Page	1531
End Page	1546
Type of Use	reuse in a thesis/dissertation
Portion	figures/tables/illustrations
Number of figures/tables/illustrations	1
Format	electronic
Are you the author of this Elsevier article?	No
Will you be translating?	No
Title	Commercially scalable fish collagen processing
Institution name	Massey University, New Zealand
Portions	Fig. 1
Requestor Location	Massey University Tennent Drive Palmerston North, 4410 New Zealand Attn: Massey University

Copyright permission for Figure 2.2

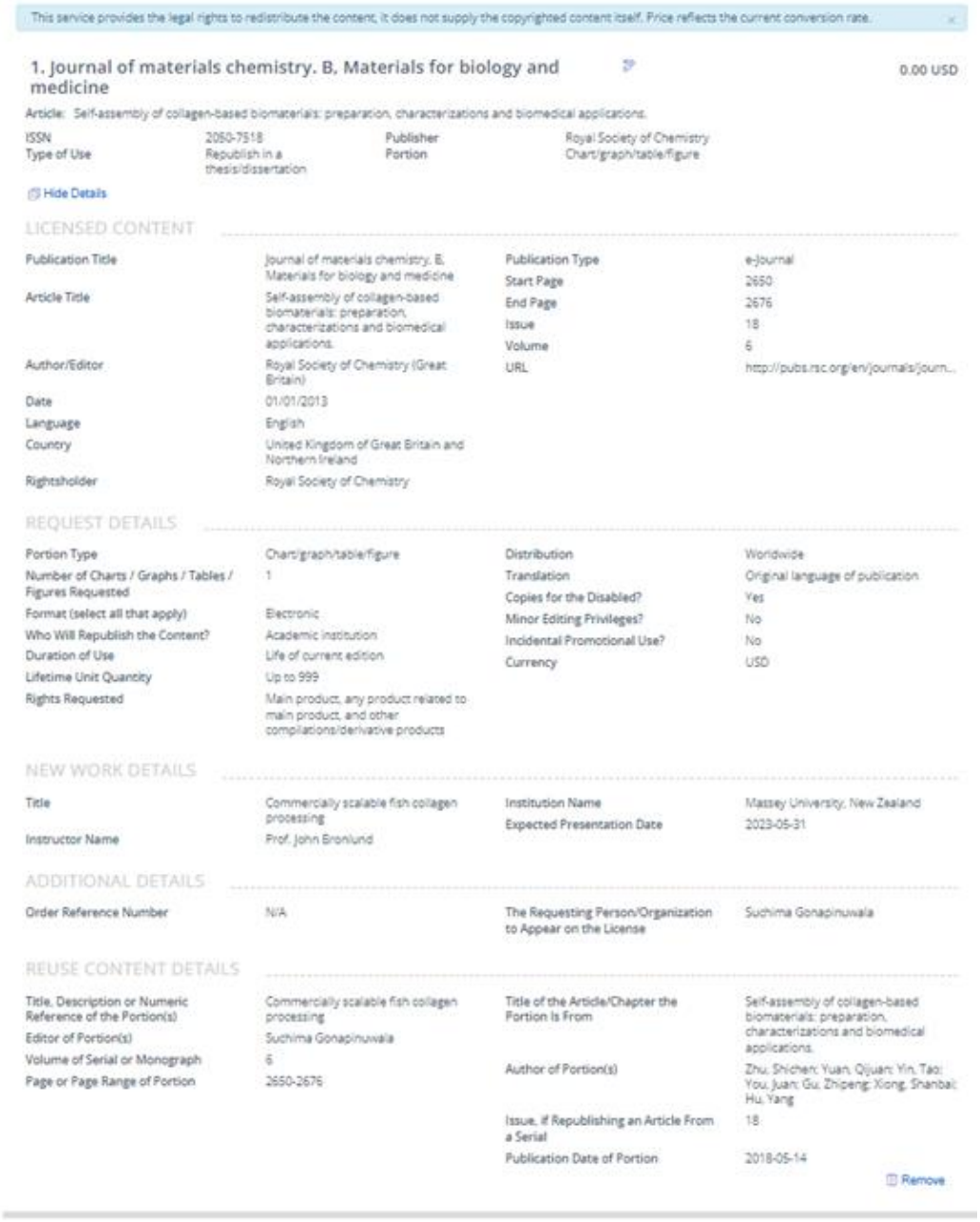

This service provides the legal rights to redistribute the content, it does not supply the copyrighted content itself. Price reflects the current conversion rate.

1. Journal of materials chemistry. B, Materials for biology and medicine 0.00 USD

Article: Self-assembly of collagen-based biomaterials: preparation, characterizations and biomedical applications.

ISSN	2050-7518	Publisher	Royal Society of Chemistry
Type of Use	Republish in a thesis/dissertation	Portion	Chart/graph/table/figure

Hide Details

LICENSED CONTENT

Publication Title	Journal of materials chemistry. B, Materials for biology and medicine	Publication Type	e-Journal
Article Title	Self-assembly of collagen-based biomaterials: preparation, characterizations and biomedical applications.	Start Page	2650
		End Page	2676
		Issue	18
		Volume	6
Author/Editor	Royal Society of Chemistry (Great Britain)	URL	http://pubs.rsc.org/en/journals/journ...
Date	01/01/2013		
Language	English		
Country	United Kingdom of Great Britain and Northern Ireland		
Rightsholder	Royal Society of Chemistry		

REQUEST DETAILS

Portion Type	Chart/graph/table/figure	Distribution	Worldwide
Number of Charts / Graphs / Tables / Figures Requested	1	Translation	Original language of publication
		Copies for the Disabled?	Yes
Format (select all that apply)	Electronic	Minor Editing Privileges?	No
Who Will Republish the Content?	Academic institution	Incidental Promotional Use?	No
Duration of Use	Life of current edition	Currency	USD
Lifetime Unit Quantity	Up to 999		
Rights Requested	Main product, any product related to main product, and other compilations/derivative products		

NEW WORK DETAILS

Title	Commercially scalable fish collagen processing	Institution Name	Massey University, New Zealand
		Expected Presentation Date	2023-05-31
Instructor Name	Prof. John Bronlund		

ADDITIONAL DETAILS

Order Reference Number	N/A	The Requesting Person/Organization to Appear on the License	Suchima Gonapinuwala

REUSE CONTENT DETAILS

Title, Description or Numeric Reference of the Portion(s)	Commercially scalable fish collagen processing	Title of the Article/Chapter the Portion Is From	Self-assembly of collagen-based biomaterials: preparation, characterizations and biomedical applications.
Editor of Portion(s)	Suchima Gonapinuwala		
Volume of Serial or Monograph	6	Author of Portion(s)	Zhu, Shichen; Yuan, Qijuan; Yin, Tao; You, Juan; Gu, Zhipeng; Xiong, Shanbai; Hu, Yang
Page or Page Range of Portion	2650-2676		
		Issue, if Republishing an Article From a Serial	18
		Publication Date of Portion	2018-05-14

Remove

Copyright permission for Figure 2.5 (A and B)

ELSEVIER LICENSE TERMS AND CONDITIONS	
Feb 05, 2023 This Agreement between Massey University -- Suchima Gonapinuwala ("You") and Elsevier ("Elsevier") consists of your license details and the terms and conditions provided by Elsevier and Copyright Clearance Center.	
License Number	5482810679239
License date	Feb 05, 2023
Licensed Content Publisher	Elsevier
Licensed Content Publication	Journal of Structural Biology
Licensed Content Title	Assembly of collagen into microribbons: effects of pH and electrolytes
Licensed Content Author	Fengzhi Jiang,Heinrich Hörber,Jonathon Howard,Daniel J. Müller
Licensed Content Date	Dec 1, 2004
Licensed Content Volume	148
Licensed Content Issue	3
Licensed Content Pages	11
Start Page	268
End Page	278
Type of Use	reuse in a thesis/dissertation
Portion	figures/tables/illustrations
Number of figures/tables/illustrations	2
Format	electronic
Are you the author of this Elsevier article?	No
Will you be translating?	No
Title	Commercially scalable fish collagen processing
Institution name	Massey University, New Zealand
Portions	Fig. 1, Fig. 3
Requestor Location	Massey University Tennent Drive Palmerston North, 4410 New Zealand Attn: Massey University

Copyright permission for Figure 2.5 (C and D)

ELSEVIER LICENSE TERMS AND CONDITIONS Feb 05, 2023	
This Agreement between Massey University -- Suchima Gonapinuwala ("You") and Elsevier ("Elsevier") consists of your license details and the terms and conditions provided by Elsevier and Copyright Clearance Center.	
License Number	5482820258761
License date	Feb 05, 2023
Licensed Content Publisher	Elsevier
Licensed Content Publication	Materials Science and Engineering: C
Licensed Content Title	pH effects on collagen fibrillogenesis in vitro: Electrostatic interactions and phosphate binding
Licensed Content Author	Yuping Li,Amran Asadi,Margo R. Monroe,Elliot P. Douglas
Licensed Content Date	Jun 1, 2009
Licensed Content Volume	29
Licensed Content Issue	5
Licensed Content Pages	7
Start Page	1643
End Page	1649
Type of Use	reuse in a thesis/dissertation
Portion	figures/tables/illustrations
Number of figures/tables/illustrations	2
Format	electronic
Are you the author of this Elsevier article?	No
Will you be translating?	No
Title	Commercially scalable fish collagen processing
Institution name	Massey University, New Zealand
Portions	Fig. 2, Fig. 3
Requestor Location	Massey University Tennent Drive Palmerston North, 4410 New Zealand Attn: Massey University